8-2017

Growth and Survivability of Microorganisms at Martian Temperatures and Pressures

Rebecca Lynne Mickol
University of Arkansas, Fayetteville

Growth and Survivability of Microorganisms at Martian Temperatures and Pressures

A dissertation submitted in partial fulfillment
of the requirements for the degree of
Doctor of Philosophy in Space and Planetary Sciences

by

Rebecca Lynne Mickol
University of Colorado
Bachelor of Arts in Astrophysics, 2010
University of Colorado
Bachelor of Arts in Ecology and Evolutionary Biology, 2010

August 2017
University of Arkansas

This dissertation is approved for recommendation to the Graduate Council.

_____
Dr. Timothy Kral
Dissertation Director

_____
Dr. John Dixon
Committee Member

_____
Dr. Dan Kennefick
Committee Member

_____
Dr. Dan Lessner
Committee Member

_____
Dr. Andrew Schuerger
Ex-officio Member

Abstract

The discovery of methane in the martian atmosphere via numerous ground- and space-based sources has prompted the study of methanogens as models for life on Mars. Methanogens are microorganisms within the domain Archaea, many of which utilize carbon dioxide (CO_2) and hydrogen to produce methane. The non-photosynthetic nature of methanogens indicates that they could exist in sub-surface environments, protected from harmful UV and ionizing radiation on the surface of Mars. These organisms also do not require organics, which are sparse on the planet.

Additionally, the wide variety of environments we find life in on Earth, as well as evidence for liquid brines on the surface of Mars, suggest that habitable environments may still exist on the planet. However, there are a variety of conditions that any extant life on Mars would need to endure, including wide variations in temperature over one sol, a low-pressure atmosphere, and a limited availability of liquid water, among others.

This dissertation encompasses various experiments that examined the ability of four species of methanogens (*Methanosarcina barkeri*, *Methanobacterium formicicum*, *Methanococcus maripaludis*, and *Methanothermobacter wolfeii*) to survive and/or grow under 1) low-pressure conditions and 2) freeze/thaw cycles. Low pressure studies include both survival and active growth experiments conducted between 7 mbar (the average surface pressure on Mars) and 143 mbar. Freeze/thaw experiments utilized short- and long-term cycles varying in temperature between the organisms' growth temperatures (22 °C, *M. maripaludis*; 37 °C, *M. barkeri* and *M. formicicum*; 55 °C, *M. wolfeii*) and -80 °C, encompassing Mars-relevant temperature changes. As a comparison to methanogen growth and survivability, additional experiments were conducted using a non-spore-forming bacterium, *Serratia liquefaciens*,

previously shown capable of growth at 7 mbar, 0 °C and within an anoxic CO_2 atmosphere. The experiments described here assessed the survivability of *S. liquefaciens* exposed to martian UV irradiation within liquid brines and ices.

The experiments discussed here demonstrate the ability of Earth microorganisms to withstand certain extreme conditions on Mars and suggest that the planet may contain relatively habitable microenvironments within the near subsurface.

Acknowledgements

Portions of this work were funded by the National Aeronautics and Space Administration (NASA) Astrobiology: Exobiology and Evolutionary Biology Program grant #NNX12AD90G and by grants from the Arkansas Space Grant Consortium. Additionally, some portions of this research were conducted at the Space Life Sciences Lab, Kennedy Space Center under grant #NNX12AJ84G from NASA's Planetary Protection Office.

I thank all of the undergraduates who conducted research with me during my graduate school career, notably, Sarah Laird and Yuta Takagi, for their assistance in parts of the research discussed here. I'd also like to acknowledge Coleman McFerrin for his unending moral support and companionship in the lab and the cities of Chicago and Boston.

Thank you to my committee members, Dr. Daniel Lessner, Dr. Daniel Kennefick and Dr. John Dixon for your support and guidance throughout my graduate career. Thank you to Walter Graupner for technical assistance with the Pegasus Planetary Simulation Chamber and construction and design of the specialized puncture device.

Thank you to Dr. Andrew Schuerger for the opportunity to conduct research with you and for your guidance through the process and successful completion of a manuscript. Your assistance regarding research, data analysis, and manuscript preparation has been greatly appreciated and often, necessary, and these skills will remain with me throughout my scientific career.

To all my family and friends, near and far, thank you for the laughter and the commiseration. I love you all dearly.

To Dr. Cassie Marnocha and Dr. Erika Kohler, there aren't words to describe how

amazing you two are, so I'll just put it in an email. Let's meet at the Drury and have Outback for dinner.

Finally, to Dr. Timothy Kral, you're welcome. I mean, thank you for being a great mentor and advisor. I greatly enjoyed my time in your lab and leaving will be bittersweet. Never a dull moment. Love, Spike.

Dedication

In loving memory of Lynne Marie Rinaldis. Mom, I love you always and forever, and you will be with me always. I wouldn't be who I am today without your endless love and devotion. May your hard work, determination, and spirit live on. Ain't no mountain high enough.

To Nick, thank you for being the best brother anyone could have and for your continuous love and support.

Table of Contents

List of Tables

List of Figures

Figure 5.1 Mars Simulation Chamber (MSC) experimental setup and slush-sputtering results for Experiment 2. Aluminum foil (**A**) or clear cellophane wrap (**B**) were used to cover the inside of the Mars Simulation Chamber (MSC) in order to mitigate slush-sputtering of the water/ice/cells/salt slurries in Experiment 2. The 6-cm water filter (wf; Fig. 5.1**A**) for UV attenuation measurements (Table 5.2) was placed immediately after the xenon lamp housing on top of the MSC. The 6-cm water filter contained filtered (0.45 µm) double-deionized (18 MΩ) water for all other experiments. (**C**) Frozen samples of $MgSO_4$ brines in Experiment 2 were dispensed in 6-cm glass dishes and placed within the central part of the UV beam (28-cm wide) on top of the LN_2 cold plate. Approximately 0.1 g of Hawaiian palagonite was added to each salt solution to provide nuclei for crystallization of the ices. (**D**) Right-side view port (vp in Fig. 5.1**A**) on the MSC with salt deposits on the inside surface of the glass port. (**E**) Salt deposits were frequently observed on the aluminum foil within the MSC during Experiment 2. The dried salt slurries created salt deposits that were primarily 0.5 to 3 mm in diameter. 214

Figure 5.2 Kill curves for *Serratia liquefaciens* cells in SDIW and liquid brines exposed to Mars equatorial UV fluence rates at 101.3 kPa. Cells of *S. liquefaciens* were inoculated into SDIW, 10 mM PO_4 buffer, 5% $MgSO_4$, or 10% $MgSO_4$ solutions at densities of ~2 x 10^6 cells/mL and exposed to UV irradiation for 0, 0.17, 0.5, 1, 5, 10, 20, 30, or 60 min (cumulative). Surviving cells (N/No) decreased 4- to 5-logs between 0 and 0.5 min, with a slower decline noted thereafter. Data from each solution were transformed independently to induce homogeneity of treatment variances (i.e., SDIW and 5% $MgSO_4$ = 0.20 power transformation; 10 mM PO_4 = 0.125 power transformation; 10% $MgSO_4$ = 0.10 power transformation). Different letters indicate significant differences among treatment means for each solution based on separate ANOVA and protected least-squares mean separation tests (n = 5; $P \leq 0.05$); bars represent standard deviations of the means. Inserted graphs represent Log(N/No) values for each solution against UVC dosage (kJ/m^2) for time-steps 0, 0.17, and 0.5 min and were used to generate F_{10} values for UVC flux (shown above) and time (data not plotted). Linear models, F_{10} values, and r^2 data for UVC flux and time are given in Table 5.1. 221

Figure 5.3 Kill curves for *Serratia liquefaciens* cells in SDIW and brine ices under martian conditions. Cells of *S. liquefaciens* were inoculated into SDIW, 10 mM PO_4 buffer, 5% $MgSO_4$, or 10% $MgSO_4$ solutions at densities of ~2 x 10^6 cells/mL. Cell suspensions were exposed to a

Mars equatorial UV flux for 0, 0.17, 1, 10, or 60 min. A second set of petri dishes were similarly prepared but shielded from UV irradiation. Results here on the inactivation of *S. liquefaciens* cells embedded in the ices were very similar to the results in Fig. 5.2 obtained in liquid assays. The most dramatic declines in the numbers of surviving cells (N/No) were observed between 0 and 1 min for all treatments. Combined results from Fig. 5.2 and here suggest that the $MgSO_4$ solutions and ices failed to attenuate UV irradiation under simulated martian conditions. Data from all solutions were transformed independently to induce homogeneity of treatment variances (i.e., SDIW and 10 mM PO_4 = 0.10 power transformation; 5% $MgSO_4$ and 10% $MgSO_4$ = 0.067 power transformation). Different letters indicate significant differences among treatment means for each solution based on separate ANOVA and protected least-squares mean separation tests (n = 3; $P \leq 0.05$); bars represent standard deviations of the means. 224

Figure 5.4 Survival of *Serratia liquefaciens* in salt solutions under frozen (-20 °C) and non-frozen (24 °C) conditions. Cells of *S. liquefaciens* were added to SDIW, 10 mM PO_4 buffer, 5% $MgSO_4$, or 10% $MgSO_4$ solutions at densities of ~2 x 10^6 viable cells/mL and exposed to either -20 or 24 °C for 24 h. Results indicate that freezing the SDIW and brine solutions at -20 °C had minimal (~1 log), but significant, effects on cell survival (N/No), except for the -20 °C 10 mM PO_4 buffer treatment which exhibited a slight decrease of 1.5 logs compared to the T = 0 controls. Data from each solution were transformed independently to induce homogeneity of treatment variances (SDIW, 10% $MgSO_4$ = log transformations; 10 mM PO_4 = 0.25 power transformation; 5% $MgSO_4$ = no transformation). Different letters indicate significant differences among treatment means for each solution within individual solutions based on separate ANOVA and protected least-squares mean separation tests (n = 4; $P \leq 0.05$); bars represent standard deviations of the means. 227

Figure 5.5 Effects of UV attenuation by Mars analog soils on the survival of *Serratia liquefaciens*. Cells of *S. liquefaciens* were added to 5% $MgSO_4$ solutions at ~2 x 10^6 cells/mL and frozen overnight for 16 h at -20 °C. Mars analog soils (i.e., basalt and Hawaiian palagonite) also were frozen at -20 °C for 16 h. The ice/analog assay dishes were exposed to a Mars UV flux for 60 min, removed, thawed, and processed with the MPN assay. Survival of *S. liquefaciens* cells (N/No) was reduced approximately 1-log and 1.5-logs for the basalt and palagonite analogs, respectively, when compared to the T = 0 controls (one T = 0 control for

List of Published Chapters

Chapter Two:
Mickol, R. L. and T. A. Kral (2016) Low Pressure Tolerance by Methanogens in an Aqueous Environment: Implications for Subsurface Life on Mars. *Origins of Life and Evolution of Biospheres*, 1-22. DOI 10.1007/s11084-016-9519-9

Chapter Four:
Mickol, R. L., J. L. Page, and A. C. Schuerger (2017) Magnesium Sulfate Salt Solutions and Ices Fail to Protect *Serratia liquefaciens* from the Biocidal Effects of UV Irradiation under Martian Conditions. *Astrobiology*, 17(5), 401-412.

Introduction

The discovery of methane in the martian atmosphere (Fonti and Marzo, 2010; Formisano et al., 2004; Geminale et al., 2008; Geminale et al., 2011; Krasnopolsky et al., 1997; Krasnopolsky et al., 2004; Maguire, 1977; Mumma et al., 2009; Webster et al., 2015) has provoked the curiosity of astrobiologists in the search for life in the solar system. Methane (CH_4) is considered an important biomarker in planetary atmospheres due to its prevalence as a metabolic end-product on Earth. Although most methane on Earth is produced biogenically (involving living organisms or formed from organic matter), it can also be produced abiogenically [involving no living organisms and only formed from inorganic matter] (Floodgate and Judd, 1992; Schoell, 1988). The search for life on other planets and moons in the solar system often utilizes atmospheric biomarkers as both a preliminary indication that life may be present on that world and as justification for further exploration. However, evidence for methane as a true biomarker requires that all other possible sources be accounted for, as methane on Earth results from a variety of sources. Thus, the discovery of methane in the martian atmosphere (Fonti and Marzo, 2010; Formisano et al., 2004; Geminale et al., 2008; Geminale et al., 2011; Krasnopolsky et al., 1997; Krasnopolsky et al., 2004; Maguire, 1977; Mumma et al., 2009; Webster et al., 2015) may be an indicator of life on the planet, although there are other possible abiotic explanations such as comet/meteorite impacts and subsequent UV photolysis (Court and Sephton, 2009; Fries et al., 2016; Keppler et al., 2012; Kress and McKay, 2004; Price et al., 2014; Schuerger et al., 2012b), clathrates (Chassefière, 2009; Chassefière and Leblanc, 2011b; Chastain and Chevrier, 2007; Max and Clifford, 2000; Max et al., 2013; Onstott et al., 2006; Prieto-Ballesteros et al., 2006), or water-rock reactions including serpentinization (Atreya et al., 2007; Atreya et al., 2011; Lyons et al., 2005; McMahon et al., 2013; Oze and Sharma, 2005).

1.1 Methane on Earth – Biological and Geological Sources

Methane on Earth is produced through a variety of biological and non-biological processes. The current total atmospheric methane abundance on Earth is 1803.2 ppb, corresponding to 4954 ± 10 Tg with a yearly production of 556 ± 56 Tg (IPCC, 2013). Although overall global abundances are fairly well constrained, and natural and anthropogenic sources are known, the specific contribution of methane from each source is not well understood (Frankenberg et al., 2005; Sheppard et al., 1982). The interconnectedness of various ecosystems and the increasing influence of humans make it difficult to distinguish between different sources of methane.

Sources of methane are often categorized into natural vs. anthropogenic emissions or biogenic vs. abiogenic emissions (Figure 1.1). Natural production of methane includes emissions from wetlands, upland soils and riparian zones, oceans, estuaries and rivers, permafrost, lakes, gas hydrates, terrestrial and marine geological sources, wildfires, vegetation, and terrestrial arthropods and wild animals (Anderson et al., 2010) and contributes 202 ± 35 Tg CH_4/yr to the atmosphere (IPCC, 2013). Anthropogenic sources of methane result from agriculture, including rice fields and ruminants, landfills, sewage treatment, biomass burning and fossil fuels (Conrad, 2009) and currently constitute 65% of the total global methane budget [354 ± 45 Tg CH_4/yr (IPCC, 2013)]. In total, biogenic sources account for over 70% of total global methane and include emissions from wetlands, rice agriculture, livestock, landfills, forests, oceans and termites (Denman et al., 2007). Many of these biogenic sources involve initial fermentation processes to produce acetate, H_2, and CO_2, which are then converted into methane by methanogenic Archaea. Non-biogenic methane (~30% total global methane) includes emissions from fossil fuels, biomass burning, waste treatment and geological sources (e.g., fossil CH_4 from

natural gas seepage and geothermal/volcanic CH_4) (Denman et al., 2007). However, there are discrepancies concerning the specific contributions of biogenic and non-biogenic methane to the total global budget, mainly due to classification of origin. For example, thermogenic methane (e.g. conversion of organic matter under high temperature and pressure) can be considered biogenic in origin since it involves organic matter (Floodgate and Judd, 1992; Kvenvolden, 1995; Kvenvolden and Rogers, 2005; Schoell, 1988). This would result in the inclusion of fossil fuels, biomass burning, and waste treatment as biogenic sources, suggesting that ~100% of Earth's global atmospheric methane is biological in origin (~80% due to methanogenic processes and ~20% from thermogenic processes), with the abiogenic contribution considered negligible (Floodgate and Judd, 1992; Kvenvolden, 1995; Kvenvolden and Rogers, 2005; Schoell, 1988).

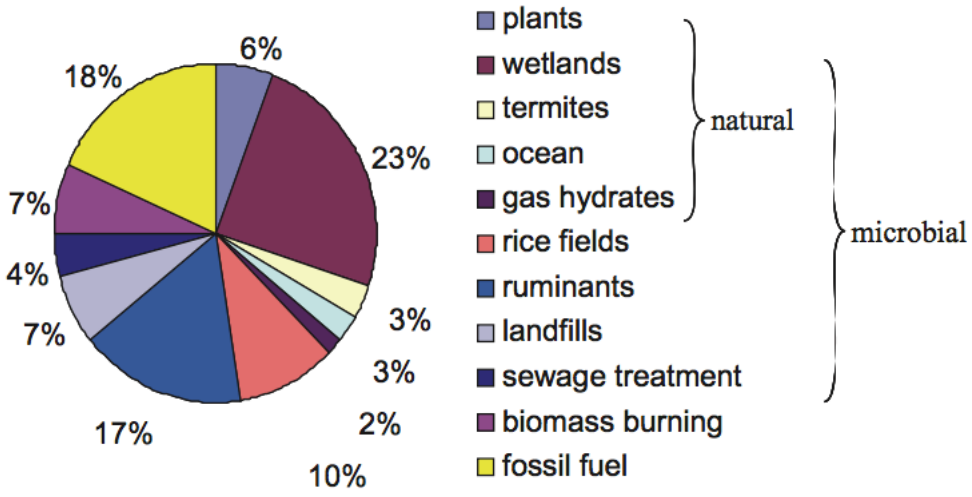

Figure 1.1 Global sources of methane in percent of the total budget of ~500-600 Tg CH_4/yr. From: Conrad (2009).

The exclusion of geological sources in global methane budgets results from the difficulty in constraining individual sources and distinguishing between biogenic and abiogenic origins. However, recent studies show increasing support for consideration of geological abiogenic

sources, citing non-negligible abundances (Etiope and Sherwood Lollar, 2013; Horita and Berndt, 1999; Sherwood Lollar et al., 2006). Geological sources of methane include two main categories: magmatic processes (typically within volcanic and high-temperature hydrothermal settings) and gas-water-rock reactions (Etiope and Sherwood Lollar, 2013). Gas-water-rock reactions are considered independent of magma or magma-derived fluid and include high-temperature reactions, alteration of carbonates via metamorphism, decomposition or methanation, uncatalyzed aqueous CO_2 reduction, and Fischer-Tropsch Type (FTT) reactions (Etiope and Sherwood Lollar, 2013). Serpentinization and Fischer-Tropsch Type reactions are considered dominant sources of geologically-produced methane. For example, Emmanuel and Ague (2007) calculated that ~55% of abiotic methane on Earth is produced through serpentinization at mid-ocean ridges, with an additional 40% resulting from continental geothermal sources (although these comprise upper limits as a significant portion of methane at these locations is likely biogenic in origin [microbial or resulting from organic matter]). Serpentinization transforms ultramafic (Mg-, Fe-rich) rocks, such as olivine, into serpentine and hydrogen (H_2), which react with carbon grains or carbon dioxide (CO_2) to form methane (Atreya et al., 2007). Fischer-Tropsch reactions produce methane and higher hydrocarbons through the interaction of CO_2 and H_2 (Berndt et al., 1996). After formation, these gases may be sequestered within clathrate hydrates, another source of atmospheric methane considered separate from geological sources (Anderson et al., 2010). Assuming geological methane is purely abiogenic, these sources, such as mud volcanoes and geothermal vents, would contribute 40 to 80 Tg CH_4/year (7% to 13% of yearly production) to the atmosphere [Table 1.1, Figure 1.2] (Etiope, 2012; Kvenvolden and Rogers, 2005). Hydrothermal vents and seeps, such as the Lost City Hydrothermal field or the Chimaera seep in Turkey, are “abiotic-dominated” systems, but

upwards of 10-20% of the produced methane is believed to be of biological origin (Bradley and Summons, 2010; Etiope et al., 2011b).

Table 1.1 Summary of estimates of CH_4 emissions to the atmosphere from various geological sources (Kvenvolden and Rogers, 2005).

Geological source	**Flux (Tg CH_4/yr)**
Natural macro-gas seeps	25
Mud volcanoes	5
Micro-seeps of natural gas	7
Gas hydrate	< 4
Magmatic volcanoes	4
Geothermal areas	3
Mid-ocean ridges	0
Total	44 (w/o gas hydrate)
	45 (w/ gas hydrate, thermogenic CH_4)
	48 (w/ gas hydrate, thermogenic and microbial CH_4)

Isotope analyses have long been used to distinguish between the abiogenic vs. biogenic origins of various atmospheric gases (Floodgate and Judd, 1992; Schoell, 1988). Two stable isotopes of carbon, ^{12}C and the heavier ^{13}C, are able to differentiate between biogenic and abiogenic origins due to the fact that organisms preferentially use the lighter, more energetically favorable ^{12}C (Floodgate and Judd, 1992). It is thought that mixing of biogenic and abiogenic methane serves to obscure abiogenic isotopic signatures (Sherwood Lollar et al., 2006), ultimately leading to an underestimation of the abundance of abiogenic methane produced. It is especially difficult to differentiate between biogenic methane and geological sources of methane at low temperatures since isotopic ratios, such as $^{13}C/^{12}C$ and D/H, are sensitive to formation temperature (Krasnopolsky, 2006). This suggests that isotopic comparisons may not be sufficient

to differentiate between biogenic and abiogenic methane [Figure 1.3] (Bradley and Summons, 2010; Etiope et al., 2011b; Horita and Berndt, 1999; Krasnopolsky, 2006; McCollom and Seewald, 2006).

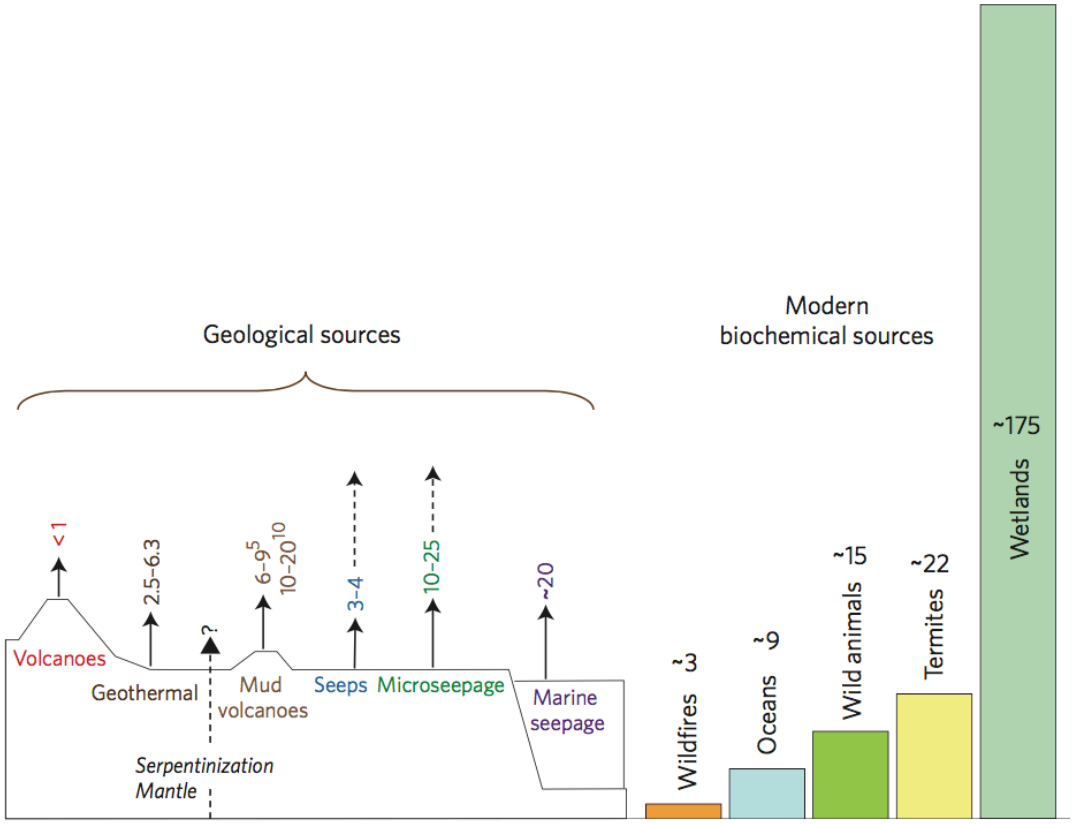

Figure 1.2 Earth degassing (abiogenic/geological sources) versus modern natural (biochemical) methane sources. Methane generated in the subsurface can escape to the atmosphere through terrestrial and marine seepage, as well as by geothermal vents and volcanoes. Geological sources contribute between 60 and 80 Tg CH_4/year. Italics denote uncertain methane sources. Dashed arrows suggest seepage that may increase significantly with warming temperatures. All fluxes provided in units of Tg CH_4 /year. From: Etiope (2012).

Oze et al. (2012) demonstrated the ability of the H_2/CH_4 ratio to distinguish between abiogenic methane from laboratory serpentinization experiments and biogenic methane resulting from serpentinization systems where life is also present (Figure 1.4). Currently, an H_2/CH_4 ratio of 40 distinguishes between abiogenic ($H_2/CH_4 > 40$) and biogenic ($H_2/CH_4 < 40$) sources of methane. The lowest abiogenic value is 42, resulting from an abiotic serpentinization laboratory

experiment, whereas the highest biogenic value is 33 (Oze et al., 2012). However, comparison with additional biogenic and abiogenic sources of methane is needed to ensure the dependability of the H_2/CH_4 ratio. The difficulty with which biogenic and abiogenic methane is differentiated on Earth bodes poorly for analysis of the origin of methane on other bodies in the solar system.

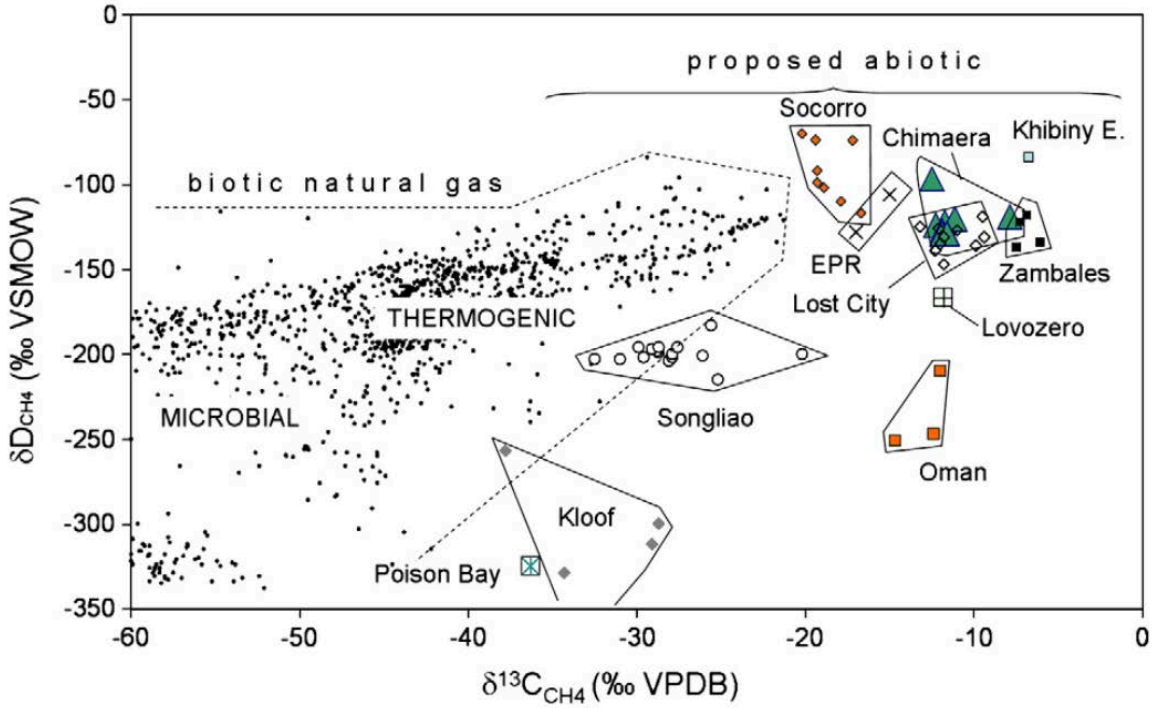

Figure 1.3 The methane $\delta 13C_{CH4}$ vs. δD_{CH4} plot. Overlap between biotic and abiotic sources occurs around $\delta 13C_{CH4}$ -20 to -40 and δD_{CH4} ~ -150 to -250. Chimaera data are compared with biotic (from a global data-set owned by the authors) and abiotic gas (East Pacific Rise – EPR; Socorro, Mexico – Socorro; Lovozero and Khibiny Eudialyte, Russia – Lovozero, Khibiny E.; Songliao, China – Songliao; Zambales, Philippines – Zambales; Kloof, Witwatersrand Basin, South Africa – Kloof; Poison Bay, New Zealand – Poison Bay). From: Etiope et al. (2011b).

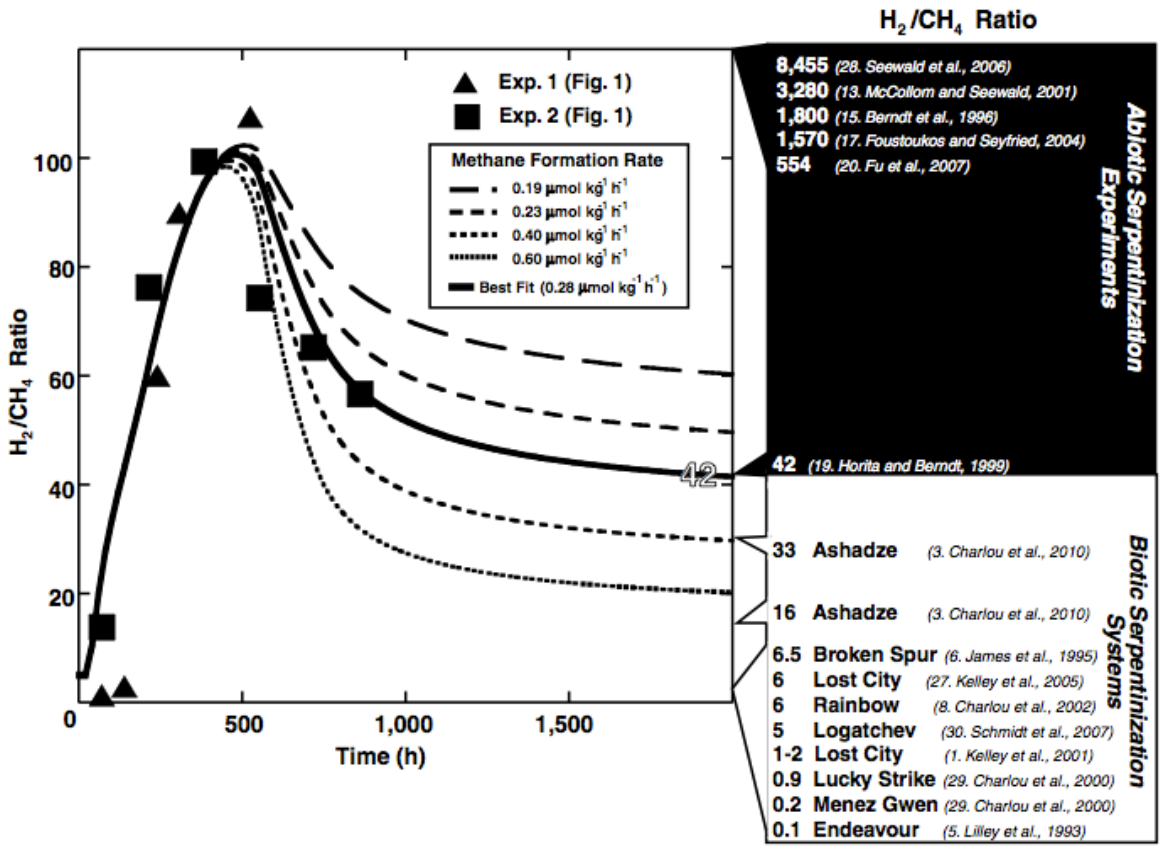

Figure 1.4 Model for serpentinization-fueled H_2 production and CH_4 formation using H_2/CH_4 ratios, data points and rates from two experiments. Data from other studies demonstrate that abiotic serpentinization systems (i.e. laboratory experiments) have H_2/CH_4 ratios equal to or greater than approximately 40 and serpentinization systems where life is present have H_2/CH_4 ratios less than approximately 40. From: Oze et al. (2012).

1.2 Methane on Mars

Methane was first detected in the atmosphere of Mars with an upper limit of 20 ppb by Mariner 9 (Maguire, 1977). Subsequent analyses have reported spatial and temporal variability of methane, including localized plumes [Figure 1.5] (Fonti and Marzo, 2010; Formisano et al., 2004; Geminale et al., 2008; Geminale et al., 2011; Krasnopolsky et al., 1997; Krasnopolsky et al., 2004; Mumma et al., 2009; Webster et al., 2015). The localization of methane on Mars is especially intriguing given that the lifetime of the gas in an atmosphere (~300 years) dictates that

methane would distribute fairly uniformly within the atmosphere (Krasnopolsky et al., 2004). Explanations for the detection of methane primarily include past or present life, including a subsurface biosphere (Atreya et al., 2007; Atreya et al., 2011; Krasnopolsky et al., 2004; Max and Clifford, 2000; Onstott et al., 2006), or abiogenic sources such as serpentinization (Atreya et al., 2007; Atreya et al., 2011; Chassefière and Leblanc, 2011a, b; Oze and Sharma, 2005). Clathrate release (Atreya et al., 2011; Chassefière, 2009; Chassefière and Leblanc, 2011b; Chastain and Chevrier, 2007; Elwood Madden et al., 2007; Gainey and Elwood Madden, 2012; Geminale et al., 2011; Max and Clifford, 2000; Max et al., 2013; Prieto-Ballesteros et al., 2006; Stevens et al., 2015; Thomas et al., 2009) remains a widely-supported source for the detected methane on Mars, however this explanation still requires an initial origin for the compound.

Additional sources and sinks of the methane on Mars have been suggested including comet and meteorite impacts (Court and Sephton, 2009; Fries et al., 2016; Kress and McKay, 2004; Price et al., 2014), photochemical reactions (Bar-Nun and Dimitrov, 2006; Bar-Nun and Dimitrov, 2007; Bartoszek et al., 2011; Moores and Schuerger, 2012; Schuerger et al., 2011; Schuerger et al., 2012b), radiolysis of ice and liquid water (Onstott et al., 2006), soil adsorption (Gough et al., 2010), magmatism and/or hydrothermal alteration of basalt (Lyons et al., 2005; McMahon et al., 2013) and as a result of wind erosion (Jensen et al., 2014) or dust storms (Farrell et al., 2006). However, these explanations remain relatively unsupported compared with a biological origin of methane or as a result of clathrate release or serpentinization. Comets and meteorites have been eliminated as sources of methane due to the low probability of impact and an insufficient flux of volatiles during impact to account for the high local concentrations of methane (~45-60 ppbv), though comets could have played a more important role earlier in Mars' history (Atreya et al., 2007; Court and Sephton, 2009; Formisano et al., 2004; Fries et al., 2016;

Geminale et al., 2008; Krasnopolsky, 2006; Krasnopolsky et al., 2004; Kress and McKay, 2004; Price et al., 2014). However, a recent study by Fries et al. (2016) has reexamined the possibility that the detected methane plumes can be explained by periodic meteor showers on Mars. The authors correlated all previous methane detections with known cometary debris streams and they suggest that the local concentrations of methane up to 60 ppbv can be explained by infall of cometary debris (Fries et al., 2016). It is important to note that previous studies contend that UV photolysis of cometary or meteoritic impacts may be sufficient to account for the globally-averaged value of 10 ppbv CH_4 detected in some observations (Keppler et al., 2012).

Adsorption of methane on the regolith has been cited as a fast-acting sink, and subsequent source, that could explain the high variability of methane in the atmosphere (Gough et al., 2010), but global climate models have failed to reproduce observations of seasonal variability (Meslin et al., 2011). Gough et al. (2011) have also dismissed H_2O_2 within the martian soil as a possible sink that could explain the variability in methane observed.

Geological analyses of regions associated with detected methane plumes (Mumma et al., 2009) indicate older terrains from the Noachian and Hesperian epochs, suggesting that methane formed on the planet long ago and is slowly being released along fractures (Etiope et al., 2011a; Wray and Ehlmann, 2011), whether from subsurface clathrates or other geological processes. However, outgassing from magma or hydrothermal systems would require high temperatures and recent volcanism, which have not been recently observed on the planet (Atreya et al., 2007; Krasnopolsky, 2005, 2006; Krasnopolsky et al., 2004). Based on comparisons to Mauna Loa, Ryan et al. (2006) dismiss the possibility of recent volcanism as a methane source on Mars. The lack of recent volcanism also dismisses the alteration of basaltic rock as a source of methane on Mars (Lyons et al., 2005).

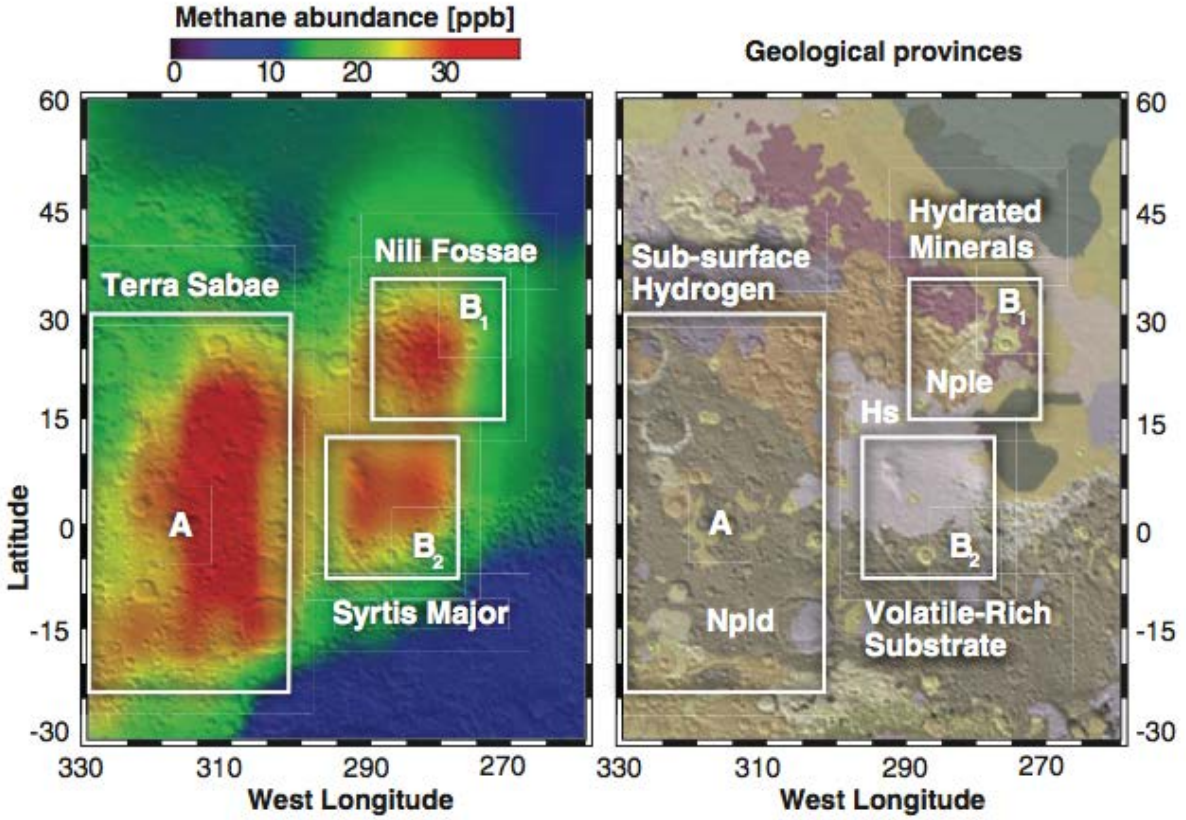

Figure 1.5 Regions where CH_4 appears notably localized in northern summer (A, B_1, and B_2) and their relationship to mineralogical and geomorphological domains. **Left:** Observations of CH_4 near the Syrtis Major volcanic district. **Right:** Geological map superimposed on the topographic shaded relief from the Mars Orbiter Laser Altimeter. The most ancient terrain units are dissected and etched Noachian plains (Npld and Nple; ~3.6 to 4.5 billion years old, when Mars was wet) and are overlain by volcanic deposits from Syrtis Major of Hesperian (Hs) age (~3.1 to 3.6 billion years old). From: Mumma et al. (2009).

Serpentinization of olivine is a favored source of methane on Mars (Atreya et al., 2007; Atreya et al., 2011; Oze and Sharma, 2005). The production of CH_4 is favorable at low temperature under martian conditions, though the presence of sulfur and aqueous carbon dioxide could be limiting factors (Oze and Sharma, 2005). Further support for serpentinization is the high abundance of olivine at Nili Fossae (Chastain and Chevrier, 2007; Wray and Ehlmann, 2011), the location of identified methane plumes (Mumma et al., 2009). However, based on the observed D/H ratio on Mars, Chassefière and Leblanc (2011a) have constrained the amount of

methane produced by serpentinization to just 20% of the estimated present release rate (~ 10^8 cm^2/s, based on an average atmospheric abundance of 20 ppbv).

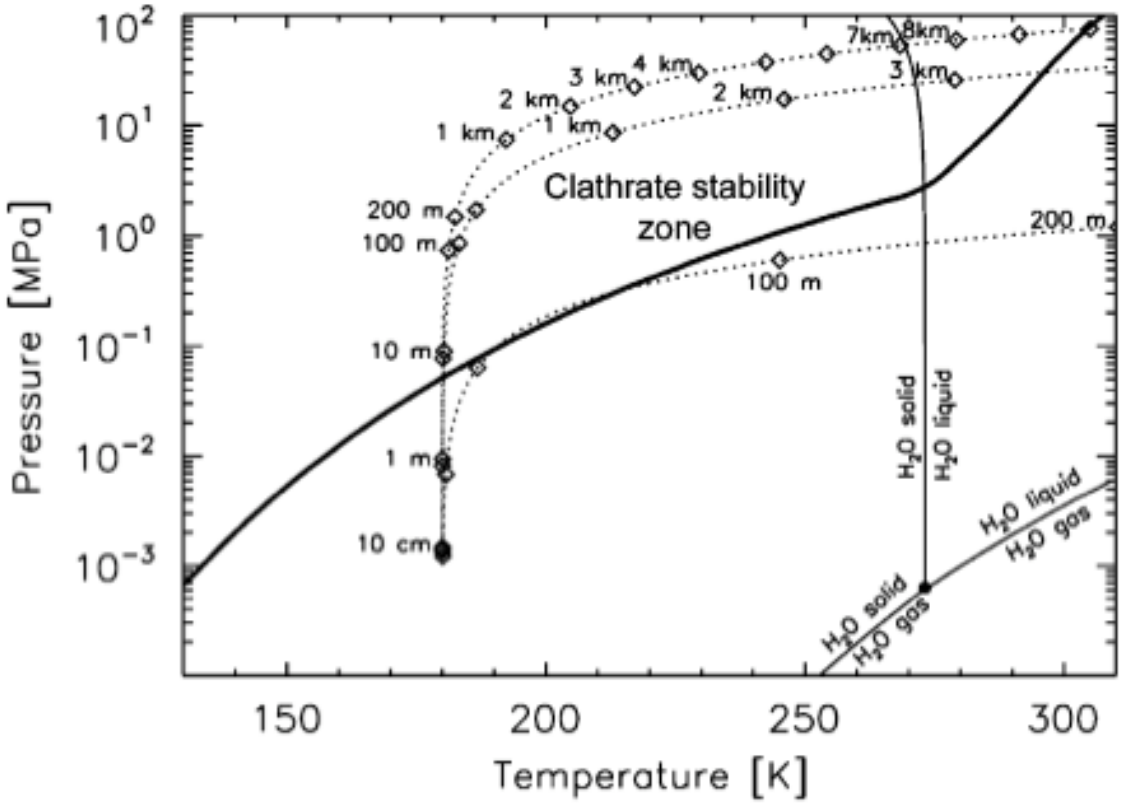

Figure 1.6 Pressure vs. temperature stability diagram of water (thin solid lines) and methane clathrate (thick solid curve). The dotted lines represent various models of martian geothermal profiles depending on the surface material, from top to bottom: ice-cemented soil, dry sandstone and dry, unconsolidated soil. From: Chastain and Chevrier (2007).

Increased abundance of methane (compared to the global average) over the northern pole of Mars during local summer suggests that the north polar cap is a source of methane (Geminale et al., 2011). Release of methane from clathrate hydrates as the north polar cap sublimates is one explanation for the observed abundances, however biology and serpentinization are not excluded (Geminale et al., 2011). Chastain and Chevrier (2007) argue for the existence of both methane and CH_4/CO_2 clathrates in the shallow subsurface (Figure 1.6). Clathrate release is further supported by the idea that glacial retreat, due to changes in Mars' obliquity, fuels dissociation

(Prieto-Ballesteros et al., 2006). In addition, these clathrates could be of primordial origin, with slow and extended release over longer periods of time (Prieto-Ballesteros et al., 2006). However, the presence of methane within clathrates still requires an initial source of the compound (Thomas et al., 2009).

1.3 Methanogens as Candidates for Life on Mars

Methanogens can be considered ideal candidates for life on Mars and could be a possible source of the discovered methane. Methanogens are microorganisms from the domain Archaea that produce methane as a metabolic byproduct. Many methanogens utilize H_2 and CO_2 in order to produce CH_4 (Equation 1).

$$CO_2 + 4H_2 \rightarrow CH_4 + 2H_2O \qquad \text{Equation 1}$$

While CO_2 is abundant in the martian atmosphere, H_2 has been detected in the upper atmosphere (Krasnopolsky and Feldman, 2001) and is incorporated into a variety of martian atmospheric models (Atreya and Gu, 1994; Krasnopolsky, 1993; Nair et al., 1994). McMahon et al. (2016) also contend that current rates of seismic activity on Mars are sufficient to release microbially-relevant abundances of H_2 stored within fault rocks. Additionally, methanogens do not require organic nutrients, which may be relatively sparse on the planet (Freissinet et al., 2015), and methanogens are also are non-photosynthetic, indicating that they could exist in a subsurface environment. Previous studies have shown that a 1-mm thick covering of regolith is enough to shield bacteria from the harmful UV and ionizing radiation that reaches the surface of

Mars (Schuerger et al., 2012a). Thus, a subsurface environment could potentially house extant methanogens, giving a source to the methane detected in Mars' atmosphere.

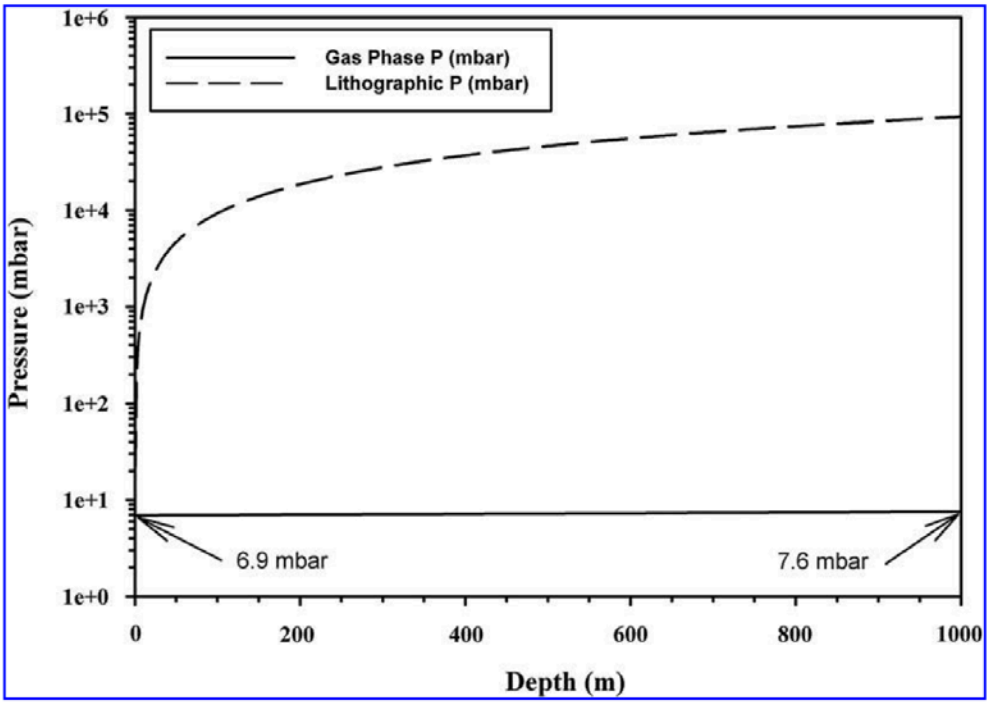

Figure 1.7 Atmospheric gas-phase (i.e., for void spaces) and lithographic (i.e., for salt, or ice inclusions) pressure lapse rates for Mars. The atmospheric gas-phase pressure increases very slowly with increasing depth in the martian lithosphere and reaches 25 mbar at a depth of 13.8 km below the martian datum. In contrast, the lithographic pressure for salt or ice inclusions in the lithosphere can achieve 25 mbar at 19.5 cm of overburden depth. The lithographic pressure is entirely dependent upon the microbial niche being completely (i.e., 100%) sealed from outgassing; otherwise, the niche would equilibrate to the atmospheric pressure predicted by the gas-phase lapse rate. From: Schuerger et al. (2013).

Should methanogens be present on Mars today, they would need to endure the harsh conditions of the planet. These include low temperatures, low atmospheric pressure, and low water availability. While Mars may once have had abundant flowing water, liquid water on the surface is now limited to recurring slope lineae (RSLs) amongst crater walls. RSLs are dark streaks that appear on the surface of the planet with apparent seasonality (McEwen et al., 2014; McEwen et al., 2011). Spectra suggest that these RSLs form from briny aquifers just below the

surface (Ojha et al., 2015). Thus, any surface liquid water available would be both a) intermittent and b) relatively briny.

Although methanogens may exist in the martian subsurface, depending on the depth, these organisms may still be subjected to the low atmospheric pressure of the planet. Schuerger et al. (2013) note that the atmospheric pressure increases only slightly with depth (Figure 1.7), based on the porosity of the soil. Any life within the top 1000 m of the surface would thus be subjected to the low atmospheric pressure of Mars (average: 7 mbar), unless the organisms were completely enclosed in rock (Figure 1.7). Interestingly, low pressure is an often-overlooked condition when considering extreme environments. On Earth, there is no naturally-occurring environment that mimics the low pressure of Mars where a stable ecosystem could form. Thus, life on Earth would have no basis for evolving to adapt to low pressure. For instance, the pressure on the top of Mount Everest is only 330 mbar (Fajardo-Cavazos et al., 2012). However, temporary habitats exist within Earth's atmosphere. Organisms have been collected from various heights in Earth's atmosphere, which offers the most similarity to Mars-like conditions. For example, at 20 km, organisms are subject to high UV radiation (59.75 W/m^2 [total UV; 200 nm – 400 nm]), low temperatures (-75 °C) and low pressures [~50 mbar] (Smith et al., 2011; Smith et al., 2010). In comparison, the solar constant for Mars is 49.95 W/m^2 [200 nm – 400 nm] (Schuerger et al., 2003). Although the atmosphere likely doesn't constitute a stable or persistent ecosystem, it does offer a comparison for survival under martian conditions when organisms are subjected to multiple extremes.

Four methanogens were used in the majority of experiments described here: *Methanosarcina barkeri* (OCM 38, ATCC 43569), *Methanobacterium formicicum* (OCM 55, ATCC 33274, *Methanothermobacter wolfeii* (OCM 36, ATCC 43096), and *Methanococcus*

maripaludis (OCM 151, ATCC 43000). These methanogens were initially chosen as representatives of the breadth of methanogenic Archaea and correspond to the type strains for their species. The Kral lab has been studying these methanogens as candidates for life on Mars for over twenty years. Studies have included growth on martian clays and soil simulants (Chastain et al., 2010; Chastain and Kral, 2010a, b; Kral et al., 2004; Mickol et al., 2016), desiccation experiments (Kendrick and Kral, 2006), survival/growth under low pressure (Kral and Altheide, 2013; Kral et al., 2011; Mickol and Kral, 2016), isotope fractionation analyses (Sinha and Kral, 2015), and the use of high-pressure environments as deep-subsurface habitats (Sinha et al., 2017), among others. The research described here expands upon these previous studies by incorporating various short- and long-term freeze/thaw experiments (Chapter 1) and various low pressure experiments ranging between 6 mbar and 143 mbar and incorporating the use of micro-environments (Chapters 2, 3).

One important distinction between the four methanogens used here is the composition of their cell walls. Unlike members of the domain Bacteria, methanogens do not contain peptidoglycan. Previous studies have revealed variations in cell envelope structure between different methanogenic genera [Figure 1.8] (Claus and König, 2010). The cell envelope makeup may account for some differences in survivability when exposed to martian conditions, specifically, low pressure, between the different methanogens. For instance, Kandler and König (1978) determined that methanogens that stain Gram-positive, including both *Methanosarcina* and *Methanobacterium*, contained cell envelopes with a "thick, rigid sacculus composed of a specific wall polymer", whereas methanogens that stain Gram-negative, such as *Methanococcus*, lacked a rigid sacculus. Additionally, the rigid cell walls of the Methanosarcinales and

Methanobacteriales orders tend to be more resistant to lysing, detergents and enzymes than the proteinaceous cells walls of the Methanococcales (Bush, 1985).

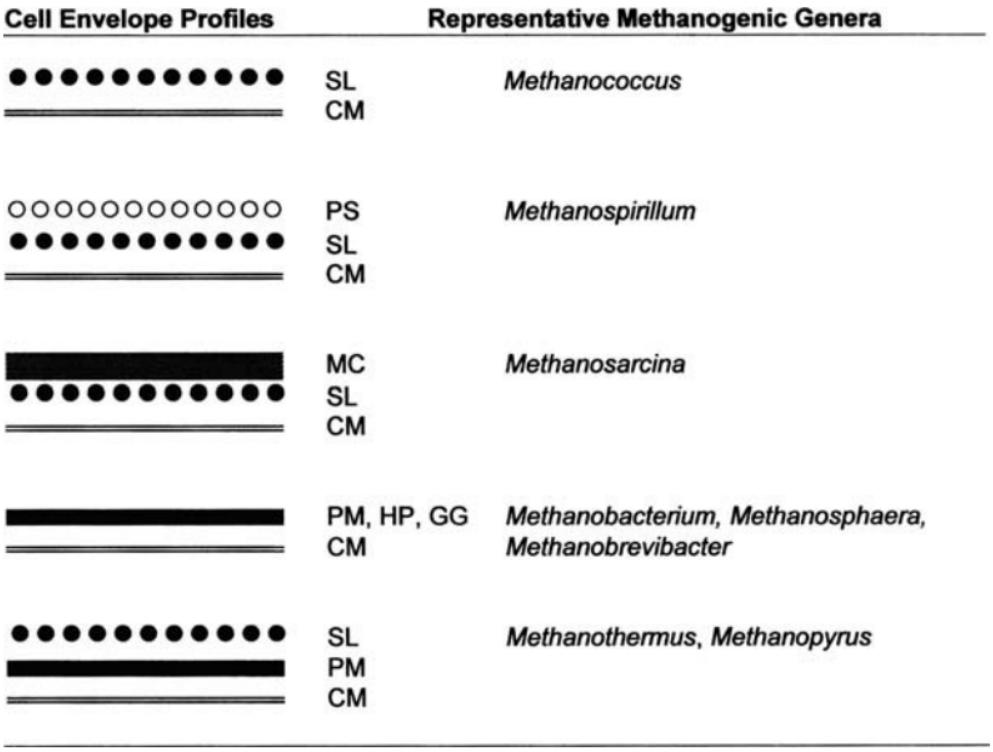

Figure 1.8 Cell wall profiles of methanogens (CM = cytoplasmic membrane, GG = glutaminylglycan, HP = heteropolysaccharide, MC = methanochondroitin, PM = pseudomurein, PS = protein sheath, SL = S layer). From: Claus and König (2010).

1.3.1 Methanosarcinales

1.3.1.1 *Methanosarcina barkeri*

Methanosarcina are considered the most metabolically diverse genus among the methanogens. Most of these organisms can utilize all four catabolic pathways for the production of methane being capable of growth by "CO_2 reduction with H_2, methyl reduction with H_2, aceticlastic fermentation of acetate, or methylotrophic catabolism of methanol, methylated amines, and dimethylsulfides" (Maeder et al., 2006). *M. barkeri*, in particular, is also capable of

utilizing carbon monoxide (CO) as both a carbon source and an energy source (O'Brien et al., 1984), which could potentially fuel microbial metabolism on Mars (King, 2015). Additionally, most *Methanosarcina* spp. can grow in a minimal medium and can fix molecular nitrogen (Maeder et al., 2006). Many members of the *Methanosarcina* genus are also capable of adapting to high intracellular solute concentrations due to their ability to synthesize or accumulate osmoprotectants and alter their outer cell envelope (Maeder et al., 2006; Sowers et al., 1993). The metabolic diversity of these species is typically attributed to their large genome sizes [e.g. 4.8 Mb, *Methanosarcina barkeri* Fusaro] (Maeder et al., 2006).

M. barkeri was initially isolated from an anaerobic sewage-sludge digestor, is coccoid in shape, and grows at an optimum temperature between 37 °C – 42 °C (Bryant and Boone, 1987a; Maestrojuán and Boone, 1991). This species typically forms irregular cellular aggregates, which may result from non-ideal growth conditions (Maestrojuán and Boone, 1991). It is important to note that while methane production and optical density are often used as proxies for growth in methanogens, that even under identical conditions, “often one subculture had a different morphology than another subculture of the same strain” (Maestrojuán and Boone, 1991). This typically accounts for large variations in optical densities and/or methane production between subcultures under the same conditions.

1.3.1.2 Methanochondroitin

Methanosarcina are unique in that they are the only methanogenic order that typically forms cell aggregates. The aggregates form in clusters and each aggregate typically includes eight cells of variable shape and size [0.5 – 3 μm] (Milkevych et al., 2015). The cell wall consists of three separate components: a cytoplasmic membrane, a surface layer (S-layer, see 1.3.2

Archaeal surface layer, below) and a heteropolysaccharide matrix (Milkevych et al., 2015). The heteropolysaccharide is composed of fibrillar polymer methanochondroitin, which resembles the chondroitin of eukaryotic cells in regard to both composition and structure (Kreisl and Kandler, 1986). This layer has a variable thickness between 20-200 nm based on growing conditions and enzymatic activity (Milkevych et al., 2015), and is only produced by aggregated cells and not individual cells (Albers and Meyer, 2011). Similar to other desiccation-resistant prokaryotes, this extracellular polysaccharide (EPS) matrix is believed to offer protection against environmental stresses such as desiccation or oxygen exposure (Anderson et al., 2012). Anderson et al. (2012) discovered that cells that produced methanochondroitin (and thus formed multicellular aggregates) had significantly higher survival rates than cells that did not produce methanochondroitin (individual cells), in response to desiccation, high temperatures and oxygen exposure. This unique morphology for *Methanosarcina* spp. likely aids in the survival of *M. barkeri* exposed to various extreme conditions, such as low-pressure (Chapters 2, 3) and freeze/thaw cycles (Chapter 1).

1.3.2 Archaeal surface layer (S-layer)

The S-layer is a proteinaceous boundary layer that forms the outermost layer of the cell wall (Milkevych et al., 2015). S-layer proteins are found within most Archaea and even range among species from all major phylogenetic groups of Bacteria. The simple composition of the S-layer and its widespread nature lends credence to the idea that it was one of the first cell wall structures to evolve (Albers and Meyer, 2011). Archaeal S-layers are typically composed of a single protein or glycoprotein species with a molecular mass between 40-200 kDa and a thickness between 5-25 nm (Albers and Meyer, 2011).

1.3.3 Methanobacteriales

1.3.3.1 *Methanobacterium formicicum*

M. formicicum is a mesophile originally isolated from an anaerobic sludge digestor (Bryant and Boone, 1987b). Cells are crooked, Gram-positive rods that are typically 0.5 μm wide and 2-15 μm long (Bryant and Boone, 1987b). This species can utilize formate as an electron donor in place of, and in addition to, H_2 (Schauer and Ferry, 1980). Cultures provided with 80/20 H_2/CO_2 in addition to formate result in greater biomass yield (Schauer and Ferry, 1980) and inform our media preparations in most of the experiments presented here. This species is also capable of nitrogen fixation (Magingo and Stumm, 1991) and may play an important role in interspecies electron transfer in anaerobic digestors due to the reversible reaction between formate synthesis and H_2 utilization [Table 1.2] (Baron and Ferry, 1989; Wu et al., 1993).

Table 1.2 Biochemical reactions occurring during metabolism of hydrogen and formate by *Methanobacterium formicicum* [modified from Wu et al. (1993)].

	Reaction	
(1)	$HCOO^- + H_2O \rightarrow H_2 + HCO_3^-$	Hydrogen production from formate
(2)	$H_2 + HCO_3^- \rightarrow HCOO^- + H_2O$	Formate synthesis from hydrogen
(3)	$H_2 + ¼\ HCO_3^- + ¼\ H^+ \rightarrow ¼\ CH_4 + ¾\ HCO_3^-$	Methanogenesis from hydrogen
(4)	$HCOO + ¼\ H^- + ¼\ H_2O \rightarrow ¼\ CH_4 + ¾\ HCO_3^-$	Methanogenesis from formate

1.3.3.2 *Methanothermobacter wolfeii*

M. wolfeii is a thermophile, originally isolated from a mixture of sewage sludge and river sediment, with an optimum growth temperature between 55 °C and 65 °C, with no growth found above 76 °C or below 37 °C (Winter et al., 1984). Cells are crooked, Gram-positive rods that are 0.35 – 0.5 μm wide and 2.5 μm long (Wasserfallen et al., 2000; Winter et al., 1984). Like *M.*

formicicum, this species can also use formate as a carbon and energy source, as well as H_2/CO_2 (Wasserfallen et al., 2000). As with members of Methanobacteriales (see Section 1.3.3.3 Pseudomurein, below), *M. wolfeii* cell wall extracts contain components of pseudomurein. However, the molar ratio of lysine to glutamic acid suggests the presence of additional galactosamine- and glucosamine-containing polymers, similar to several *Methanobacterium thermoautotrophicum* strains (Winter et al., 1984). In general, the cell wall is 22 nm thick (Winter et al., 1984). Interestingly, cells of this species are subject to lysing following the exhaustion of the H_2 supply within the medium (König et al., 1985).

1.3.3.3 Pseudomurein

Members of Methanobacteriales contain a unique type of peptidoglycan called pseudomurein (Claus and König, 2010). Resembling peptidoglycan, cell walls within this order typically contain three amino acids: lysine, alanine or threonine, and glutamic acid. Pseudomurein lacks muramic acid, utilizing glucosamine and/or galactosamine instead (Kandler and König, 1978). The molar ratio of the amino acids (Lys:Ala:Glu) also differs between pseudomurein (1:1.2:2) and peptidoglycan [1:2:1] (Kandler and König, 1978). Although pseudomurein is similar to bacterial peptidoglycan, there is no homology between archaeal pseudomurein-producing proteins and bacterial peptidoglycan synthesis, which suggests that these pathways evolved separately (Albers and Meyer, 2011; König et al., 1989). Additionally, in contrast to peptidoglycan, the amino acids present in pseudomurein are all L-amino acids (Kandler and König, 1978).

1.3.4 Methanococcales

1.3.4.1 *Methanococcus maripaludis*

M. maripaludis was initially isolated from a salt marsh in South Carolina. Cells are pleomorphic coccoid-rod in shape and typically 1.2 μm by 1.6 μm (Jones et al., 1983a). *M. maripaludis* stains Gram-negative, is weakly motile and can utilize formate or H_2/CO_2 for methane production (Jones et al., 1983a). This species is classified as a mesophile, growing at temperatures between 18 °C and 47 °C (Jones et al., 1983a). Although optimum growth occurs near 38 °C, *M. maripaludis* cells are cultured at room temperature (22 °C) in our lab, allowing us to utilize a comparatively lower-temperature methanogen in our studies. This organism is also classified as a halophile, requiring elevated magnesium chloride and sodium chloride concentrations similar to seawater (Jones et al., 1983a; Jones et al., 1983b).

The cell wall of *M. maripaludis* consists of a single electron dense outer layer, approximately 10 nm in size, that is osmotically fragile and highly susceptible to detergents (Jones et al., 1983a). The relatively weaker cell wall of *M. maripaludis* may explain the apparent sensitivity to certain extreme conditions, as compared to the other three methanogens used (see Chapters 2, 3, 4).

1.4 Dissertation Goals and Significance

The research presented here examined the ability of four species of methanogens to survive and/or metabolize under martian conditions, specifically, low pressures down to 6 mbar and freeze/thaw cycles between -80 °C and 22 °C. The over-arching goal was to expand the parameter space of martian habitability for methanogens. Previous studies in this lab have considered the effect of various martian conditions on the growth and survivability of

methanogens. The research formulating this dissertation intended to further examine the ability of four specific methanogens to withstand and/or thrive under certain martian conditions including within low-pressure environments and exposed to vigorous freeze/thaw cycles.

NASA has always been at the forefront of the search for life in the universe. From the Viking experiments to the Mars Science Laboratory, Mars has piqued the curiosity of scientists for decades. With evidence of a warm, wet past (Jakosky and Phillips, 2001; Pollack et al., 1987), scientists continue to analyze the 'Red Planet' for past and present signs of life. The search for life on Mars remains one of the main goals for NASA as indicated in both Visions and Voyages for Planetary Science in the Decade 2013-2022 (Committee, 2011) as well as the NASA 2014 Science Plan (NASA, 2014) and 2015 NASA Astrobiology Strategy (Hays, 2015). One of the three main themes for the next decade concerns planetary habitats and searching for the requirements of life. The main goal for the 2014 Science Plan for planetary science states that "NASA's strategic objective in planetary science is to ascertain the content, origin, and evolution of the solar system and the potential for life elsewhere" (NASA, 2014). The fourth chapter of the 2015 NASA Astrobiology Strategy focuses on "co-evolution of life and the physical environment" (Hays, 2015). Within this chapter, the authors note that "understanding the limits of life on Earth, both in the present and the past, is critical for where and how we should search for life elsewhere" (Hays, 2015). The study of microbial life on Earth has uncovered multiple mechanisms for survival under extreme conditions. Thus, the research described here directly contributes to various goals within the NASA Astrobiology Strategy.

Current goals of the Curiosity rover and the future 2020 Mars rovers are to determine both past and present habitability of the planet (Grotzinger et al., 2012; Mustard et al., 2013). One specific objective of the Mars 2020 rover seeks to "explore an astrobiologically relevant

ancient environment on Mars to decipher its geological processes and history, including the assessment of past habitability" (Mustard et al., 2013). The experiments conducted here serve to inform our understanding of the habitability of specific environments on Mars and could guide discussions for prospective landing sites. The Mars 2020 rover mission also intends to demonstrate technology capable of returning Mars samples to Earth. Thus, planetary protection will play an important role in the execution of this and future missions concerning both forward contamination (bringing Earth life to Mars on one of the many rovers or landers) and backward contamination (in the case of a sample return mission). Planetary protection and martian simulation experiments often utilize characteristic aerobic organisms commonly found on Earth that have the potential for forward contamination by adhering to spacecraft (Berry et al., 2010; Fajardo-Cavazos et al., 2010; Kerney and Schuerger, 2011; Moeller et al., 2012; Newcombe et al., 2005; Nicholson et al., 2012; Nicholson and Schuerger, 2005; Osman et al., 2008; Rettberg et al., 2004; Schuerger et al., 2012a; Schuerger et al., 2003; Schuerger and Nicholson, 2006; Schuerger and Nicholson, 2016; Schuerger et al., 2005; Schuerger et al., 2006; Schuerger et al., 2013; Tauscher et al., 2006; Vaishampayan et al., 2012; Venkateswaran et al., 2014). However, the anaerobic nature of methanogens may make these organisms more likely candidates for the ability to withstand the environment of space or other planets. More specifically, the "Special Regions" of interest on Mars have recently been re-evaluated based on "the existence of environmental conditions that may be conducive to terrestrial microbial growth" (Rettberg et al., 2016). Thus, it is important to understand the ability of Earth organisms to both survive and grow under martian conditions for both planetary protection concerns and as evidence for the possibility of past or present life on Mars.

This dissertation features unique research focusing on novel laboratory experiments that complements NASA's vision. The growth/survival studies discussed here have demonstrated the limits at which survival and growth are possible for methanogens under low pressure (~50 mbar) and freeze/thaw cycles. The anaerobic, non-photosynthetic nature of methanogens makes them ideal candidates for life on Mars, and the study of these organisms fully supports NASA's search for life. Not only could methanogens possibly exist on Mars today, the prevalence of methanogens in the Earth's early history (Kasting, 2004; Woese and Fox, 1977) supports the possibility of early life on Mars as well.

1.5 Dissertation Outline

Chapter 2 incorporates experiments testing the ability of four methanogens to survive or metabolize during and after exposure to temperatures down to -80 °C. These experiments include long-term freeze/thaw cycling over the course of months as well as short-term diurnal and 48-h cycles that more closely resemble the present environment of Mars. Chapter 3 is a series of experiments ranging from 143 mbar down to 6 mbar and was published in *Origins of Life and Evolution of Biospheres* in 2016. These experiments examined the methanogens' survivability under low-pressure conditions in aqueous media. This chapter also includes an experiment testing longer exposure to low pressure using a "micro-environment" setup. This experiment leads into the next chapter, Chapter 4, which discusses micro-environment experiments in order to demonstrate growth at low pressures. These experiments use both optical density and methane production as proxies for growth directly before and directly after exposure to low pressure. The last chapter serves as a comparison for microbial survival under martian conditions and will be published in *Astrobiology* in May 2017. In this chapter, *Serratia liquefaciens*, a bacterium

previously shown to actively grow at 7 mbar, 0 °C and under a CO_2 environment, was exposed to martian UV irradiation within magnesium sulfate brines and ices.

1.6 References

Albers, S.-V., Meyer, B.H. (2011) The archaeal cell envelope. *Nature Reviews Microbiology* 9, 414-426.

Anderson, B., Bartlett, K., Frolking, S., Hayhoe, K., Jenkins, J., Salas, W. (2010) *Methane and Nitrous Oxide Emissions From Natural Sources*. Office Of Atmospheric Programs, US EPA, EPA 430-R-10-001, Washington, D.C.

Anderson, K.L., Apolinario, E.E., Sowers, K.R. (2012) Desiccation as a long-term survival mechanism for the archaeon *Methanosarcina barkeri*. *Applied and Environmental Microbiology* 78, 1473-1479.

Atreya, S.K., Gu, Z.G. (1994) Stability of the Martian atmosphere: Is heterogeneous catalysis essential? *Journal of Geophysical Research: Planets (1991–2012)* 99, 13133-13145.

Atreya, S.K., Mahaffy, P.R., Wong, A.-S. (2007) Methane and related trace species on Mars: Origin, loss, implications for life, and habitability. *Planetary and Space Science* 55, 358-369.

Atreya, S.K., Witasse, O., Chevrier, V.F., Forget, F., Mahaffy, P.R., Price, B.P., Webster, C.R., Zurek, R.W. (2011) Methane on Mars: Current observations, interpretation, and future plans. *Planetary and Space Science* 59, 133-136.

Bar-Nun, A., Dimitrov, V. (2006) Methane on Mars: A product of H_2O photolysis in the presence of CO. *Icarus* 181, 320-322.

Bar-Nun, A., Dimitrov, V. (2007) "Methane on Mars: A product of H_2O photolysis in the presence of CO" Response to V.A. Krasnopolsky. *Icarus* 188, 543-545.

Baron, S.F., Ferry, J.G. (1989) Reconstitution and properties of a coenzyme F_{420}-mediated formate hydrogenlyase system in *Methanobacterium formicicum*. *Journal of Bacteriology* 171, 3854-3859.

Bartoszek, M., Wecks, M., Jakobs, G., Möhlmann, D. (2011) Photochemically induced formation of Mars relevant oxygenates and methane from carbon dioxide and water. *Planetary and Space Science* 59, 259-263.

Berndt, M.E., Allen, D.E., Seyfried Jr., W.E. (1996) Reduction of CO_2 during serpentinization of olivine at 300 °C and 500 bar. *Geology* 24, 351-354.

Berry, B.J., Jenkins, D.G., Schuerger, A.C. (2010) Effects of simulated Mars conditions on the survival and growth of *Escherichia coli* and *Serratia liquefaciens*. *Applied and Environmental Microbiology* 76, 2377-2386.

Bradley, A.S., Summons, R.E. (2010) Multiple origins of methane at the Lost City Hydrothermal Field. *Earth and Planetary Science Letters* 297, 34-41.

Bryant, M.P., Boone, D.R. (1987a) Emended description of strain MS^T ($DSM\ 800^T$), the type strain of *Methanosarcina barkeri*. *International Journal of Systematic Bacteriology* 37, 169-170.

Bryant, M.P., Boone, D.R. (1987b) Isolation and characterization of *Methanobacterium formicicum* MF. *International Journal of Systematic Bacteriology* 37, 171-171.

Bush, J.W. (1985) Enzymatic lysis of the pseudomurein-containing methanogen *Methanobacterium formicicum*. *Journal of Bacteriology* 163, 27-36.

Chassefière, E. (2009) Metastable methane clathrate particles as a source of methane to the martian atmosphere. *Icarus* 204, 137-144.

Chassefière, E., Leblanc, F. (2011a) Constraining methane release due to serpentinization by the observed D/H ratio on Mars. *Earth and Planetary Science Letters* 310, 262-271.

Chassefière, E., Leblanc, F. (2011b) Methane release and the carbon cycle on Mars. *Planetary and Space Science* 59, 207-217.

Chastain, B., Kral, T., Chevrier, V., Altheide, T. (2010) Growth and Biomediated Mineral Alterations by Methanogens Under Geochemical Conditions Similar to the Martian Subsurface. *LPI Contributions* 1538, 5234.

Chastain, B.K., Chevrier, V. (2007) Methane clathrate hydrates as a potential source for martian atmospheric methane. *Planetary and Space Science* 55, 1246-1256.

Chastain, B.K., Kral, T.A. (2010a) Approaching Mars-like geochemical conditions in the laboratory: omission of artificial buffers and reductants in a study of biogenic methane production on a smectite clay. *Astrobiology* 10, 889-897.

Chastain, B.K., Kral, T.A. (2010b) Zero-valent iron on Mars: An alternative energy source for methanogens. *Icarus* 208, 198-201.

Claus, H., König, H. (2010) Cell Envelopes of Methanogens, In: König, H., Claus, H., Varma, A. (Eds.), Prokaryotic Cell Wall Compounds: Structure and Biochemistry. Springer Berlin Heidelberg, pp. 231-251.

Committee on the Planetary Science Decadal Survey (2011) *Vision and Voyages for Planetary Science in the Decade 2013-2022*. National Academies Press, Washington, D.C., pp. 398.

Conrad, R. (2009) The global methane cycle: recent advances in understanding the microbial processes involved. *Environmental Microbiology Reports* 1, 285-292.

Court, R.W., Sephton, M.A. (2009) Investigating the contribution of methane produced by ablating micrometeorites to the atmosphere of Mars. *Earth and Planetary Science Letters* 288, 382-385.

Denman, K., Brasseur, G., Chidthaisong, A., Ciais, P., Cox, P., Dickinson, R., Hauglustaine, D., Heinze, C., Holland, E., Jacob, D. (2007) *Climat Change 2007: The Physical Science Basis., edited by: Contribution of Working Group I to the Fourth Assesment Report on the INtergovernmental Panel on Climate Change*. Cambridge University Press, Cambridge, United Kingdom and New York, USA.

Elwood Madden, M.E., Ulrich, S.M., Onstott, T.C., Phelps, T.J. (2007) Salinity-induced hydrate dissociation: A mechanism for recent CH_4 release on Mars. *Geophysical Research Letters* 34.

Emmanuel, S., Ague, J.J. (2007) Implications of present- day abiogenic methane fluxes for the early Archean atmosphere. *Geophysical Research Letters* 34.

Etiope, G. (2012) Methane uncovered. *Nature Geoscience* 5, 373-374.

Etiope, G., Oehler, D.Z., Allen, C.C. (2011a) Methane emissions from Earth's degassing: Implications for Mars. *Planetary and Space Science* 59, 182-195.

Etiope, G., Schoell, M., Hosgörmez, H. (2011b) Abiotic methane flux from the Chimaera seep and Tekirova ophiolites (Turkey): Understanding gas exhalation from low temperature serpentinization and implications for Mars. *Earth and Planetary Science Letters* 310, 96-104.

Etiope, G., Sherwood Lollar, B. (2013) Abiotic methane on Earth. *Reviews of Geophysics* 51, 276-299.

Fajardo-Cavazos, P., Schuerger, A.C., Nicholson, W.L. (2010) Exposure of DNA and *Bacillus subtilis* spores to simulated martian environments: use of quantitative PCR (qPCR) to measure inactivation rates of DNA to function as a template molecule. *Astrobiology* 10, 403-411.

Fajardo-Cavazos, P., Waters, S.M., Schuerger, A.C., George, S., Marois, J.J., Nicholson, W.L. (2012) Evolution of *Bacillus subtilis* to Enhanced Growth at Low Pressure: Up-Regulated Transcription of *des-desKR*, Encoding the Fatty Acid Desaturase System. *Astrobiology* 12, 258-270.

Farrell, W.M., Delory, G.T., Atreya, S.K. (2006) Martian dust storms as a possible sink of atmospheric methane. *Geophysical Research Letters* 33.

Floodgate, G.D., Judd, A.G. (1992) The origins of shallow gas. *Continental Shelf Research* 12, 1145-1156.

Fonti, S., Marzo, G. (2010) Mapping the methane on Mars. *Astronomy and Astrophysics* 512.

Formisano, V., Atreya, S., Encrenaz, T., Ignatiev, N., Giuranna, M. (2004) Detection of methane in the atmosphere of Mars. *Science* 306, 1758-1761.

Frankenberg, C., Meirink, J.F., van Weele, M., Platt, U., Wagner, T. (2005) Assessing methane emissions from global space-borne observations. *Science* 308, 1010-1014.

Freissinet, C., Glavin, D.P., Mahaffy, P.R., Miller, K.E., Eigenbrode, J.L., Summons, R.E., Brunner, A.E., Buch, A., Szopa, C., Archer Jr., P.D., Franz, H.B., Atreya, S.K., Brinckerhoff, W.B., Cabane, M., Coll, P., Conrad, P.G., Des Marais, D.J., Dworkin, J.P., Fairén, A.G., François, P., Grotzinger, J.P., Kashyap, S., ten Kate, I.L., Leshin, L.A., Malespin, C.A., Martin, M.G., Martin-Torres, F.J., McAdam, A.C., Ming, D.W., Navarro-González, R., Pavlov, A.A., Prats, B.D., Squyres, S.W., Steele, A., Stern, J.C., Sumner, D.Y., Sutter, B., Zorzano, M.-P., the MSL Science Team (2015) Organic molecules in the sheepbed mudstone, gale crater, mars. *Journal of Geophysical Research: Planets* 120, 495-514.

Fries, M., Christou, A., Archer, D., Conrad, P., Cooke, W., Eigenbrode, J., ten Kate, I.L., Matney, M., Niles, P., Sykes, M., Steele, A., Treiman, A. (2016) A cometary origin for martian atmospheric methane. *Geochemical Perspectives Letters* 2, 10-23.

Gainey, S.R., Elwood Madden, M.E. (2012) Kinetics of methane clathrate formation and dissociation under Mars relevant conditions. *Icarus* 218, 513-524.

Geminale, A., Formisano, V., Giuranna, M. (2008) Methane in Martian atmosphere: average spatial, diurnal, and seasonal behaviour. *Planetary and Space Science* 56, 1194-1203.

Geminale, A., Formisano, V., Sindoni, G. (2011) Mapping methane in Martian atmosphere with PFS-MEX data. *Planetary and Space Science* 59, 137-148.

Gough, R.V., Tolbert, M.A., McKay, C.P., Toon, O.B. (2010) Methane adsorption on a martian soil analog: An abiogenic explanation for methane variability in the martian atmosphere. *Icarus* 207, 165-174.

Gough, R.V., Turley, J.J., Ferrell, G.R., Cordova, K.E., Wood, S.E., DeHaan, D.O., McKay, C.P., Toon, O.B., Tolbert, M.A. (2011) Can rapid loss and high variability of martian methane be explained by surface H_2O_2? *Planetary and Space Science* 59, 238-246.

Grotzinger, J.P., Crisp, J., Vasavada, A.R., Anderson, R.C., Baker, C.J., Barry, R., Blake, D.F., Conrad, P., Edgett, K.S., Ferdowski, B., Gellert, R., Gilbert, J.B., Golombek, M., Gómez-Elvira, J., Hassler, D.M., Jandura, L., Litvak, M., Mahaffy, P., Maki, J., Meyer, M., Malin, M.C., Mitrofanov, I., Simmonds, J.J., Vaniman, D., Welch, R.V., Wiens, R.C. (2012) Mars Science Laboratory Mission and Science Investigation. *Space Science Reviews* 170, 5-56.

Hays, L. (Ed.) (2015) *NASA Astrobiology Strategy*. National Aeronautics and Space Administration, Washington, D.C., pp. 256.

Horita, J., Berndt, M.E. (1999) Abiogenic methane formation and isotopic fractionation under hydrothermal conditions. *Science* 285, 1055-1057.

IPCC (2013) *Climate Change 2013: The Physical Science Basis: Working Group I Contribution to the Fifth Assessment Report of the Intergovernmental Panel on Climate Change* [Stocker, T.F., D. Qin, G.-K. Plattner, M. Tignor, S.K. Allen, J. Boschung, A. Nauels, Y. Xia, V. Bex and P.M. Midgley (Eds.)]. Cambridge University Press, Cambridge, United Kingdom and New York, NY, USA, pp. 1535.

Jakosky, B.M., Phillips, R.J. (2001) Mars' volatile and climate history. *Nature* 412, 237-244.

Jensen, S.J.K., Skibsted, J., Jakobsen, H.J., ten Kate, I.L., Gunnlaugsson, H.P., Merrison, J.P., Finster, K., Bak, E., Iversen, J.J., Kondrup, J.C., Nørnberg, P. (2014) A sink for methane on Mars? The answer is blowing in the wind. *Icarus* 236, 24-27.

Jones, W.J., Paynter, M.J.B., Gupta, R. (1983a) Characterization of *Methanococcus maripaludis* sp. nov., a new methanogen isolated from salt marsh sediment. *Archives of Microbiology* 135, 91-97.

Jones, W.J., Whitman, W.B., Fields, R.D., Wolfe, R.S. (1983b) Growth and plating efficiency of methanococci on agar media. *Applied and Environmental Microbiology* 46, 220-226.

Kandler, O., König, H. (1978) Chemical composition of the peptidoglycan-free cell walls of methanogenic bacteria. *Archives of Microbiology* 118, 141-152.

Kasting, J.F. (2004) Paleoclimatology: Archaean atmosphere and climate. *Nature* 432.

Kendrick, M.G., Kral, T.A. (2006) Survival of methanogens during desiccation: implications for life on Mars. *Astrobiology* 6, 546-551.

Keppler, F., Vigano, I., McLeod, A., Ott, U., Früchtl, M., Röckmann, T. (2012) Ultraviolet-radiation-induced methane emissions from meteorites and the Martian atmosphere. *Nature* 486, 93-96.

Kerney, K.R., Schuerger, A.C. (2011) Survival of *Bacillus subtilis* endospores on ultraviolet-irradiated rover wheels and Mars regolith under simulated martian conditions. *Astrobiology* 11, 477-485.

King, G.M. (2015) Carbon monoxide as a metabolic energy source for extremely halophilic microbes: implications for microbial activity in Mars regolith. *Proceedings of the National Academy of Sciences of the United States of America* 112, 4465-4470.

König, H., Kandler, O., Hammes, W. (1989) Biosynthesis of pseudomurein: isolation of putative precursors from *Methanobacterium thermoautotrophicum*. *Canadian Journal of Microbiology* 35, 176-181.

König, H., Semmler, R., Lerp, C., Winter, J. (1985) Evidence for the occurrence of autolytic enzymes in *Methanobacterium wolfei*. *Archives of Microbiology* 141, 177-180.

Kral, T.A., Altheide, T.S. (2013) Methanogen survival following exposure to desiccation, low pressure and martian regolith analogs. *Planetary and Space Science* 89, 167-171.

Kral, T.A., Altheide, T.S., Lueders, A.E., Schuerger, A.C. (2011) Low pressure and desiccation effects on methanogens: Implications for life on Mars. *Planetary and Space Science* 59, 264-270.

Kral, T.A., Bekkum, C.R., McKay, C.P. (2004) Growth of methanogens on a Mars soil simulant. *Origins of Life and Evolution of the Biosphere* 34, 615-626.

Krasnopolsky, V.A. (1993) Photochemistry of the Martian atmosphere (mean conditions). *Icarus* 101, 313-332.

Krasnopolsky, V.A. (2005) A sensitive search for SO_2 in the martian atmosphere: Implications for seepage and origin of methane. *Icarus* 178, 487-492.

Krasnopolsky, V.A. (2006) Some problems related to the origin of methane on Mars. *Icarus* 180, 359-367.

Krasnopolsky, V.A., Bjoraker, G.L., Mumma, M.J., Jennings, D.E. (1997) High-resolution spectroscopy of Mars at 3.7 and 8 μm: A sensitive search for H_2O_2, H_2CO, HCl, and CH_4, and detection of HDO. *Journal of Geophysical Research* 102, 6525-6534.

Krasnopolsky, V.A., Feldman, P.D. (2001) Detection of molecular hydrogen in the atmosphere of Mars. *Science* 294, 1914-1917.

Krasnopolsky, V.A., Maillard, J.P., Owen, T.C. (2004) Detection of methane in the martian atmosphere: evidence for life? *Icarus* 172, 537-547.

Kreisl, P., Kandler, O. (1986) Chemical structure of the cell wall polymer of *Methanosarcina*. *Systematic and Applied Microbiology* 7, 293-299.

Kress, M.E., McKay, C.P. (2004) Formation of methane in comet impacts: implications for Earth, Mars, and Titan. *Icarus* 168, 475-483.

Kvenvolden, K.A. (1995) A review of the geochemistry of methane in natural gas hydrate. *Organic Geochemistry* 23, 997-1008.

Kvenvolden, K.A., Rogers, B.W. (2005) Gaia's breath—global methane exhalations. *Marine and Petroleum Geology* 22, 579-590.

Lyons, J.R., Manning, C., Nimmo, F. (2005) Formation of methane on Mars by fluid-rock interaction in the crust. *Geophysical Research Letters* 32.

Maeder, D.L., Anderson, I., Brettin, T.S., Bruce, D.C., Gilna, P., Han, C.S., Lapidus, A., Metcalf, W.W., Saunders, E., Tapia, R., Sowers, K.R. (2006) The *Methanosarcina barkeri* genome: comparative analysis with *Methanosarcina acetivorans* and

Methanosarcina mazei reveals extensive rearrangement within methanosarcinal genomes. *Journal of Bacteriology* 188, 7922-7931.

Maestrojuán, G.M., Boone, D.R. (1991) Characterization of *Methanosarcina barkeri* MS^T and 227, *Methanosarcina mazei* S-6^T, and *Methanosarcina vacuolata* Z-761^T. *International Journal of Systematic Bacteriology* 41, 267-274.

Magingo, F.S.S., Stumm, C.K. (1991) Nitrogen fixation by *Methanobacterium formicicum*. *FEMS Microbiology Letters* 81, 273-277.

Maguire, W.C. (1977) Martian isotopic ratios and upper limits for possible minor constituents as derived from Mariner 9 infrared spectrometer data. *Icarus* 32, 85-97.

Max, M.D., Clifford, S.M. (2000) The state, potential distribution, and biological implications of methane in the Martian crust. *Journal of Geophysical Research: Planets (1991-2012)* 105, 4165-4171.

Max, M.D., Clifford, S.M., Johnson, A.H. (2013) Hydrocarbon system analysis for methane hydrate exploration on Mars, In: Ambrose, W.A., Reilly II, J.F., Peters, D.C. (Eds.), Energy resources for human settlement in the solar system and Earth's future in space: AAPG Memoir, pp. 99-114.

McCollom, T.M., Seewald, J.S. (2006) Carbon isotope composition of organic compounds produced by abiotic synthesis under hydrothermal conditions. *Earth and Planetary Science Letters* 243, 74-84.

McEwen, A.S., Dundas, C.M., Mattson, S.S., Toigo, A.D., Ojha, L., Wray, J.J., Chojnacki, M., Byrne, S., Murchie, S.L., Thomas, N. (2014) Recurring slope lineae in equatorial regions of Mars. *Nature Geoscience* 7, 53-58.

McEwen, A.S., Ojha, L., Dundas, C.M., Mattson, S.S., Byrne, S., Wray, J.J., Cull, S.C., Murchie, S.L., Thomas, N., Gulick, V.C. (2011) Seasonal flows on warm martian slopes. *Science* 333, 740-743.

McMahon, S., Parnell, J., Blamey, N.J. (2013) Sampling methane in basalt on Earth and Mars. *International Journal of Astrobiology* 12, 113-122.

McMahon, S., Parnell, J., Blamey, N.J. (2016) Evidence for seismogenic hydrogen gas, a potential microbial energy source on Earth and Mars. *Astrobiology* 16, 690-702.

Meslin, P.-Y., Gough, R., Lef√®vre, F., Forget, F. (2011) Little variability of methane on Mars induced by adsorption in the regolith. *Planetary and Space Science* 59, 247-258.

Mickol, R., Craig, P., Kral, T. (2016) *Nontronite and Montmorillonite as Nutrient Sources for Life on Mars*, Biosignature Preservation and Detection in Mars Analog Environments, Lake Tahoe, NV.

Mickol, R.L., Kral, T.A. (2016) Low Pressure Tolerance by Methanogens in an Aqueous Environment: Implications for Subsurface Life on Mars. *Origins of Life and Evolution of Biospheres*, 1-22.

Milkevych, V., Donose, B.C., Juste-Poinapen, N., Batstone, D.J. (2015) Mechanical and cell-to-cell adhesive properties of aggregated *Methanosarcina*. *Colloids and Surfaces B: Biointerfaces* 126, 303-312.

Moeller, R., Schuerger, A.C., Reitz, G., Nicholson, W.L. (2012) Protective role of spore structural components in determining *Bacillus subtilis* spore resistance to simulated mars surface conditions. *Applied and Environmental Microbiology* 78, 8849-8853.

Moores, J.E., Schuerger, A.C. (2012) UV degradation of accreted organics on Mars: IDP longevity, surface reservoir of organics, and relevance to the detection of methane in the atmosphere. *Journal of Geophysical Research* 117.

Mumma, M.J., Villanueva, G.L., Novak, R.E., Hewagama, T., Bonev, B.P., DiSanti, M.A., Mandell, A.M., Smith, M.D. (2009) Strong release of methane on Mars in northern summer 2003. *Science* 323, 1041-1045.

Mustard, J.F., Adler, M., Allwood, A., Bass, D.S., Beaty, D.W., Bell III, J.F., Brinckerhoff, W.B., Carr, M., Des Marais, D.J., Drake, B., Edgett, K.S., Eigenbrode, J., Elkins-Tanton, L.T., Grant, J.A., Milkovich, S.M., Ming, D., Moore, C., Murchie, S., Onstott, T.C., Ruff, S.W., Sephton, M.A., Steele, A., Treiman, A. (2013) Report of the Mars 2020 Science Definition Team. 154 pp., posted July, 2013, by the Mars Exploration Program Analysis Group (MEPAG) at http://mepag.jpl.nasa.gov/reports/MEP/Mars_2020_SDT_Report_Final.pdf.

Nair, H., Allen, M., Anbar, A.D., Yung, Y.L., Clancy, R.T. (1994) A photochemical model of the martian atmosphere. *Icarus* 111, 124-150.

NASA (2014) *NASA Science Plan 2014*. National Aeronautics and Space Administration, Washington, D.C., pp. 124.

Newcombe, D.A., Schuerger, A.C., Benardini, J.N., Dickinson, D., Tanner, R., Venkateswaran, K. (2005) Survival of spacecraft-associated microorganisms under simulated martian UV irradiation. *Applied and Environmental Microbiology* 71, 8147-8156.

Nicholson, W.L., Moeller, R., the Protect Team, Horneck, G. (2012) Transcriptomic responses of germinating *Bacillus subtilis* spores exposed to 1.5 years of space and simulated martian conditions on the EXPOSE-E experiment PROTECT. *Astrobiology* 12, 469-486.

Nicholson, W.L., Schuerger, A.C. (2005) *Bacillus subtilis* spore survival and expression of germination-induced bioluminescence after prolonged incubation under simulated Mars atmospheric pressure and composition: implications for planetary protection and lithopanspermia. *Astrobiology* 5, 536-544.

O'Brien, J.M., Wolkin, R.H., Moench, T.T., Morgan, J.B., Zeikus, J.G. (1984) Association of hydrogen metabolism with unitrophic or mixotrophic growth of *Methanosarcina barkeri* on carbon monoxide. *Journal of Bacteriology* 158, 373-375.

Ojha, L., Wilhelm, M.B., Murchie, S.L., McEwen, A.S., Wray, J.J., Hanley, J., Massé, M., Chojnacki, M. (2015) Spectral evidence for hydrated salts in recurring slope lineae on Mars. *Nature Geoscience* 8, 829-832.

Onstott, T.C., McGown, D., Kessler, J., Sherwood Lollar, B., Lehmann, K.K., Clifford, S.M. (2006) Martian CH_4: sources, flux, and detection. *Astrobiology* 6, 377-395.

Osman, S., Peeters, Z., La Duc, M.T., Mancinelli, R., Ehrenfreund, P., Venkateswaran, K. (2008) Effect of shadowing on survival of bacteria under conditions simulating the martian atmosphere and UV radiation. *Applied and Environmental Microbiology* 74, 959-970.

Oze, C., Jones, L.C., Goldsmith, J.I., Rosenbauer, R.J. (2012) Differentiating biotic from abiotic methane genesis in hydrothermally active planetary surfaces. *Proceedings of the National Academy of Sciences of the United States of America* 109, 9750-9754.

Oze, C., Sharma, M. (2005) Have olivine, will gas: Serpentinization and the abiogenic production of methane on Mars. *Geophysical Research Letters* 32.

Pollack, J.B., Kasting, J.F., Richardson, S.M., Poliakoff, K. (1987) The case for a wet, warm climate on early Mars. *Icarus* 71, 203-224.

Price, M.C., Ramkissoon, N.K., McMahon, S., Miljković, K., Parnell, J., Wozniakiewicz, P.J., Kearsley, A.T., Blamey, N.J.F., Cole, M.J., Burchell, M.J. (2014) Limits on methane release and generation via hypervelocity impact of Martian analogue materials. *International Journal of Astrobiology* 13, 132-140.

Prieto-Ballesteros, O., Kargel, J.S., Fairén, A.G., Fernández-Remolar, D.C., Dohm, J.M., Amils, R. (2006) Interglacial clathrate destabilization on Mars: Possible contributing source of its atmospheric methane. *Geology* 34, 149-152.

Rettberg, P., Anesio, A.M., Baker, V.R., Baross, J.A., Cady, S.L., Detsis, E., Foreman, C.M., Hauber, E., Ori, G.G., Pearce, D.A., Renno, N.O., Ruvkun, G., Sattler, B., Saunders, M.P., Smith, D.H., Wagner, D., Westall, F. (2016) Planetary Protection and Mars Special Regions—A Suggestion for Updating the Definition. *Astrobiology* 16, 119-125.

Rettberg, P., Rabbow, E., Panitz, C., Horneck, G. (2004) Biological space experiments for the simulation of Martian conditions: UV radiation and Martian soil analogues. *Advances in Space Research* 33, 1294-1301.

Ryan, S., Dlugokencky, E.J., Tans, P.P., Trudeau, M.E. (2006) Mauna Loa volcano is not a methane source: Implications for Mars. *Geophysical Research Letters* 33.

Schauer, N.L., Ferry, J.G. (1980) Metabolism of formate in *Methanobacterium formicicum*. *Journal of Bacteriology* 142, 800-807.

Schoell, M. (1988) Multiple origins of methane in the earth. *Chemical Geology* 71, 1-10.

Schuerger, A.C., Clausen, C., Britt, D. (2011) Methane evolution from UV-irradiated spacecraft materials under simulated martian conditions: Implications for the Mars Science Laboratory (MSL) mission. *Icarus* 213, 393-403.

Schuerger, A.C., Golden, D.C., Ming, D.W. (2012a) Biotoxicity of Mars soils: 1. Dry deposition of analog soils on microbial colonies and survival under Martian conditions. *Planetary and Space Science* 72, 91-101.

Schuerger, A.C., Mancinelli, R.L., Kern, R.G., Rothschild, L.J., McKay, C.P. (2003) Survival of endospores of *Bacillus subtilis* on spacecraft surfaces under simulated martian environments: implications for the forward contamination of Mars. *Icarus* 165, 253-276.

Schuerger, A.C., Moores, J.E., Clausen, C.A., Barlow, N.G., Britt, D.T. (2012b) Methane from UV-irradiated carbonaceous chondrites under simulated Martian conditions. *Journal of Geophysical Research* 117.

Schuerger, A.C., Nicholson, W.L. (2006) Interactive effects of hypobaria, low temperature, and CO_2 atmospheres inhibit the growth of mesophilic *Bacillus* spp. under simulated martian conditions. *Icarus* 185, 143-152.

Schuerger, A.C., Nicholson, W.L. (2016) Twenty Species of Hypobarophilic Bacteria Recovered from Diverse Soils Exhibit Growth under Simulated Martian Conditions at 0.7 kPa. *Astrobiology* 16, 964-976.

Schuerger, A.C., Richards, J.T., Hintze, P.E., Kern, R.G. (2005) Surface characteristics of spacecraft components affect the aggregation of microorganisms and may lead to different survival rates of bacteria on Mars landers. *Astrobiology* 5, 545-559.

Schuerger, A.C., Richards, J.T., Newcombe, D.A., Venkateswaran, K. (2006) Rapid inactivation of seven *Bacillus* spp. under simulated Mars UV irradiation. *Icarus* 181, 52-62.

Schuerger, A.C., Ulrich, R., Berry, B.J., Nicholson, W.L. (2013) Growth of *Serratia liquefaciens* under 7 mbar, 0 degrees C, and CO_2-enriched anoxic atmospheres. *Astrobiology* 13, 115-131.

Sheppard, J., Westberg, H., Hopper, J., Ganesan, K., Zimmerman, P. (1982) Inventory of global methane sources and their production rates. *Journal of Geophysical Research: Oceans (1978-2012)* 87, 1305-1312.

Sherwood Lollar, B., Lacrampe-Couloume, G., Slater, G., Ward, J., Moser, D., Gihring, T., Lin, L.-H., Onstott, T. (2006) Unravelling abiogenic and biogenic sources of methane in the Earth's deep subsurface. *Chemical Geology* 226, 328-339.

Sinha, N., Kral, T.A. (2015) Stable carbon isotope fractionation by methanogens growing on different Mars regolith analogs. *Planetary and Space Science* 112, 35-41.

Sinha, N., Nepal, S., Kral, T., Kumar, P. (2017) Survivability and growth kinetics of methanogenic archaea at various pHs and pressures: Implications for deep subsurface life on Mars. *Planetary and Space Science* 136, 15-24.

Smith, D.J., Griffin, D.W., McPeters, R.D., Ward, P.D., Schuerger, A.C. (2011) Microbial survival in the stratosphere and implications for global dispersal. *Aerobiologia* 27, 319-332.

Smith, D.J., Griffin, D.W., Schuerger, A.C. (2010) Stratospheric microbiology at 20 km over the Pacific Ocean. *Aerobiologia* 26, 35-46.

Sowers, K.R., Boone, J.E., Gunsalus, R.P. (1993) Disaggregation of *Methanosarcina* spp. and growth as single cells at elevated osmolarity. *Applied and Environmental Microbiology* 59, 3832-3839.

Stevens, A.H., Patel, M.R., Lewis, S.R. (2015) Numerical modelling of the transport of trace gases including methane in the subsurface of Mars. *Icarus* 250, 587-594.

Tauscher, C., Schuerger, A.C., Nicholson, W.L. (2006) Survival and germinability of *Bacillus subtilis* spores exposed to simulated Mars solar radiation: implications for life detection and planetary protection. *Astrobiology* 6, 592-605.

Thomas, C., Mousis, O., Picaud, S., Ballenegger, V. (2009) Variability of the methane trapping in martian subsurface clathrate hydrates. *Planetary and Space Science* 57, 42-47.

Vaishampayan, P.A., Rabbow, E., Horneck, G., Venkateswaran, K.J. (2012) Survival of *Bacillus pumilus* spores for a prolonged period of time in real space conditions. *Astrobiology* 12, 487-497.

Venkateswaran, K., La Duc, M.T., Horneck, G. (2014) Microbial existence in controlled habitats and their resistance to space conditions. *Microbes and Environments* 29, 243-249.

Wasserfallen, A., Nölling, J., Pfister, P., Reeve, J., De Macario, E.C. (2000) Phylogenetic analysis of 18 thermophilic *Methanobacterium* isolates supports the proposals to create a new genus, *Methanothermobacter* gen. nov., and to reclassify several isolates in three species, *Methanothermobacter thermautotrophicus* comb. nov., *Methanothermobacter wolfeii* comb. nov., and *Methanothermobacter marburgensis* sp. nov. *International Journal of Systematic and Evolutionary Microbiology* 50, 43-53.

Webster, C.R., Mahaffy, P.R., Atreya, S.K., Flesch, G.J., Mischna, M.A., Meslin, P.-Y., Farley, K.A., Conrad, P.G., Christensen, L.E., Pavlov, A.A., Martín-Torres, J., Zorzano, M.-P., McConnochie, T.H., Owen, T., Eigenbrode, J.L., Glavin, D.P., Steele, A., Malespin, C.A., Archer Jr., P.D., Sutter, B., Coll, P., Freissinet, C., McKay, C.P., Moores, J.E., Schwenzer, S.P., Bridges, J.C., Navarro-Gonzalez, R., Gellert, R., Lemmon, M.T., the MSL Science Team (2015) Mars methane detection and variability at Gale crater. *Science* 347, 415-417.

Winter, J., Lerp, C., Zabel, H.-P., Wildenauer, F.X., König, H., Schindler, F. (1984) *Methanobacterium wolfei*, sp. nov., a new tungsten-requiring, thermophilic, autotrophic methanogen. *Systematic and Applied Microbiology* 5, 457-466.

Woese, C.R., Fox, G.E. (1977) Phylogenetic structure of the prokaryotic domain: the primary kingdoms. *Proceedings of the National Academy of Sciences of the United States of America* 74, 5088-5090.

Wray, J.J., Ehlmann, B.L. (2011) Geology of possible Martian methane source regions. *Planetary and Space Science* 59, 196-202.

Wu, W.-M., Hickey, R.F., Jain, M.K., Zeikus, J.G. (1993) Energetics and regulations of formate and hydrogen metabolism by *Methanobacterium formicicum*. *Archives of Microbiology* 159, 57-65.

Chapter 2. Survival of Non-psychrophilic Methanogens Exposed to Extreme Temperature Changes.

R. L. Mickol[1], Y. A. Takagi[2], S. K. Laird[3], and T. A. Kral[1,3]

[1]Arkansas Center for Space and Planetary Sciences, University of Arkansas, Fayetteville, AR; [2]Dept. of Biology, Oberlin College, Oberlin, OH; [3]Dept. of Biological Sciences, University of Arkansas, Fayetteville, AR; [rebecca.mickol@gmail.com]

Contributions of authors: S. K. Laird prepared the Original sets for Experiments 2, 3, and 4, and performed the first 11, 9, and 6 methane measurements, respectively, under the guidance of R.L. Mickol during Spring 2013. All transfer sets were prepared by R.L. Mickol and subsequent methane readings for both Original and Transfer sets were performed by R.L. Mickol. Y. A. Takagi performed Experiments 4 and 5 under the guidance of R. L. Mickol during Summer 2014. Additional experiments and data analysis were performed by R.L. Mickol.

2.1 Abstract

Polygonal ground and other geomorphological features reminiscent of recent freeze/thaw cycling are evident on Mars. Permafrost on Mars may constitute a habitable environment considering the existence of active microbial communities on Earth. The overlap between patterned ground and detections of localized methane plumes on Mars suggest the compound may have been released from thawing permafrost. On Earth, permafrost communities are often active at subfreezing temperatures and consist of methane-producing Archaea. Analysis of ice cores and soil samples on Earth notes that (1) archaeal communities often contain both mesophiles and psychrophiles at different depths and (2) active methane is being produced at subfreezing temperatures over geological timescales. In this study, non-psychrophilic methanogens were tested for their ability to survive extreme weekly and daily temperature changes, similar to those on Mars.

2.2 Introduction

Mars experiences wide temperature variations over one sol, often ranging from temperatures just above freezing to -100 °C and lower (Kieffer et al., 1977). Any microorganisms that could potentially inhabit Mars would at least need to be able to survive these temperatures, and also make use of any available liquid water or temporary increases in temperature in order to metabolize. Due to the very thin atmosphere and lack of other insulating factors, temperatures vary widely on Mars based on location and season. Temperatures from the primary Viking mission ranged between 130 K (-143 °C) and 290 K [~17 °C] (Kieffer et al., 1977). Measurements from the Thermal Emission Spectrometer (TES) depicted nighttime temperatures ranging between 150 K and 220 K [-123 °C and -53 °C] (Christensen et al., 2001).

Additional temperature measurements from the Thermal Emission Imaging System (THEMIS) aboard Mars Odyssey place nighttime temperatures in Chryse basin (22.5°N; 324°E) in the range of 187.8 K to 203.7 K (-85.4 °C to -69.5 °C), while daytime temperatures range between 232.5 K to 248.5 K [-40.7 °C to -24.7 °C] (Christensen et al., 2003). Temperatures in Russell crater (54°S; 13°E) reached up to 260 K (-13 °C) in the daytime and down to 170 K (-103 °C) at night (Christensen et al., 2003). One major goal of THEMIS was to search for locations of possible geothermal activity on Mars. However, the widespread thermal variation and temperature anomalies due to high rock abundance have complicated the search for hotspots or coldspots (Christensen et al., 2003).

Although certain psychrophilic organisms are capable of active metabolism below freezing temperatures where water may still remain liquid, most organisms require temperatures above 0 °C for active growth, and there are currently no organisms that can actively grow below -20 °C (Clarke, 2014). Additionally, growth may be relatively slow at lower temperatures (Franzmann et al., 1997; Rivkina et al., 2000) due to reduced molecular kinetic energy and the subsequent lower rate of metabolic reactions (Clarke, 2014). The freezing temperatures of Mars may not be conducive to continued active metabolism, but exposure to these temperatures is not necessarily lethal to the organism. Many organisms have freeze tolerances that enable them to survive freezing temperatures down to -196 °C (Clarke, 2014). Active metabolism is then resumed once warmer temperatures are achieved.

On Earth, permafrost is defined by temperature and refers to any rocks, soil, or sediments that remain at or below 0 °C for at least two years in a row (Wagner, 2008; Wagner et al., 2002). Permafrost environments typically range between -50 °C and 30 °C, subjecting their microbial communities to large freeze/thaw cycles not encountered elsewhere. Permafrost consists of three

temperature-dependent layers: 1. An active layer (0.2 – 2 m thick), the uppermost layer, which experiences the widest range in temperatures (-50 – 30 °C), depending on fluctuations in air temperature; 2. Perennially-frozen permafrost sediments (10 – 20 m thick) subject to smaller temperature variations (-15 – 0 °C above the zero annual amplitude [constant temperature]); and 3. Deeper permafrost sediments that are characterized by more stable temperatures between -10 and -5 °C (Wagner, 2008; Wagner et al., 2002). Microbial communities within the active layer are thus subject to yearly freezing and thawing, correlating with seasonal temperatures.

Experiments utilizing freeze/thaw cycles have come under scrutiny for not accurately representing temperature changes seen in nature (Henry, 2007). However, temperatures can vary widely based on location, season, and whether measurements are taken from the air or soil at varying depths (Henry, 2007). For example, Zhang et al. (2003) analyzed temperature data from 1997-1999 within the contiguous United States. The authors discovered that duration of soil freezing ranges between one and eight months, and the number of freeze-thaw cycles that occurs ranges from one to more than eleven, based on location (Zhang et al., 2003). Additionally, the frozen period of freeze-thaw cycles varied in length from less than twenty days to over 220 days (Zhang et al., 2003). In regard to a more Mars-like environment, soils at a depth of 5 cm in Antarctica (Signy Island, South Orkney Islands, maritime Antarctic; 60°43'S, 45°38'W) experienced 42 freeze-thaw cycles during a three-month period, with an average of 15 freeze/thaw cycles per month (Yergeau and Kowalchuk, 2008). The average soil temperature (5 cm below the surface) was 1.1 °C, ranging between the minimum -5.6 °C and the maximum of 15.8 °C (Yergeau and Kowalchuk, 2008). Thus, over a single season, “a soil freeze/thaw cycle can occur several times, and the length of freeze and thaw within one freeze/thaw cycle may not be symmetric” (Zhang et al., 2003). As such, previous freeze/thaw experiments have used a

variety of cycle lengths, number of cycles, and temperatures [Table 1; see also (Henry, 2007)]. The diurnal freeze/thaw experiment included in this study (Expt. 5) is similar to the diurnal temperature changes utilized in the martian simulation experiment of Morozova et al. (2007).

On Mars, surface temperatures range widely over just one sol (0 °C to -100 °C). As on Earth, temperatures may be more stable under the martian surface due to insulation from the overlying layers (Henry, 2007). However, stability does not necessitate warmer temperatures. The globally-averaged annual mean soil temperature on Mars is 204 K (-69 °C), varying between 234 K (-39 °C) at the equator to 159 K (-114 °C) at the poles (Mellon et al., 2008; Mellon et al., 2004). Although surface temperatures do rise above 0 °C at the equator, it is believed that near-subsurface (within 6 cm) soil temperatures never rise above freezing (Mellon et al., 2008). However, models utilizing different thermal conductivities and soil densities suggest that temperatures above 273 K may be possible 3-7 km beneath the martian surface (Mellon and Phillips, 2001). Additionally, on Earth, consistent snowpacks can insulate soil communities and result in higher microbial activities than soils that are not well-insulated, and thus, subject to colder temperatures (Henry, 2007). However, on Mars, only the polar caps would constitute semi-permanent insulated habitats.

Despite the consistently cold temperatures on the planet, Page (2007) notes the existence of various geomorphological landforms that are reminiscent of relatively recent freeze/thaw cycles on Mars. Interestingly, the author suggests that thawing permafrost may result in the loss of volatiles from the soil and thus could form a source for the localized methane plumes detected over the Cerberus plains on Mars – a region that also features polygonal ground (Page, 2007). Further, Ulrich et al. (2012) have noted periglacial landforms on Mars, suggesting that methanogens, specifically, could potentially exist there. On Earth, permafrost communities are

considered fairly active at subfreezing temperatures (Rivkina et al., 2004; Rivkina et al., 2007; Wagner et al., 2007) and the same could potentially be true for regions on Mars (Gilichinsky et al., 2007; Steven et al., 2009; Wagner et al., 2002).

Table 2.1 Examples of previous freeze/thaw studies.

Number of Cycles	Temperatures During Cycles	Length at Temp.	Total Experiment Length	Sample	Reference
18	2 °C -4 °C	9 h 15 h	18 days	Abisko, northern Swedish Lapland, vegetation and soil blocks	Larsen et al. (2002)
1 or 4	-9 °C and 4 °C	12 h each	1 day or 4 days	Western Alps, the Pennines, alpine soil	Freppaz et al. (2007)
14	-10 °C and 0 °C	12 h each	14 days	Canadian arctic soil	Kumar et al. (2013)
3	4 °C, 2 °C, 0 °C, -2 °C, -5 °C	24 h each	20 days	Arctic intertidal mud flat sediment	Sawicka et al. (2010)
2	-20 °C and 10 °C	3 weeks each	12 weeks	Arctic intertidal mud flat sediment	Sawicka et al. (2010)
8	-20 °C 10 °C	12 h 18 h	10 days	Arctic intertidal mud flat sediment	Sawicka et al. (2010)
4	-17 °C 4 °C	5 days 7 days	48 weeks	Finnish agricultural soil (loamy sand, peat)	Koponen et al. (2006)
3	-25 °C 1 °C	15 h 9 h	3 days	Wisconsin soil, seeds of *Elymus canadensis*	Connolly and Orrock (2015)
10	-15 °C 17 °C	1 day 6 days	70 days	Canadian grassland soil	Feng et al. (2007)
6	5 °C -40 °C	12 min 48 min	6 hours	Cloud water isolates	Joly et al. (2015)
4	-15 °C, -10 °C, -5 °C, 5 °C, 10 °C	1 week each	8 weeks	Chinese agricultural grassland soil	Lu et al. (2015)

(continued)

Table 2.1 Examples of previous freeze/thaw cycles (continued)

Number of Cycles	Temperatures During Cycles	Length at Temp.	Total Experiment Length	Sample	Reference
3	-5 °C 5 °C	5 days 2 days	21 days	Glas Maol (summit plateau), East Scotland, soil cores	Wipf et al. (2015)
1	-5 °C	5 days	5 days	Glas Maol soil cores	Wipf et al. (2015)
1	-5 °C	19 days	19 days	Glas Maol soil cores	Wipf et al. (2015)
3, 12, 24, 36, or 48[a]	10 °C -15 °C	15 h 9 h	12 weeks	Antarctic soil cores	Yergeau and Kowalchuk (2008)

[a]Number of cycles corresponds to frequency treatment during a 12-week period: 3 cycles = frequency of one month, 12 cycles = frequency of one week, 24 cycles = 2 cycles per week, 36 cycles = 3 cycles per week, 48 cycles = 4 cycles per week. Cycles were only conducted four out of seven days per week (Yergeau and Kowalchuk, 2008).

Methanogens are microorganisms in the domain Archaea that utilize hydrogen (H_2) and carbon dioxide (CO_2) to produce methane (CH_4) and are often prominent in permafrost communities on Earth (Blake et al., 2015; Gilichinsky et al., 2007; Kobabe et al., 2004; Koch et al., 2009; Liebner et al., 2015; Rivkina et al., 2007; Shcherbakova et al., 2016; Wagner et al., 2007; Wagner et al., 2005). The discovery of methane in the martian atmosphere (Fonti and Marzo, 2010; Formisano et al., 2004; Geminale et al., 2008; Geminale et al., 2011; Krasnopolsky et al., 1997; Krasnopolsky et al., 2004; Maguire, 1977; Mumma et al., 2009; Webster et al., 2015) reinforces the study of methanogens as candidates for life on Mars. A few studies have assessed the growth and survivability of methanogens under low temperature conditions, focusing on methanogens isolated from permafrost habitats in comparison with both psychrotolerant and non-psychrophilic methanogens from non-permafrost environments (Morozova et al., 2007; Morozova and Wagner, 2007; Schirmack et al., 2014a). Morozova et al.

(2007) compared survival within pure cultures under martian conditions for three methanogen strains isolated from permafrost and three reference organisms: *Methanosarcina barkeri*, *Methanogenium frigidium* (isolated from Ace Lake, Antarctica) and *Methanobacterium* spec. MC-20. This study consisted of 22 days of diurnal freeze/thaw cycles between -75 °C and 20 °C. Morozova et al. (2007) discovered that the three permafrost strains had the highest survival (60.6% - 90.4%, cell counts), whereas the survival rate for the reference organisms was exceptionally low (5.8% survival for *M. frigidum*, 0.3% survival for *M. barkeri*). Additionally, methane production following exposure was significantly decreased for the three reference strains, whereas the permafrost strains had similar methane production before and after exposure (Morozova et al., 2007). In a separate study, Schirmack et al. (2014a) were able to demonstrate methane production by *Methanosarcina soligelidi* (Wagner et al., 2013), a permafrost methanogen also used in the Morozova et al. (2007) study, at temperatures down to -5 °C and at a pressure of 50 kPa (0.5 bar), which the authors suggest may be achievable in the martian subsurface.

Analysis of methane within permafrost ice cores has also led to the suggestion that methane is being produced at subfreezing temperatures [-9 °C, -11 °C] (Tung et al., 2005; Tung et al., 2006) and [-3 °C, -6 °C] (Wagner et al., 2007). The calculated metabolic rates associated with excess methane, based on cell counts within the ice core, suggest that this metabolic energy is typically expended to repair damaged DNA and amino acids (Tung et al., 2005). These findings correspond to the idea of “survival metabolism”, illustrated by Price and Sowers (2004). This differs from both “growth” and “maintenance metabolism”, but is evident as a survival tactic for microbes in deep glacial ice, subsurface sediments, and ocean sediments (Price and Sowers, 2004). From their analysis, the authors also suggest that organisms may be capable of

survival metabolism at temperatures down to –40 °C (Price and Sowers, 2004). As such, freeze/thaw cycles within subfreezing environments on Mars may prove relatively habitable in terms of survival of extant organisms.

The experiments described here exposed four methanogen species (*Methanothermobacter wolfeii*, *Methanobacterium formicicum*, *Methanosarcina barkeri*, *Methanococcus maripaludis*) to temperature changes between -80 °C and 55 °C. These experiments are reminiscent of recent studies analyzing the effect of freeze/thaw cycles on microbial communities within terrestrial permafrost (Lu et al., 2015; Sawicka et al., 2010), but the range of temperatures also has relevance to Mars.

2.3 Materials and Methods

2.3.1 Microbial Procedures

Methanogens were originally obtained from the Oregon Collection of Methanogens (OCM), Portland State University, Oregon. Each methanogen was initially cultured in its respective anaerobic growth medium and kept at a temperature within the organisms' ideal growth range: *Methanococcus maripaludis* (OCM 151), MSH medium (Ni and Boone, 1991), 22 °C; *Methanosarcina barkeri* (OCM 38), MS medium (Boone et al., 1989), 37 °C; *Methanobacterium formicicum* (OCM 55), MSF medium (MS medium supplemented with formate), 37 °C; *Methanothermobacter wolfeii* (OCM 36), MM medium (Xun et al., 1988), 55 °C. Media were prepared according to Kendrick and Kral (2006). Following preparation in an anaerobic chamber, media were dispensed into anaerobic culture tubes, fitted with rubber stoppers, and sealed with aluminum crimps as described in Boone et al. (1989). The media were then autoclaved for sterilization. Prior to inoculation with the respective organisms, 2.5% sterile

sodium sulfide (~125 μL per 10 mL) was added to each culture tube to remove residual oxygen (Boone et al., 1989). The tubes were then pressurized with 2 bar H_2 and incubated at the organisms' respective growth temperatures. For each experiment, growth was monitored via methane production using a Varian Micro-GC (Model CP4900). In Experiments 5 and 6, optical density (OD_{600}) was also monitored using a Spectronic 20D+ (Spectronic Instruments, USA) over time as a proxy for growth.

2.3.2 Experiment 1: Growth at 4 °C and 22 °C

Media were prepared as described (see 2.3.1 Microbial Procedures) for each of four methanogen species. For each species, there were four replicates for each temperature (4 °C and 22 °C). Organisms were inoculated with 0.5 mL culture and test tubes were kept at the desired temperature for the duration of the experiment. Growth was monitored over 140 days by methane production via gas chromatography.

2.3.3 Experiment 2: 5 g sand, 10 mL medium

Two types of methanogen growth media (MSF, MM) were prepared as described (see 2.3.1 Microbial Procedures). Two separate sets were prepared (one for each of two organisms) and transfer sets were also prepared as described below.

Five grams of sand were added to each of 10 test tubes, with five tubes containing 10 mL MSF medium, and five tubes containing 10 mL MM methanogen growth medium (see 2.3.1 Microbial Procedures). The MSF tubes were inoculated with 0.5 mL of MSF medium containing *M. formicicum* (n = 4). The MM test tubes were inoculated with 0.5 mL of MM medium containing *M. wolfeii* (n = 4). One test tube for each medium type was not inoculated. After

inoculation, each tube was pressurized with 2 bar H_2 gas. The tubes were next subjected to varying freeze/thaw cycles at temperatures of 55 °C, 37 °C, 22 °C, 4 °C, -15 °C, and -80 °C (Table 2.2).

After 104 days, a transfer set was prepared following the same method as above. On Day 105, the five transfer tubes with MM medium were each inoculated with 0.5 mL from one tube from the MM Original Set (n = 5; see Fig. 2.1). The four tubes with MSF medium were each inoculated with 0.5 mL from one tube from the MSF Original Set (n = 4; see Fig. 2.2). On Day 179, a second transfer set was prepared following the methods above. In this set, each MM transfer tube was inoculated with 0.5 mL culture from the corresponding MM tube in Transfer Set 1 (see Fig. 2.1). Two MSF transfer tubes were inoculated from one tube in MSF Transfer Set and two additional MSF transfer tubes were inoculated from two different tube in MSF Transfer Set 1 (see Fig. 2.2). On Day 1490, a third transfer set was prepared following the methods above. This set contained only 10 mL medium (either MSF or MM), and did not include any sand. In this set, on Day 1494, each of the tubes (MSF: n = 4; MM: n = 5) was inoculated with 0.5 mL from the corresponding tube in Transfer Set 2 (see Figs. 2.1, 2.2).

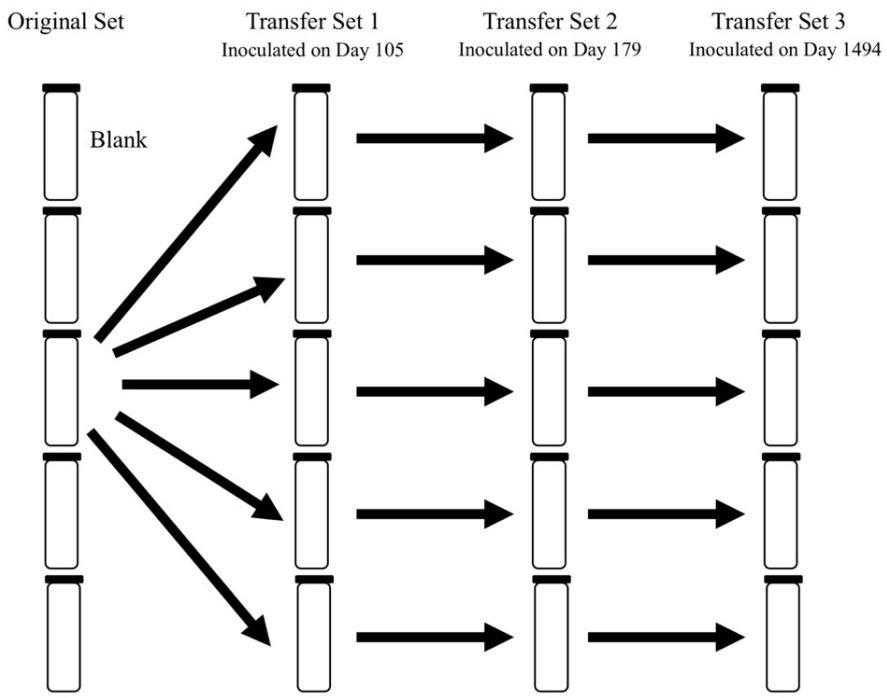

Figure 2.1 Inoculation scheme for Transfer Sets 1, 2, and 3 for cultures of *Methanothermobacter wolfeii* in Experiment 2 (5 g sand, 10 mL medium).

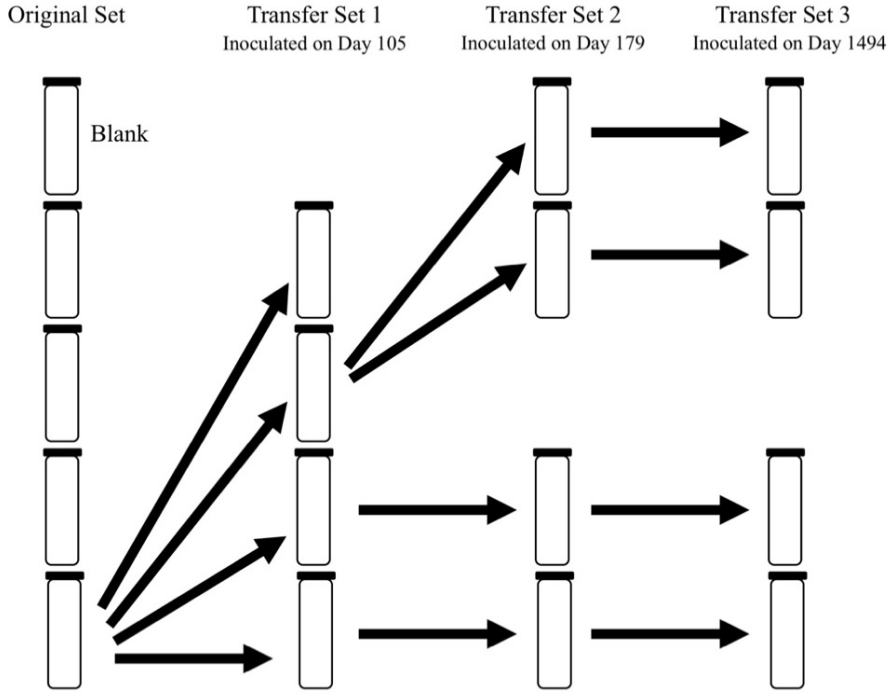

Figure 2.2 Inoculation scheme for Transfer Sets 1, 2, and 3 for cultures of *Methanobacterium formicicum* in Experiment 2 (5 g sand, 10 mL medium).

Table 2.2 Time intervals and temperatures for freeze/thaw cycling for Experiment 2.

			Original Set		Transfer Set 1		Transfer Set 2		Transfer Set 3	
	Cumulative Days of Cycling[a]	Cumulative Years of Cycling	Time at Temperature (days)	Temperature[b] (°C)	Time at Temperature (days)	Temperature[b] (°C)	Time at Temperature (days)	Temperature (°C)	Time at Temperature (days)	Temperature (°C)
	5	0.014	5	37 or 55						
	14	0.038	9	37 or 55						
	19	0.052	5	4						
	26	0.071	7	4						
	40	0.110	14	-15						
	47	0.129	7	4						
	63	0.173	16	-15						
	70	0.192	7	4						
	77	0.211	7	-15						
	96	0.263	19	4						
	103	0.282	7	22	Inoculated from Original Set on Day 105					
	112	0.307			7	22				
	127	0.348			15	22				
	138	0.378			11	-15				
	165	0.452			27	22				
	179	0.490			14	4	Inoculated from Transfer Set 1 on Day 179			
	196	0.537			17	37 or 55	17	37 or 55		
	211	0.578			15	-80	15	-80		
	231	0.633			20	4	20	4		
	252	0.690			21	22	21	22		
	267	0.732			15	-80	15	-80		
	297	0.814					30	4		
	334	0.915					37	-15		
	1487	4.074					1153	-80		
	1494	4.093					7	22	Inoculated from Transfer Set 2 on Day 1494	
	1508	4.132							14	37 or 55
	1522	4.170							14	37 or 55
Total	1508	4.170	103		162		1315		28	

Colors correspond to temperature of cycle: Incubation temperature (red [37 °C, *M. formicicum*; 55 °C, *M. wolfeii*]), room temperature (orange, 22 °C), 4 °C (yellow), -15 °C (blue), -80 °C (white). Original set tubes were re-pressurized with 2 bar H_2 on Day 96 during cycling.
[a]Cumulative Days of Cycling correspond to the number of days elapsed since the Original Set was first inoculated.
[b]Instances where temperatures are identical for two adjacent cycles indicate that the cultures were removed from incubation, tested for methane production, and replaced at that temperature for an additional incubation period.

2.3.4 Experiment 3: 10 g sand, 5 mL medium

Two types of methanogen growth media (MSF, MM) were prepared, as noted above (see 2.3.1 Microbial Procedures). Two separate sets were prepared (one for each of two organisms) and transfer sets were also prepared as described below. Ten grams of sand were added to each

of seven test tubes, with four tubes containing 5 mL MSF medium, and three tubes containing 5 mL MM methanogen growth medium (see 2.3.1 Microbial Procedures, above). The MSF tubes were inoculated with 0.5 mL of MSF medium containing *M. formicicum* (n = 4). The MM test tubes were inoculated with 0.5 mL of MM medium containing *M. wolfeii* (n = 3). After inoculation, each tube was pressurized with 2 bar H_2 gas. The tubes were next subjected to varying freeze/thaw cycles at temperatures of 55 °C, 37 °C, 22 °C, 4 °C, -15 °C, and -80 °C (Tables 2.3, 2.4).

After 90 days, a transfer set was prepared following the same method as above. On Day 91, two transfer tubes with MM medium were each inoculated with 0.3 mL from one tube from the MM Original Set. The remaining transfer tube with MM medium was inoculated with 0.3 mL from a different tube from the MM Original Set (see Fig. 2.3, n = 3). The four tubes with MSF medium were each inoculated with 0.3 mL from one tube from the MSF Original Set (see Fig. 2.4, n = 4). On Day 190, a second transfer set was prepared following the methods above. In this set, three MM tubes were inoculated with 0.5 mL from one MM Transfer Set 1 tube and two MM tubes were inoculated with 0.5 mL from a different MM Transfer Set 1 tube (see Fig. 2.3, n = 5). Three MSF tubes were inoculated with 0.5 mL from one MSF Transfer Set 1 tube and one MSF tube was inoculated with 0.5 mL from a different MSF Transfer Set 1 tube (see Fig. 2.4, n = 4). On Day 1467, Transfer Set 2 tubes were removed from a -80 °C freezer and thawed at room temperature for seven days (Tables 2.3, 2.4). A third transfer set was prepared with 10 mL medium (no sand) for both organisms as mentioned above (see 2.3.1 Microbial Procedures). On Day 1474, each tube within Transfer Set 3 was inoculated with 0.5 mL culture from the corresponding tube in Transfer Set 2 (see Figs. 2.3, 2.4). The tubes were incubated at the organisms' respective growth temperatures and monitored for methane production.

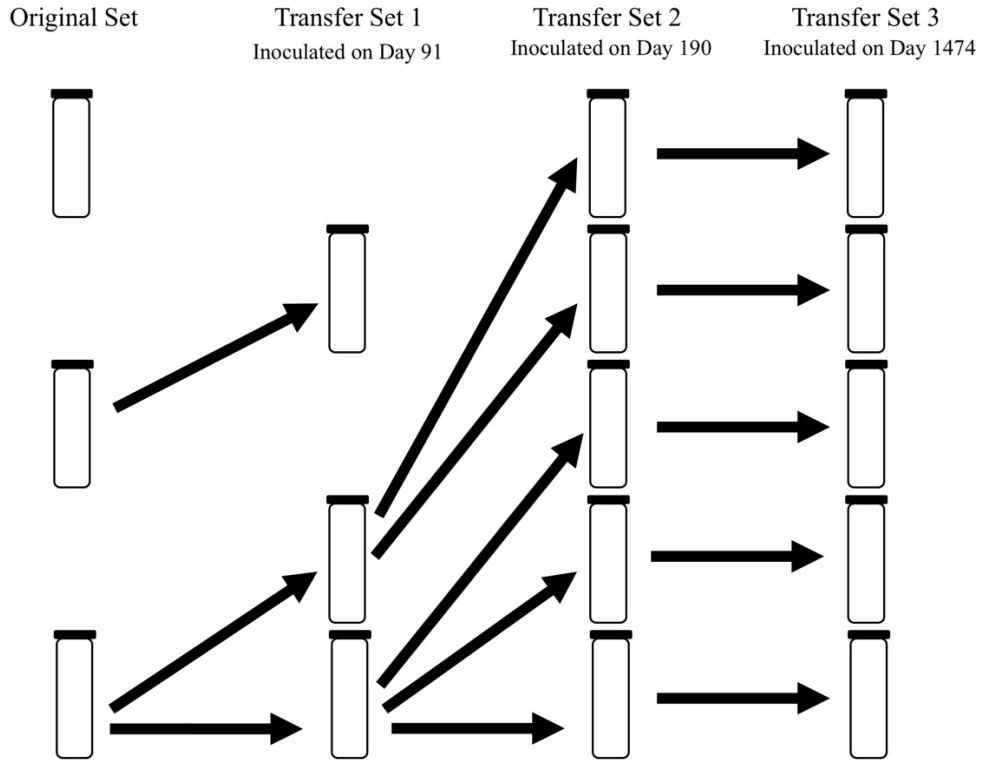

Figure 2.3 Inoculation scheme for Transfer Sets 1, 2, and 3 for cultures of *Methanothermobacter wolfeii* in Experiment 3 (10 g sand, 5 mL medium).

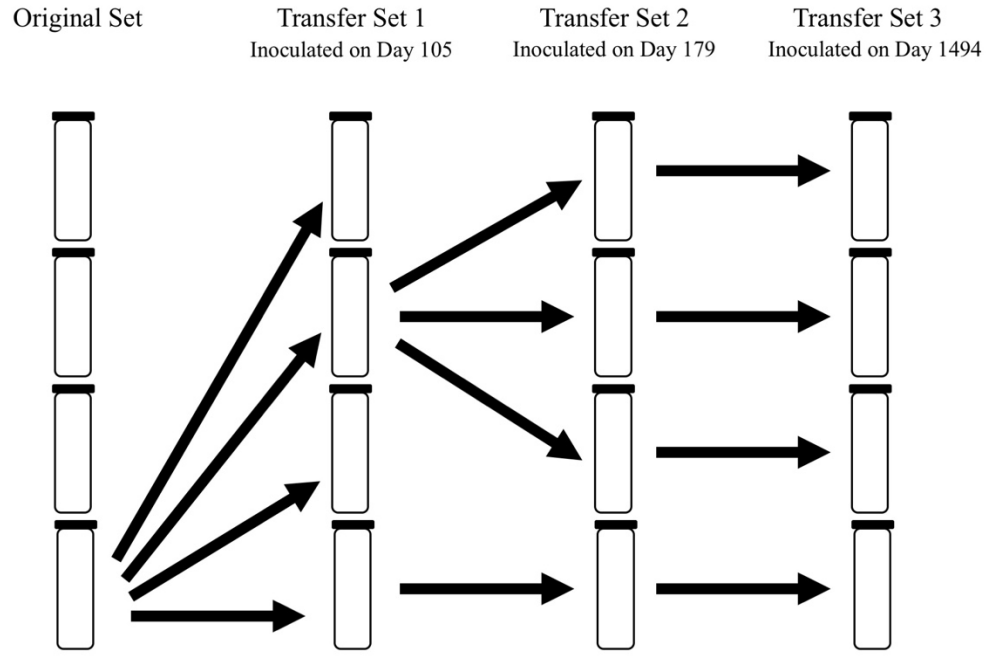

Figure 2.4 Inoculation scheme for Transfer Sets 1, 2, and 3 for cultures of *Methanobacterium formicicum* in Experiment 3 (10 g sand, 5 mL medium).

Table 2.3 Time intervals and temperatures for freeze/thaw cycling for Experiment 3 for *Methanobacterium formicicum* cultures.

		Original Set		Transfer Set 1		Transfer Set 2		Transfer Set 3	
Cumulative Days of Cycling[a]	Cumulative Years of Cycling	Time at Temperature (days)	Temperature (°C)	Time at Temperature (days)	Temperature (°C)	Time at Temperature (days)	Temperature (°C)	Time at Temperature (days)	Temperature (°C)
18	0.049	18	4						
25	0.068	7	37						
41	0.112	16	-15						
48	0.132	7	4						
55	0.151	7	-15						
74	0.203	19	4						
81	0.222	7	22						
				Inoculated from Original Set on Day 91					
146	0.400			55	37				
160	0.438			14	-15				
179	0.490			19	22				
196	0.537			17	4	Inoculated from Transfer Set 1 on Day 190			
207	0.567					17	37		
214	0.586			18	-15				
228	0.625					21	-80		
246	0.674			32	22				
284	0.778					56	37		
316	0.866					32	-15		
1467	4.02					1151	-80		
1474	4.04					7	22	Inoculated from Transfer Set 2 on Day 1474	
1488	4.08							14	37
1502	4.12							14	37
1502	4.08	81		155		1284		28	

Colors correspond to temperature of cycle: Incubation temperature (red, 37 °C), room temperature (orange, 22 °C), 4 °C (yellow), -15 °C (blue), -80 °C (white). Original set tubes were re-pressurized with 2 bar H_2 on Day 74 during cycling. Instances where temperatures are identical for two adjacent cycles indicate that the cultures were removed from incubation, tested for methane production, and replaced at that temperature for an additional incubation period. [a]Cumulative Days of Cycling correspond to the number of days elapsed since the Original Set was first inoculated.

Table 2.4 Time intervals and temperatures for freeze/thaw cycling for Experiment 3 for *Methanothermobacter wolfeii* cultures.

		Original Set		Transfer Set 1		Transfer Set 2		Transfer Set 3	
Cumulative Days of Cycling[a]	Cumulative Years of Cycling	Time at Temperature (days)	Temperature (°C)	Time at Temperature (days)	Temperature (°C)	Time at Temperature (days)	Temperature (°C)	Time at Temperature (days)	Temperature (°C)
18	0.049	18	4						
25	0.068	7	55						
41	0.112	16	-15						
48	0.132	7	4						
55	0.151	7	-15						
74	0.203	19	4						
81	0.222	7	22						
				Inoculated from Original Set on Day 91					
146	0.400			55	37				
160	0.438			14	55				
179	0.490			19	4				
196	0.537			17	55	Inoculated from Transfer Set 1 on Day 190			
207	0.567					17	55		
214	0.586			18	-15				
228	0.625					21	-80		
246	0.674			32	22				
284	0.778					56	55		
316	0.866					32	-15		
1467	4.02					1151	-80		
1474	4.04					7	22	Inoculated from Transfer Set 2 on Day 1474	
1488	4.08							14	55
1502	4.12							14	55
1502	4.12	81		155		1284		28	

Colors correspond to temperature of cycle: Incubation temperature (red, 55 °C), 37 °C (green), room temperature (orange, 22 °C), 4 °C (yellow), -15 °C (blue), -80 °C (white). Original set tubes were re-pressurized with 2 bar H_2 on Day 74 during cycling. Instances where temperatures are identical for two adjacent cycles indicate that the cultures were removed from incubation, tested for methane production, and replaced at that temperature for an additional incubation period.

[a]Cumulative Days of Cycling correspond to the number of days elapsed since the Original Set was first inoculated.

2.3.5 Experiment 4: 5 mL medium

This experiment focused on long-term survival to freeze/thaw cycles in media alone. Cultures of *M. formicicum* (n = 5) and *M. wolfeii* (n = 5) were initially grown in their respective anaerobic growth media (see 2.3.1 Microbial Procedures). Test tubes contained 5 mL media (MSF, *M. formicicum*; MM, *M. wolfeii*) and were inoculated with 0.5 mL culture. Tubes were pressurized with 2 bar H_2 and incubated at the organisms' growth temperature (*M. wolfeii*: 55 °C*; M. formicicum*: 37 °C) for 17 days. The cultures were then exposed to varying freeze/thaw cycles for 126 days (see Table 2.5). On Day 126, the cultures were transferred to an -80 °C freezer for 1151 days (3 years, 1 month). On Day 1154, fresh media (10 mL per test tube) were prepared as described above (see 2.3.1 Microbial Procedures). This transfer set was inoculated with 0.5 mL culture from the corresponding tube in the original set on Day 1158 (see Fig. 2.5). The tubes were kept at the organisms' respective growth temperatures for 14 days.

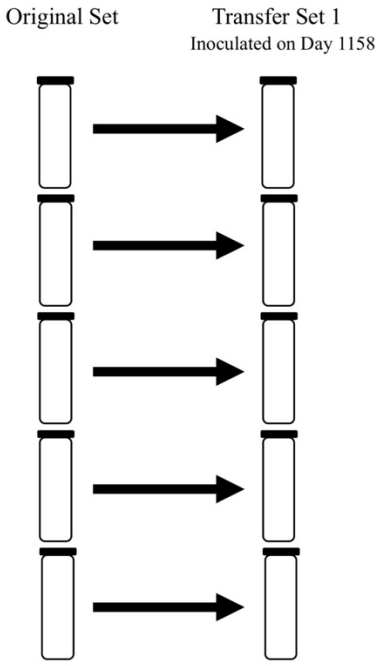

Figure 2.5 Inoculation scheme for Transfer Sets 1, 2, and 3 for cultures of *Methanobacterium formicicum* and *Methanothermobacter wolfeii* in Experiment 4 (5 mL medium).

Table 2.5 Time intervals and temperatures for freeze/thaw cycling for Experiment 4.

			Original Set		Transfer Set 1	
	Cumulative Days of Cycling[a]	Cumulative Years of Cycling	Time at Temperature (days)	Temperature (°C)	Time at Temperature (days)	Temperature (°C)
	17	0.47	17	37 or 55		
	38	0.104	21	-80		
	94	0.258	56	37 or 55		
	126	0.345	32	-15		
	1277	3.50	1151	-80		
	1284	3.52	7	22	Inoculated from Original Set on Day 1284	
	1298	3.56	14	37 or 55	14	37 or 55
	1312	3.60			14	37 or 55
Total	1312	3.60	1298		28	

Colors correspond to temperature of cycle: Incubation temperature (red, *M. formicicum*: 37 °C, or *M. wolfeii*: 55 °C), room temperature (orange, 22 °C), -15 °C (blue), -80 °C (white). Instances where temperatures are identical for two adjacent cycles indicate that the cultures were removed from incubation, tested for methane production, and replaced at that temperature for an additional incubation period.
[a]Cumulative Days of Cycling correspond to the number of days elapsed since the Original Set was first inoculated.

2.3.6 Experiments 5, 6: 24-h, 48-h Cycles

Two separate experiments were performed: in the first experiment (Expt. 5), a diurnal (24-h) temperature cycle was used; the second experiment (Expt. 6) used a 48-h cycle (Table 2.6). Each methanogen was initially grown in its respective anaerobic growth medium (see 2.3.1 Microbial Procedures). An aliquot of 0.5 mL of culture was inoculated into 10 mL of fresh medium for experimentation. Tubes were pressurized with 2 bar H_2 and incubated at a temperature within each organism's growth range (*M. wolfeii*: 55 °C*; M. formicicum*, *M. barkeri*: 37 °C; *M. maripaludis:* 22 °C) for 5 days, then incubated at room temperature (22 °C) for an additional 6 days, in order to acclimate the cultures to the highest temperature within the freeze/thaw cycles. Cultures were then exposed to a specific freeze/thaw cycle (Table 2.6) for 10

days (Expt. 5; n = 4) or 12 days (Expt. 6; n = 3). After the exposure period, cultures were incubated at their respective growth temperatures. Growth was monitored by methane production via gas chromatography and optical density.

Table 2.6 Temperature cycling for Experiment 5 (24-h) and Experiment 6 (48-h).

Expt. 5: 24-h Cycling		**Expt. 6: 48-h Cycling**	
-15 °C	2 hours	-15 °C	5 hours
4 °C	2 hours	4 °C	4 hours
22 °C	2 hours	22 °C	15 hours
4 °C	2 hours	4 °C	5 hours
-15 °C	2 hours	-15 °C	4 hours
-80 °C	14 hours	-80 °C	15 hours

2.4 Results

2.4.1 Experiment 1: Growth at 4 °C and 22 °C

Methane production did not occur for any of the four methanogen species after 140 days' incubation at 4 °C (data not shown). Three of the four methanogens were able to produce methane at 22 °C; *M. wolfeii* was not capable of any methane production after 140 days at 22 °C (Fig. 2.6).

2.4.2 Experiment 2: 5 g sand, 10 mL medium

The original sets for both *M. wolfeii* and *M. formicicum* consisted of n = 4 replicates (one tube in each set of 5 was not inoculated). Both transfer sets for *M. wolfeii* consisted of n = 5 tubes. The transfer sets for *M. formicicum* both consisted of n = 4 tubes.

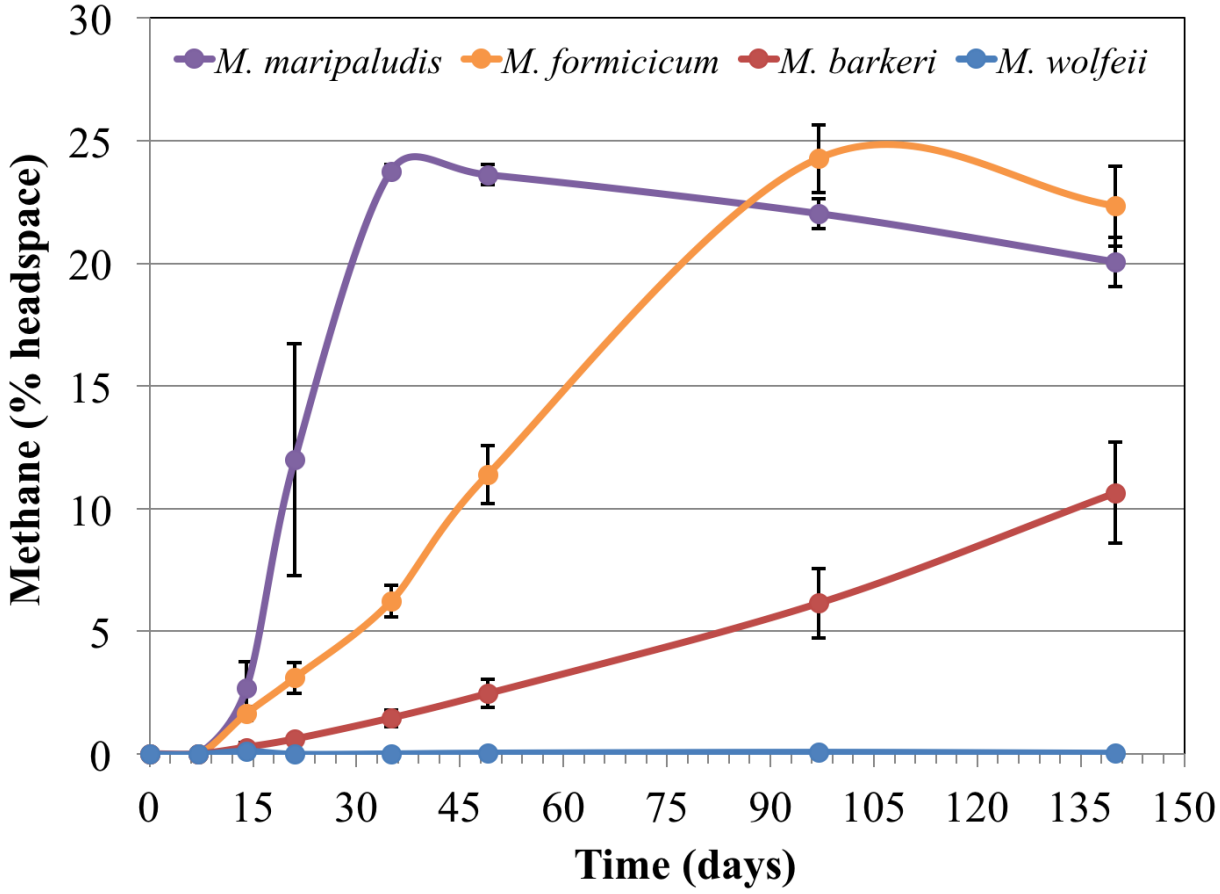

Figure 2.6 Methane production (% headspace) over time for four species of methanogens (*Methanococcus maripaludis*, *Methanobacterium formicicum*, *Methanosarcina barkeri*, *Methanothermobacter wolfeii*) at 22 °C. Error bars indicate ± one standard deviation (n = 4).

Methane production for the four cultures within the original set of *M. formicicum* all displayed ~3% methane production after 5 days (data not shown). After an additional 9 days at 37 °C, methane abundance was much more varied between replicates (~22-42%, Fig. 2.7). After Transfer Set 1 was inoculated and incubated at room temperature for 22 days, methane production within the four replicates ranged between 26% and 34% methane (Fig. 2.7). Additionally, after inoculation and incubation at 37 °C for 17 days, four cultures within Transfer

Set 2 displayed methane amounts between 22-25% (Fig. 2.7). The lower amount of methane produced by the cultures within Transfer Set 2 may be the result of a lower number of cells in the transfer inoculum and does not necessarily represent cell death.

Initial methane production for cultures of *M. wolfeii* reached ~38% methane following 14 days of incubation at 55 °C (Fig. 2.8). After Transfer Set 1 was inoculated, four of the five cultures displayed methane amounts between 2-4% after 7 days' incubation at room temperature (data not shown). After an additional 15 days, all five cultures increased in methane production, but amounts varied between 17% and 28% (Fig. 2.8). The culture with lowest methane value (17%) after 22 days corresponds to the culture that showed no methane production (0%) after 7 days' incubation at room temperature. In the second transfer set, all five cultures displayed methane production after 17 days at 55 °C (19-24%; Fig. 2.8). Similar to the cultures of *M. formicicum*, the decrease in methane amount between the three sets of replicates is not necessarily attributable to cell death and may be the result of fewer cells in the transfer inocula.

This experiment also examined survival following long-term exposure to freezing temperatures. Tubes with Transfer Set 2 were subjected to various freeze/thaw cycles, then kept at -80 °C for ~3 years (Table 2.2). The tubes were removed from the freezer, thawed at room temperature for 7 days, and then transfers were made to 10 mL fresh media. These new transfer tubes (Transfer Set 3) were stored at the organisms' respective incubation temperatures and monitored for methane production. For *M. formicicum*, none of the cultures produced methane up to 28 days following inoculation (Fig. 2.7). For *M. wolfeii*, four out of five cultures displayed high methane production (30-33% headspace) after 14 days' incubation at 55 °C (Fig. 2.8). One culture failed to produce any methane after 14 days' incubation and is not included in the data shown here.

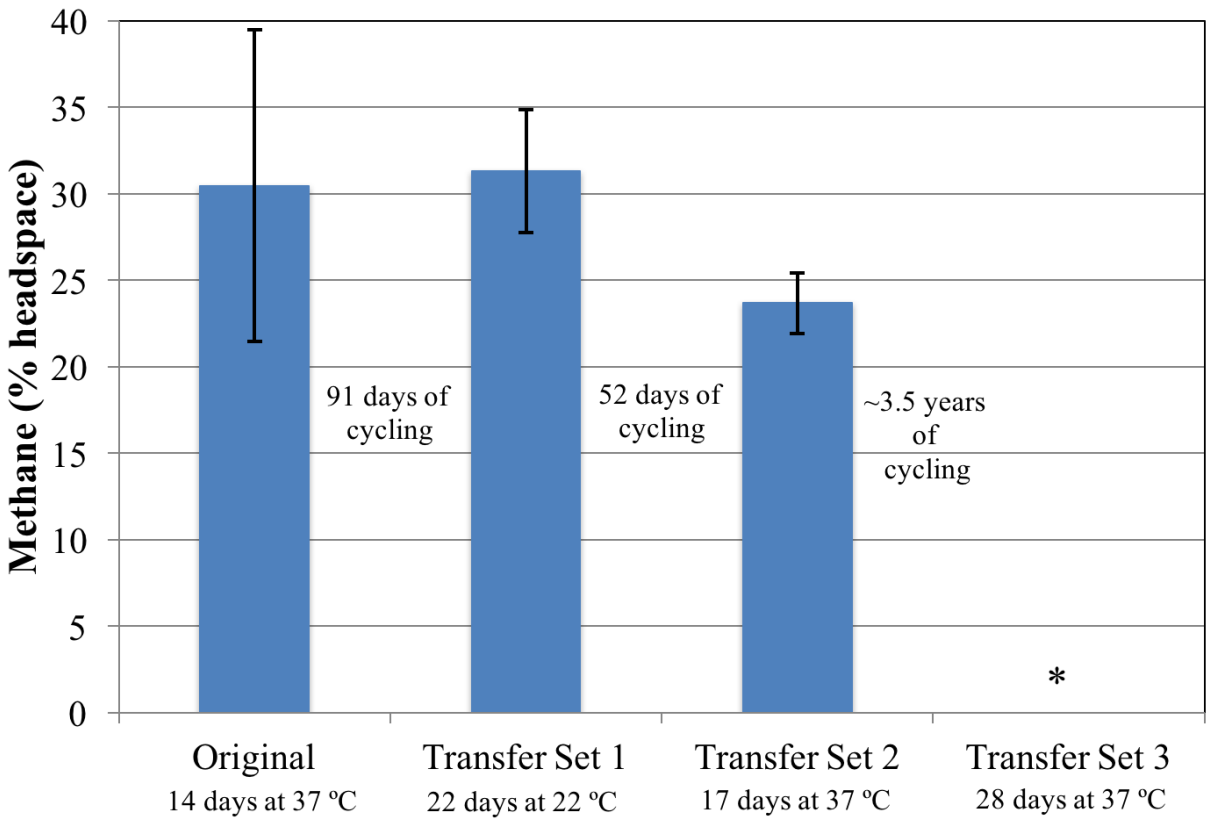

Figure 2.7 Methane production by *Methanobacterium formicicum* following initial incubation period for each of three sets. Test tubes contain 5 g sand and 10 mL MSF medium. Transfer Set 1 tubes (n = 4) were inoculated from one tube in the Original Set (n = 4) following 105 days of freeze/thaw cycles (see Table 2.2). Transfer Set 2 tubes (n = 4) were inoculated from three separate test tubes from Transfer Set 1 following 74 days of freeze/thaw cycles (see Table 2.2). Transfer Set 3 tubes (n = 4) were inoculated from the corresponding tube in Transfer Set 2 (see Table 2.2). The asterisk indicates that no methane was produced. Error bars indicate ± one standard deviation.

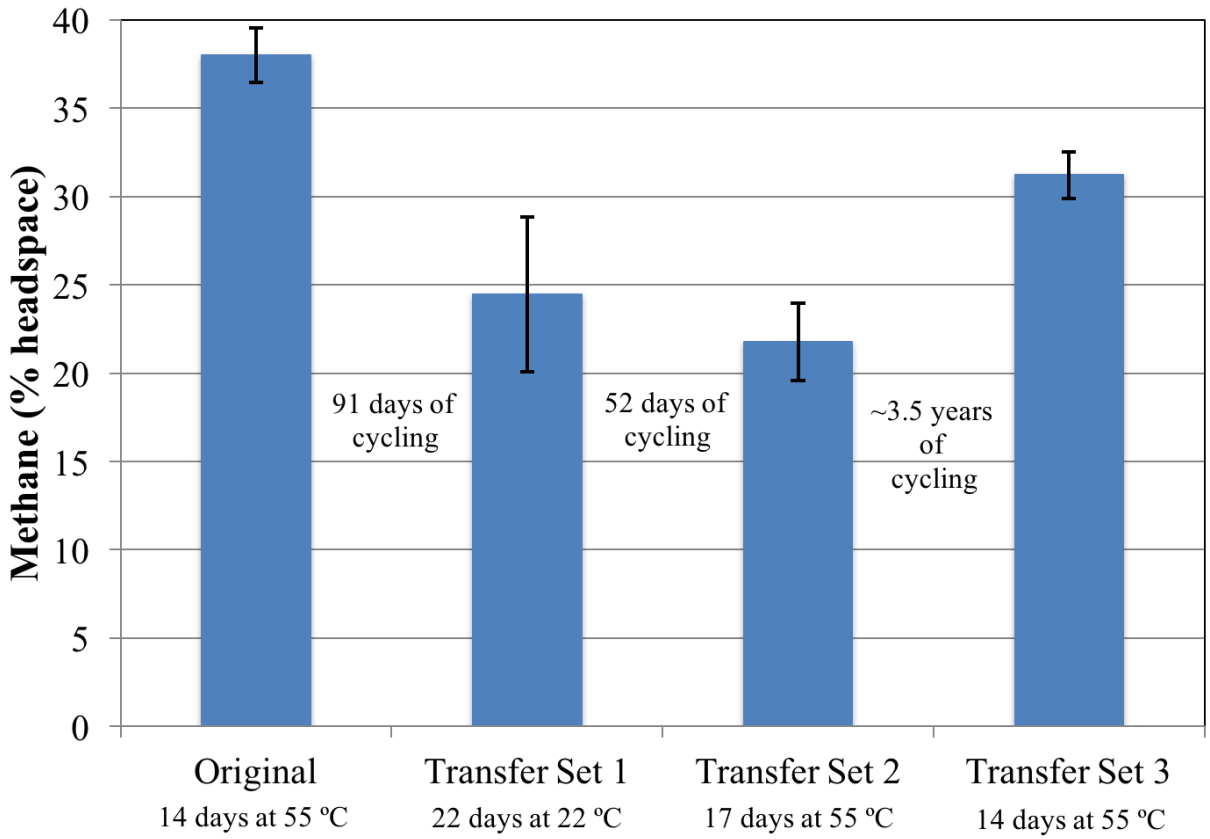

Figure 2.8 Methane production by *Methanothermobacter wolfeii* following initial incubation period for each of three sets. Test tubes for Original Set and Transfer Sets 1 and 2 contain 5 g sand and 10 mL MM medium. Transfer Set 3 tubes contain 10 mL MM medium. Transfer Set 1 tubes (n = 5) were inoculated from one tube in the Original Set (n = 4) following 105 days of freeze/thaw cycles (see Table 2.2). Transfer Set 2 tubes (n = 5) were inoculated from the corresponding tube within Transfer Set 1 following 74 days of freeze/thaw cycles (see Table 2.2). Transfer Set 3 tubes (n = 5*) were inoculated from the corresponding tube within Transfer Set 2 on Day 1494 (see Table 2.2). Error bars indicate ± one standard deviation. *One replicate did not produce any methane and is not included in the data shown here.

2.4.3 Experiment 3: 10 g sand, 5 mL medium

There were n = 4 tubes each for the Original Set, Transfer Set 1, and Transfer Set 2 for cultures of *M. formicicum*. For *M. formicicum*, methane production was nearly negligible (< 1% headspace) for the four tubes within the Original Set after the initial incubation period of 18 days at 4 °C followed by 7 days at 37 °C (Fig. 2.9). In Transfer Set 1, after 55 days' incubation at 37 °C, three cultures measured 20-26% methane while one measured ~6% methane, resulting in

the large error bar for the data shown for Transfer Set 1 (Fig. 2.4). In Transfer Set 2, the four cultures produced varied amounts of methane ranging between 2-13% (Fig. 2.9).

For *M. wolfeii*, three cultures produced an average of ~28% methane following the initial incubation period of 18 days at 4 °C followed by 7 days at 55 °C. In Transfer Set 1 for *M. wolfeii*, the three cultures failed to produce methane following inoculation from the Original Set following 55 days at 37 °C. After an additional 14 days at 55 °C, methane production resumed ranging between 4% and 19% for the three replicate, resulting in a large error bar seen in Figure 2.10. In Transfer Set 2, of the five cultures for *M. wolfeii*, two produced 22-25% methane after the initial incubation period (17 days at 55 °C), while the other three produced 6-11% methane, resulting in a large error bar for this set as shown in Figure 2.10.

It is important to note that the freeze/thaw cycling for Transfer Set 2 for both *M. wolfeii* and *M. formicicum* were not identical (Tables 2.3, 2.4). The reason for the difference was to allow additional time for *M. wolfeii* cultures to grow, should they be able, after methane production was not seen following the initial incubation period of 55 days at 37 °C for this set.

Replicates within Transfer Set 3 were used to determine if any cells survived freeze/thaw cycling followed by ~3 years at -80 °C. No cultures of either *M. formicicum* or *M. wolfeii* displayed methane production after 28 days' incubation (Figs. 2.9, 2.10).

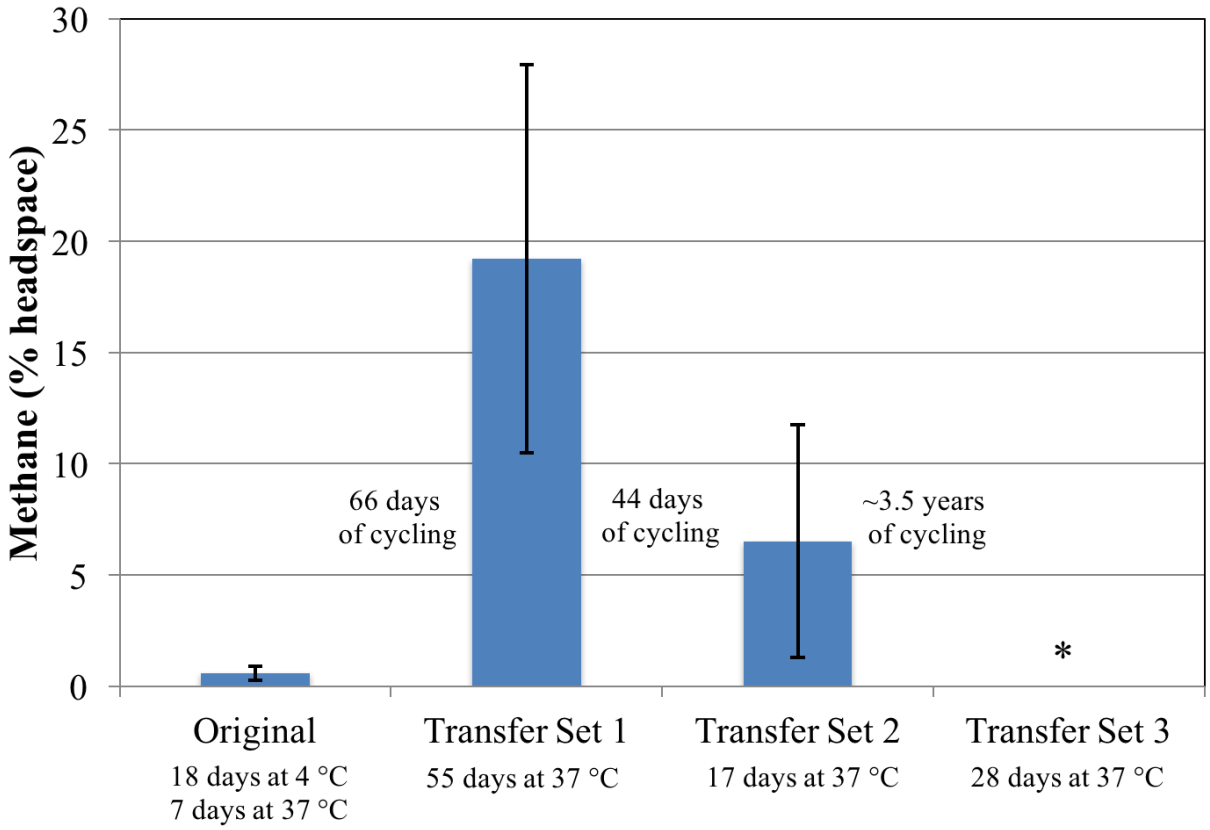

Figure 2.9 Methane production by *Methanobacterium formicicum* following initial incubation period for each of three sets. Test tubes contain 10 g sand and 5 mL MSF medium. Transfer Set 1 tubes (n = 4) were inoculated from one tube in the Original Set (n = 4) following 91 days of freeze/thaw cycles (see Table 2.3). Transfer Set 2 tubes (n = 4) were inoculated from three separate test tubes from Transfer Set 1 following 99 days of freeze/thaw cycles (see Table 2.3). Transfer Set 3 tubes (n = 4) were inoculated from the corresponding tube in Transfer Set 2 after 1474 days of freeze/thaw cycles (see Table 2.3). Error bars indicate ± one standard deviation.

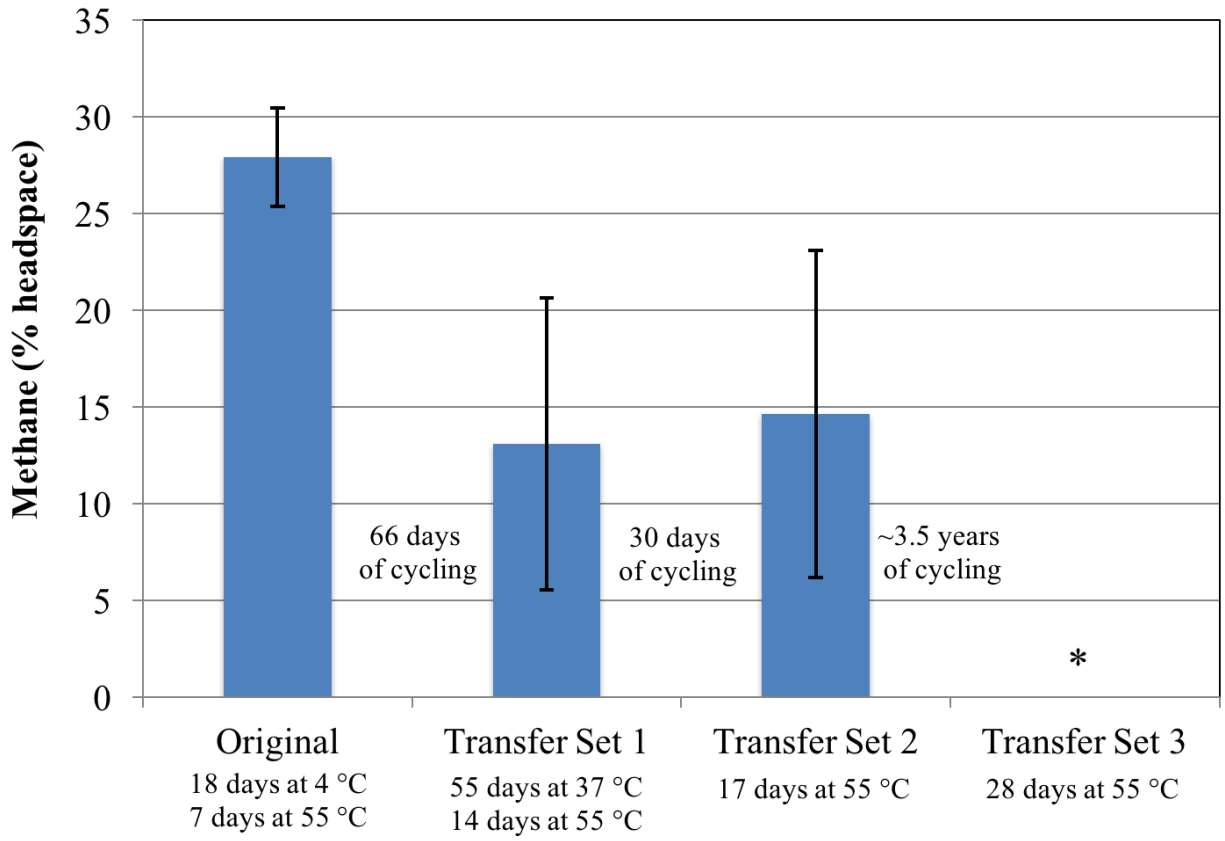

Figure 2.10 Methane production by *Methanothermobacter wolfeii* following initial incubation period for each of three sets. Test tubes contain 10 g sand and 5 mL MM medium. Transfer Set 1 tubes (n = 3) were inoculated from two separate test tubes in the Original Set (n = 3) following 91 days of freeze/thaw cycles (see Table 2.4). Transfer Set 2 tubes (n = 5) were inoculated from two separate test tubes from Transfer Set 1 following 99 days of freeze/thaw cycles (see Table 2.4). Transfer Set 3 tubes (n = 5) were inoculated from the corresponding tube in Transfer Set 2 after 1474 days of freeze/thaw cycles (see Table 2.4). Error bars indicate ± one standard deviation.

2.4.4 Experiment 4: 5 mL medium

This experiment aimed to assess survival under long-term freeze/thaw conditions. Tubes were subjected to 126 days of freeze/thaw cycles, then stored at -80 °C. After ~3 years at -80 °C and transfer to fresh media, two out of five cultures of *M. wolfeii* showed appreciable methane production (12.8%, 31.0% headspace) after 14 days' incubation at 55 °C. The methane abundance within these two cultures increased with another 14 days' incubation at 55 °C (28.5%,

33.6% methane, respectively), with a third culture producing ~7% methane (Fig. 2.11). The two remaining replicates showed no methane production after 28 days and are not included in the data shown in Fig. 2.11. No methane was produced by cultures of *M. formicicum* after 28 days' incubation at 37 °C (Fig. 12).

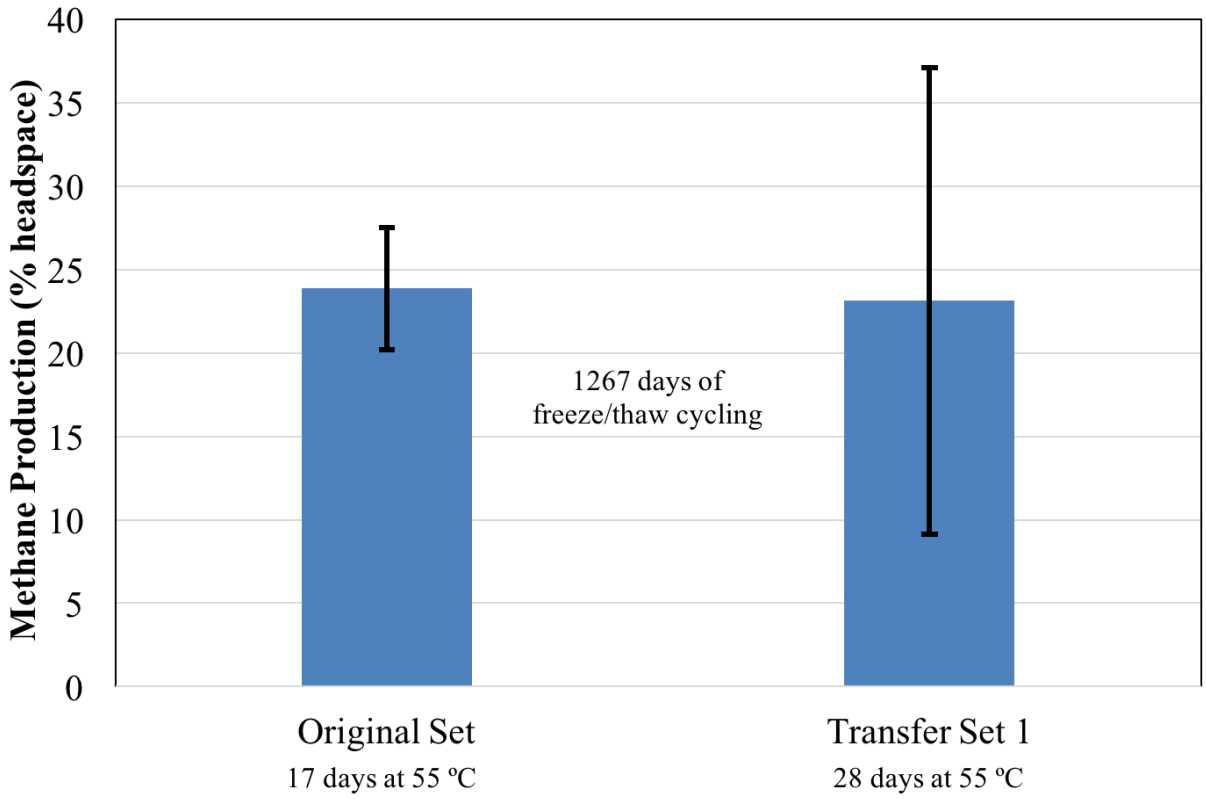

Figure 2.11 Methane production by *Methanothermobacter wolfeii* following initial incubation period for each of two sets. Original Set test tubes contained 5 mL MM medium. Transfer Set 1 test tubes contained 10 mL MM medium. Transfer Set 1 tubes (n = 5*) were inoculated from the corresponding replicate in the Original Set (n = 5) following 1284 days of freeze/thaw cycles (see Table 2.5). Error bars indicate ± one standard deviation. *Two of five replicates within Transfer Set 1 failed to produce methane after 28 days' incubation and are not included in the data shown here.

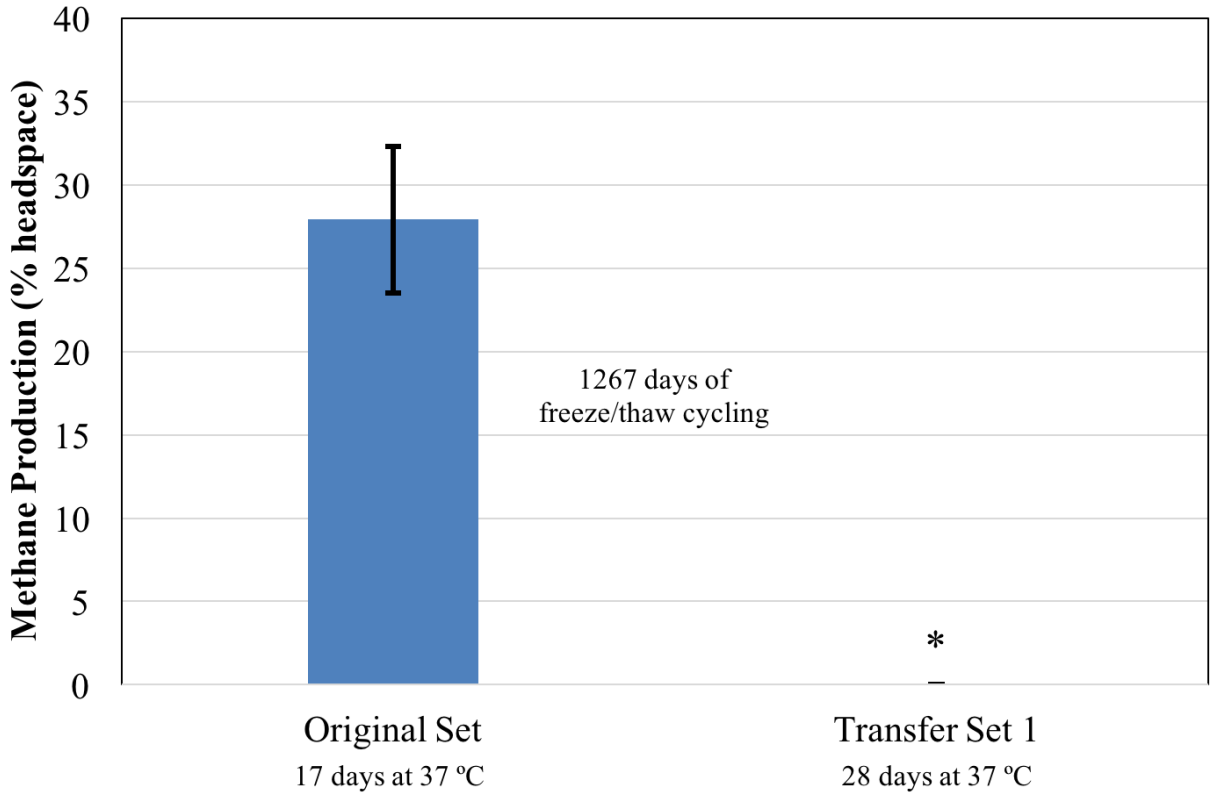

Figure 2.12 Methane production by Methanobacterium formicicum following initial incubation period for each of two sets. Original Set test tubes contained 5 mL MSF medium. Transfer Set 1 test tubes contained 10 mL MSF medium. Transfer Set 1 tubes (n = 5) were inoculated from the corresponding replicate in the Original Set (n = 5) following 1284 days of freeze/thaw cycles (see Table 2.5). Error bars indicate ± one standard deviation.

2.4.5 Experiments 5, 6: 24-h, 48-h Cycles

Three of the four methanogen species (except *M. maripaludis*) survived both the diurnal and 48-h temperature cycles (Figs. 2.13-2.18). For both experiments, some tubes "exploded" during the cycling period and were excluded from additional growth monitoring.

For *M. wolfeii*, one of the replicates in the 24-h experiment "exploded" after Day 3 and thus, this tube was not included in any of the data shown here (n = 3). Following the freeze/thaw cycling, after being placed back at their incubation temperatures (55 °C), 24-h cultures of *M. wolfeii* resumed active methane production as evidenced by the increase in methane between

days 10 and 16 (Fig. 2.13). Of all the methanogens tested, *M. wolfeii* has the highest incubation temperature (55 °C); interestingly, this species produced much greater amounts of methane following the 24-h cycling period (~33% headspace) as compared to the initial methane produced during pre-cycling incubation period (~9% headspace, Fig. 2.13).

The 48-h cultures of *M. wolfeii* also demonstrated increased methane production following the freeze/thaw cycling (Fig. 2.14), but results among replicates were more varied and not as large as the methane produced by the 24-h cultures. Another interesting aspect of the *M. wolfeii* cultures was the increase in optical density during the freeze/thaw cycling for both the 24-h and 48-h replicates (Figs. 2.13, 2.14). Generally, optical density increases in accordance with methane production. However, the optical density did not continue to increase during the post-cycling incubation period when methane production rose, suggesting that optical density and methane production are uncoupled in this scenario. The initial increase in optical density during the freeze/thaw cycling could be the result of physical alteration to the cells.

Methane production by *M. formicicum* rose very slightly during incubation after 24-h and 48-h freeze/thaw cycling, as compared to pre-cycling abundances (Figs. 2.15, 2.16). For *M. formicicum*, two of the four replicates in the 24-h experiment became contaminated with oxygen after the initial 11-day incubation period and they are not included in the data (n = 2). In terms of optical density, one of the three replicates of *M. formicicum* for the 48-h experiment measured negative optical density values for the last two data points (Day 15, Day 22), and so for these two points, the optical density is the average of only two replicates (Fig. 2.16). Similar to the cultures of *M. wolfeii*, cultures of *M. formicicum* did not display optical density values in accordance with increasing methane production. Cultures in both the 24-h and 48-h experiments experienced a significant decline in optical density following exposure to the freeze/thaw cycles during the

post-cycling incubation period, while methane abundance rose slightly (Figs. 2.15, 2.16). The increase in optical density during the 24-h freeze/thaw cycling (Fig. 2.15) also suggests that the changes in optical density are independent from methane production in these cultures.

Average methane production within cultures of *M. barkeri* increased during the incubation period following the 24-h and 48-h freeze/thaw cycling (Figs. 2.17, 2.18), with individual replicates experiencing increases in methane production and others experiencing decreases over the same time period. Cultures demonstrated extensive variation in optical density especially during the post-cycling incubation period for the 24-h experiment (Fig. 2.17). In the 48-h experiment, cultures of *M. barkeri* increased in optical density during the freeze/thaw cycling period (Fig. 2.18). Cells of *M. barkeri* often form irregular multicellular aggregates, especially under stressed conditions, which can cause large variations in optical density readings (Maestrojuán and Boone, 1991).

Survival of *M. maripaludis* following 24-h and 48-h freeze/thaw cycling remains unknown due to the explosion of test tubes during the experimental period. Methane production and optical density for these cultures were only measured following the initial 11-day incubation period before the replicates were subjected to the freeze/thaw cycling (data not shown). Experimental data can be found in Appendix A.

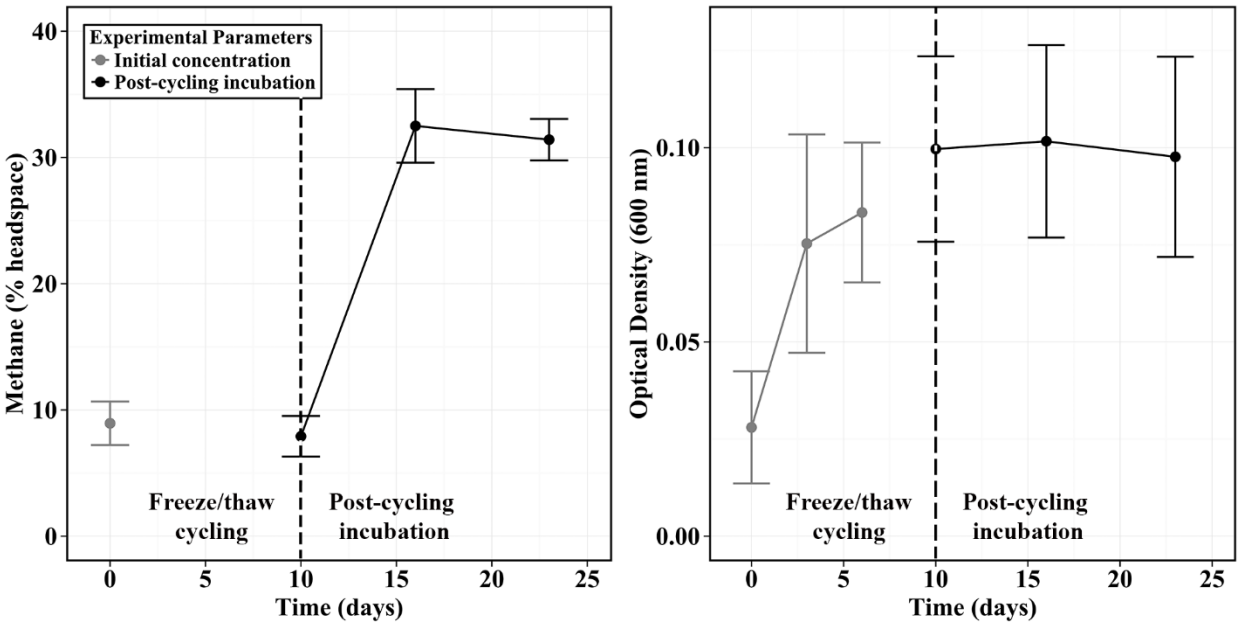

Figure 2.13 Methane production (% headspace; left panel) and optical density (OD_{600}; right panel) by *Methanothermobacter wolfeii* following an initial incubation period and exposure to 24-h (n = 3) temperature changes between -80 °C and 22 °C (see Table 2.6). The dashed black line separates the freeze/thaw cycling period (10 days, gray symbols) from the post-cycling incubation period (13 days, black symbols). Error bars indicate ± one standard deviation.

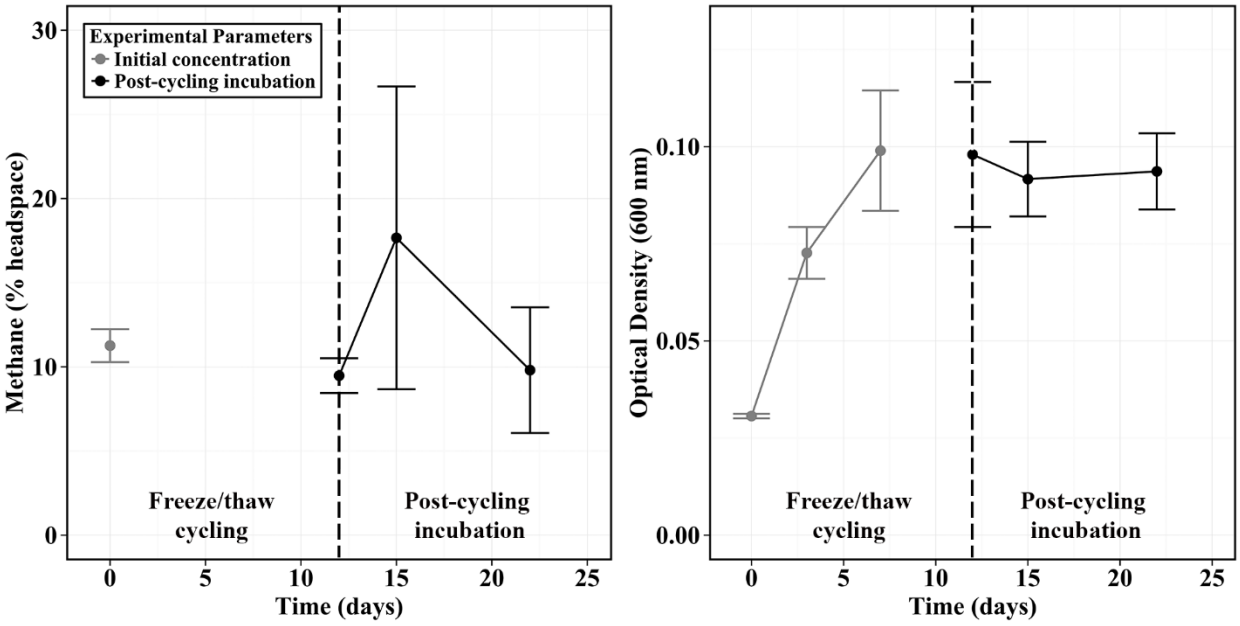

Figure 2.14 Methane production (% headspace; left panel) and optical density (OD_{600}; right panel) by *Methanothermobacter wolfeii* following an initial incubation period and exposure to 48-h (n = 3) temperature changes between -80 °C and 22 °C (see Table 2.6). The dashed black line separates the freeze/thaw cycling period (12 days, gray symbols) from the post-cycling incubation period (13 days, black symbols). Error bars indicate ± one standard deviation.

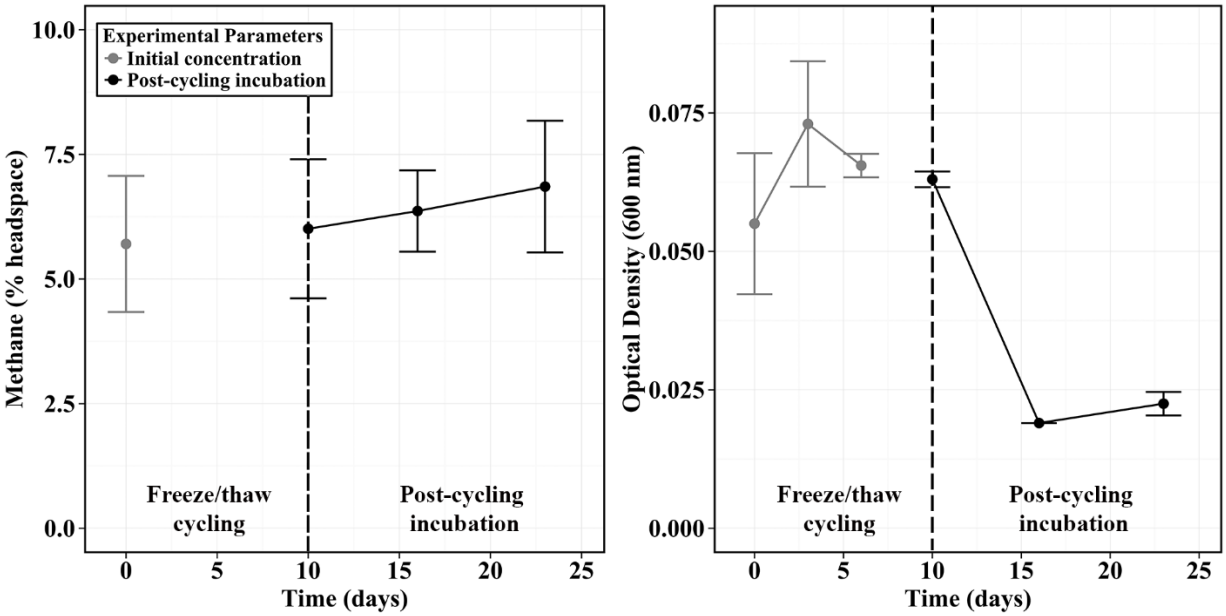

Figure 2.15 Methane production (% headspace; left panel) and optical density (OD_{600}; right panel) by *Methanobacterium formicicum* following an initial incubation period and exposure to 24-h (n = 2) temperature changes between -80 °C and 22 °C (see Table 2.6). The dashed black line separates the freeze/thaw cycling period (10 days, gray symbols) from the post-cycling incubation period (13 days, black symbols). Error bars indicate ± one standard deviation.

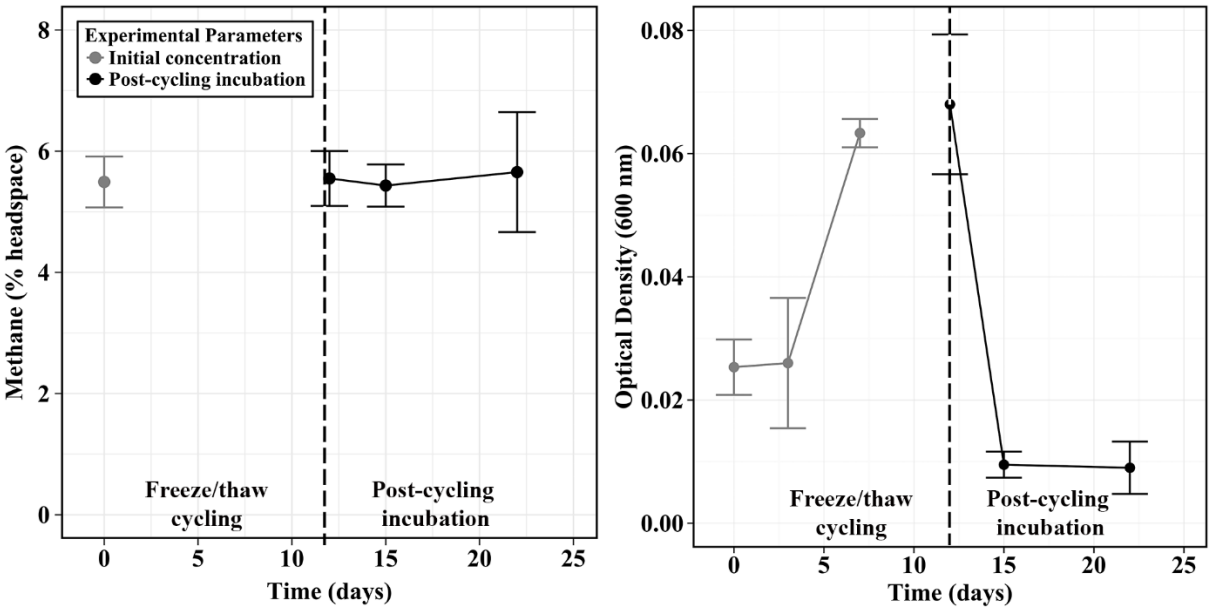

Figure 2.16 Methane production (% headspace; left panel) and optical density (OD_{600}; right panel) by *Methanobacterium formicicum* following an initial incubation period and exposure to 48-h (n = 3*) temperature changes between -80 °C and 22 °C (see Table 2.6). The dashed black line separates the freeze/thaw cycling period (12 days, gray symbols) from the post-cycling incubation period (10 days, black symbols). Error bars indicate ± one standard deviation. *The last two data points (Day 15, Day 22) consist of n = 2 replicates for the optical density measurements only.

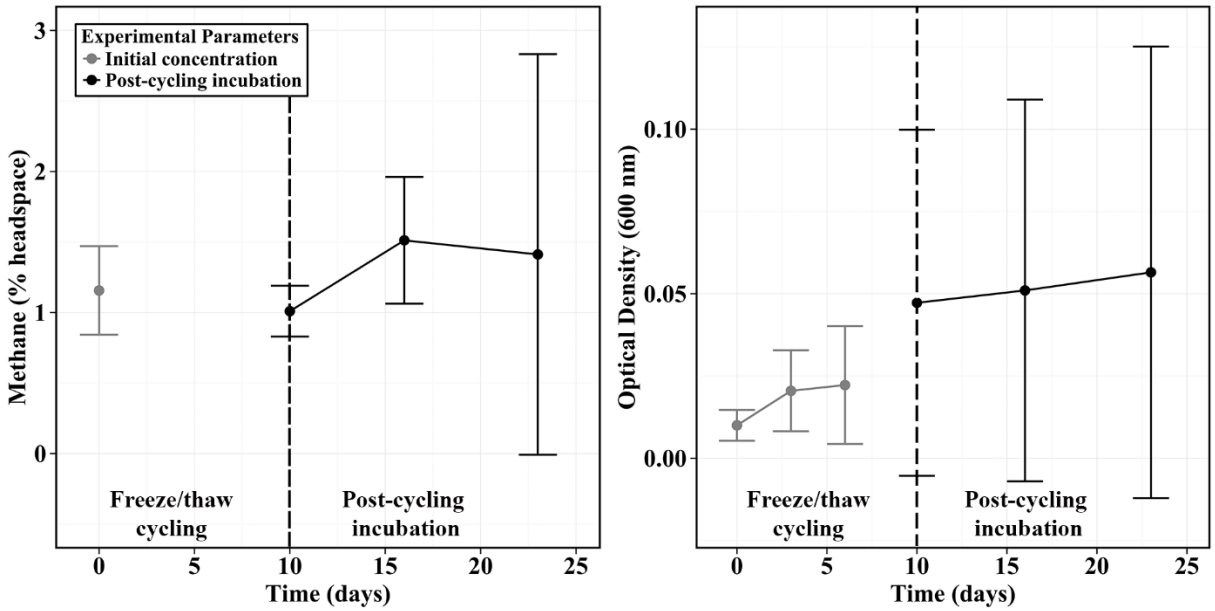

Figure 2.17 Methane production (% headspace; left panel) and optical density (OD_{600}; right panel) by *Methanosarcina barkeri* following an initial incubation period and exposure to 24-h (n = 4*) temperature changes between -80 °C and 22 °C (see Table 2.6). The dashed black line separates the freeze/thaw cycling period (10 days, gray symbols) from the post-cycling incubation period (13 days, black symbols). Error bars indicate ± one standard deviation. *The last two data points (Day 15, Day 22) consist of n = 2 replicates for the optical density measurements only.

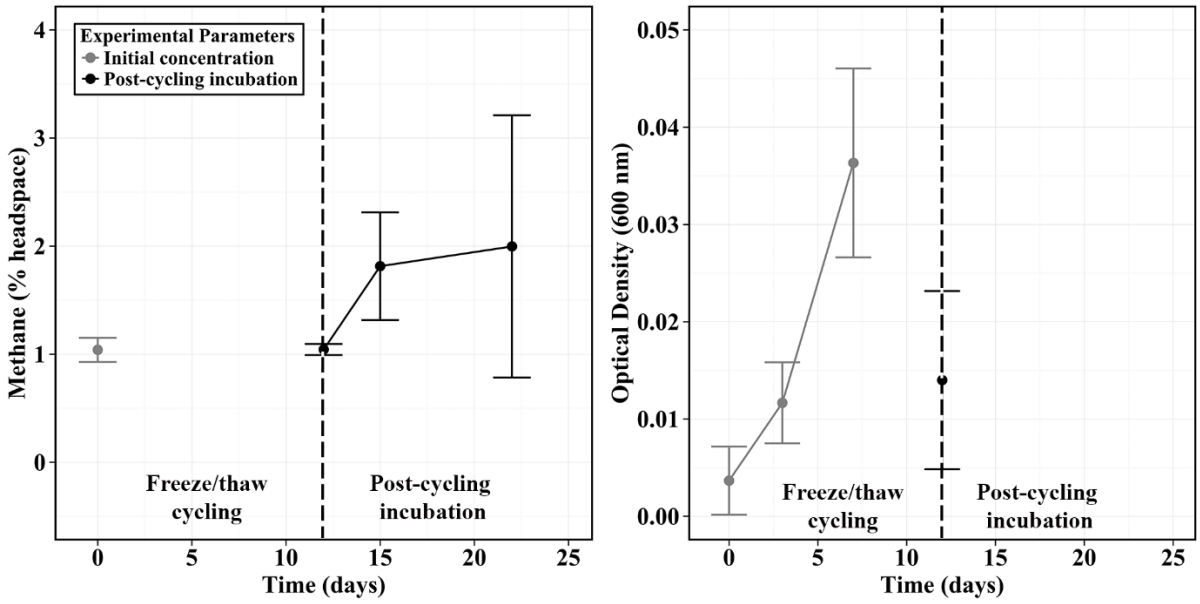

Figure 2.18 Methane production (% headspace; left panel) and optical density (OD_{600}; right panel) by *Methanosarcina barkeri* following an initial incubation period and exposure to 48-h (n = 3) temperature changes between -80 °C and 22 °C (see Table 2.6). The dashed black line separates the freeze/thaw cycling period (12 days, gray symbols) from the post-cycling incubation period (10 days, black symbols). Error bars indicate ± one standard deviation. Note: there is no optical density data past Day 12 for this experiment.

2.5 Discussion

Methane production was monitored over the freeze/thaw cycling period for each experiment, but active methanogenesis is difficult to demonstrate at low temperatures due to the slow rate of growth of the organisms and thus, low production values over long periods of time. Additionally, methane solubility, as well as the effects of temperature on the tightness of the stoppers and crimps within the test tubes may also play a role in altering true methane measurements. To elucidate the effect of freeze/thaw cycles on methane abundance within test tubes, a control study was performed. Anaerobic test tubes were filled with 10 mL deionized water and sealed with rubber stoppers and aluminum crimps. Tubes were injected with 10 mL CH_4 and three replicates were left at room temperature (22 °C) for 60 min, while another three replicates were stored at -15 °C for 60 min. Both sets of replicates were then subjected to freeze/thaw cycles between 22 °C and -15 °C for over two months. Methane measurements were recorded over time and demonstrate significant variability between cycles, although the general trend shows methane abundance decreasing over time (due to removal of headspace gas samples; Fig. 2.18). Thus, methane abundances during cycling were not displayed here.

Permafrost methanogen communities may be able to rapidly resume growth and metabolism when warmer temperatures are achieved (Blake et al., 2015). In experiments utilizing microcosms featuring permafrost soil, incubation at higher temperatures resulted in a shifted methanogenic community structure and increased methane production within ~24 hours (Blake et al., 2015). These results suggest that the production of methane could have resumed during periods of higher temperature in the cycling experiments conducted here. However, comparison between pure culture and microcosm experiments is difficult considering the various additional factors such as community member interaction and nutrient availability present in the

microcosms. Microcosms supplemented with H_2/CO_2 also exhibited greater rates of methane production than with addition of other substrates at all temperatures (Blake et al., 2015).

Methanogen diversity within permafrost is also seen to increase with increasing soil depth, likely due to the increasingly anaerobic conditions (Shcherbakova et al., 2016). This could have significance for Mars if methanogens were able to arise on the planet earlier in its' history, and have either gone extinct or still exist in the deep subsurface.

One interesting note concerning methanogenic communities in permafrost is the preference for hydrogenotrophic methanogenesis over acetoclastic methanogenesis in certain environments (Blake et al., 2015; Ganzert et al., 2007; Karaevskaya et al., 2014; Wagner et al., 2007; Wagner et al., 2005). For example, in a permafrost core from the Siberian Arctic, methane production from samples incubated with H_2/CO_2 as substrates at subfreezing temperatures (-3 °C, -6 °C) was up to 3.5 times higher than samples supplemented with acetate (Wagner et al., 2007). In the experiments described here, all methanogens were pressurized with hydrogen as an energy source. Ganzert et al. (2007) also discovered that methanogenic permafrost communities transition from mesophilic organisms to psychrotolerant or psychrophilic organisms with increasing soil depth. As the temperatures are much colder on Mars, it may be possible that any life on the planet has had the ability to adapt to more extreme temperatures.

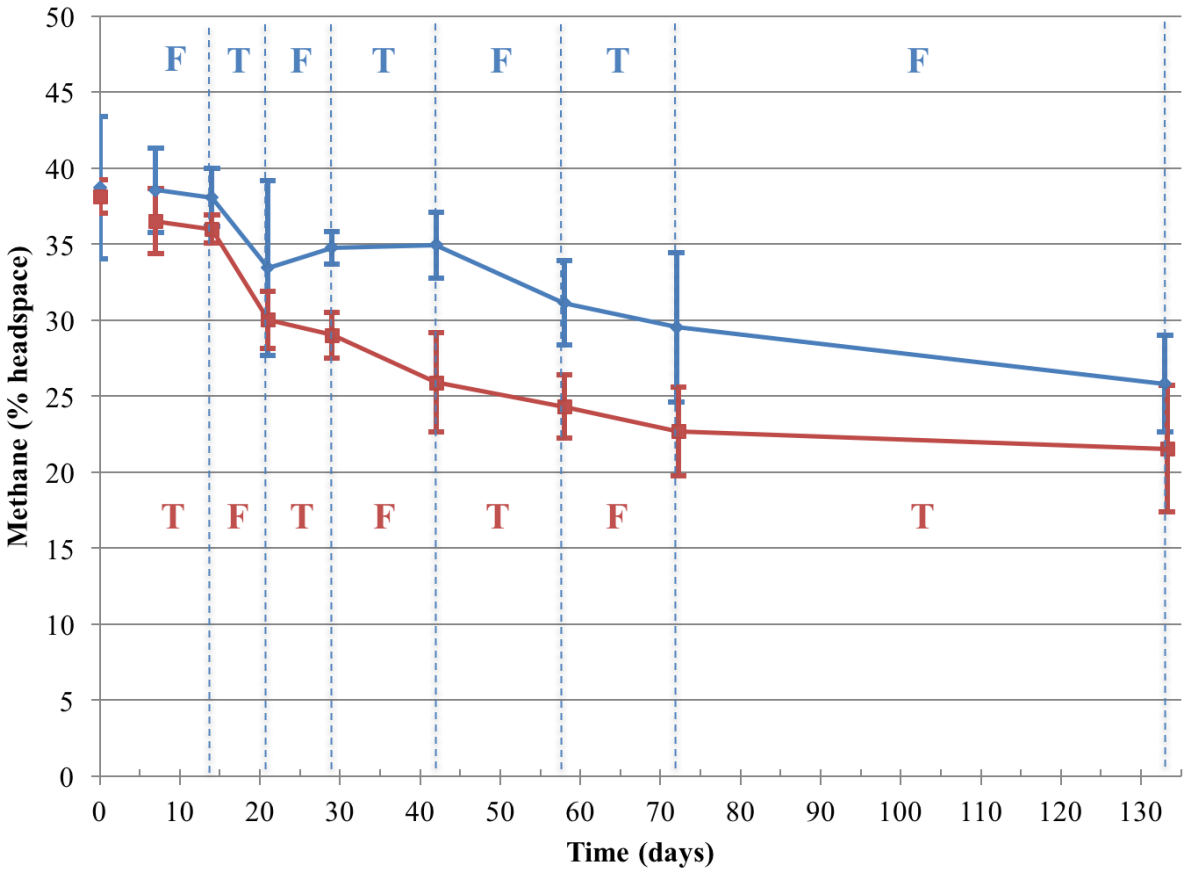

Figure 2.19 Control study showing variation in methane abundance within replicates subjected to alternating freeze/thaw cycles. Tubes contain 10 mL water and were injected with 100% methane gas. Blue symbols and red symbols refer to two separate groups (n = 3) which were subjected to opposite cycles. Freezes (F) occurred at -15 °C, thawing (T) occurred at 22 °C. Error bars indicate ± one standard deviation.

2.5.1 Experiment 1: Growth at 4 °C and 22 °C

These data provide a comparison for the subsequent freeze/thaw cycle data. No growth was possible at 4 °C after 140 days for any of the four methanogens, and thus, methane production (cell growth) could not occur during the brief exposures to 4 °C during the subsequent freeze/thaw cycling experiments. Growth was possible at room temperature (22 °C) for three of the four methanogens (*M. barkeri*, *M. formicicum*, *M. maripaludis*), although growth rates varied (Fig. 2.1). As such, the subsequent freeze/thaw cycling experiments constitute

survival experiments, although the return of active metabolism (methane production, growth) may be possible during brief exposures to 22 °C or higher. Growth at 22 °C was not possible for *M. wolfeii*, a thermophile, with the highest optimum growth temperature tested here. When initially isolated, cultures of *M. wolfeii* did not display growth below 37 °C with optimal growth occurring between 55-65 °C (Winter et al., 1984). The optimum temperature for growth for *M. formicicum* is 37 °C, but certain strains are capable of growth down to 20-25 °C (Battumur et al., 2016). The optimum growth temperature for *M. barkeri* is also 37 °C, but this organism is capable of growth using a variety of substrates and also appears to grow over a wide temperature range (Maestrojuán and Boone, 1991; Westermann et al., 1989). A recent study showed that a methanol-adapted strain, *M. barkeri* DSMZ 800^T, was capable of growth at 15 °C, but that growth was severely limited with solely H_2 and CO_2 as substrates (Gunnigle et al., 2013). Additionally, the optical density for the cultures grown at 15 °C on H_2/CO_2 did not correlate with methane production (Gunnigle et al., 2013). Gunnigle et al. (2013) discovered that optical density best correlated with methane production when cells were grown on H_2/CO_2 plus methanol or methanol alone and at 37 °C. Cells that were grown on purely H_2/CO_2 at 37 °C displayed a general correlation between optical density and methane production, but cultures grown on H_2/CO_2 plus methanol or methanol alone at 15 °C showed a delay of about 20 days in methane production, compared to the increases in optical density, whereas this lag was much greater for cultures grown solely on H_2/CO_2 (Gunnigle et al., 2013). Additionally, although it is not a psychrophilic methanogen, a recent metagenomic analysis of Alaskan permafrost soils discovered that *M. barkeri* was the dominant species within thawed samples (Coolen and Orsi, 2015). Further, Wagner et al. (2007) detected significant amounts of *Methanosarcina* spp. phospholipid etherlipids within upper Late Holocene ice sediments. This correlates with the

isolation of unique *Methanosarcina* spp. with demonstrated tolerance to extreme conditions (Morozova and Wagner, 2007). The authors suggest that the ability of *Methanosarcina* spp. to form multicellular aggregates assists in their ability to withstand environmental stresses, compared with other methanogens (Wagner et al., 2007). *Methanosarcina* spp. have also been detected as the dominant species within a methane-poor region of an Antarctic permafrost marine deposit (Karaevskaya et al., 2014). The dominance of a mesophilic methanogen in a permafrost setting supports the freeze/thaw experiments conducted here with non-psychrophilic methanogens.

Cultures of *M. maripaludis* are capable of growth between 18-47 °C, with optimum growth displayed between 35-39 °C (Jones et al., 1983). However, based on the organisms' relatively high optical density and methane production, we culture *M. maripaludis* at room temperature (~22 °C), which allows us to incorporate relatively lower temperatures (compared to 37 °C and 55 °C) into our experiments.

Psychrotolerant methanogens exist in pure culture that can actively grow at temperatures down to 1 °C (Franzmann et al., 1992; Schirmack et al., 2014b; Simankova et al., 2003; Simankova et al., 2001; Wagner et al., 2013), but most isolated species have maximum growth temperatures above 23 °C [see Table 7; (Chong et al., 2002; Kotelnikova et al., 1998; Krivushin et al., 2010; Rivkina et al., 2007; Shcherbakova et al., 2011; Shimizu et al., 2015; Shlimon et al., 2004; von Klein et al., 2002)]. Two exceptions are *Methanogenium frigidum*, which grows maximally at 15 °C with a doubling time of 2.9 days (Franzmann et al., 1997) and *Methanolobus psychrophilus*, with an optimum temperature of 18 °C (Zhang et al., 2008). At low temperatures, the growth rates of both psychrophilic and psychrotolerant species are exceptionally slow such that experiments with these organisms are not conducive to student research timeframes.

Additionally, other psychrophilic methanogens, such as *Methanococcoides burtonii*, isolated from Ace Lake in Antarctica, are capable of growth at low temperatures (e.g., 1.7 °C) only after growth is initiated at higher temperature [20 °C] (Franzmann et al., 1992). Attempts to culture older stocks of *M. frigidum* at 4 °C using H_2/CO_2 with and without acetate were unsuccessful in this lab.

Table 2.7 Isolated psychrophilic and psychrotolerant methanogens.

Methanogen	Growth Range	Optimum Temperature	Reference
Methanogenium frigidum	0[a] - 17 °C	15 °C	Franzmann et al. (1997)
Methanolobus psychrophilus	0 - 25 °C	18 °C	Zhang et al. (2008)
Methanococcoides alaskense			Singh et al. (2005)
Strain AK-4	-2.3[b] - 28.4 °C	21 °C	
Strain AK-5	-2.3[b] - 30.6 °C	23.6 °C	
Strain AK-9	-10.7[b] - 30.1 °C	26 °C	
Methanococcoides burtonii	-2.5[c] - 29 °C	23 °C	Franzmann et al. (1992)
Methanosarcina lacustris	1 - 35 °C	25 °C	Simankova et al. (2001)
Methanosarcina baltica	4 – 27 °C	25 °C	von Klein et al. (2002)
Methanogenium marinum	5 - 25 °C	25 °C	Chong et al. (2002)
Methanosarcina soligelidi	0 - 54 °C	28 °C	Wagner et al. (2013)
Methanobacterium veterum	10 - 46 °C	28 °C	Krivushin et al. (2010)
Methanobacterium movilense	0 - 44 °C	33 °C	Schirmack et al. (2014b)
Methanosarcina subterranea	10 - 40 °C	35 °C	Shimizu et al. (2015)
Methanobacterium arcticum	15 - 45 °C	37 °C	Shcherbakova et al. (2011)
Methanobacterium subterraneum	3.6 - 45 °C	20 - 40 °C	Kotelnikova et al. (1998)
Methanobacterium aarhusense	5 - 48 °C	45 °C	Shlimon et al. (2004)
Strain *MM*	1 - 32 °C	25 °C	Simankova et al. (2003)
Strain *MS*	1 - 32 °C	25 °C	Simankova et al. (2003)
Strain *MSP*	5 - 35 °C	25 °C	Simankova et al. (2003)

(continued)

Table 2.7 Isolated psychrophilic and psychrotolerant methanogens (continued).

Methanogen	Growth Range	Optimum Temperature	Reference
Strain *ZB*	1 - 38 °C	30 °C	Simankova et al. (2003)
Strain *MT*	5 - 40 °C	35 °C	Simankova et al. (2003)
Strain JL01	10 - 37 °C	24 - 28 °C	Rivkina et al. (2007)
Strain MK4	10 - 45 °C	28 °C	Rivkina et al. (2007)
Strain M2	15 - 45 °C	37 °C	Rivkina et al. (2007)

[a]Growth is possible until medium freezes (Franzmann et al., 1997).
[b]Based on the Ratkowsky model (Ratkowsky et al., 1983; Singh et al., 2005).
[c]The Ratkowsky model suggests the T_{min} for this species is -2.54 °C, however, cultures incubated at 1.7 °C or 3.2 °C were not capable of growth unless growth was first initiated at 20 °C (Franzmann et al., 1992).

2.5.2 Experiment 2: 5 g sand, 10 mL medium, Experiment 3: 10 g sand, 5 mL medium, Experiment 4: 5 mL medium

Sand was utilized in Experiments 2 and 3 to mimic a near-subsurface environment. Experiments 2, 3 and 4 utilized a mesophile, *M. formicicum*, and a thermophile, *M. wolfeii*. As evidenced by Experiment 1, growth was not expected at 4 °C nor 22 °C for *M. wolfeii*. Growth was not expected at 4 °C for *M. formicicum*, but was possible at room temperature (22 °C, Fig. 2.1). Thus, the freeze/thaw cycling for Experiments 2 and 3 constitute survival experiments for two non-psychrophilic methanogen species subjected to temperatures between 37 or 55 °C and -80 °C (Tables 2.2-2.4). The production of methane within transfer tubes indicates that cells of both *M. formicicum* (Figs. 2.2, 2.4) and *M. wolfeii* (Figs. 2.3, 2.5) were able to tolerate freeze/thaw cycling and resume active metabolism (methane production) once appropriate temperatures were reached. These studies did not include cell counts and so the specific percentage of survival from the original inoculum is unknown. It also may not be possible to

directly compare the amount of methane produced by each set (Original, Transfer 1, Transfer 2, Transfer 3; Figs. 2.2-2.5) based on possible differences in inoculum size (i.e., the exact number of cells contained within 0.5 mL culture that served as inoculum). However, the main point remains that a certain percentage of cells of both *M. formicicum* and *M. wolfeii* were able to tolerate the length and extent of freeze/thaw cycles and could resume metabolism at warmer temperatures in fresh media.

These experiments also included long-term survival, with tubes exposed to freeze/thaw cycles, then stored at -80 °C for over three years (see Tables 2.2-2.5). In Experiment 2, after transfer to fresh media and 14 days' incubation at their respective growth temperatures, four out of five replicates of *M. wolfeii* demonstrated high methane production (~30% headspace). This is surprising given the extent of freeze/thaw cycling and the classification of the organism as a thermophile. Replicates of *M. formicicum* subjected to the same conditions failed to produce appreciable methane (>1%) after 14 days' incubation at 37 °C. In Experiment 3, one replicate of *M. wolfeii* produced 0.70% methane, but all the remaining replicates, as well as the five replicates for *M. formicicum,* failed to produce any methane. Methane production for cultures of *M. wolfeii* in Experiment 4 was more varied with one replicate measuring 12.8% methane, another replicate measuring 31.0% methane and three replicates measuring 0% methane after 14 days' incubation at 55 °C. Cultures of *M. formicicum* in Expt. 4 failed to produce any methane following incubation. There are a couple possible explanations for this: 1. There were no surviving cells within those cultures, or 2. The cells are subject to as significant lag phase and methane production may be delayed. In a study using *M. barkeri*, Gunnigle et al. (2013) noticed that growth was much slower at 15 °C compared to 37 °C, and that H_2/CO_2 as substrates produced the lowest optical density and methane measurements, compared to methanol as a

substrate. However, the strain of *M. barkeri* used was previously adapted for use of methanol as a substrate and that may account for the poor performance of the organism under H_2/CO_2 conditions (Gunnigle et al., 2013).

The reasons for the increased survival of *M. wolfeii* cells under extreme cold temperatures, as compared to the other three methanogens tested here, remain unknown. Enhanced survival may be attributable to the presence of DEAD-box RNA helicases, which are believed to function as cold stress proteins within other methanogenic species including the psychrotolerant *Methanococcoides burtonii* (Lim et al., 2000), the psychrophile *Methanolobus psychrophilus* (Chen et al., 2012), and the hyperthermophile *Methanococcus jannaschii* (Boonyaratanakornkit et al., 2005). Shimada et al. (2009) suggest that DEAD-box RNA helicases allow hyperthermophilic archaea the ability to adapt to lower temperatures. This is evidenced by the presence of these genes within *Thermococcus kodakaraensis*, which typically grows at lower temperatures (optimum growth temperature range for genus *Thermococcus*: 75-95 °C) than the hyperthermophiles within the closely-related genus *Pyrococcus* (optimum growth temperature range: 95-103 °C), which lack any orthologs (Fukui et al., 2005; Shimada et al., 2009). However, extensive additional research would be required to confirm both the presence and expression of these proteins in *M. wolfeii*. Ding et al. (2008) have also demonstrated the up-regulation of a protein disulfide isomerase within *Methanothermobacter thermoautotrophicus* ΔH during growth at temperatures below optimal (50 °C, optimal: 65 °C) and after cold shock at 4 °C. Ultimately, additional experiments are required to assess the true nature of cold-tolerance in *M. wolfeii*.

2.5.3 Experiments 5, 6: 24-h and 48-h Cycles

Experiments 5 and 6 aimed to more closely replicate the daily temperature changes on Mars and consisted of 24-hr cycling (Expt. 5) and 48-hr cycling (Expt. 6) between 22 °C and -80 °C. These experiments monitored optical density over the course of the cycling in order to assess the growth potential or morphological alterations to the cells due to the freeze/thaw process. Although optical density didn't mirror methane production, this is not unusual for methanogens in pure culture [see 2.5.1 Experiment 1, above] (Gunnigle et al., 2013; Maestrojuán and Boone, 1991). Although results are varied, these experiments demonstrate that martian diurnal freeze/thaw cycles are not necessarily lethal to non-psychrophilic methanogens. Most replicates for each of three species (*M. barkeri*, *M. wolfeii*, *M. formicicum*) demonstrated an increase in either methane or optical density over the course of the experiment, though these two growth proxies were not necessarily correlated. Also, the variation between replicates of the same species under identical conditions, as has been noted previously (Maestrojuán and Boone, 1991), can hinder analysis. Ultimately, direct cell counts may shed more light on the true extent of survival within each replicate. However, direct cell counts are also difficult for *Methanosarcina* spp., which tend to form multicellular aggregates, especially under extreme conditions (Maestrojuán and Boone, 1991).

2.6 Conclusions

Non-psychrophilic methanogens are capable of survival during extreme weekly and daily temperature changes, similar to those on Mars. Variation was seen for both optical density and methane production for identical replicates of each species, but this is not uncommon for pure methanogenic cultures. The survival of non-psychrophilic methanogens under extreme

freeze/thaw cycles, as well as their anaerobic and non-photosynthetic nature and their ability to use simple substrates such as H_2 and CO_2 for energy and carbon sources, respectively, makes them ideal candidates for extinct or extant life on Mars. The prevalence of methanogenic communities in arctic regions on Earth and the existence of permafrost on Mars and the evidence for relatively recent freeze/thaw episodes on the planet suggests that these locations may form habitable environments on Mars. Future work will attempt to explore methanogen growth and survivability under additional martian conditions. These experiments will include combinations of temperature and pressure in order to better simulate current environments on Mars.

2.7 Acknowledgements

R. L. Mickol was supported by NASA Astrobiology: Exobiology and Evolutionary Biology Program, #NNX12AD90G. Y. Takagi was funded through NSF Grant No. 1157002.

2.8 References

Battumur, U., Yoon, Y.-M., Kim, C.-H. (2016) Isolation and Characterization of a New *Methanobacterium formicicum* KOR-1 from an Anaerobic Digester Using Pig Slurry. *Asian-Australasian Journal of Animal Sciences* 29, 586-593.

Blake, L.I., Tveit, A., Øvreås, L., Head, I.M., Gray, N.D. (2015) Response of methanogens in Arctic sediments to temperature and methanogenic substrate availability. *PLoS ONE* 10, e0129733.

Boone, D.R., Johnson, R.L., Liu, Y. (1989) Diffusion of the interspecies electron carriers H_2 and formate in methanogenic ecosystems and its implications in the measurement of K_m for H_2 or formate uptake. *Applied and Environmental Microbiology* 55, 1735-1741.

Boonyaratanakornkit, B.B., Simpson, A.J., Whitehead, T.A., Fraser, C.M., El- Sayed, N.M.A., Clark, D.S. (2005) Transcriptional profiling of the hyperthermophilic methanarchaeon *Methanococcus jannaschii* in response to lethal heat and non- lethal cold shock. *Environmental Microbiology* 7, 789-797.

Chen, Z., Yu, H., Li, L., Hu, S., Dong, X. (2012) The genome and transcriptome of a newly described psychrophilic archaeon, *Methanolobus psychrophilus* R15, reveal its cold adaptive characteristics. *Environmental Microbiology Reports* 4, 633-641.

Chong, S.C., Liu, Y., Cummins, M., Valentine, D.L., Boone, D.R. (2002) *Methanogenium marinum* sp. nov., a H_2-using methanogen from Skan Bay, Alaska, and kinetics of H_2 utilization. *Antonie van Leeuwenhoek* 81, 263-270.

Christensen, P.R., Bandfield, J.L., Bell III, J.F., Gorelick, N., Hamilton, V.E., Ivanov, A., Jakosky, B.M., Kieffer, H.H., Lane, M.D., Malin, M.C., McConnochie, T., McEwen, A.S., McSween Jr., H.Y., Mehall, G.L., Moersch, J.E., Nealson, K.H., Rice Jr., J.W., Richardson, M.I., Ruff, S.W., Smith, M.D., Titus, T.N., Wyatt, M.B. (2003) Morphology and composition of the surface of Mars: Mars Odyssey THEMIS results. *Science* 300, 2056-2061.

Christensen, P.R., Bandfield, J.L., Hamilton, V.E., Ruff, S.W., Kieffer, H.H., Titus, T.N., Malin, M.C., Morris, R.V., Lane, M.D., Clark, R.L., Jakosky, B.M., Mellon, M.T., Pearl, J.C., Conrath, B.J., Smith, M.D., Clancy, R.T., Kuzmin, R.O., Roush, T., Mehall, G.L., Gorelick, N., Bender, K., Murray, K., Dason, S., Greene, E., Silverman, S., Greenfield, M. (2001) Mars Global Surveyor Thermal Emission Spectrometer experiment: investigation description and surface science results. *Journal of Geophysical Research: Planets* 106, 23823-23871.

Clarke, A. (2014) The thermal limits to life on Earth. *International Journal of Astrobiology* 13, 141-154.

Connolly, B.M., Orrock, J.L. (2015) Climatic variation and seed persistence: freeze–thaw cycles lower survival via the joint action of abiotic stress and fungal pathogens. *Oecologia* 179, 609-616.

Coolen, M.J.L., Orsi, W.D. (2015) The transcriptional response of microbial communities in thawing Alaskan permafrost soils. *Frontiers in Microbiology* 6, 197.

Ding, X., Lv, Z.-M., Zhao, Y., Min, H., Yang, W.-J. (2008) MTH1745, a protein disulfide isomerase-like protein from thermophilic archaea, *Methanothermobacter thermoautotrophicum* involving in stress response. *Cell Stress and Chaperones* 13, 239-246.

Feng, X., Nielsen, L.L., Simpson, M.J. (2007) Responses of soil organic matter and microorganisms to freeze–thaw cycles. *Soil Biology and Biochemistry* 39, 2027-2037.

Fonti, S., Marzo, G.A. (2010) Mapping the methane on Mars. *Astronomy and Astrophysics* 512.

Formisano, V., Atreya, S., Encrenaz, T., Ignatiev, N., Giuranna, M. (2004) Detection of methane in the atmosphere of Mars. *Science* 306, 1758-1761.

Franzmann, P.D., Liu, Y., Balkwill, D.L., Aldrich, H.C., De Macario, E.C., Boone, D.R. (1997) *Methanogenium frigidum* sp. nov., a psychrophilic, H_2-using methanogen from Ace Lake, Antarctica. *International Journal of Systematic Bacteriology* 47, 1068-1072.

Franzmann, P.D., Springer, N., Ludwig, W., De Macario, E.C., Rohde, M. (1992) A methanogenic archaeon from Ace Lake, Antarctica: *Methanococcoides burtonii* sp. nov. *Systematic and Applied Microbiology* 15, 573-581.

Freppaz, M., Williams, B.L., Edwards, A.C., Scalenghe, R., Zanini, E. (2007) Simulating soil freeze/thaw cycles typical of winter alpine conditions: implications for N and P availability. *Applied Soil Ecology* 35, 247-255.

Fukui, T., Atomi, H., Kanai, T., Matsumi, R., Fujiwara, S., Imanaka, T. (2005) Complete genome sequence of the hyperthermophilic archaeon *Thermococcus kodakaraensis* KOD1 and comparison with *Pyrococcus* genomes. *Genome Research* 15, 352-363.

Ganzert, L., Jurgens, G., Münster, U., Wagner, D. (2007) Methanogenic communities in permafrost-affected soils of the Laptev Sea coast, Siberian Arctic, characterized by 16S rRNA gene fingerprints. *FEMS Microbiology Ecology* 59, 476-488.

Geminale, A., Formisano, V., Giuranna, M. (2008) Methane in Martian atmosphere: average spatial, diurnal, and seasonal behaviour. *Planetary and Space Science* 56, 1194-1203.

Geminale, A., Formisano, V., Sindoni, G. (2011) Mapping methane in Martian atmosphere with PFS-MEX data. *Planetary and Space Science* 59, 137-148.

Gilichinsky, D.A., Wilson, G.S., Friedmann, E.I., McKay, C.P., Sletten, R.S., Rivkina, E.M., Vishnivetskaya, T.A., Erokhina, L.G., Ivanushkina, N.E., Kochkina, G.A., Shcherbakova, V.A., Soina, V.S., Spirina, E.V., Vorobyova, E.A., Fyodorov-Davydov, D.G., Hallet, B., Ozerskaya, S.M., Sorokovikov, V.A., Laurinavichyus, K.S., Shatilovich, A.V., Chanton, J.P., Ostroumov, V.E., Tiedje, J.M. (2007) Microbial populations in Antarctic permafrost: biodiversity, state, age, and implication for astrobiology. *Astrobiology* 7, 275-311.

Gunnigle, E., McCay, P., Fuszard, M., Botting, C.H., Abram, F., O'Flaherty, V. (2013) A functional approach to uncover the low-temperature adaptation strategies of the archaeon *Methanosarcina barkeri*. *Applied and Environmental Microbiology* 79, 4210-4219.

Henry, H.A.L. (2007) Soil freeze–thaw cycle experiments: Trends, methodological weaknesses and suggested improvements. *Soil Biology and Biochemistry* 39, 977-986.

Joly, M., Amato, P., Sancelme, M., Vinatier, V., Abrantes, M., Deguillaume, L., Delort, A.-M. (2015) Survival of microbial isolates from clouds toward simulated atmospheric stress factors. *Atmospheric Environment* 117, 92-98.

Jones, W.J., Paynter, M.J.B., Gupta, R. (1983) Characterization of *Methanococcus maripaludis* sp. nov., a new methanogen isolated from salt marsh sediment. *Archives of Microbiology* 135, 91-97.

Karaevskaya, E.S., Demchenko, L.S., Demidov, N.E., Rivkina, E.M., Bulat, S.A., Gilichinsky, D.A. (2014) Archaeal diversity in permafrost deposits of Bunger Hills Oasis and King George Island (Antarctica) according to the 16S rRNA gene sequencing. *Microbiology* 83, 398-406.

Kendrick, M.G., Kral, T.A. (2006) Survival of methanogens during desiccation: implications for life on Mars. *Astrobiology* 6, 546-551.

Kieffer, H.H., Martin, T.Z., Peterfreund, A.R., Jakosky, B.M., Miner, E.D., Palluconi, F.D. (1977) Thermal and albedo mapping of Mars during the Viking primary mission. *Journal of Geophysical Research* 82, 4249-4291.

Kobabe, S., Wagner, D., Pfeiffer, E.-M. (2004) Characterisation of microbial community composition of a Siberian tundra soil by fluorescence in situ hybridisation. *FEMS Microbiology Ecology* 50, 13-23.

Koch, K., Knoblauch, C., Wagner, D. (2009) Methanogenic community composition and anaerobic carbon turnover in submarine permafrost sediments of the Siberian Laptev Sea. *Environmental Microbiology* 11, 657-668.

Koponen, H.T., Jaakkola, T., Keinänen-Toivola, M.M., Kaipainen, S., Tuomainen, J., Servomaa, K., Martikainen, P.J. (2006) Microbial communities, biomass, and activities in soils as affected by freeze thaw cycles. *Soil Biology and Biochemistry* 38, 1861-1871.

Kotelnikova, S., Macario, A.J.L., Pedersen, K. (1998) *Methanobacterium subterraneum* sp. nov., a new alkaliphilic, eurythermic and halotolerant methanogen isolated from deep granitic groundwater. *International Journal of Systematic Bacteriology* 48, 357-367.

Krasnopolsky, V.A., Bjoraker, G.L., Mumma, M.J., Jennings, D.E. (1997) High-resolution spectroscopy of Mars at 3.7 and 8 μm: A sensitive search for H_2O_2, H_2CO, HCl, and CH_4, and detection of HDO. *Journal of Geophysical Research* 102, 6525-6534.

Krasnopolsky, V.A., Maillard, J.P., Owen, T.C. (2004) Detection of methane in the martian atmosphere: evidence for life? *Icarus* 172, 537-547.

Krivushin, K.V., Shcherbakova, V.A., Petrovskaya, L.E., Rivkina, E.M. (2010) *Methanobacterium veterum* sp. nov., from ancient Siberian permafrost. *International Journal of Systematic and Evolutionary Microbiology* 60, 455-459.

Kumar, N., Grogan, P., Chu, H., Christiansen, C.T., Walker, V.K. (2013) The effect of freeze-thaw conditions on arctic soil bacterial communities. *Biology* 2, 356-377.

Larsen, K.S., Jonasson, S., Michelsen, A. (2002) Repeated freeze–thaw cycles and their effects on biological processes in two arctic ecosystem types. *Applied Soil Ecology* 21, 187-195.

Liebner, S., Ganzert, L., Kiss, A., Yang, S., Wagner, D., Svenning, M.M. (2015) Shifts in methanogenic community composition and methane fluxes along the degradation of discontinuous permafrost. *Frontiers in Microbiology* 6, 356.

Lim, J., Thomas, T., Cavicchioli, R. (2000) Low temperature regulated DEAD-box RNA helicase from the Antarctic archaeon, *Methanococcoides burtonii*. *Journal of Molecular Biology* 297, 553-567.

Lu, Z., Du, R., Du, P., Qin, S., Liang, Z., Li, Z., Wang, Y., Wang, Y. (2015) Influences of Land Use/Cover Types on Nitrous Oxide Emissions during Freeze-Thaw Periods from Waterlogged Soils in Inner Mongolia. *PLoS ONE* 10, e0139316.

Maestrojuán, G.M., Boone, D.R. (1991) Characterization of *Methanosarcina barkeri* MS^T and 227, *Methanosarcina mazei* S-6^T, and *Methanosarcina vacuolata* Z-761^T. *International Journal of Systematic Bacteriology* 41, 267-274.

Maguire, W.C. (1977) Martian isotopic ratios and upper limits for possible minor constituents as derived from Mariner 9 infrared spectrometer data. *Icarus* 32, 85-97.

Mellon, M.T., Boynton, W.V., Feldman, W.C., Arvidson, R.E., Titus, T.N., Bandfield, J.L., Putzig, N.E., Sizemore, H.G. (2008) A prelanding assessment of the ice table depth and ground ice characteristics in Martian permafrost at the Phoenix landing site. *Journal of Geophysical Research* 113, E00A25.

Mellon, M.T., Feldman, W.C., Prettyman, T.H. (2004) The presence and stability of ground ice in the southern hemisphere of Mars. *Icarus* 169, 324-340.

Mellon, M.T., Phillips, R.J. (2001) Recent gullies on Mars and the source of liquid water. *Journal of Geophysical Research* 106, 23165-23179.

Morozova, D., Möhlmann, D., Wagner, D. (2007) Survival of Methanogenic Archaea from Siberian Permafrost under Simulated Martian Thermal Conditions. *Origins of Life and Evolution of Biospheres* 37, 189-200.

Morozova, D., Wagner, D. (2007) Stress response of methanogenic archaea from Siberian permafrost compared with methanogens from nonpermafrost habitats. *FEMS Microbiology Ecology* 61, 16-25.

Mumma, M.J., Villanueva, G.L., Novak, R.E., Hewagama, T., Bonev, B.P., DiSanti, M.A., Mandell, A.M., Smith, M.D. (2009) Strong release of methane on Mars in northern summer 2003. *Science* 323, 1041-1045.

Ni, S., Boone, D.R. (1991) Isolation and characterization of a dimethyl sulfide-degrading methanogen, *Methanolobus siciliae* HI350, from an oil well, characterization of *M. siciliae* T4/M^T, and emendation of *M. siciliae*. *International Journal of Systematic Bacteriology* 41, 410-416.

Page, D.P. (2007) Recent low-latitude freeze–thaw on Mars. *Icarus* 189, 83-117.

Price, P.B., Sowers, T. (2004) Temperature dependence of metabolic rates for microbial growth, maintenance, and survival. *Proceedings of the National Academy of Sciences of the United States of America* 101, 4631-4636.

Ratkowsky, D.A., Lowry, R.K., McMeekin, T.A., Stokes, A.N., Chandler, R.E. (1983) Model for bacterial culture growth rate throughout the entire biokinetic temperature range. *Journal of Bacteriology* 154, 1222-1226.

Rivkina, E., Laurinavichius, K., McGrath, J., Tiedje, J., Shcherbakova, V., Gilichinsky, D. (2004) Microbial life in permafrost. *Advances in Space Research* 33, 1215-1221.

Rivkina, E., Shcherbakova, V., Laurinavichius, K., Petrovskaya, L., Krivushin, K., Kraev, G., Pecheritsina, S., Gilichinsky, D. (2007) Biogeochemistry of methane and methanogenic archaea in permafrost. *FEMS Microbiology Ecology* 61, 1-15.

Rivkina, E.M., Friedmann, E.I., McKay, C.P., Gilichinsky, D.A. (2000) Metabolic activity of permafrost bacteria below the freezing point. *Applied and Environmental Microbiology* 66, 3230-3233.

Sawicka, J.E., Robador, A., Hubert, C., Jørgensen, B.B., Brüchert, V. (2010) Effects of freeze–thaw cycles on anaerobic microbial processes in an Arctic intertidal mud flat. *The ISME Journal* 4, 585-594.

Schirmack, J., Böhm, M., Brauer, C., Löhmannsröben, H.-G., de Vera, J.-P., Möhlmann, D., Wagner, D. (2014a) Laser spectroscopic real time measurements of methanogenic activity under simulated Martian subsurface analog conditions. *Planetary and Space Science* 98, 198-204.

Schirmack, J., Mangelsdorf, K., Ganzert, L., Sand, W., Hillebrand-Voiculescu, A., Wagner, D. (2014b) *Methanobacterium movilense* sp. nov., a hydrogenotrophic, secondary-alcohol-utilizing methanogen from the anoxic sediment of a subsurface lake. *International Journal of Systematic and Evolutionary Microbiology* 64, 522-527.

Shcherbakova, V., Rivkina, E., Pecheritsyna, S., Laurinavichius, K., Suzina, N., Gilichinsky, D. (2011) *Methanobacterium arcticum* sp. nov., a methanogenic archaeon from Holocene Arctic permafrost. *International Journal of Systematic and Evolutionary Microbiology* 61, 144-147.

Shcherbakova, V., Yoshimura, Y., Ryzhmanova, Y., Taguchi, Y., Segawa, T., Oshurkova, V., Rivkina, E. (2016) Archaeal communities of Arctic methane-containing permafrost. *FEMS Microbiology Ecology* 92, fiw135.

Shimada, Y., Fukuda, W., Akada, Y., Ishida, M., Nakayama, J., Imanaka, T., Fujiwara, S. (2009) Property of cold inducible DEAD-box RNA helicase in hyperthermophilic archaea. *Biochemical and Biophysical Research Communications* 389, 622-627.

Shimizu, S., Ueno, A., Naganuma, T., Kaneko, K. (2015) *Methanosarcina subterranea* sp. nov., a methanogenic archaeon isolated from a deep subsurface diatomaceous shale formation. *International Journal of Systematic and Evolutionary Microbiology* 65, 1167-1171.

Shlimon, A.G., Friedrich, M.W., Niemann, H., Ramsing, N.B., Finster, K. (2004) *Methanobacterium aarhusense* sp. nov., a novel methanogen isolated from a marine

sediment (Aarhus Bay, Denmark). *International Journal of Systematic and Evolutionary Microbiology* 54, 759-763.

Simankova, M.V., Kotsyurbenko, O.R., Lueders, T., Nozhevnikova, A.N., Wagner, B., Conrad, R., Friedrich, M.W. (2003) Isolation and characterization of new strains of methanogens from cold terrestrial habitats. *Systematic and Applied Microbiology* 26, 312-318.

Simankova, M.V., Parshina, S.N., Tourova, T.P., Kolganova, T.V., Zehnder, A.J.B., Nozhevnikova, A.N. (2001) *Methanosarcina lacustris* sp. nov., a new psychrotolerant methanogenic archaeon from anoxic lake sediments. *Systematic and Applied Microbiology* 24, 362-367.

Singh, N., Kendall, M.M., Liu, Y., Boone, D.R. (2005) Isolation and characterization of methylotrophic methanogens from anoxic marine sediments in Skan Bay, Alaska: description of *Methanococcoides alaskense* sp. nov., and emended description of *Methanosarcina baltica*. *International Journal of Systematic and Evolutionary Microbiology* 55, 2531-2538.

Steven, B., Niederberger, T.D., Whyte, L.G. (2009) Bacterial and Archaeal Diversity in Permafrost, In: Margesin, R. (Ed.), Permafrost Soils. Springer-Verlag, pp. 59-72.

Tung, H.C., Bramall, N.E., Price, P.B. (2005) Microbial origin of excess methane in glacial ice and implications for life on Mars. *Proceedings of the National Academy of Sciences of the United States of America* 102, 18292-18296.

Tung, H.C., Price, P.B., Bramall, N.E., Vrdoljak, G. (2006) Microorganisms metabolizing on clay grains in 3-km-deep Greenland basal ice. *Astrobiology* 6, 69-86.

Ulrich, M., Wagner, D., Hauber, E., de Vera, J.-P., Schirrmeister, L. (2012) Habitable periglacial landscapes in martian mid-latitudes. *Icarus* 219, 345-357.

von Klein, D., Arab, H., Völker, H., Thomm, M. (2002) *Methanosarcina baltica*, sp. nov., a novel methanogen isolated from the Gotland Deep of the Baltic Sea. *Extremophiles* 6, 103-110.

Wagner, D. (2008) Microbial Communities and Processes in Arctic Permafrost Environments, In: Dion, P., Nautiyal, C.S. (Eds.), Microbiology of Extreme Soils. Springer Berlin, pp. 133-154.

Wagner, D., Gattinger, A., Embacher, A., Pfeiffer, E.-M., Schloter, M., Lipski, A. (2007) Methanogenic activity and biomass in Holocene permafrost deposits of the Lena Delta, Siberian Arctic and its implication for the global methane budget. *Global Change Biology* 13, 1089-1099.

Wagner, D., Lipski, A., Embacher, A., Gattinger, A. (2005) Methane fluxes in permafrost habitats of the Lena Delta: effects of microbial community structure and organic matter quality. *Environmental Microbiology* 7, 1582-1592.

Wagner, D., Schirmack, J., Ganzert, L., Morozova, D., Mangelsdorf, K. (2013) *Methanosarcina soligelidi* sp. nov., a desiccation- and freeze-thaw-resistant methanogenic archaeon from a Siberian permafrost-affected soil. *International Journal of Systematic and Evolutionary Microbiology* 63, 2986-2991.

Wagner, D., Spieck, E., Bock, E., Pfeiffer, E.-M. (2002) Microbial Life in Terrestrial Permafrost: Methanogenesis and Nitrification in Gelisols as Potentials for Exobiological Process, In: Horneck, G., Baumstark-Khan, C. (Eds.), Astrobiology: The Quest for the Conditions of Life. Springer Berlin, pp. 143-159.

Webster, C.R., Mahaffy, P.R., Atreya, S.K., Flesch, G.J., Mischna, M.A., Meslin, P.-Y., Farley, K.A., Conrad, P.G., Christensen, L.E., Pavlov, A.A., Martín-Torres, J., Zorzano, M.-P., McConnochie, T.H., Owen, T., Eigenbrode, J.L., Glavin, D.P., Steele, A., Malespin, C.A., Archer Jr., P.D., Sutter, B., Coll, P., Freissinet, C., McKay, C.P., Moores, J.E., Schwenzer, S.P., Bridges, J.C., Navarro-Gonzalez, R., Gellert, R., Lemmon, M.T., the MSL Science Team (2015) Mars methane detection and variability at Gale crater. *Science* 347, 415-417.

Westermann, P., Ahring, B.K., Mah, R.A. (1989) Temperature compensation in *Methanosarcina barkeri* by modulation of hydrogen and acetate affinity. *Applied and Environmental Microbiology* 55, 1262-1266.

Winter, J., Lerp, C., Zabel, H.-P., Wildenauer, F.X., König, H., Schindler, F. (1984) *Methanobacterium wolfei*, sp. nov., a new tungsten-requiring, thermophilic, autotrophic methanogen. *Systematic and Applied Microbiology* 5, 457-466.

Wipf, S., Sommerkorn, M., Stutter, M.I., Wubs, E.R.J., Van Der Wal, R. (2015) Snow cover, freeze‐thaw, and the retention of nutrients in an oceanic mountain ecosystem. *Ecosphere* 6, 1-16.

Xun, L., Boone, D.R., Mah, R.A. (1988) Control of the life cycle of *Methanosarcina mazei* S-6 by manipulation of growth conditions. *Applied and Environmental Microbiology* 54, 2064-2068.

Yergeau, E., Kowalchuk, G.A. (2008) Responses of Antarctic soil microbial communities and associated functions to temperature and freeze–thaw cycle frequency. *Environmental Microbiology* 10, 2223-2235.

Zhang, G., Jiang, N., Liu, X., Dong, X. (2008) Methanogenesis from methanol at low temperatures by a novel psychrophilic methanogen, "*Methanolobus psychrophilus*" sp. nov., prevalent in Zoige wetland of the Tibetan plateau. *Applied and Environmental Microbiology* 74, 6114-6120.

Zhang, T., Armstrong, R.L., Smith, J. (2003) Investigation of the near-surface soil freeze-thaw cycle in the contiguous United States: Algorithm development and validation. *Journal of Geophysical Research: Atmospheres* 10.

2.9 Appendix A: Experimental Data

2.9.1 Experiment 1: Growth at 4 ºC and 22 ºC

Table 2.8 Data for Experiment 1: Growth at 4 ºC and 22 ºC

Temperature[a]	Tube	Medium[b]	Day[c]	Methane[d]
22	1	MS	0	0
22	2	MS	0	0
22	3	MS	0	0
22	4	MS	0	0
22	5	MSH	0	0
22	6	MSH	0	0
22	7	MSH	0	0
22	8	MSH	0	0
22	9	MSF	0	0
22	10	MSF	0	0
22	11	MSF	0	0
22	12	MSF	0	0
22	13	MM	0	0
22	14	MM	0	0
22	15	MM	0	0
22	16	MM	0	0
22	1	MS	7	0
22	2	MS	7	0
22	3	MS	7	0
22	4	MS	7	0
22	5	MSH	7	0
22	6	MSH	7	0
22	7	MSH	7	0
22	8	MSH	7	0
22	9	MSF	7	0
22	10	MSF	7	0
22	11	MSF	7	0
22	12	MSF	7	0
22	13	MM	7	0
22	14	MM	7	0
22	15	MM	7	0
(continued)				

Temperature[a]	Tube	Medium[b]	Day[c]	Methane[d]
22	16	MM	7	0
22	1	MS	14	0.001979
22	2	MS	14	0.374185
22	3	MS	14	0.330864
22	4	MS	14	0.380043
22	5	MSH	14	2.589
22	6	MSH	14	1.907
22	7	MSH	14	4.2179
22	8	MSH	14	2.0817
22	9	MSF	14	2.1061
22	10	MSF	14	1.508
22	11	MSF	14	1.4791
22	12	MSF	14	1.5208
22	13	MM	14	0.095877
22	1	MS	21	0.7256
22	2	MS	21	0.572
22	3	MS	21	0.5303
22	4	MS	21	0.5902
22	5	MSH	21	10.9959
22	6	MSH	21	8.0618
22	7	MSH	21	18.8277
22	8	MSH	21	10.1188
22	9	MSF	21	3.6764
22	10	MSF	21	2.6077
22	11	MSF	21	3.5992
22	12	MSF	21	2.5413
22	13	MM	21	0.0093
22	14	MM	21	0
22	15	MM	21	0
22	16	MM	21	0
22	1	MS	35	1.8665
22	2	MS	35	1.3395
22	3	MS	35	1.0776
22	4	MS	35	1.573
22	5	MSH	35	23.6906
22	6	MSH	35	23.4954
22	7	MSH	35	24.1062
(continued)				

Temperature[a]	Tube	Medium[b]	Day[c]	Methane[d]
22	8	MSH	35	23.7482
22	9	MSF	35	7.0753
22	10	MSF	35	5.7373
22	11	MSF	35	5.7651
22	12	MSF	35	6.3542
22	13	MM	35	0
22	14	MM	35	0.0041
22	15	MM	35	0.0035
22	16	MM	35	0.0503
22	1	MS	49	3.1933
22	2	MS	49	2.2431
22	3	MS	49	1.8334
22	4	MS	49	2.5677
22	5	MSH	49	24.172
22	6	MSH	49	23.2331
22	7	MSH	49	23.3975
22	8	MSH	49	23.6171
22	9	MSF	49	12.9854
22	10	MSF	49	10.2332
22	11	MSF	49	10.8204
22	12	MSF	49	11.5089
22	13	MM	49	0.0394
22	14	MM	49	0.0371
22	15	MM	49	0.0393
22	16	MM	49	0.0362
22	1	MS	97	7.648
22	2	MS	97	4.9543
22	3	MS	97	4.9323
22	4	MS	97	7.0597
22	5	MSH	97	22.8886
22	6	MSH	97	21.6715
22	7	MSH	97	22.0483
22	8	MSH	97	21.4899
22	9	MSF	97	22.8135
22	10	MSF	97	26.1366
22	11	MSF	97	24.1818
22	12	MSF	97	23.9539
(continued)				

Temperature[a]	Tube	Medium[b]	Day[c]	Methane[d]
22	13	MM	97	0.1087
22	14	MM	97	0.0432
22	15	MM	97	0.052
22	16	MM	97	0.0549
22	1	MS	140	11.9112
22	2	MS	140	7.8972
22	3	MS	140	10.3079
22	4	MS	140	12.4878
22	5	MSH	140	21.4619
22	6	MSH	140	20.054
22	7	MSH	140	19.3987
22	8	MSH	140	19.3222
22	9	MSF	140	22.9106
22	10	MSF	140	24.214
22	11	MSF	140	21.7711
22	12	MSF	140	20.4315
22	13	MM	140	0.0845
22	14	MM	140	0.0529
22	15	MM	140	0.0046
22	16	MM	140	0
4	17	MS	0	0
4	18	MS	0	0
4	19	MS	0	0
4	20	MS	0	0
4	21	MSH	0	0
4	22	MSH	0	0
4	23	MSH	0	0
4	24	MSH	0	0
4	25	MSF	0	0
4	26	MSF	0	0
4	27	MSF	0	0
4	28	MSF	0	0
4	29	MM	0	0
4	30	MM	0	0
4	31	MM	0	0
4	32	MM	0	0
4	17	MS	7	0
(continued)				

Temperature[a]	Tube	Medium[b]	Day[c]	Methane[d]
4	18	MS	7	0
4	19	MS	7	0
4	20	MS	7	0
4	21	MSH	7	0
4	22	MSH	7	0.407
4	23	MSH	7	0
4	24	MSH	7	0
4	25	MSF	7	0
4	26	MSF	7	0
4	27	MSF	7	0
4	28	MSF	7	0.3452
4	29	MM	7	0
4	30	MM	7	0
4	31	MM	7	0
4	32	MM	7	0
4	17	MS	14	0.02575
4	18	MS	14	0.186
4	19	MS	14	0
4	20	MS	14	0.0407
4	21	MSH	14	0.0112
4	22	MSH	14	0.01456
4	23	MSH	14	0.015787
4	24	MSH	14	0.013419
4	25	MSF	14	0.01786
4	26	MSF	14	0.02214
4	27	MSF	14	0.02122
4	28	MSF	14	0.01924
4	29	MM	14	0.02234
4	30	MM	14	0.011396
4	31	MM	14	0.02954
4	32	MM	14	0.00592
4	17	MS	21	0.039
4	18	MS	21	0.036
4	19	MS	21	0.034
4	20	MS	21	0.0363
4	21	MSH	21	0.0342
4	22	MSH	21	0.0199
(continued)				

Temperature[a]	Tube	Medium[b]	Day[c]	Methane[d]
4	23	MSH	21	0.0183
4	24	MSH	21	0.0156
4	25	MSF	21	0
4	26	MSF	21	0.0226
4	27	MSF	21	0.0121
4	28	MSF	21	0.0162
4	29	MM	21	0.009
4	30	MM	21	0
4	31	MM	21	0.0274
4	32	MM	21	0.0103
4	17	MS	35	0.0306
4	18	MS	35	0.0414
4	19	MS	35	0.053
4	20	MS	35	0
4	21	MSH	35	0.0142
4	22	MSH	35	0.0155
4	23	MSH	35	0
4	24	MSH	35	0.0135
4	25	MSF	35	0.0432
4	26	MSF	35	0.0239
4	27	MSF	35	0.0154
4	28	MSF	35	0.0271
4	29	MM	35	0.0394
4	30	MM	35	0.0125
4	31	MM	35	0.0234
4	32	MM	35	0
4	17	MS	49	0.0593
4	18	MS	49	0.0454
4	19	MS	49	0.0607
4	20	MS	49	0.065
4	21	MSH	49	0.01
4	22	MSH	49	0.0085
4	23	MSH	49	0.0181
4	24	MSH	49	0.0143
4	25	MSF	49	0.0196
4	26	MSF	49	0.0247
4	27	MSF	49	0.022
(continued)				

Temperature[a]	Tube	Medium[b]	Day[c]	Methane[d]
4	28	MSF	49	0.0222
4	29	MM	49	0.0232
4	30	MM	49	0.0121
4	31	MM	49	0.0292
4	32	MM	49	0.0128
4	17	MS	97	0.3586
4	18	MS	97	0.0523
4	19	MS	97	0.0803
4	20	MS	97	0
4	21	MSH	97	0.0729
4	22	MSH	97	0.0094
4	23	MSH	97	0.0136
4	24	MSH	97	0.011
4	25	MSF	97	0.0114
4	26	MSF	97	0.0202
4	27	MSF	97	0
4	28	MSF	97	0.0146
4	30	MM	97	0.0088
4	31	MM	97	0
4	32	MM	97	0
4	17	MS	140	0.0808
4	18	MS	140	0
4	19	MS	140	0.0746
4	20	MS	140	0.0834
4	21	MSH	140	0
4	22	MSH	140	0.0074
4	23	MSH	140	0.0116
4	24	MSH	140	0
4	25	MSF	140	0.0139
4	26	MSF	140	0
4	27	MSF	140	0.0056
4	28	MSF	140	0
4	29	MM	140	0
4	30	MM	140	0
4	31	MM	140	0.0077
4	32	MM	140	0.0087

[a]Temperature refers to the temperature at which the cultures were incubated for the duration of the experiment.

[b]Medium corresponds to the specific medium (and organism) contained in each test tube. MM = *Methanothermobacter wolfeii*; MS = *Methanosarcina barkeri*; MSF = *Methanobacterium formicicum*; MSH = *Methanococcus maripaludis* (see 2.3.1 Microbial Procedures for specific media components).
[c]Day refers to the days elapsed since inoculation of the cultures.
[d]Methane is given in % headspace.

2.9.2 Experiment 2: 5 g sand, 10 mL medium

Table 2.9 Data for Experiment 2: 5 g sand, 10 mL medium

Set	Tube	Medium[a]	Days Since Inoculation	Cumulative Days[b]	Methane[c]
Original	2	MSF	0	0	0
Original	3	MSF	0	0	0
Original	4	MSF	0	0	0
Original	5	MSF	0	0	0
Original	7	MM	0	0	0
Original	8	MM	0	0	0
Original	9	MM	0	0	0
Original	10	MM	0	0	0
Original	2	MSF	5	5	3.0789
Original	3	MSF	5	5	3.1329
Original	4	MSF	5	5	2.9079
Original	5	MSF	5	5	2.4538
Original	7	MM	5	5	14.3488
Original	8	MM	5	5	39.6527
Original	9	MM	5	5	31.8195
Original	10	MM	5	5	40.0935
Original	2	MSF	14	14	21.8227
Original	3	MSF	14	14	41.9792
Original	4	MSF	14	14	33.0374
Original	5	MSF	14	14	24.9905
Original	7	MM	14	14	36.0931
Original	8	MM	14	14	38.2859
Original	9	MM	14	14	37.8306
Original	10	MM	14	14	39.8564
Transfer Set 1	11	MSF	7	112	0
Transfer Set 1	12	MSF	7	112	0.011
(continued)					

Set	Tube	Medium[a]	Days Since Inoculation	Cumulative Days[b]	Methane[c]
Transfer Set 1	13	MSF	7	112	0
Transfer Set 1	14	MSF	7	112	0
Transfer Set 1	15	MM	7	112	0
Transfer Set 1	16	MM	7	112	3.3177
Transfer Set 1	17	MM	7	112	4.8049
Transfer Set 1	18	MM	7	112	2.3424
Transfer Set 1	19	MM	7	112	3.4259
Transfer Set 1	11	MSF	22	127	26.0179
Transfer Set 1	12	MSF	22	127	32.7367
Transfer Set 1	13	MSF	22	127	33.6145
Transfer Set 1	14	MSF	22	127	32.8483
Transfer Set 1	15	MM	22	127	17.3794
Transfer Set 1	16	MM	22	127	27.7524
Transfer Set 1	17	MM	22	127	28.3215
Transfer Set 1	18	MM	22	127	23.7366
Transfer Set 1	19	MM	22	127	25.1286
Transfer Set 2	20	MSF	17	196	25.1346
Transfer Set 2	21	MSF	17	196	22.0187
Transfer Set 2	22	MSF	17	196	25.2432
Transfer Set 2	23	MSF	17	196	22.3083
Transfer Set 2	24	MM	17	196	21.3916
Transfer Set 2	25	MM	17	196	20.4197
Transfer Set 2	26	MM	17	196	24.4157
Transfer Set 2	27	MM	17	196	23.5051
Transfer Set 2	28	MM	17	196	19.1122
Transfer Set 3	29	MSF	14	1508	0
Transfer Set 3	30	MSF	14	1508	0
Transfer Set 3	31	MSF	14	1508	0
Transfer Set 3	33	MM	14	1508	30.5565
Transfer Set 3	34	MM	14	1508	33.1978
Transfer Set 3	35	MM	14	1508	30.4533
Transfer Set 3	36	MM	14	1508	0.0308
Transfer Set 3	37	MM	14	1508	30.6614
Transfer Set 3	29	MSF	28	1522	0
Transfer Set 3	30	MSF	28	1522	0
Transfer Set 3	31	MSF	28	1522	0
Transfer Set 3	32	MSF	28	1522	0
(continued)					

Set	Tube	Medium[a]	Days Since Inoculation	Cumulative Days[b]	Methane[c]
Transfer Set 3	33	MM	28	1522	30.1424
Transfer Set 3	34	MM	28	1522	32.5183
Transfer Set 3	35	MM	28	1522	31.6231
Transfer Set 3	36	MM	28	1522	0.5447
Transfer Set 3	37	MM	28	1522	27.6778

[a]Medium corresponds to the specific medium (and organism) contained in each test tube. MM = MSF = *Methanobacterium formicicum* (see 2.3.1 Microbial Procedures for specific media components).
[b]Cumulative Days refers to the days elapsed since the cultures within the Original Set were inoculated.
[c]Methane is given in % headspace.

2.9.3 Experiment 3: 10 g sand, 5 mL medium

Table 2.10 Data for Experiment 3: 10 g sand, 5 mL medium

Set	Tube	Medium[a]	Days Since Inoculation	Cumulative Days[b]	Methane[c]
Original	1	MSF	0	0	0
Original	2	MSF	0	0	0
Original	3	MSF	0	0	0
Original	4	MSF	0	0	0
Original	5	MM	0	0	0
Original	6	MM	0	0	0
Original	7	MM	0	0	0
Original	1	MSF	4	4	0
Original	2	MSF	4	4	0
Original	3	MSF	4	4	0
Original	4	MSF	4	4	0
Original	5	MM	4	4	0
Original	6	MM	4	4	0
Original	7	MM	4	4	0
Original	1	MSF	18	18	0
Original	2	MSF	18	18	0
Original	3	MSF	18	18	0
Original	4	MSF	18	18	0
Original	5	MM	18	18	0
Original	6	MM	18	18	0
(continued)					

Set	Tube	Medium[a]	Days Since Inoculation	Cumulative Days[b]	Methane[c]
Original	7	MM	18	18	0
Original	7	MM	18	18	0
Original	1	MSF	25	25	0.6105
Original	2	MSF	25	25	0.3671
Original	3	MSF	25	25	0.3255
Original	4	MSF	25	25	0.9917
Original	5	MM	25	25	26.2313
Original	6	MM	25	25	30.8385
Original	7	MM	25	25	26.6494
Transfer Set 1	8	MSF	19	110	0
Transfer Set 1	9	MSF	19	110	0
Transfer Set 1	10	MSF	19	110	0
Transfer Set 1	11	MSF	19	110	0.02674
Transfer Set 1	12	MM	19	110	0
Transfer Set 1	13	MM	19	110	0
Transfer Set 1	14	MM	19	110	0
Transfer Set 1	8	MSF	55	146	20.475
Transfer Set 1	9	MSF	55	146	6.6083
Transfer Set 1	10	MSF	55	146	23.3775
Transfer Set 1	11	MSF	55	146	26.3754
Transfer Set 1	12	MM	55	146	0
Transfer Set 1	13	MM	55	146	0
Transfer Set 1	14	MM	55	146	0
Transfer Set 1	12	MM	69	160	4.7119
Transfer Set 1	13	MM	69	160	15.0968
Transfer Set 1	14	MM	69	160	19.4291
Transfer Set 2	15	MSF	17	207	13.8088
Transfer Set 2	16	MSF	17	207	3.149
Transfer Set 2	17	MSF	17	207	2.3164
Transfer Set 2	18	MSF	17	207	6.7967
Transfer Set 2	19	MM	17	207	8.361
Transfer Set 2	20	MM	17	207	21.9208
Transfer Set 2	21	MM	17	207	10.8703
Transfer Set 2	22	MM	17	207	6.6087
Transfer Set 2	23	MM	17	207	25.3368
Transfer Set 3	24	MSF	14	1488	0
Transfer Set 3	25	MSF	14	1488	0
(continued)					

Set	Tube	Medium[a]	Days Since Inoculation	Cumulative Days[b]	Methane[c]
Transfer Set 3	26	MSF	14	1488	0
Transfer Set 3	27	MSF	14	1488	0
Transfer Set 3	29	MM	14	1488	0
Transfer Set 3	30	MM	14	1488	0
Transfer Set 3	31	MM	14	1488	0
Transfer Set 3	32	MM	14	1488	0
Transfer Set 3	24	MSF	28	1502	0
Transfer Set 3	25	MSF	28	1502	0
Transfer Set 3	26	MSF	28	1502	0
Transfer Set 3	27	MSF	28	1502	0
Transfer Set 3	28	MM	28	1502	0.015
Transfer Set 3	29	MM	28	1502	0
Transfer Set 3	30	MM	28	1502	0
Transfer Set 3	31	MM	28	1502	0
Transfer Set 3	32	MM	28	1502	0

[a]Medium corresponds to the specific medium (and organism) contained in each test tube. MM = *Methanothermobacter wolfeii*; MSF = *Methanobacterium formicicum* (see 2.3.1 Microbial Procedures for specific media components).
[b]Cumulative Days refers to the days elapsed since the cultures within the Original Set were inoculated.
[c]Methane is given in % headspace.

2.9.4 Experiment 4: 5 mL medium

Table 2.11 Data for Experiment 4: 5 mL medium

Set	Tube	Medium[a]	Days Since Inoculation	Cumulative Days[b]	Methane[c]
Original	1	MSF	0	0	0
Original	2	MSF	0	0	0
Original	3	MSF	0	0	0
Original	4	MSF	0	0	0
Original	5	MSF	0	0	0
Original	6	MM	0	0	0
Original	7	MM	0	0	0
Original	8	MM	0	0	0
Original	9	MM	0	0	0
Original	10	MM	0	0	0
(continued)					

Set	Tube	Medium[a]	Days Since Inoculation	Cumulative Days[b]	Methane[c]
Original	1	MSF	17	17	29.102
Original	2	MSF	17	17	22.3741
Original	3	MSF	17	17	32.2623
Original	4	MSF	17	17	24.2937
Original	5	MSF	17	17	31.4958
Original	6	MM	17	17	19.7713
Original	7	MM	17	17	20.4306
Original	8	MM	17	17	24.3714
Original	9	MM	17	17	27.4447
Original	10	MM	17	17	27.2843
Transfer Set 1	11	MSF	14	1298	0
Transfer Set 1	12	MSF	14	1298	0
Transfer Set 1	13	MSF	14	1298	0
Transfer Set 1	14	MSF	14	1298	0
Transfer Set 1	15	MSF	14	1298	0
Transfer Set 1	16	MM	14	1298	12.7903
Transfer Set 1	17	MM	14	1298	30.9841
Transfer Set 1	18	MM	14	1298	0
Transfer Set 1	19	MM	14	1298	0
Transfer Set 1	20	MM	14	1298	0
Transfer Set 1	11	MSF	28	1312	0
Transfer Set 1	12	MSF	28	1312	0
Transfer Set 1	13	MSF	28	1312	0
Transfer Set 1	14	MSF	28	1312	0
Transfer Set 1	15	MSF	28	1312	0
Transfer Set 1	16	MM	28	1312	28.5209
Transfer Set 1	17	MM	28	1312	33.5981
Transfer Set 1	18	MM	28	1312	7.2304
Transfer Set 1	19	MM	28	1312	0
Transfer Set 1	20	MM	28	1312	0

[a]Medium corresponds to the specific medium (and organism) contained in each test tube. MM = *Methanothermobacter wolfeii*; MSF = *Methanobacterium formicicum* (see 2.3.1 Microbial Procedures for specific media components).
[b]Cumulative Days refers to the days elapsed since the cultures within the Original Set were inoculated.
[c]Methane is given in % headspace.

2.9.5 Experiments 5, 6: 24-h, 48-h Cycles

Table 2.12 Data for Experiments 5, 6: 24-h, 48-h Cycles

Experiment	Tube	Medium[a]	Days Since Inoculation	Methane[b]	OD[c]
24-hr	1	MM	0	0	0
24-hr	2	MM	0	0	0
24-hr	3	MM	0	0	0
24-hr	4	MS	0	0	0
24-hr	5	MS	0	0	0
24-hr	6	MS	0	0	0
24-hr	7	MS	0	0	0
24-hr	8	MSF	0	0	0
24-hr	9	MSF	0	0	0
24-hr	10	MSH	0	0	0
24-hr	11	MSH	0	0	0
24-hr	12	MSH	0	0	0
24-hr	13	MSH	0	0	0
24-hr	1	MM	11	10.0408	0.044
24-hr	2	MM	11	6.9526	0.016
24-hr	3	MM	11	9.8315	0.024
24-hr	4	MS	11	1.6220	0.015
24-hr	5	MS	11	1.0674	0.004
24-hr	6	MS	11	0.9789	0.009
24-hr	7	MS	11	0.9570	0.012
24-hr	8	MSF	11	6.6688	0.064
24-hr	9	MSF	11	4.7389	0.046
24-hr	10	MSH	11	10.3536	0.076
24-hr	11	MSH	11	6.7792	0.026
24-hr	12	MSH	11	5.2840	0.058
24-hr	13	MSH	11	13.6610	0.110
24-hr	1	MM	14	9.1600	0.102
24-hr	2	MM	14	6.6075	0.046
24-hr	3	MM	14	9.2748	0.078
24-hr	4	MS	14	1.5832	0.021
24-hr	5	MS	14	0.8243	0.006
24-hr	6	MS	14	0.8093	0.019
(continued)					

Experiment	Tube	Medium[a]	Days Since Inoculation	Methane[b]	OD[c]
24-hr	7	MS	14	0.9348	0.036
24-hr	8	MSF	14	7.0572	0.081
24-hr	9	MSF	14	5.7132	0.065
24-hr	10	MSH	14	11.2530	0.004
24-hr	11	MSH	14	7.2320	0.017
24-hr	12	MSH	14	5.9905	0.006
24-hr	13	MSH	14	13.9535	0.037
24-hr	1	MM	17	9.0824	0.084
24-hr	2	MM	17	6.3168	0.101
24-hr	3	MM	17	8.8960	0.065
24-hr	4	MS	17	2.2219	0.025
24-hr	5	MS	17	1.5496	0.002
24-hr	6	MS	17	1.0306	0.017
24-hr	7	MS	17	0.8890	0.045
24-hr	8	MSF	17	6.6523	0.067
24-hr	9	MSF	17	5.2881	0.064
24-hr	13	MSH	17	13.4438	0.034
24-hr	1	MM	21	8.9884	0.119
24-hr	2	MM	21	6.0572	0.107
24-hr	3	MM	21	8.6748	0.073
24-hr	4	MS	21	1.2777	0.033
24-hr	5	MS	21	0.9502	0.005
24-hr	6	MS	21	0.9171	0.027
24-hr	7	MS	21	0.8930	0.124
24-hr	8	MSF	21	6.9946	0.064
24-hr	9	MSF	21	5.0225	0.062
24-hr	1	MM	27	30.7360	0.124
24-hr	2	MM	27	30.9009	0.106
24-hr	3	MM	27	35.8649	0.075
24-hr	4	MS	27	1.9893	0.010
24-hr	5	MS	27	1.5850	ND[d]
24-hr	6	MS	27	1.5689	ND
24-hr	7	MS	27	0.9049	0.092
24-hr	8	MSF	27	6.9399	0.019
24-hr	9	MSF	27	5.7878	0.019
24-hr	1	MM	34	30.3313	0.121
(continued)					

Experiment	Tube	Medium[a]	Days Since Inoculation	Methane[b]	OD[c]
24-hr	2	MM	34	30.6045	0.102
24-hr	3	MM	34	33.2937	0.070
24-hr	4	MS	34	3.5227	0.008
24-hr	5	MS	34	0.9779	ND
24-hr	6	MS	34	0.6011	ND
24-hr	7	MS	34	0.5463	0.105
24-hr	8	MSF	34	7.7891	0.024
24-hr	9	MSF	34	5.9194	0.021
48-hr	14	MM	0	0	0
48-hr	15	MM	0	0	0
48-hr	16	MM	0	0	0
48-hr	17	MS	0	0	0
48-hr	18	MS	0	0	0
48-hr	19	MS	0	0	0
48-hr	20	MSF	0	0	0
48-hr	21	MSF	0	0	0
48-hr	22	MSF	0	0	0
48-hr	23	MSH	0	0	0
48-hr	24	MSH	0	0	0
48-hr	25	MSH	0	0	0
48-hr	14	MM	11	12.1782	0.03
48-hr	15	MM	11	10.2266	0.031
48-hr	16	MM	11	11.3806	0.031
48-hr	17	MS	11	0.9307	0
48-hr	18	MS	11	1.0369	0.007
48-hr	19	MS	11	1.1536	0.004
48-hr	20	MSF	11	5.0627	0.025
48-hr	21	MSF	11	5.9034	0.021
48-hr	22	MSF	11	5.5130	0.03
48-hr	23	MSH	11	7.7427	0.075
48-hr	24	MSH	11	7.2533	0.073
48-hr	25	MSH	11	9.1863	0.08
48-hr	14	MM	14	10.4938	0.071
48-hr	15	MM	14	9.7149	0.067
48-hr	16	MM	14	10.7693	0.08
48-hr	17	MS	14	1.1211	0.015
(continued)					

Experiment	Tube	Medium[a]	Days Since Inoculation	Methane[b]	OD[c]
48-hr	18	MS	14	0.8522	0.013
48-hr	19	MS	14	0.9853	0.007
48-hr	20	MSF	14	5.1523	0.034
48-hr	21	MSF	14	5.8558	0.014
48-hr	22	MSF	14	5.4477	0.03
48-hr	23	MSH	14	7.8923	ND
48-hr	24	MSH	14	7.2766	ND
48-hr	25	MSH	14	9.7670	0.007
48-hr	14	MM	18	9.8958	0.114
48-hr	15	MM	18	8.9851	0.1
48-hr	16	MM	18	10.3938	0.083
48-hr	17	MS	18	1.1189	0.034
48-hr	18	MS	18	1.0663	0.047
48-hr	19	MS	18	1.3047	0.028
48-hr	20	MSF	18	5.8616	0.066
48-hr	21	MSF	18	6.2293	0.062
48-hr	22	MSF	18	5.3014	0.062
48-hr	23	MSH	18	8.3131	0.008
48-hr	25	MSH	18	8.8628	0.015
48-hr	14	MM	23	9.7812	0.095
48-hr	15	MM	23	8.3239	0.118
48-hr	16	MM	23	10.3224	0.081
48-hr	17	MS	23	1.0178	0.006
48-hr	18	MS	23	1.0097	0.024
48-hr	19	MS	23	1.1026	0.012
48-hr	20	MSF	23	5.0759	0.076
48-hr	21	MSF	23	5.9800	0.073
48-hr	22	MSF	23	5.5949	0.055
48-hr	23	MSH	23	7.8326	0
48-hr	14	MM	27	20.7726	0.102
48-hr	15	MM	27	7.5276	0.09
48-hr	16	MM	27	24.6958	0.083
48-hr	17	MS	27	1.2409	ND
48-hr	18	MS	27	2.0665	ND
48-hr	19	MS	27	2.1357	ND
48-hr	20	MSF	27	5.1050	0.008
(continued)					

Experiment	Tube	Medium[a]	Days Since Inoculation	Methane[b]	OD[c]
48-hr	21	MSF	27	5.7993	0.011
48-hr	22	MSF	27	5.3949	ND
48-hr	23	MSH	27	8.2600	ND
48-hr	14	MM	34	5.5649	0.105
48-hr	15	MM	34	12.6231	0.088
48-hr	16	MM	34	11.2245	0.088
48-hr	17	MS	34	3.3884	ND
48-hr	18	MS	34	1.4442	ND
48-hr	19	MS	34	1.1591	ND
48-hr	20	MSF	34	4.5129	0.006
48-hr	21	MSF	34	6.2127	0.012
48-hr	22	MSF	34	6.2394	ND
48-hr	23	MSH	34	4.6834	ND

[a]Medium corresponds to the specific medium (and organism) contained in each test tube. MM = *Methanothermobacter wolfeii*; MS = *Methanosarcina barkeri*; MSF = *Methanobacterium formicicum*; MSH = *Methanococcus maripaludis* (see 2.3.1 Microbial Procedures for specific media components).
[b]Methane is given in % headspace.
[c]OD = Optical Density (600 nm).
[d]ND = No Data.

Chapter 3. Low Pressure Tolerance by Methanogens in an Aqueous Environment: Implications for Subsurface Life on Mars

R. L. Mickol[1] and T. A. Kral[1,2]

[1]Arkansas Center for Space and Planetary Sciences, University of Arkansas, Fayetteville, Arkansas, 72701, USA.

[2]Dept. of Biological Sciences, University of Arkansas, Fayetteville, Arkansas, 72701, USA.

This chapter has been published.
Mickol, R. L. and T. A. Kral (2016) Low Pressure Tolerance by Methanogens in an Aqueous Environment: Implications for Subsurface Life on Mars. ***Origins of Life and Evolution of Biospheres*****, 1-22. DOI 10.1007/s11084-016-9519-9**

3.1 Abstract

The low pressure at the surface of Mars (average: 6 mbar) is one potentially biocidal factor that any extant life on the planet would need to endure. Near subsurface life, while shielded from ultraviolet radiation, would also be exposed to this low pressure environment, as the atmospheric gas-phase pressure increases very gradually with depth. Few studies have focused on low pressure as inhibitory to the growth or survival of organisms. However, recent work has uncovered a potential constraint to bacterial growth below 25 mbar. The study reported here tested the survivability of four methanogen species (*Methanothermobacter wolfeii*, *Methanosarcina barkeri*, *Methanobacterium formicicum*, *Methanococcus maripaludis*) under low pressure conditions approaching average martian surface pressure (6 mbar – 143 mbar) in an aqueous environment. Each of the four species survived exposure of varying length (3 days – 21 days) at pressures down to 6 mbar. This research is an important stepping-stone to determining if methanogens can actively metabolize/grow under these low pressures. Additionally, the recently discovered recurring slope lineae suggest that liquid water columns may connect the surface to deeper levels in the subsurface. If that is the case, any organism being transported in the water column would encounter the changing pressures during the transport.

3.2 Introduction

The potential discovery of methane in the martian atmosphere by both space-based missions (Fonti and Marzo, 2010; Formisano et al., 2004; Geminale et al., 2008; Geminale et al., 2011; Maguire, 1977) and ground-based telescopes (Krasnopolsky et al., 1997; Krasnopolsky et al., 2004; Mumma et al., 2009) has fueled the study of methanogens as ideal organisms for life on Mars. While there are possible abiotic sources for the methane on Mars (Chassefière and Leblanc, 2011; Chastain and Chevrier, 2007; Lyons et al., 2005; Maguire, 1977; Onstott et al., 2006; Oze and Sharma, 2005), a biological source cannot be ruled out. Although Curiosity initially failed to detect methane in the martian atmosphere (Webster et al., 2013), previous reports note very localized sources of methane on the planet (Fonti and Marzo, 2010; Mumma et al., 2009). However, more recent results released by the Mars Science Laboratory team have illustrated an increase in methane abundance over time (Webster et al., 2015).

Methanogens are microorganisms within the domain Archaea that produce methane. Some methanogens are chemoautotrophic, producing methane through the metabolism of hydrogen (H_2) as an energy source and carbon dioxide (CO_2) as a carbon source. Methanogens can be considered ideal organisms for life on Mars because they are anaerobic, do not require organic nutrients, and are non-photosynthetic, indicating they could exist in a subsurface environment. Methanogens have previously been shown to metabolize or survive under various martian conditions, including metabolism at low pressure [50 mbar (Kral et al., 2011)], metabolism on JSC Mars-1, a martian soil simulant (Kral et al., 2011; Kral et al., 2004), and survival following desiccation at Earth and Mars surface pressures (Kral and Altheide, 2013; Kral et al., 2011). A distinction between growth, metabolism and survival should be noted. Growth is typically thought of as an increase in size or numbers in the case of microorganisms

(Tortora et al., 2015). Growth typically accompanies metabolism, and in the research reported here, prior to and following exposure to low pressure, they are occurring concomitantly. Survival would indicate that the organism has remained viable (capable of metabolism/growth when more favorable conditions are restored) during challenging conditions, but may not have demonstrated any measureable metabolism/growth during those challenging conditions. The experiments conducted in the research reported here were testing for survival only under low-pressure conditions.

The surface pressure of Mars is approximately $1/100^{th}$ the surface pressure of Earth, averaging between one and ten millibar over one martian year over the martian surface, based on differences in topography and the exchange of CO_2 between the atmosphere and the polar caps (Hess et al., 1979; Hess et al., 1980; Spiga et al., 2007). There are no locations on Earth's surface that reach such low levels (the pressure at the top of Mount Everest is 330 mbar; Fajardo-Cavazos, 2012), thus there are no surface environments on Earth within which organisms could adapt to low pressure. It is possible, however, that low-pressure atmospheric environments exist that house microorganisms. At sufficiently high altitudes (~20 km), the atmospheric pressure is low enough to be Mars-like (~5 mbar). Studies by Griffin (2004, 2008) and Smith et al. (2010) have collected air samples at these heights which contain microorganisms including bacteria, fungi and viruses capable of growth, isolation and identification under Earth-normal lab conditions between 22-30 °C. Various mechanisms can transport bacteria from Earth's surface through the highest reaches of the atmosphere, but general atmospheric retention time (3-10 days) and cold temperatures (-75 °C) suggest that these altitudes do not comprise permanent ecosystems (Smith et al., 2010). Additionally, the studies by Griffin (2004, 2008) and Smith (2010) did not include archaeal identification. In a recent review, Gandolfi et al. (2013) note that

of eight studies that did include archaeal sequencing, only one sequence (*Euryarchaeota*) was retrieved. Thus, in terms of atmospheric biology and low pressure environments, more data including archaeal species is needed.

Schuerger et al. (2013) cited 17 biocidal/inhibitory factors that any extant life on Mars would need to endure in order to remain viable. Although the synergistic effects of these biocidal factors are not explored within the experiments conducted here, certain assumptions can be made to increase the validity of these studies: 1. The organisms are protected from UV radiation. 2. There is H_2 gas available for metabolism. 3. There is sufficient liquid water for active metabolism. These three assumptions are not improbable when a subsurface environment is considered. In regard to UV radiation, Schuerger et al. (2012) note that a one-millimeter thick layer of crushed basalt (analog martian regolith) provides sufficient attenuation of UV radiation allowing for the survival of *Bacillus subtilis* HA101 endospores and *Enterococcus faecalis* ATCC 29212 cells. Although H_2 has only been detected in the upper atmosphere (Krasnopolsky and Feldman, 2001) and not definitively identified at the surface, it is believed to exist on Mars and is incorporated into a number of atmospheric models (Atreya and Gu, 1994; Krasnopolsky, 1993; Nair et al., 1994). Possible sources of H_2 on Mars include downward diffusion from the upper atmosphere (Weiss et al., 2000), volcanic and hydrothermal activity (Boston et al., 1992; Wray and Ehlmann, 2011), radiolysis of subsurface ice and water (Onstott et al., 2006), and water-rock interactions, specifically, serpentinization (Atreya et al., 2007; McCollom and Bach, 2009; Oze and Sharma, 2005). Significant H_2 can be produced through serpentinization, but reaction rates are severely limited at low temperatures (< ~200 °C). However, at low temperatures conducive to life (< 130 °C), a steady source of H_2 may result from the decomposition of Fe-rich brucite, as H_2 is lost from the system. In this scenario, the total amount

of H_2 produced could eventually equal the amount produced at high temperature, although the production would be very gradual over time (McCollom and Bach, 2009).

It is important to note that the absence of detection of H_2 does not necessarily rule out its existence in the martian atmosphere or within the subsurface. Kral et al. (1998) have shown that *Methanobacterium formicicum* is capable of H_2 uptake at levels down to 15 ppm. The low concentration of H_2 on Mars may not be detectable when the entire atmosphere is taken into account. Thus, the absence of H_2 in the martian atmosphere may be more consistent with the presence of methanogens than with their absence. However, in the case that H_2 is not available on Mars, carbon monoxide has also been reported in the martian atmosphere (Barth et al., 1969; Clancy et al., 1983; Krasnopolsky, 2007; Lellouch et al., 1991), which certain methanogens can use in place of H_2 as an energy source (Daniels et al., 1977; O'Brien et al., 1984). Recently, King (2015) has demonstrated the ability of two microorganisms to oxidize carbon monoxide at concentrations much lower than that contained in the martian atmosphere, under conditions of high salt and low water activity. One of these organisms, *Halorubrum* str. BV1, is a member of the Euryarchaeota, a phylum to which methanogens also belong (King, 2015). Lastly, there is evidence that there is water, albeit frozen, on Mars in the near subsurface (Boynton et al., 2002; Feldman et al., 2002; Haberle et al., 2001; Malin and Edgett, 2000; Mitrofanov et al., 2002; Rennó et al., 2009; Smith et al., 2009). The presence of recurring slope lineae (RSLs) has reignited the idea that there is liquid water, in the form of brines, available on or near the planet surface (Grimm et al., 2014; McEwen et al., 2014; McEwen et al., 2011; Ojha et al., 2015; Stillman et al., 2014). More recently, thermodynamic modeling, in conjunction with temperature and humidity measurements at the martian surface, suggest that nighttime transient brines may form in the very near subsurface (< 5 cm). However, the nighttime temperatures and the water

activity of the brines are likely much too low to support life as we know it (Martín-Torres et al., 2015). Additionally, meteoritic evidence suggests the presence of a subsurface water reservoir either in the form of a hydrated crust or embedded ground ice (Usui et al., 2015).

Of the various conditions on Mars that contribute to its seeming inhospitality, low pressure is typically included in Mars simulation experiments, but the effect of low pressure itself is often overlooked when compared to more lethal effects, such as UV radiation and desiccation. However, the low pressure environment cannot be ignored, as the atmospheric gas-phase pressure increases only very gradually with depth and there appears to be a "25 mbar limit" below which many bacteria fail to grow (Schuerger et al., 2013).

This research encompasses seven experiments testing the survival of four species of methanogens (*Methanothermobacter wolfeii, Methanosarcina barkeri, M. formicicum, Methanococcus maripaludis*) at low pressures approaching 6 mbar, the average surface pressure on Mars, in liquid media.

3.3 Methods

3.3.1 Cultures and Growth Media

Methanogen cultures were originally obtained from the Oregon Collection of Methanogens, Portland State University, Oregon. Each methanogen was grown in its own anaerobic medium for optimum growth: *Methanosarcina barkeri* [OCM 38], MS medium [yeast extract, trypticase peptone, mercaptoethanesulfonic acid, potassium phosphate, ammonium chloride, magnesium chloride, calcium chloride, and additional trace minerals (Boone et al., 1989; Kendrick and Kral, 2006)]; *Methanobacterium formicicum* [OCM 55], MS medium supplemented with sodium formate [designated MSF medium; (Boone et al., 1989)];

Methanothermobacter wolfeii [OCM 36], MM medium [a minimal medium containing the same components as MS medium except yeast extract, trypticase peptone and mercaptoethanesulfonic acid (Kendrick and Kral, 2006; Xun et al., 1988)]; and *Methanococcus maripaludis* [OCM 151], MSH medium [MS medium containing additional sodium chloride, magnesium chloride and potassium chloride (Ni and Boone, 1991)]. These media provide the nutrients and minerals necessary for growth, and are not intended to represent the available concentration of nutrients on Mars.

Microbial procedures for each of the seven experiments were as follows: Growth media were prepared under anaerobic conditions in a 90:10 CO_2:H_2 gas Coy Anaerobic Chamber (Coy Laboratory Products Inc., Grass Lake Charter Township, MI) following the procedure of Kendrick and Kral (2006). Ten milliliters of each of the four media were added to each of five anaerobic culture tubes, for a total of twenty tubes (see Table 3.1). This provided five replicates for each of the four methanogen species for each of the seven experiments. The tubes were fitted with rubber stoppers and aluminum crimps (Boone et al., 1989), sealing the tubes under anaerobic conditions and eliminating exposure to the ambient atmosphere. A sterile solution of ~125 μL of 2.5% sodium sulfide was added to the media following sterilization via autoclave (Boone et al., 1989). Each culture tube was inoculated with 0.5 mL of the corresponding methanogen. The anaerobic nature and slow doubling time of methanogens makes them difficult to grow on agar or to provide accurate cell counts without the use of expensive and/or involved techniques. Common methods used to determine methanogen growth are optical density measurements and methane measurements using gas chromatography (Sowers and Schreier, 1995). In all experiments explained here, 0.5 mL of culture was used as a standard inoculum. The tubes were pressurized with 2 bar H_2 gas and placed at their respective incubation

temperatures (25 °C for *M. maripaludis*, 37 °C for *M. barkeri* and *M. formicicum*, 55 °C for *M. wolfeii*). This incubation period allowed for the initial growth of the organisms for use in each experiment, which was verified via methane detection by gas chromatography.

Table 3.1 Experimental conditions for each of seven experiments, including pressures, time punctured and time exposed to low pressure. Each experiment consisted of five replicates for each of four methanogen species in 10 mL of their respective anaerobic growth medium. Incubations both pre- and post-exposure were conducted at the methanogens' respective growth temperatures (*Methanosarcina barkeri*, 37 °C, MS medium; *Methanobacterium formicicum*, 37 °C, MSF medium; *Methanothermobacter wolfeii*, 55 °C, MM medium; *Methanococcus maripaludis*, 24 °C, MSH medium).

Expt.	Amount of regolith analog per tube	Time for equilibration of chamber[a] (days)	Pressure range during exposure[b] (mbar)	Time exposed to low pressure (days)	Time between filling chamber with CO_2 and removing tubes[c] (days)	Average temperature inside Pegasus Chamber during exposure (°C)	Overall time punctured (days)	Incubation times following exposure (days)
1	NA[d]	1	138 ± 5	8	NA	28	8	96
2	NA	2	69 ± 3	11	4	30	12	111
3	NA	2	69 ± 3	11	5	30	14	37
4	NA	2	35 ± 3	6	3	31	7	44
5	NA	1	8 ± 2	3	1	30	4	56
6	5 g JSC Mars-1	1	14 ± 7	5	3	27	7	40
7	NA	1 hour	49.1 ± 0.1	21	1 hour	28	1 hour	157

[a]The time for equilibration corresponds to the length of time between when the chamber was set at the desired pressure and the tubes were punctured.
[b]A pressure range is given based on the capabilities of our chamber.
[c]The chamber was filled with CO_2 before removal of the needles from the tubes to ensure that the tubes were not under negative pressure when removed from the chamber.
[d]NA = Not Applicable.

3.3.2 Pegasus Planetary Simulation Chamber and Experimental Procedures

Seven low pressure experiments were conducted in the Pegasus Planetary Simulation Chamber, previously described (Kral et al., 2011). In Experiments 1 through 5 and Experiment 7,

anaerobic tubes contained only cultures in liquid media, as prepared above (Section 2.1). The major variable was pressure.

In Experiment 6, cultures consisted of liquid media, as prepared above (Section 3.3.1), with an additional five grams of JSC Mars-1 regolith simulant situated atop a sterile cotton plug (Fig. 3.1A). This served to keep the liquid cultures separated from the regolith, in order to eliminate the possibility of soil-water interactions or clumping of cells adhering to soil particles.

For the preparation of the cultures for Experiment 6, five grams of JSC Mars-1 simulant regolith were placed into each of twenty empty, anaerobic culture tubes and sterilized via autoclave. Previously prepared growth media containing cultures of each methanogen species (10 mL of liquid media) and the tubes containing the sterilized regolith simulant were placed into a Coy Anaerobic Chamber. Within the chamber, the aluminum crimps and rubber stoppers were removed from each of the twenty tubes containing the methanogens. A sterile cotton ball was placed into each of these tubes above the liquid medium. Five grams of sterile regolith simulant were transferred to each tube and allowed to sit on top of the cotton. The tubes were re-stoppered with their original stoppers and re-crimped with new crimps (Fig. 3.1A).

For Experiments 1 through 6, before being placed in the Pegasus Planetary Simulation Chamber, cultures were tested for methane production (Varian Micro-GC, model CP-4900, Palo Alto, CA) and optical density (600 nm; Spectronic 20D+, Spectronic Instruments, USA; Experiments 5, 6 only) to confirm active metabolism and growth. Methane production and optical density are typically used as a proxy for methanogen growth when both are seen to increase over time (Sowers and Schreier, 1995). The tubes were placed into the chamber with a palladium catalyst box to remove residual oxygen. Within the chamber, the twenty tubes for each experiment were situated inside a test tube rack, sorted randomly, but grouped by species (five

replicates for each of the four species). A second test tube rack was placed over the top of the tubes to secure their position for use with a specialized puncture device (Fig. 3.1B). The chamber door was closed and duct seal putty (Rainbow Technology, Pelham, AL) was applied around the seal as a further safeguard against oxygen contamination. The chamber was evacuated, filled with 80:20 H_2:CO_2 gas and evacuated again. This cycle was repeated three times to ensure removal of the ambient atmosphere. On the third cycle, H_2/CO_2 gas was added to the chamber in a continuous flow while under vacuum for a total of three minutes to ensure removal of the atmosphere. The chamber was then set at the desired pressure for the duration of the experiment.

Pressure setpoints (Table 3.1) were maintained using a DU 200 capacitive sensor and Center One controller (Oerlikon Leybold Vacuum, Export, PA). Following a prescribed time for each experiment, the tubes were punctured with a specialized device containing one-inch, 22-gauge syringe needles (Fig. 3.1B) to allow equilibration between the chamber pressure and the pressure inside the tubes. The seal between the puncture device and the chamber was also covered with duct seal putty to minimize oxygen contamination. All experiments were conducted at room temperature. Pressures and exposure times are seen in Table 3.1.

Following the prescribed exposure times (limited by evaporation of the liquid media), the needles were removed from the tubes using the same device. The puncturing of the tubes and removal of the needles before and after exposure to low pressure were performed in order to limit oxygen exposure to the methanogens, which are strict anaerobes. This also limited exposure to the ambient atmosphere, keeping the methanogens in contact with solely H_2/CO_2 gas. After another set of designated times (Table 3.1), the chamber was filled to atmospheric pressure with CO_2. Following removal from the chamber, additional 2.5% sodium sulfide solution (~125 μL) was added to each test tube to remove residual oxygen. A second set of sterile methanogen

growth media was prepared as above (five test tubes for each of the four types of media). Each of these twenty tubes was inoculated with 0.5 mL of methanogen media from one of the original tubes (e.g., 0.5 mL from original tube #1 was used to inoculate transfer tube #1). Both the original and transfer sets were pressurized with 2 bar H_2 gas and kept at the organisms' respective incubation temperatures (Table 3.1). For each experiment, growth was monitored by methane production (gas chromatography) and optical density (Experiments 5, 6 only).

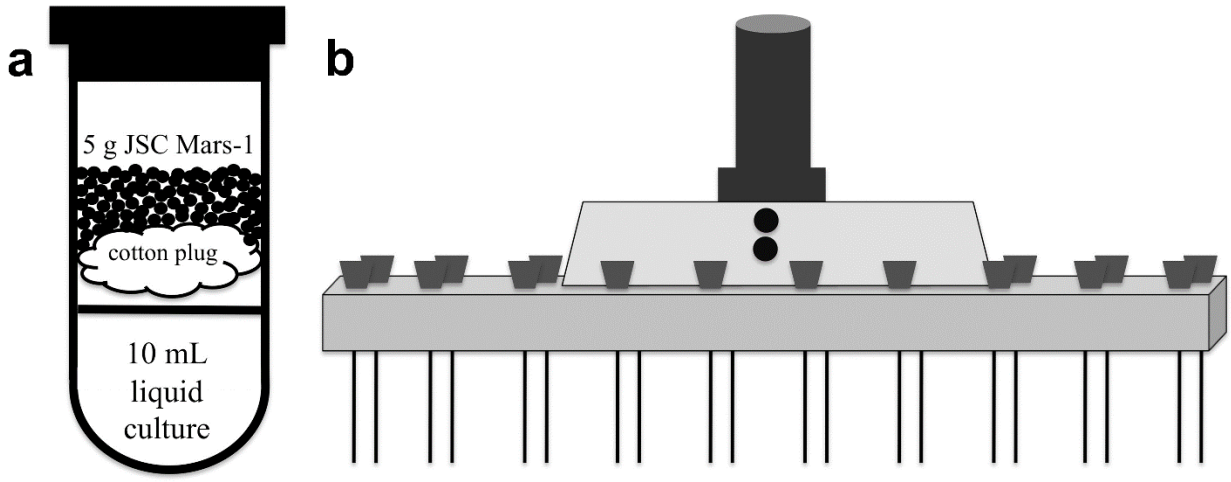

Figure 3.1 (a) Diagram illustrating anaerobic tube contents for Experiment 6 only. Tubes were sealed with a rubber stopper and crimp, and contained 10 mL liquid culture, a cotton plug situated just above the liquid, and five grams JSC Mars-1 atop the cotton. **(b)** Diagram of the specialized puncture device. Twenty holes were cut into a piece of Plexiglas within which 1-inch 22-gauge syringe needles were inserted and removed for each experiment. The device was connected to a cylindrical manipulator via two screws. The cylindrical manipulator was fitted through one of the top ports of the Pegasus Planetary Simulation Chamber, and allowed for manual operation of the device (puncture of tubes, removal of needles) during experiments.

For Experiments 1 through 6, following designated post-exposure incubation periods (Table 3.1), electrical conductivity, salinity and total dissolved solids (TDS) were measured for both the original and transfer sets for each experiment (Tables 3.2-3.4), where applicable, using

an EcoSense EC300 Conductivity/Temperature probe (YSI Inc., Yellow Springs, OH). In order to have sufficient liquid for measurements, tubes within each set, for each experiment, were combined.

In Experiment 7, in order to limit evaporation and extend the length of the experiment, a different procedure was used. Media in anaerobic test tubes were prepared as above (Section 3.3.1). As with Experiments 1 through 6, the test tubes were measured for methane production via gas chromatography (Shimadzu Scientific Instruments Inc., model GC-2014, Columbia, MD), as well as optical density (Expts. 5 through 7 only) before the start of the experiment. The tubes were placed into the Pegasus Planetary Simulation Chamber with a palladium catalyst box to remove residual oxygen. Within the chamber, the twenty tubes were situated inside a test tube rack, sorted randomly (five replicates for each of the four species). A second test tube rack was placed over the top of the tubes to secure their position for use with a specialized puncture device (Fig. 3.1B). The chamber door was closed, and the chamber was evacuated to 50 mbar while 80:20 H_2:CO_2 gas was bled into the chamber. Pressure setpoints (Table 3.1) were maintained using a MKS Type 651C pressure controller and MKS Type 253B throttling valve (MKS Instruments Inc., Andover, MA). After 30 min, the test tubes were punctured with the specialized device mentioned above (Fig. 3.1B) to allow equilibration between the chamber pressure and the pressure inside the tubes. This equilibration period lasted for 1 h, after which the needles were removed from the tubes, effectively creating “micro-environments” within each culture tube. The 80:20 H_2:CO_2 gas source continued to bleed into the chamber during the 1 h period of equilibration. The tubes remained sealed within the chamber for the duration of the experiment, which dictates that the actual pressure within the tubes was dependent upon the temperature of the tubes within the chamber. However, the resulting vapor pressure based on the temperature

within the chamber (27-30 °C) was calculated to be between 36 and 42 mbar, lower than the experimental pressure (50 mbar) initially sealed in the tubes. Therefore, the chamber temperature would not have increased the pressure in the tubes. There is a somewhat foolproof aspect of this procedure. If there is a leak in the septum following the removal of the needle, the pressure will remain in equilibrium with the low pressure in the chamber. If the leak is large enough to allow any measureable evaporation, it will be visually obvious.

After 21 days (Table 3.1), the chamber was filled to atmospheric pressure with CO_2 gas and the test tubes were re-punctured to equilibrate them with the chamber environment. After 20 min, the needles were removed from the test tubes and the tubes were removed from the chamber. Following removal, additional 2.5% sodium sulfide solution (~125 μL) was added to each test tube to remove residual oxygen. A second set of sterile methanogen growth media was prepared as above (five test tubes for each of the four types of media). Each of these twenty tubes was inoculated with 0.5 mL of methanogen media from one of the original tubes (e.g., 0.5 mL from original tube #1 was used to inoculate transfer tube #1). Both the original and transfer sets were pressurized with 2 bar H_2 gas and kept at the organisms' respective incubation temperatures (Table 3.1). Growth was monitored over 157 days by methane production (gas chromatography) and optical density.

3.4 Results

For each of the seven experiments, viable cells of each of the four methanogen species (*M. barkeri*, *M. formicicum*, *M. maripaludis*, *M. wolfeii*) were successfully transferred to new media (transfer cultures) following exposure to low pressure. Methane production was generally similar between original and transfer cultures in Experiments 1-4 and 7, although *M. formicicum*

and *M. maripaludis* experienced slightly higher methane production within transfer tubes than in original tubes for all seven experiments (Figs. 3.2-3.4). *M. formicicum* produced the highest and most consistent amounts of methane across all seven experiments (40-60% headspace; Figs. 3.2-3.4).

3.4.1 Experiment 1: 133 – 143 mbar

For each species, at least one original culture continued to show an increase in methane production during the post-exposure incubation period (Fig. 3.2). However, at least one original culture for each species also failed to produce any significant methane following exposure to low pressure (> 1%).

Transfer cultures for each species produced greater amounts of methane than the original cultures during the post-exposure incubation period (Fig. 3.2), with methane being produced in all five transfer culture replicates. Methane produced in transfer cultures of *M. wolfeii* and *M. formicicum* was initially high (29.5 ± 4.1% and 33.9 ± 3.4%, respectively). Electrical conductivities, salinities and total dissolved solids were relatively similar between original and transfer cultures for *M. barkeri*, *M. formicicum* and *M. wolfeii* (Tables 3.2-3.4).

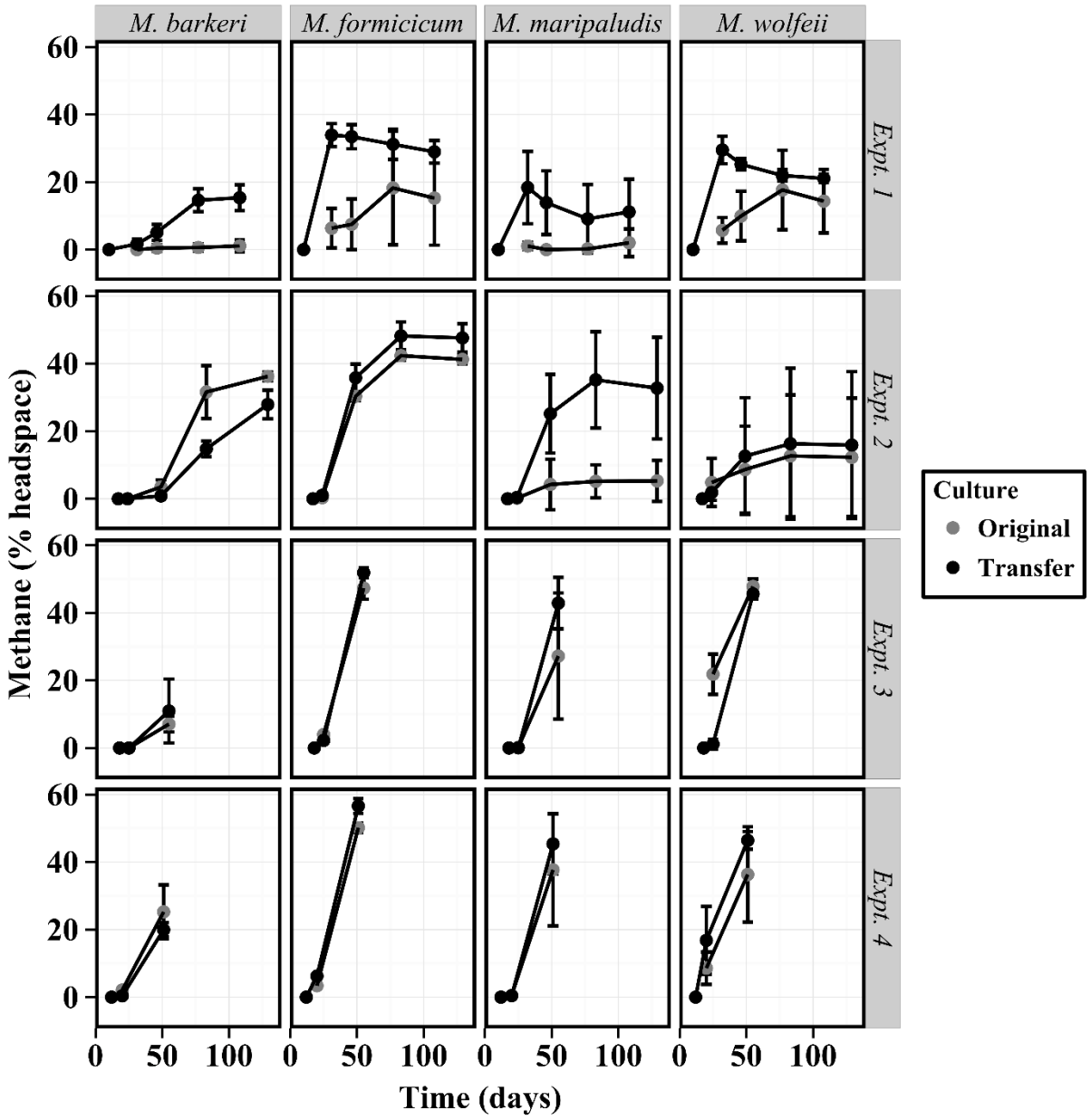

Figure 3.2 Average methane (% headspace) produced for four methanogen species (*Methanosarcina barkeri*, *Methanobacterium formicicum*, *Methanococcus maripaludis* and *Methanothermobacter wolfeii*) after exposure to low pressure for four separate experiments (Experiment 1: 133 –143 mbar, Experiments 2, 3: 67 – 72 mbar, Experiment 4: 33 – 38 mbar). Original tubes (gray circles) contained active cultures producing methane before being placed into the Pegasus Planetary Simulation Chamber (Day 0). Transfer cultures (black circles) were inoculated on the day the original tubes were removed from the chamber. Prior to and following the low-pressure exposure period, cultures were kept at the organisms' growth temperatures (25 °C for *M. maripaludis*, 37 °C for *M. barkeri* and *M. formicicum*, and 55 °C for *M. wolfeii*). Error bars indicate +/- one standard deviation.

3.4.2 Experiment 2: 67 – 72 mbar

All five original culture replicates for *M. barkeri*, *M. formicicum* and *M. maripaludis* continued to produce methane following exposure to low pressure (Fig. 3.2). Only two original cultures for *M. wolfeii* produced significant methane (>1%) during the post-exposure incubation period. For *M. maripaludis*, one original culture continued to produce methane but to a much lesser extent than the other four cultures (~10% vs. ~40%).

Only two transfer cultures for *M. wolfeii* produced significant methane during the post-exposure incubation period, which are sub-cultures from the two original cultures mentioned above.

Electrical conductivities, salinities and TDS differed between original and transfer cultures for each methanogen, although there was not significant evaporation within the original cultures during this experiment. All three measurements were slightly higher in transfer cultures than in original cultures for *M. formicicum*, whereas measurements were higher in original cultures than transfer cultures for *M. wolfeii*. Electrical conductivity and salinity were higher in original cultures than transfer cultures for *M. barkeri* (Tables 3.2-3.4).

3.4.3 Experiment 3: 67 – 72 mbar

All five original cultures and all five transfer cultures for all four species produced methane after the start of the experiment.

Electrical conductivity, salinity and TDS were greater in transfer cultures than original cultures for both *M. formicicum* and *M. maripaludis*, despite insignificant evaporation during the experiment. Measurements were relatively similar between original and transfer cultures for *M. barkeri* and *M. wolfeii*, with slightly higher values in transfer cultures (Tables 3.2-3.4).

3.4.4 Experiment 4: 33 – 37 mbar

All five replicates for both original and transfer cultures for all four species produced methane after the original cultures were removed from the chamber and the transfer cultures were inoculated (Fig. 3.2).

Varying rates of evaporation occurred within original cultures throughout the experiment (0.5-5.6 mL decrease in volume of liquid media over six days). Evaporation was three times greater in the front row of cultures tubes than in the back row (decrease in volume of liquid media of 3.83 ± 1.33 mL vs. 1.15 ± 0.53 mL).

Electrical conductivity, salinity and TDS were greater in original cultures than transfer cultures for *M. formicicum* and *M. wolfeii*. Measurements were essentially identical between original and transfer cultures for *M. barkeri*. Electrical conductivity was higher in original cultures than transfer cultures for *M. maripaludis* (Tables 3.2-3.4; salinity and TDS were not measured in transfer cultures).

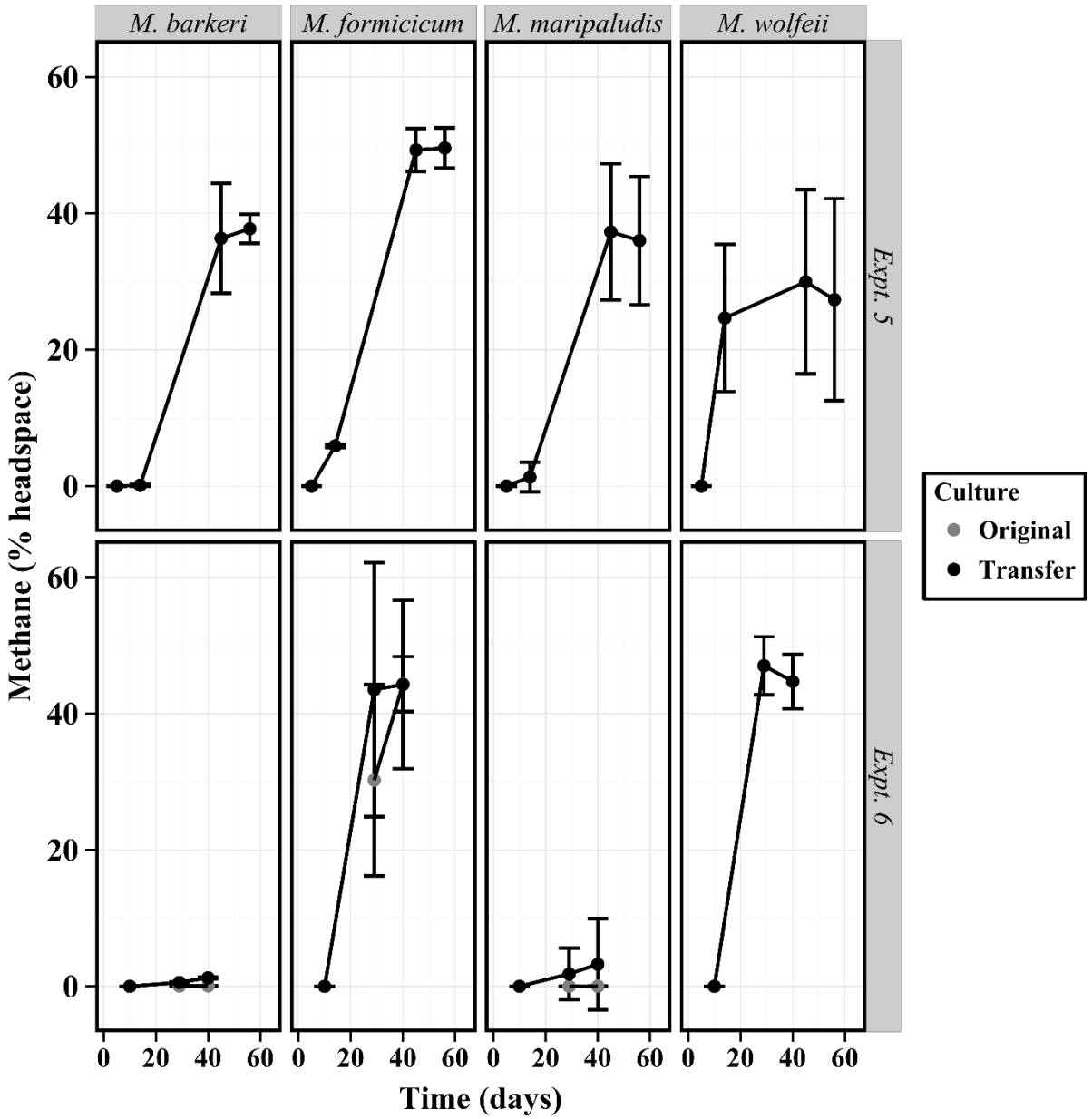

Figure 3.3 Average methane (% headspace) produced for four methanogen species (*Methanosarcina barkeri*, *Methanobacterium formicicum*, *Methanococcus maripaludis* and *Methanothermobacter wolfeii*) after exposure to low pressure for two separate experiments (Experiment 5: 6 – 10 mbar, Experiment 6: 7 – 20 mbar). Original tubes (gray circles) contained active cultures producing methane before being placed into the Pegasus Planetary Simulation Chamber (Day 0). Transfer cultures (black circles) were inoculated on the day the original tubes were removed from the chamber. Prior to and following the low-pressure exposure period, cultures were kept at the organisms' growth temperatures (25 °C for *M. maripaludis*, 37 °C for *M. barkeri* and *M. formicicum*, and 55 °C for *M. wolfeii*). Error bars indicate +/- one standard deviation.

3.4.5 Experiment 5: 6 – 10 mbar

All four methanogen species survived three days' exposure to 8 mbar, close to the average martian surface pressure (Fig. 3.3), despite heavy evaporation (~10 mL in 3 days). Sufficient liquid remained to perform transfers from at least two original cultures to fresh media for each of the four species. However, original tubes were depleted of liquid media after transfer, measured zero percent methane after 16 days, and were discarded.

Electrical conductivity, salinity and TDS were only measured in transfer cultures for *M. barkeri, M. wolfeii* and *M. maripaludis* (measurements were not taken in transfer cultures for *M. formicicum* due to an insufficient amount of liquid following evaporation in original cultures). Measurements for *M. barkeri* cultures were comparable to measurements in uninoculated MS medium. Electrical conductivity, salinity and TDS were all higher in transfer cultures for *M. wolfeii* and *M. maripaludis* than for uninoculated MM (*M. wolfeii*) and MSH (*M. maripaludis*) media (Tables 3.2-3.4).

Transfer cultures for each of the four species all produced methane after inoculation. Optical density values within transfer cultures increased for all four methanogens after inoculation (data not shown). Measurements were comparable to pre-exposure values for *M. barkeri, M. maripaludis* and *M. formicicum* (~0.07, ~0.1, and ~0.2 respectively). *M. wolfeii* transfer cultures displayed greater optical density values, as compared to pre-exposure numbers (0.12 ± 0.02 vs. 0.05 ± 0.01).

3.4.6 Experiment 6: 7 – 20 mbar

All four methanogen species survived five days' exposure to pressures approaching average martian surface pressures (Fig. 3.3). JSC Mars-1 was utilized as a diffusion barrier,

which prolonged the experiment by two days (compared to Experiment 5). Although each culture experienced heavy evaporation (~10 mL in 5 days), at least three replicates for each species retained a sufficient amount of culture to perform transfers to fresh media following exposure to low pressure.

Due to a lack of media as a result of evaporation in the original cultures, electrical conductivity, salinity and TDS measurements were only taken in transfer cultures of *M. maripaludis*, *M. barkeri* and *M. formicicum* (measurements were not possible in original cultures for all four methanogens, nor in transfer cultures for *M. wolfeii*). Values for electrical conductivity, salinity and TDS were all higher in transfer cultures than for uninoculated media (Tables 3.2-3.4).

Original cultures of *M. maripaludis* (n = 4), *M. barkeri* (n = 3) and *M. formicicum* (n = 2) retained enough liquid culture following transfer to continue being monitored for methane production during the post-exposure incubation period. The original cultures of *M. maripaludis* and *M. barkeri* produced methane to a much lesser extent than cultures in previous experiments, but contained methane amounts similar to transfer cultures of the same experiment (Fig. 3.3). Original cultures of *M. formicicum* initially produced high amounts of methane after being removed from the chamber (~30-45%). *M. formicicum* and *M. wolfeii* transfer cultures initially produced high amounts of methane (~45%) after inoculation (Fig. 3.3).

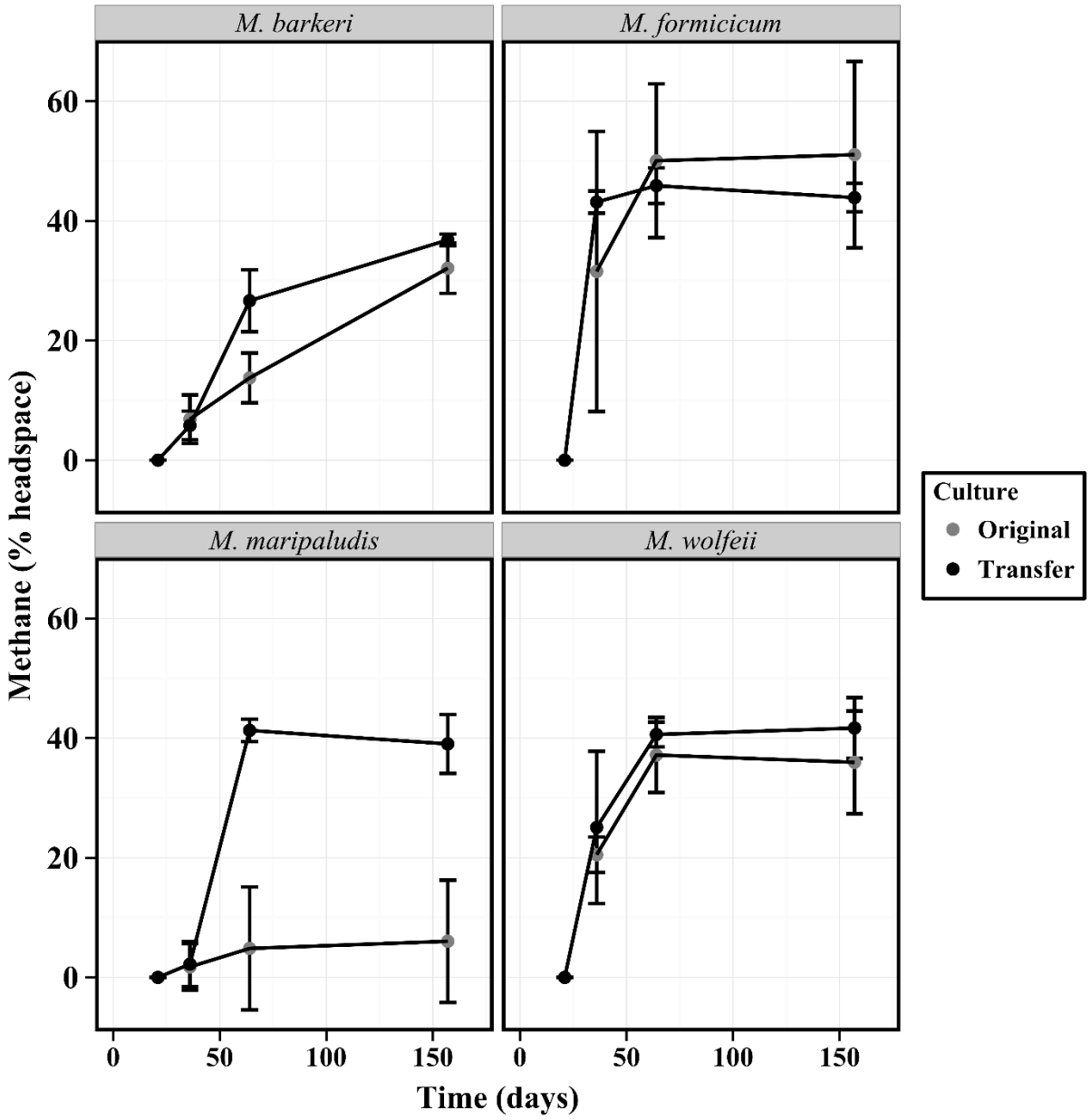

Figure 3.4 Average methane (% headspace) produced for four methanogen species (*Methanosarcina barkeri*, *Methanobacterium formicicum*, *Methanococcus maripaludis* and *Methanothermobacter wolfeii*) after exposure to low pressure (Experiment 7: 21 days, 47 – 50 mbar). Original tubes (gray circles) contained active cultures producing methane before being placed into the Pegasus Planetary Simulation Chamber (Day 0). Transfer cultures (black circles) were inoculated on the day the original tubes were removed from the chamber. Prior to and following the low-pressure exposure period, cultures were kept at the organisms' growth temperatures (25 °C for *M. maripaludis*, 37 °C for *M. barkeri* and *M. formicicum*, and 55 °C for *M. wolfeii*). Error bars indicate +/- one standard deviation.

Optical density values within transfer cultures for *M. barkeri*, *M. formicicum*, and *M. wolfeii* were initially higher than the values measured in the original cultures before the start of the experiment (data not shown). All three transfer cultures for *M. wolfeii* increased in optical density after inoculation, whereas only two of five transfer cultures for *M. maripaludis* increased in optical density during the post-exposure incubation period.

3.4.7 Experiment 7: 47 – 50 mbar

All five original culture replicates for *M. barkeri*, *M. formicicum* and *M. wolfeii* survived 21 days at 50 mbar and produced methane following exposure to low pressure (Fig. 3.4). Only one original culture of *M. maripaludis* produced significant methane (~8%) at the beginning of the post-exposure incubation period, and continued to increase in methane abundance over this period. One original culture of *M. maripaludis* did not begin to produce significant methane (~1%) until the second measurement taken on Day 64 (Fig. 3.4). The other three original cultures of *M. maripaludis* failed to produce any methane during the post-exposure incubation period.

All five transfer cultures for all four species produced methane after inoculation from original cultures following exposure to low pressure. Transfer cultures containing *M. formicicum* initially produced high amounts of methane (~43%, Fig. 3.4). After 157 days of post-exposure incubation, transfer cultures of all four species produced ~40% methane. Original cultures of *M. barkeri*, *M. formicicum* and *M. wolfeii* produced methane amounts similar to transfer cultures. Transfer cultures of *M. maripaludis* produced significantly more methane than original cultures (~40% vs. ~5%, Fig. 3.4).

Optical density values (data not shown) for both original and transfer cultures verify the growth demonstrated via methane production above.

Table 3.2 Electrical conductivity measurements (milliSiemens/centimeter; mS/cm) for four methanogens for Experiments 1 through 6, including uninoculated media. Measurements are from the combined media from each culture tube for each set (original and transfer), and were taken following both exposure to low pressure (original cultures) and inoculation of methanogens from original to transfer cultures.

	M. barkeri		*M. formicicum*		*M. wolfeii*		*M. maripaludis*	
Expt.	O[a]	T[b]	O	T	O	T	O	T
1	10.6	10.66	11.5	11.11	9.65	9.52	47.76	49.95
2	10.45	9.41	10.68	11.2	10.32	9.97	47.42	52.46
3	10.12	10.39	10.42	12.15	9.66	9.83	50.52	48.7
4	10.78	10.74	12.68	11.89	11.05	10.23	53.6	50.64
5	ND[c]	9.02	ND	ND	ND	10.99	ND	58.4
6	ND	11.8	ND	13.33	ND	ND	ND	57.6
Media	9.6		10.18		9.68		44.9	

[a]O = original cultures.
[b]T = transfer cultures.
[c]ND = No Data.

Table 3.3 Salinity measurements (parts per thousand; ppt) for four methanogens for Experiments 1 through 6, including uninoculated media. Measurements are from the combined media from each culture tube for each set (original and transfer), and were taken following both exposure to low pressure (original cultures) and inoculation of methanogens from original to transfer cultures.

	M. barkeri		*M. formicicum*		*M. wolfeii*		*M. maripaludis*	
Expt.	O[a]	T[b]	O	T	O	T	O	T
1	6.1	6.0	6.5	6.3	5.3	5.2	31.6	33.2
2	5.9	5.2	6.0	6.3	5.7	5.5	31.3	35.0
3	5.6	6.0	6.0	7.1	5.3	5.4	33.6	32.3
4	6.1	6.1	7.3	6.8	6.3	5.7	36.1	ND
5	ND[c]	5.2	ND	ND	ND	6.2	ND	39.6
6	ND	6.7	ND	7.6	ND	ND	ND	39.1
Media	5.5		5.9		5.5		29.3	

[a]O = original cultures.
[b]T = transfer cultures.
[c]ND = No data.

Table 3.4 Total dissolved solids (TDS) measurements (g/L) for four methanogens for Experiments 1 through 6, including uninoculated media. Measurements are from the combined media from each culture tube for each set (original and transfer), and were taken following both exposure to low pressure (original cultures) and inoculation of methanogens from original to transfer cultures.

	M. barkeri		*M. formicicum*		*M. wolfeii*		*M. maripaludis*	
Expt.	O[a]	T[b]	O	T	O	T	O	T
1	7.16	6.94	7.46	7.18	6.38	6.28	31.09	32.55
2	6.80	6.93	6.91	7.25	6.77	6.45	30.90	34.17
3	6.58	6.79	6.80	7.92	6.25	6.36	32.95	31.82
4	6.92	6.94	8.25	7.73	7.22	6.64	35.2	ND
5	ND[c]	6.00	ND	ND	ND	7.01	ND	38.2
6	ND	7.73	ND	8.7	ND	ND	ND	37.7
Media	6.24		6.67		5.5		28.96	

[a]O = original cultures.
[b]T = transfer cultures.
[c]ND = No data.

3.5 Discussion

The results shown here indicate that methanogen cells within aqueous media can remain viable after exposure to a low pressure environment, as well as the consequent evaporation of the liquid media, for the time periods tested. While survival during relatively long-term desiccation at low pressures has already been shown (Kral and Altheide, 2013; Kral et al., 2011), the effect of low pressure on cells in aqueous media represents novel research and an important stepping stone toward observing active growth of methanogens at low pressure. The results reported here are also important from the standpoint of methanogens possibly inhabiting a liquid water column below the surface of Mars. The recently discovered recurring slope lineae (Grimm et al., 2014; McEwen et al., 2014; McEwen et al., 2011; Stillman et al., 2014) suggest that liquid water is moving from the subsurface to the surface and, very likely, vice versa. That being the case, those

methanogens might be encountering substantially different pressures, and survival at those varying pressures would be paramount for their continued existence.

The assumptions made in these experiments (availability of water, protection from UV radiation, availability of H_2) are not unreasonable with respect to Mars when considering a subsurface environment. Similar to Earth, it is possible that Mars contains deep subsurface habitats conducive to life. These habitats may contain H_2 and warmer temperatures due to geothermal or volcanic activity (Boston et al., 1992). As such, these experiments provide possible insight into the survival of methanogens under subsurface martian conditions.

Few studies have characterized the effects of low pressure on the growth and survivability of microorganisms (Fajardo-Cavazos et al., 2012; Nicholson et al., 2013; Schuerger et al., 2013), whereas the only studies investigating the effects of martian conditions on methanogens at Mars surface pressures have used desiccated cells (Johnson et al., 2011; Kral and Altheide, 2013; Kral et al., 2011) or pelleted cells (Morozova et al., 2007). A recent study by Schirmack et al. (2014) incorporated in situ measurements of methane production by methanogens under Mars-like conditions, but the pressure used was 500 mbar, which the authors cite as an achievable pressure in the near subsurface (< 20 m), based on modeling by Jones et al. (2011). However, Schuerger et al. (2013) described two separate pressure models for the martian subsurface using either the lithographic pressure (of the overlying rock) or the gas-phase pressure (due to void spaces within the regolith). The gas-phase model predicts that pressure within the martian subsurface increases only slightly with depth, reaching 25 mbar at 13.9 km (Schuerger et al., 2013). In contrast, the lithographic pressure requires complete seclusion from the atmosphere, such as within rock and ice grains, and reaches 25 mbar at only 19.5 cm below the surface. The model by Jones et al. (2011) agrees with the lithographic pressure model

described by (Schuerger et al., 2013), indicating that any microorganisms at this pressure would need to be completely shielded from the martian atmosphere.

Morozova et al. (2007) have previously demonstrated the effects of a simulated Mars environment on pelleted cells of three methanogen strains isolated from Siberian permafrost (*Methanosarcina* spec. SMA-21, *Methanosarcina* spec. SMA-16, *Methanosarcina* spec. SMA-23) compared to three non-permafrost reference methanogens (*Methanobacterium* spec. MC-20, *Methanosarcina barkeri* [DSM 8687], and *Methanogenium frigidum* [DSM 16458]). Morozova and colleagues (2007) discovered that the methanogens isolated from permafrost habitats showed increased survival under martian conditions when compared to the reference organisms (60-90% vs. 0.3-5.8%). Interestingly, whereas *M. barkeri* exhibited the least resistance to martian conditions (0.3% survival) during the Morozova et al. (2007) experiments, during our low pressure experiment at 8 mbar (Experiment 5), *M. barkeri* produced similar amounts of methane post-exposure as compared to pre-exposure values (Fig. 3.3). In addition, for Experiments 5, 6 and 7, the optical density values for *M. barkeri* post-exposure were equal to or greater than the values pre-exposure (data not shown). Although the survival of *M. barkeri* cannot be directly compared between the Morozova et al. (2007) experiment and this paper due to differences in methods and experimental setup, these conflicting results illustrate the need for further study of microorganisms under martian conditions, taking into account martian environmental factors (temperature, pressure, etc.), as well as cell state (desiccated, pellet, active, etc.).

Considering that hydrated cells, as opposed to desiccated cells, were exposed to the low pressure environment, it is not extreme to suggest that methanogens *might* be able to metabolize under these conditions, given the availability of liquid water. However, it is more likely, given the relatively slow metabolism of methanogens and thus, long generation times, that the cells

simply entered an inactive state for the short duration of the experiments. Additionally, it could be considered a large assumption to expect that liquid water is consistently available in the martian subsurface, either in terms of prolonged availability or suitable salt concentration.

These experiments were conducted in anaerobic culture tubes, within which the liquid media initially formed a 10 mL water column. The hydrostatic pressure of the water column could have increased the pressure at the bottom of the liquid environment. Equation 1 gives the formula for the pressure at a given depth in a static liquid, where P_{atm} is the pressure of the atmosphere acting on the liquid, ρ is the density of the liquid, g is gravity (9.8 m/s^2) and h is the height of the liquid:

$$P = P_{atm} + \rho g h \quad (1)$$

The height of the 10 mL water column within the tubes was about 6 cm. Using the density of water and substituting the appropriate values into Equation 1, the hydrostatic pressure of the liquid medium, before any evaporation, is 5.9 mbar. As such, should the methanogen cells have collected at the bottom of the test tube during each experiment (the tubes were kept upright during the course of the experiments), the minimum pressures for each experiment are, in reality, ~6 mbar greater than the pressures quoted in each experiment. Thus, the minimum pressure for Experiments 5 and 6, which aimed to incorporate the average martian surface pressure of 6 mbar, was initially slightly higher (~12-13 mbar). However, as the liquid continued to evaporate, the decrease in the height of the water column would also decrease the hydrostatic pressure. Although these pressures are slightly higher than desired, they are still comparable to pressures at the martian surface, specifically in the Hellas basin region (Spiga et al., 2007).

The evaporation of the liquid media [~2 mm/hr at 7 mbar and 20 °C; Sears and Moore (2005)] constitutes the limiting factor to experiment length for experiments below 37 mbar (Expts. 4, 5, 6). This necessitates either the replenishment of liquid water throughout the duration of the experiment or the use of diffusion barriers to slow the rate of evaporation (as in Experiment 6). The use of five grams JSC Mars-1 in Experiment 6 did prolong the experiment by two days (compared to Experiment 5), though the pressure was slightly higher in Experiment 6 (7-20 mbar vs. 6-10 mbar). One option to reduce the rate of evaporation is to reduce the temperature of the chamber to 0 °C. Another option would be to use brines, such as $MgSO_4$ or $CaCl_2$, which can significantly reduce the rate of evaporation (Altheide et al., 2009; Sears and Chittenden, 2005), although these would both introduce additional stressors to the methanogens.

In order to assess the effect of evaporation, the electrical conductivity, salinity and TDS of the remaining liquid media within the original cultures, as well as the transfer cultures, were measured. Significant evaporation occurred in Experiments 4, 5, and 6, as expected, but sufficient liquid remained in Experiment 4 to measure both the original and transfer cultures. The twenty culture tubes in Experiment 4 experienced variable rates of evaporation, with greater evaporation occurring in the front row of test tubes. This discrepancy in evaporation may be due to the airflow through the chamber as a result of the fan within the palladium catalyst apparatus. The original cultures in Experiments 5 and 6 retained sufficient liquid media to perform transfers to new media, although electrical conductivity, salinity and TDS measurements were not possible in these tubes (Tables 3.2-3.4). For Experiments 1-4, there was no clear trend or increase in electrical conductivity, salinity or TDS values between the original and transfer cultures, or between experiments. The electrical conductivity, salinity and TDS of uninoculated media were also measured for comparison. Values for original and transfer cultures within each

experiment were typically greater than uninoculated media. In general, differences in values between original and transfer cultures within each experiment did not vary greatly (Expts. 1-4; Tables 3.2-3.4). The greatest differences occurred in cultures of *M. maripaludis*, which is expected due to the higher salt content of this medium.

The most significant evaporation occurred in Experiments 5 and 6 and insufficient liquid remained to analyze the resulting salinity of the media within the original cultures, although it is certain the salinities would increase. Electrical conductivity, salinity and TDS values for transfer cultures of Experiments 5 and 6 (where applicable) were typically higher than values for original and transfer cultures of Experiments 1-4, as well as values for uninoculated media. A better assessment of methanogen tolerance to brines, however, requires a much more in-depth assessment of electrical conductivity, salinity, and TDS values over time, in conjunction with methane production.

The creation of low-pressure "micro-environments" in Experiment 7 eliminated the risk of evaporation and allowed for a much longer exposure period (21 days), compared to the other six experiments (Table 3.1). Future experiments attempting to demonstrate survival at pressures lower than 50 mbar would require adequate temperature control to also maintain the vapor pressure of the liquid media.

The four methanogens tested in these experiments were chosen as the type strains of their species while also representing three (*Methanobacteriales*, *Methanococcales*, and *Methanosarcinales)* of the seven methanogenic orders. The aim was to address the possible stress responses to low pressure from a variety of methanogenic Archaea. However, methane production was relatively similar for both pre-exposure and post-exposure cultures for each of the four species. Previous studies in this lab have demonstrated the hardiness of *M. barkeri*, *M.*

formicicum, and *M. wolfeii* when exposed to relatively harsh conditions, whereas *M. maripaludis* often displays lower tolerability (Kendrick and Kral, 2006; Kral and Altheide, 2013; Kral et al., 2011; Kral et al., 2004). Previously, Kral et al. (2011) investigated the effect of low pressure on active and desiccated cells. *M. barkeri*, *M. wolfeii*, and *M. formicicum* all produced methane at both 400 mbar and 50 mbar on JSC Mars-1, although methane production was reduced at 50 mbar compared to 400 mbar. In terms of desiccation at 1 bar, *M. barkeri* survived 330 days, *M. wolfeii* survived 180 days, *M. formicicum* survived 120 days and *M. maripaludis* did not survive at all. At 6 mbar, desiccated cells of *M. barkeri*, *M. wolfeii*, and *M. formicicum* survived 120 days desiccation, while *M. maripaludis* only survived for 60 days (Kral et al., 2011). The differences in survivability may be attributable to the differences in cell wall composition and morphology of the cells. *Methanosarcina* species are known for their large genomes with many redundant coding sequences (Anderson et al., 2012). These redundancies are believed to be responsible for the organisms' abilities to endure a broader range of environments through both the ability to use multiple substrates for metabolism (H_2/CO_2, carbon monoxide, methanol, methyl compounds, acetate), as well as the formation of complex structures that could aid in protection. For example, *Methanosarcina* are the only methanogens that typically form multicellular aggregates embedded in an extracellular polysaccharide, which aids in protection against desiccation and oxygen exposure (Anderson et al., 2012). Additionally, *Methanosarcina* have thick (~0.18 microns) and rigid cell walls (Kandler and Hippe, 1977). In contrast, the cell wall of *M. maripaludis* consists of a single electron dense layer (~10 nm) and the cell envelope is relatively fragile (Jones et al., 1983). The apparent higher sensitivity of *M. maripaludis* to low pressure as seen here (see Figs. 3.3, 3.4; Experiments 6, 7), and desiccation, as in previous studies (Kral and Altheide, 2013; Kral et al., 2011), may be attributable to the relatively weaker

cell wall, whereas *Methanosarcina* and *Methanobacterium* both contain thick, rigid cell walls composed of specific polymers (Kandler and König, 1978). Overall, however, archaeal lipid membranes typically have higher rigidity and stability, as well as lower permeability to protons and higher salt tolerance, as compared to those of bacteria and eukarya, which promotes tolerance of harsher environments (van de Vossenberg et al., 1998).

Methanogens also contain a number of unique mechanisms for dealing with osmoadaptation and osmoregulation. Even in low-salt conditions, Archaea typically contain high concentrations of intracellular potassium ions (K^+). As such, many Archaea have evolved salt-tolerant enzymes that consist of mainly acidic amino acids, which gives an overall negative charge to the protein and prevents folding unless K^+ is available (Martin et al., 1999). Aside from the typical response of osmosis in order to counterbalance salt concentration, many methanogens also incorporate compatible solutes, or osmolytes, as a long-term adaptation technique. However, due to the normally high concentration of K^+ ions in the cell, potassium is an inadequate compatible solute and other solutes are typically used (Martin et al., 1999). There are two main ways that compatible solutes stabilize proteins. First, osmolytes tend to destabilize the unfolded protein compared to the folded structure, which keeps the protein intact. Also, osmolytes utilize differences in physical properties, such as the density of water, to maintain equilibrium at interface regions (Roberts, 2004).

The lack of experiments studying the effects of low pressure on growth, metabolism and survival of organisms suggests that low pressure has not necessarily been deemed an important biocidal factor when considering life on other planets, specifically Mars. Few studies have very recently begun to address the issue of low pressure with the conclusions noting that pressure may have more of an effect on growth than has previously been believed (Fajardo-Cavazos et al.,

2012; Nicholson et al., 2013; Schuerger et al., 2013). Schuerger et al. (2013) tested the ability of 26 strains of 22 bacterial species to grow under low pressure (7 mbar), low temperature (0 °C), and a CO_2-dominated anoxic atmosphere. Of these 26 strains, only *Serratia liquefaciens* ATCC 27592 exhibited obvious growth under these conditions. Although the synergistic effects of pressure, temperature, and anoxia may have contributed to the death of many of these species, Schuerger et al. (2013) also discovered that when looking at pressure separately, most species were inhibited at 25 mbar. In addition, of the six bacterial strains that grew at 25 mbar, all of them exhibited smaller colonies compared to those grown at 1013 mbar or 100 mbar (Schuerger et al., 2013). The inability for a number of strains to grow at low pressure, along with changes in colony morphology, signify the importance of studying the effects of low pressure as an inhibitor of growth and survival.

The recent and ongoing studies of low pressure focus on various bacterial strains commonly found on spacecraft or in clean rooms, in terms of planetary protection. However, the synergistic effects of multiple potentially biocidal factors (low pressure, low temperature, CO_2 atmosphere) can overwhelm the organism, resulting in death (Schuerger et al., 2013). Methanogens are ideal candidates for life on Mars because they are anaerobic, non-photosynthetic, and do not require organic nutrients. These factors alone warrant further investigation into the survivability and growth of methanogens under martian conditions. In the work of Schuerger et al. (2013), 12 of the 26 bacterial strains tested were unable to grow in a CO_2 atmosphere at any pressure. The anaerobic nature of methanogens removes the CO_2 atmosphere of Mars as a potential biocidal factor considering the fact that many methanogens require CO_2 as a carbon source. Although this characteristic also makes methanogens unlikely to persist on spacecraft within clean rooms, if cells did remain on spacecraft prior to launch,

survival following long-term desiccation of these microorganisms has already been shown (Kral and Altheide, 2013; Kral et al., 2011). The ability of methanogens to remain viable following desiccation and actively grow under CO_2 atmospheres warrants further investigation in terms of planetary protection, mainly forward contamination, alone.

As stated previously (Kral and Altheide, 2013; Kral et al., 2014; Kral et al., 2016), these experiments were not intended to mimic actual martian conditions, but rather, in this case, to study survival of methanogens exposed to pressures approaching those at the martian surface.

Future work will attempt in situ methane measurements within the Pegasus Planetary Simulation Chamber to determine if the methanogens are actively metabolizing under low pressure conditions. These experiments will make use of one or more of the options above (low temperature, regolith as diffusion barrier, brines, "micro-environments") in order to slow the evaporation rate of the liquid media and prolong the experiment.

3.6 Conclusions

Four species of methanogen (*M. barkeri*, *M. formicicum*, *M. wolfeii*, *M. maripaludis*) were tested for their ability to survive pressures approaching average martian surface pressures. Hydrated cells from all four methanogen species survived varying lengths of exposure (3 days – 21 days) to pressures between 6 mbar and 143 mbar. The limiting factor in most of the experiments was the evaporation of the liquid media. Future work will attempt to prolong experiment length (by decreasing the rate of evaporation) through the use of brines and analog regolith as diffusion barriers, and/or creating "micro-environments" as described.

3.7 Acknowledgements

The authors thank Dr. Chris McKay for his helpful suggestions during the review process. The authors would like to acknowledge Walter Graupner at the Arkansas Center for Space and Planetary Sciences for his research assistance. The authors would also like to thank Larry Joe Steeley Jr. (Rainbow Technology, Pelham, AL) for his donation of duct seal putty. This research was supported by a grant from the National Aeronautics and Space Administration (NASA) Astrobiology: Exobiology and Evolutionary Biology Program, grant #NNX12AD90G and by grants from the Arkansas Space Grant Consortium.

3.8 References

Altheide, T., Chevrier, V., Nicholson, C., Denson, J. (2009) Experimental investigation of the stability and evaporation of sulfate and chloride brines on Mars. *Earth and Planetary Science Letters* 282, 69-78.

Anderson, K.L., Apolinario, E.E., Sowers, K.R. (2012) Desiccation as a long-term survival mechanism for the archaeon *Methanosarcina barkeri*. *Applied and Environmental Microbiology* 78, 1473-1479.

Atreya, S.K., Gu, Z.G. (1994) Stability of the Martian atmosphere: Is heterogeneous catalysis essential? *Journal of Geophysical Research: Planets (1991–2012)* 99, 13133-13145.

Atreya, S.K., Mahaffy, P.R., Wong, A.-S. (2007) Methane and related trace species on Mars: Origin, loss, implications for life, and habitability. *Planetary and Space Science* 55, 358-369.

Barth, C.A., Fastie, W.G., Hord, C.W., Pearce, J.B., Kelly, K.K., Stewart, A.I., Thomas, G.E., Anderson, G.P., Raper, O.F. (1969) Mariner 6: Ultraviolet spectrum of Mars upper atmosphere. *Science* 165, 1004-1005.

Boone, D.R., Johnson, R.L., Liu, Y. (1989) Diffusion of the interspecies electron carriers H_2 and formate in methanogenic ecosystems and its implications in the measurement of K_m for H_2 or formate uptake. *Applied and Environmental Microbiology* 55, 1735-1741.

Boston, P.J., Ivanov, M.V., McKay, C.P. (1992) On the possibility of chemosynthetic ecosystems in subsurface habitats on Mars. *Icarus* 95, 300-308.

Boynton, W.V., Feldman, W.C., Squyres, S.W., Prettyman, T.H., Brückner, J., Evans, L.G., Reedy, R.C., Starr, R., Arnold, J.R., Drake, D.M., Engler, P. A. J., Metzger, A.E., Mitrofanov, I., Trombka, J. I., d'Uston, C., Wänke, H., Gasnault, O., Hamara, D.K., Janes, D.M., Marcialis, R.L., Maurice, S., Mikheeva, I., Taylor, G.J., Tokar, R., Shinohara, C. (2002) Distribution of hydrogen in the near surface of Mars: Evidence for subsurface ice deposits. *Science* 297, 81-85.

Chassefière, E., Leblanc, F. (2011) Constraining methane release due to serpentinization by the observed D/H ratio on Mars. *Earth and Planetary Science Letters* 310, 262-271.

Chastain, B.K., Chevrier, V. (2007) Methane clathrate hydrates as a potential source for martian atmospheric methane. *Planetary and Space Science* 55, 1246-1256.

Clancy, R.T., Muhleman, D.O., Jakosky, B.M. (1983) Variability of carbon monoxide in the Mars atmosphere. *Icarus* 55, 282-301.

Daniels, L., Fuchs, G., Thauer, R.K., Zeikus, J.G. (1977) Carbon monoxide oxidation by methanogenic bacteria. *Journal of Bacteriology* 132, 118-126.

Fajardo-Cavazos, P., Waters, S.M., Schuerger, A.C., George, S., Marois, J.J., Nicholson, W.L. (2012) Evolution of *Bacillus subtilis* to Enhanced Growth at Low Pressure: Up-Regulated Transcription of *des-desKR*, Encoding the Fatty Acid Desaturase System. *Astrobiology* 12, 258-270.

Feldman, W.C., Boynton, W.V., Tokar, R.L., Prettyman, T.H., Gasnault, O., Squyres, S.W., Elphic, R.C., Lawrence, D.J., Lawson, S.L., Maurice, S. (2002) Global distribution of neutrons from Mars: Results from Mars Odyssey. *Science* 297, 75-78.

Fonti, S., Marzo, G.A. (2010) Mapping the methane on Mars. *Astronomy and Astrophysics* 512.

Formisano, V., Atreya, S., Encrenaz, T., Ignatiev, N., Giuranna, M. (2004) Detection of methane in the atmosphere of Mars. *Science* 306, 1758-1761.

Gandolfi, I., Bertolini, V., Ambrosini, R., Bestetti, G., Franzetti, A. (2013) Unravelling the bacterial diversity in the atmosphere. *Applied microbiology and biotechnology* 97, 4727-4736.

Geminale, A., Formisano, V., Giuranna, M. (2008) Methane in Martian atmosphere: average spatial, diurnal, and seasonal behaviour. *Planetary and Space Science* 56, 1194-1203.

Geminale, A., Formisano, V., Sindoni, G. (2011) Mapping methane in Martian atmosphere with PFS-MEX data. *Planetary and Space Science* 59, 137-148.

Griffin, D.W. (2004) Terrestrial microorganisms at an altitude of 20,000 m in Earth's atmosphere. *Aerobiologia* 20, 135-140.

Griffin, D.W. (2008) Non-spore forming eubacteria isolated at an altitude of 20,000 m in Earth's atmosphere: extended incubation periods needed for culture-based assays. *Aerobiologia* 24, 19-25.

Grimm, R.E., Harrison, K.P., Stillman, D.E. (2014) Water budgets of martian recurring slope lineae. *Icarus* 233, 316-327.

Haberle, R.M., McKay, C.P., Schaeffer, J., Cabrol, N.A., Grin, E.A., Zent, A.P., Quinn, R. (2001) On the possibility of liquid water on present-day Mars. *Journal of Geophysical Research: Planets (1991-2012)* 106, 23317-23326.

Hess, S.L., Henry, R.M., Tillman, J.E. (1979) The seasonal variation of atmospheric pressure on Mars as affected by the south polar cap. *Journal of Geophysical Research: Solid Earth (1978–2012)* 84, 2923-2927.

Hess, S.L., Ryan, J.A., Tillman, J.E., Henry, R.M., Leovy, C.B. (1980) The annual cycle of pressure on Mars measured by Viking landers 1 and 2. *Geophysical Research Letters* 7, 197-200.

Johnson, A.P., Pratt, L.M., Vishnivetskaya, T., Pfiffner, S., Bryan, R.A., Dadachova, E., Whyte, L., Radtke, K., Chan, E., Tronick, S. (2011) Extended survival of several organisms and amino acids under simulated martian surface conditions. *Icarus* 211, 1162-1178.

Jones, E.G., Lineweaver, C.H., Clarke, J.D. (2011) An extensive phase space for the potential martian biosphere. *Astrobiology* 11, 1017-1033.

Jones, W.J., Paynter, M.J.B., Gupta, R. (1983) Characterization of *Methanococcus maripaludis* sp. nov., a new methanogen isolated from salt marsh sediment. *Archives of Microbiology* 135, 91-97.

Kandler, O., Hippe, H. (1977) Lack of peptidoglycan in the cell walls of *Methanosarcina barkeri*. *Archives of Microbiology* 113, 57-60.

Kandler, O., König, H. (1978) Chemical composition of the peptidoglycan-free cell walls of methanogenic bacteria. *Archives of Microbiology* 118, 141-152.

Kendrick, M.G., Kral, T.A. (2006) Survival of methanogens during desiccation: implications for life on Mars. *Astrobiology* 6, 546-551.

King, G.M. (2015) Carbon monoxide as a metabolic energy source for extremely halophilic microbes: implications for microbial activity in Mars regolith. *Proceedings of the National Academy of Sciences of the United States of America* 112, 4465-4470.

Kral, T.A., Altheide, T.S. (2013) Methanogen survival following exposure to desiccation, low pressure and martian regolith analogs. *Planetary and Space Science* 89, 167-171.

Kral, T.A., Altheide, T.S., Lueders, A.E., Schuerger, A.C. (2011) Low pressure and desiccation effects on methanogens: Implications for life on Mars. *Planetary and Space Science* 59, 264-270.

Kral, T.A., Bekkum, C.R., McKay, C.P. (2004) Growth of methanogens on a Mars soil simulant. *Origins of Life and Evolution of the Biosphere* 34, 615-626.

Kral, T.A., Birch, W., Lavender, L.E., Virden, B.T. (2014) Potential use of highly insoluble carbonates as carbon sources by methanogens in the subsurface of Mars. *Planetary and Space Science* 101, 181-185.

Kral, T.A., Brink, K.M., Miller, S.L., McKay, C.P. (1998) Hydrogen consumption by methanogens on the early Earth. *Origins of Life and Evolution of Biospheres* 28, 311-319.

Kral, T.A., Goodhart, T.H., Harpool, J.D., Hearnsberger, C.E., McCracken, G.L., McSpadden, S.W. (2016) Sensitivity and adaptability of methanogens to perchlorates: Implications for life on Mars. *Planetary and Space Science* 120, 87-95.

Krasnopolsky, V.A. (1993) Photochemistry of the Martian atmosphere (mean conditions). *Icarus* 101, 313-332.

Krasnopolsky, V.A. (2007) Long-term spectroscopic observations of Mars using IRTF/CSHELL: Mapping of O_2 dayglow, CO, and search for CH_4. *Icarus* 190, 93-102.

Krasnopolsky, V.A., Bjoraker, G.L., Mumma, M.J., Jennings, D.E. (1997) High-resolution spectroscopy of Mars at 3.7 and 8 μm: A sensitive search for H_2O_2, H_2CO, HCl, and CH_4, and detection of HDO. *Journal of Geophysical Research* 102, 6525-6534.

Krasnopolsky, V.A., Feldman, P.D. (2001) Detection of molecular hydrogen in the atmosphere of Mars. *Science* 294, 1914-1917.

Krasnopolsky, V.A., Maillard, J.P., Owen, T.C. (2004) Detection of methane in the martian atmosphere: evidence for life? *Icarus* 172, 537-547.

Lellouch, E., Encrenaz, T., Phillips, T., Falgarone, E., Billebaud, F. (1991) Submillimeter observations of CO in Mars' atmosphere. *Planetary and Space Science* 39, 209-212.

Lyons, J.R., Manning, C., Nimmo, F. (2005) Formation of methane on Mars by fluid-rock interaction in the crust. *Geophysical Research Letters* 32.

Maguire, W.C. (1977) Martian isotopic ratios and upper limits for possible minor constituents as derived from Mariner 9 infrared spectrometer data. *Icarus* 32, 85-97.

Malin, M.C., Edgett, K.S. (2000) Evidence for recent groundwater seepage and surface runoff on Mars. *Science* 288, 2330-2335.

Martin, D.D., Ciulla, R.A., Roberts, M.F. (1999) Osmoadaptation in Archaea. *Applied and Environmental Microbiology* 65, 1815-1825.

Martín-Torres, F.J., Zorzano, M.-P., Valentín-Serrano, P., Harri, A.-M., Genzer, M., Kemppinen, O., Rivera-Valentin, E.G., Jun, I., Wray, J., Madsen, M.B., Goetz, W., McEwen, A.S., Hardgrove, C., Renno, N., Chevrier, V.F., Mischna, M., Navarro-González, R., Martínez-Frías, J., Conrad, P., McConnochie, T., Cockell, C., Berger, G., Vasavada, A.R., Sumner, D., Vaniman, D. (2015) Transient liquid water and water activity at Gale crater on Mars. *Nature Geoscience* 8, 357-361.

McCollom, T.M., Bach, W. (2009) Thermodynamic constraints on hydrogen generation during serpentinization of ultramafic rocks. *Geochimica et Cosmochimica Acta* 73, 856-875.

McEwen, A.S., Dundas, C.M., Mattson, S.S., Toigo, A.D., Ojha, L., Wray, J.J., Chojnacki, M., Byrne, S., Murchie, S.L., Thomas, N. (2014) Recurring slope lineae in equatorial regions of Mars. *Nature Geoscience* 7, 53-58.

McEwen, A.S., Ojha, L., Dundas, C.M., Mattson, S.S., Byrne, S., Wray, J.J., Cull, S.C., Murchie, S.L., Thomas, N., Gulick, V.C. (2011) Seasonal flows on warm martian slopes. *Science* 333, 740-743.

Mitrofanov, I., Anfimov, D., Kozyrev, A., Litvak, M., Sanin, A., Tret'yakov, V., Krylov, A., Shvetsov, V., Boynton, W., Shinohara, C., Hamara, D., Saunders, R.S. (2002) Maps of subsurface hydrogen from the high energy neutron detector, Mars Odyssey. *Science* 297, 78-81.

Morozova, D., Möhlmann, D., Wagner, D. (2007) Survival of Methanogenic Archaea from Siberian Permafrost under Simulated Martian Thermal Conditions. *Origins of Life and Evolution of Biospheres* 37, 189-200.

Mumma, M.J., Villanueva, G.L., Novak, R.E., Hewagama, T., Bonev, B.P., DiSanti, M.A., Mandell, A.M., Smith, M.D. (2009) Strong release of methane on Mars in northern summer 2003. *Science* 323, 1041-1045.

Nair, H., Allen, M., Anbar, A.D., Yung, Y.L., Clancy, R.T. (1994) A photochemical model of the martian atmosphere. *Icarus* 111, 124-150.

Ni, S., Boone, D.R. (1991) Isolation and characterization of a dimethyl sulfide-degrading methanogen, *Methanolobus siciliae* HI350, from an oil well, characterization of *M. siciliae* T4/M^T, and emendation of *M. siciliae*. *International Journal of Systematic Bacteriology* 41, 410-416.

Nicholson, W.L., Krivushin, K., Gilichinsky, D., Schuerger, A.C. (2013) Growth of *Carnobacterium* spp. from permafrost under low pressure, temperature, and anoxic atmosphere has implications for Earth microbes on Mars. *Proceedings of the National Academy of Sciences of the United States of America* 110, 666-671.

O'Brien, J.M., Wolkin, R.H., Moench, T.T., Morgan, J.B., Zeikus, J.G. (1984) Association of hydrogen metabolism with unitrophic or mixotrophic growth of *Methanosarcina barkeri* on carbon monoxide. *Journal of Bacteriology* 158, 373-375.

Ojha, L., Wilhelm, M.B., Murchie, S.L., McEwen, A.S., Wray, J.J., Hanley, J., Massé, M., Chojnacki, M. (2015) Spectral evidence for hydrated salts in recurring slope lineae on Mars. *Nature Geoscience* 8, 829-832.

Onstott, T.C., McGown, D., Kessler, J., Sherwood Lollar, B., Lehmann, K.K., Clifford, S.M. (2006) Martian CH_4: sources, flux, and detection. *Astrobiology* 6, 377-395.

Oze, C., Sharma, M. (2005) Have olivine, will gas: Serpentinization and the abiogenic production of methane on Mars. *Geophysical Research Letters* 32.

Rennó, N.O., Bos, B.J., Catling, D., Clark, B.C., Drube, L., Fisher, D., Goetz, W., Hviid, S.F., Keller, H.U., Kok, J.F., Kounaves, S.P., Leer, K., Lemmon, M., Madsen, M.B., Markiewicz, W.J., Marshall, J., McKay, C., Mehta, M., Smith, M., Zorzano, M.P., Smith, P.H., Stoker, C., Young, S.M.M. (2009) Possible physical and thermodynamical evidence for liquid water at the Phoenix landing site. *Journal of Geophysical Research: Planets (1991–2012)* 114.

Roberts, M.F. (2004) Osmoadaptation and osmoregulation in Archaea: update 2004. *Frontiers in Bioscience* 9, 1999-2019.

Schirmack, J., Böhm, M., Brauer, C., Löhmannsröben, H.-G., de Vera, J.-P., Möhlmann, D., Wagner, D. (2014) Laser spectroscopic real time measurements of methanogenic activity under simulated Martian subsurface analog conditions. *Planetary and Space Science* 98, 198-204.

Schuerger, A.C., Golden, D.C., Ming, D.W. (2012) Biotoxicity of Mars soils: 1. Dry deposition of analog soils on microbial colonies and survival under Martian conditions. *Planetary and Space Science* 72, 91-101.

Schuerger, A.C., Ulrich, R., Berry, B.J., Nicholson, W.L. (2013) Growth of *Serratia liquefaciens* under 7 mbar, 0 degrees C, and CO_2-enriched anoxic atmospheres. *Astrobiology* 13, 115-131.

Sears, D.W., Chittenden, J.D. (2005) On laboratory simulation and the temperature dependence of the evaporation rate of brine on Mars. *Geophysical Research Letters* 32.

Sears, D.W., Moore, S.R. (2005) On laboratory simulation and the evaporation rate of water on Mars. *Geophysical Research Letters* 32.

Smith, D.J., Griffin, D.W., Schuerger, A.C. (2010) Stratospheric microbiology at 20 km over the Pacific Ocean. *Aerobiologia* 26, 35-46.

Smith, P.H., Tamppari, L.K., Arvidson, R.E., Bass, D., Blaney, D., Boynton, W.V., Carswell, A., Catling, D.C., Clark, B.C., Duck, T., DeJong, E., Fisher, D., Goetz, W., Gunnlaugsson, H.P., Hecht, M.H., Hipkin, V., Hoffman, J., Hviid, S.F., Keller, H.U., Kounaves, S.P., Lange, C.F., Lemmon, M.T., Madsen, M.B., Markiewicz, W.J., Marshall, J., McKay, C.P., Mellon, M.T., Ming, D.W., Morris, R.V., Pike, W.T., Renno, N., Staufer, U.,

Stoker, C., Taylor, P., Whiteway, J.A., Zent, A.P. (2009) H_2O at the Phoenix landing site. *Science* 325, 58-61.

Sowers, K.R., Schreier, H. (1995) *Archaea. A Laboratory Manual. Methanogens*. Cold Spring Harbor Laboratory Press.

Spiga, A., Forget, F., Dolla, B., Vinatier, S., Melchiorri, R., Drossart, P., Gendrin, A., Bibring, J.-P., Langevin, Y., Gondet, B. (2007) Remote sensing of surface pressure on Mars with the Mars Express/OMEGA spectrometer: 2. Meteorological maps. *Journal of Geophysical Research: Planets (1991–2012)* 112.

Stillman, D.E., Michaels, T.I., Grimm, R.E., Harrison, K.P. (2014) New observations of martian southern mid-latitude recurring slope lineae (RSL) imply formation by freshwater subsurface flows. *Icarus* 233, 328-341.

Tortora, G.J., Funke, B.R., Case, C.L. (2015) *Microbiology: An Introduction, 12th Ed.*

Usui, T., Alexander, C.M.D., Wang, J., Simon, J.I., Jones, J.H. (2015) Meteoritic evidence for a previously unrecognized hydrogen reservoir on Mars. *Earth and Planetary Science Letters* 410, 140-151.

van de Vossenberg, J.L., Driessen, A.J., Konings, W.N. (1998) The essence of being extremophilic: the role of the unique archaeal membrane lipids. *Extremophiles* 2, 163-170.

Webster, C.R., Mahaffy, P.R., Atreya, S.K., Flesch, G.J., Farley, K.A., the MSL Science Team (2013) Low Upper Limit to Methane Abundance on Mars. *Science* 342, 355-357.

Webster, C.R., Mahaffy, P.R., Atreya, S.K., Flesch, G.J., Mischna, M.A., Meslin, P.-Y., Farley, K.A., Conrad, P.G., Christensen, L.E., Pavlov, A.A., Martín-Torres, J., Zorzano, M.-P., McConnochie, T.H., Owen, T., Eigenbrode, J.L., Glavin, D.P., Steele, A., Malespin, C.A., Archer Jr., P.D., Sutter, B., Coll, P., Freissinet, C., McKay, C.P., Moores, J.E., Schwenzer, S.P., Bridges, J.C., Navarro-Gonzalez, R., Gellert, R., Lemmon, M.T., the MSL Science Team (2015) Mars methane detection and variability at Gale crater. *Science* 347, 415-417.

Weiss, B.P., Yung, Y.L., Nealson, K.H. (2000) Atmospheric energy for subsurface life on Mars? *Proceedings of the National Academy of Sciences* 97, 1395-1399.

Wray, J.J., Ehlmann, B.L. (2011) Geology of possible Martian methane source regions. *Planetary and Space Science* 59, 196-202.

Xun, L., Boone, D.R., Mah, R.A. (1988) Control of the life cycle of *Methanosarcina mazei* S-6 by manipulation of growth conditions. *Applied and Environmental Microbiology* 54, 2064-2068.

Chapter 4. Low Pressure Microenvironments: Methane Production at 50 mbar and 100 mbar

R. L. Mickol[1] and T.A. Kral[1,2]

[1]Arkansas Center for Space and Planetary Sciences, University of Arkansas, Fayetteville, AR;

[2]Dept. of Biological Sciences, University of Arkansas, Fayetteville, AR;

4.1 Abstract

Low pressure is often overlooked in terms of possible biocidal effects when considering a habitable environment on Mars. Few experiments have investigated the ability for microorganisms to actively grow under low pressure conditions, despite the atmosphere being the only location on Earth where organisms could be exposed to these pressures. Three species of methanogens (*Methanobacterium formicicum, Methanosarcina barkeri*, *Methanococcus maripaludis*) were tested for their ability to actively grow (demonstrate an increase in methane production and optical density) within low-pressure microenvironments at 50 mbar or 100 mbar. *M. formicicum* was the only species to demonstrate both an increase in methane and an increase in optical density during the low-pressure exposure period for experiments conducted at 50 mbar and 100 mbar. In certain experiments, *M. barkeri* showed an increase in optical density during the low-pressure exposure period, but a decrease in methane abundance, likely due to the formation of multicellular aggregates. During incubation following exposure to low pressure, cultures of all species resumed methane production and increased in optical density. Thus, low pressure may not be a biocidal factor for certain methanogen species, with growth possible under low-pressure conditions. Results indicate that low pressure exposure may just be inhibitory during the exposure itself, and metabolism may resume following incubation under more ideal

conditions. Further work is needed to address growth/survival under more Mars-relevant pressures and temperatures.

4.2 Introduction

Few experiments have considered the biocidal nature of the low-pressure atmosphere of Mars or the effect that low pressure (<100 mbar) might have on microorganism growth or metabolism (Fajardo-Cavazos et al., 2012; Kral et al., 2011; Mickol and Kral, 2016; Nicholson et al., 2010; Nicholson et al., 2013; Schuerger and Nicholson, 2006; Schuerger and Nicholson, 2016; Schuerger et al., 2013; Waters et al., 2014; Waters et al., 2015). Schuerger and Nicholson (2016) and Schuerger et al. (2013) have previously proposed a potential "25 mbar limit" to growth at low pressure based on the analysis of over 150 bacterial strains. However, recent experiments suggest that survival and growth at low-pressure may be more common amongst certain genera such as *Serratia* or *Carnobacterium* (Nicholson et al., 2013; Schuerger and Nicholson, 2016). The effect on growth and metabolism of Archaea, however, remains relatively unknown as most studies have focused on bacterial isolates from diverse soils or spacecraft cleanrooms and do not include Archaea (Fajardo-Cavazos et al., 2012; Nicholson et al., 2010; Nicholson et al., 2013; Schuerger and Nicholson, 2006; Schuerger and Nicholson, 2016; Schuerger et al., 2013; Waters et al., 2014; Waters et al., 2015). Only four studies have analyzed archaeal growth or survival under low-pressure conditions, all of which have focused on methanogens and three of which have come from this lab (Kral and Altheide, 2013; Kral et al., 2011; Mickol and Kral, 2016; Schirmack et al., 2014).

Interest in methanogen growth at low pressure relates to the discovery of methane in the martian atmosphere (Fonti and Marzo, 2010; Formisano et al., 2004; Geminale et al., 2008;

Geminale et al., 2011; Krasnopolsky et al., 1997; Krasnopolsky et al., 2004; Maguire, 1977; Mumma et al., 2009; Webster et al., 2015) and that methanogenic activity is responsible for the majority of methane in Earth's atmosphere (Conrad, 2009; IPCC, 2013). The surface pressure on Mars averages between 1-10 mbar (Hess et al., 1979; Hess et al., 1980; Spiga et al., 2007) and increases very slowly with depth (Schuerger et al., 2013). Methanogens are anaerobic and non-photosynthetic chemolithotrophs, many of which utilize hydrogen (H_2) and carbon dioxide (CO_2) to produce methane (CH_4). The harsh ionizing radiation at the surface of Mars dictates that any extant life would likely be subsurface. Despite the overlying regolith, pore space between soil grains would still resemble the low-pressure conditions at the planet's surface, only reaching 25 mbar at 13.8 km below the martian surface (Schuerger et al., 2013). Higher pressures can be achieved in the near-subsurface of Mars, but this would require complete seclusion from the atmosphere so that gas-exchange and equilibration is not possible (Schuerger et al., 2013).

Methane production at 400 mbar and 50 mbar by two of the three methanogens (*Methanobacterium formicicum*, *Methanosarcina barkeri*) tested here has been shown previously by experiments in this lab, although experiments only lasted 12 days (50 mbar) or 18 days [400 mbar] (Kral et al., 2011). Additionally, the chamber environment was heated to 35 °C to promote growth and cultures were subject to desiccation over the course of the experiment. Schirmack et al. (2014) have also assessed methanogen growth under low pressure conditions. These experiments utilized the permafrost isolate, *Methanosarcina soligelidi*, and assessed methane production at low temperatures (-5 to 20 °C) at 500 mbar. In two experiments, cultures were initially incubated for one day at either 20 °C or 10 °C, during which most methane was produced. The temperature was then stepped down to 10 °C or 0 °C for 12 hours, before the temperature was lowered to 0 °C or -5 °C for the remainder of the experiment (5 days). Cultures

of *M. soligelidi* produced about 100 ppm methane at 0 °C for five days and about 350 ppm methane during five days at -5 °C, both at 500 mbar (Schirmack et al., 2014).

Three species of methanogens (*M. formicicum*, *M. barkeri*, *Methanococcus maripaludis*) were tested for their ability to actively grow (increase in methane production/optical density) within low-pressure microenvironments at 50 mbar or 100 mbar. The experiments conducted here were modeled after the microenvironment experiment in Mickol and Kral (2016). Previous experiments conducted at low pressure with methanogens in their typical, liquid, anaerobic growth media were subject to rapid evaporation due to the instability of water, when temperature is not maintained at low enough values (~0 °C). To resolve this issue, experiments discussed here only incorporated pressures down to 50 mbar (above the vapor pressure of water at ~30 °C) and test tubes were equilibrated to low pressure, then re-sealed, effectively creating individual microenvironments within each test tube.

4.3 Materials and Methods

4.3.1 Microbial Procedures

Methanogens were initially obtained from the American Type Culture Collection (ATCC; Manassas, VA), cultured in their respective anaerobic growth media, and kept at a temperature within the organisms' ideal growth range: *Methanococcus maripaludis* (ATCC 43000), MSH medium (Ni and Boone, 1991), 22 °C; *Methanosarcina barkeri* (ATCC 43569), MS medium (Boone et al., 1989), 37 °C; *Methanobacterium formicicum* (ATCC 33274), MSF medium (MS medium supplemented with formate), 37 °C. Media were prepared as described in Kendrick and Kral (2006) under anaerobic conditions in a 90:10 CO_2:H_2 gas Coy Anaerobic Chamber (Coy Laboratory Products Inc., Grass Lake Charter Township, MI) and dispensed into anaerobic

culture tubes at a rate of 10 mL per tube. The tubes were fitted with rubber stoppers and sealed with aluminum crimps as described in Boone et al. (1989), and autoclaved for sterilization. Prior to inoculation with the respective organisms, a solution of 2.5% sodium sulfide (~125 μL per 10 mL medium) was added to each culture tube to remove residual oxygen (Boone et al., 1989). The tubes were then pressurized with 2 bar H_2 and incubated at the organisms' respective growth temperatures. For each experiment, growth was monitored by methane production via gas chromatography (Shimadzu Scientific Instruments Inc., model GC-2014, Columbia, MD) and via optical density (OD_{600}, Spectronic 20D+, Spectronic Instruments, USA).

4.3.2 Pegasus Planetary Simulation Chamber

Low pressure experiments were conducted in the Pegasus Planetary Simulation Chamber, housed within the Arkansas Center for Planetary Sciences at the University of Arkansas, previously described (Kral et al., 2011). Experiments described here were initially modeled after the microenvironment experiment in Mickol and Kral (2016). Pressure setpoints (Table 4.1) were maintained using a MKS Type 651C pressure controller and MKS Type 253B throttling valve (MKS Instruments Inc., Andover, MA). All experiments were conducted at room temperature and the chamber was vented with room air following the period of exposure to low pressure. Pressures and exposure times are seen in Table 4.1.

Table 4.1 Experimental conditions for each of five experiments, including pressures and time exposed to low pressure. Each experiment consisted of five replicates for each of the methanogen species tested in 10 mL of their respective anaerobic growth medium. Incubations both pre- and post-exposure were conducted at the methanogens' respective growth temperatures

(*Methanosarcina barkeri* (*M.b.*), 37 °C, MS medium; *Methanobacterium formicicum* (*M.f.*), 37 °C, MSF medium; *Methanococcus maripaludis* (*M.m.*), 22 °C, MSH medium).

Expt.	Species used	Inoculum age (days)	Initial Incubation Period (days)	Evacuation/ Experimental Pressure (mbar)	# of evacuation cycles	Time for Equilibration of Chamber at Low Pressure (min)	Time for Equilibration Between Punctured Tubes and Chamber (min)	Length of Exposure to Low Pressure (days)	Average Temperature Inside Pegasus Chamber (°C)	Incubation Times Following Exposure (days)
1	*M. barkeri*, *M. formicicum*, *M. maripaludis*	87 (*M.f.*, *M.m.*, *M.b.*) 109 (*M.m.*2)	7	100.4±0.1	0	30	60	28	26.6±0.5	91
2	*M. barkeri*, *M. formicicum*, *M. maripaludis*	37 (*M.m.*, *M.b.*) 10 (*M.f.*)	7	49.8±0.1	2	30	60	35	28.9±2.0	63
3	*M. formicicum*	30, washed	7	50.1±0.1	1, CO_2 2, H_2/CO_2	30	60	49	27.7±1.7	77
4	*M. formicicum*	60, washed	7	49.9±0.2*	1, CO_2 2, H_2/CO_2	30	60	49	27.5±1.7	14

*The pressure control valve malfunctioned on Day 30 (of 49), dropping the chamber pressure to ~0.8 mbar. The tubes remained sealed and no significant evaporation was witnessed in any tubes. Thus, it is believed the ~50 mbar microenvironments remained intact for the duration of the experiment.

4.3.3 Experiment 1: Exposure of *M. barkeri*, *M. formicicum*, and *M. maripaludis* to 100 mbar for 28 days

Methanogens were initially grown in their respective anaerobic growth media, as described above (4.3.1 Microbial Procedures). The tubes were incubated at the methanogens' respective growth temperatures for 7 days. After the initial incubation period, each tube was tested for both methane production and optical density to determine initial growth.

Next, tubes were placed inside the Pegasus Planetary Simulation Chamber with a palladium catalyst box to remove residual oxygen (Fig. 1A). Within the chamber, twenty tubes (five replicates each for *M. barkeri* and *M. formicicum*, ten replicates for *M. maripaludis*; see Table 4.1) were situated inside a test tube rack, sorted randomly. A second test tube rack was placed over the top of the tubes to secure their position for use with a specialized puncture device (see Mickol and Kral [2016] for a description of the device; also see Fig. 1B). As a control, an additional seventeen tubes (five replicates each for *M. barkeri* and *M. formicicum*, five replicates for the 89-day-old cultures of *M. maripaludis* and two replicates for the 109-day-old cultures of

M. maripaludis; see Table 4.1) were situated inside an adjacent test tube rack. These tubes would not be punctured (i.e., exposed to low pressure), but would be exposed to the same temperature as the punctured (low-pressure) test tubes. Within both sets, one test tube was not initially inoculated to serve as a blank for optical density measurements. The chamber door was closed and duct seal putty (Rainbow Technology, Pelham, AL) was applied around the seal as a further safeguard against oxygen contamination. The seal between the puncture device and the chamber was also covered with duct seal putty. The chamber was evacuated to 100 mbar, 80:20 H_2:CO_2 gas was bled into the chamber and the system was left to equilibrate for 30 minutes. Next, the experimental tubes were punctured with the specialized puncture device containing one-inch, 22-gauge syringe needles for 60 minutes to allow equilibration between the chamber pressure and the pressure inside the tubes (see Mickol and Kral, 2016). After 60 min, the needles were removed from the tubes, effectively creating "low-pressure microenvironments" within each test tube, and the H_2:CO_2 gas was turned off. The chamber was actively maintained at 100 mbar for the duration of the experiment. After 28 days, the chamber was slowly vented with room air to atmospheric pressure. Test tubes were removed from the chamber and immediately tested for methane production and optical density. All tubes were re-pressurized with 1.9 bar H_2 and put at the organisms' respective incubation temperatures. Tubes were then monitored over time for methane production and optical density.

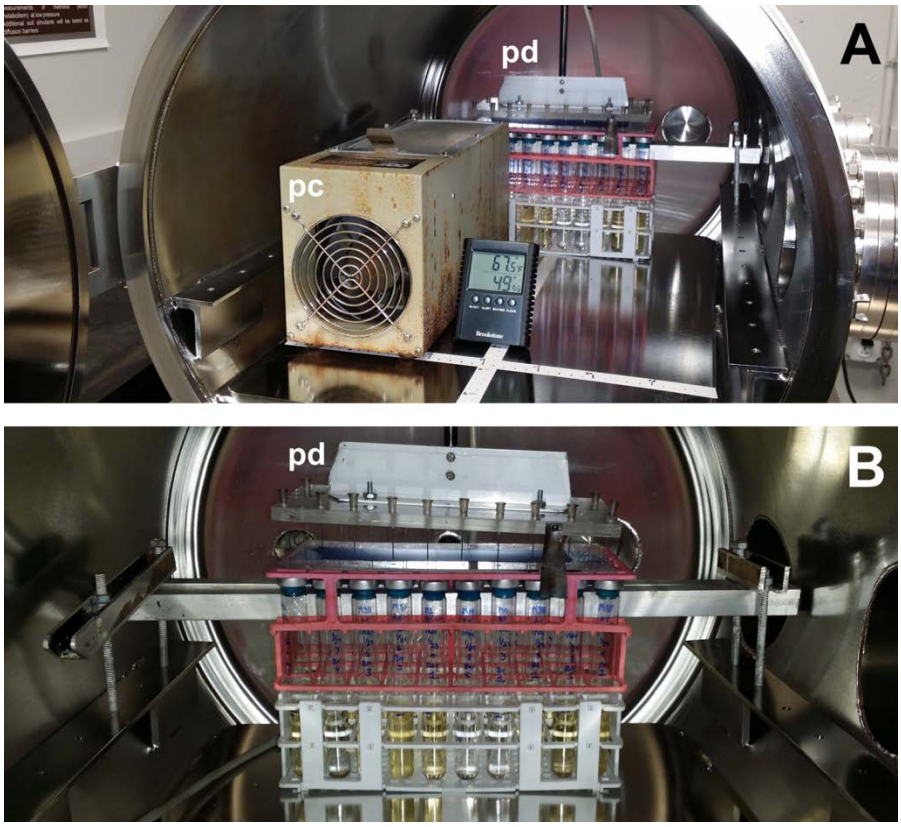

Figure 4.1 Photos depicting arrangement of test tubes within the Pegasus Planetary Simulation Chamber for each experiment. **A.** Experimental setup for each experiment: pd = puncture device, pc = palladium catalyst. **B.** Close-up view of the puncture device. The puncture device contains 22-gauge 1-inch syringe needles to puncture tubes and allow equilibration with the chamber atmosphere.

4.3.4 Experiment 2: Exposure of *M. barkeri*, *M. formicicum*, and *M. maripaludis* to 50 mbar for 35 days

Media were prepared as described in 4.3.1 Microbial Procedures, however, the oxygen indicator, resazurin, was not included. Although this removed the ability to determine extent of oxygen contamination within each test tube, it allowed for continued optical density measurements over time as the color of the media remained unchanged.

Experimental procedures were similar to those for Expt. 1, except for cycling between low pressure and atmospheric pressure before the tubes were punctured in order to ensure

removal of the ambient atmosphere. Test tubes were inoculated with 0.5 mL culture, pressurized with 2 bar H_2 and incubated for 7 days. Tubes were then measured for methane production and optical density to determine initial growth. Tubes were placed inside the chamber as described above for Expt. 1. The chamber was closed and evacuated to 50 mbar while CO_2 gas was bled in to the system. The chamber was then filled with CO_2 to atmospheric pressure and evacuated again. This cycle was repeated, the chamber was again evacuated to 50 mbar and the system was left to equilibrate for 30 min. Next, the CO_2 gas was turned off and the H_2/CO_2 (80:20) gas was turned on, while the chamber was maintained at 50 mbar. The test tubes were punctured as in Expt. 1. After 60 min, the needles were removed from the test tubes and the H_2/CO_2 gas was turned off. The chamber was actively maintained at 50 mbar for the duration of the experiment. After 35 days, the chamber was vented to the atmosphere and the test tubes were removed. All test tubes were immediately measured for methane production and optical density. After measurement, tubes were re-pressurized with 2 bar H_2 and stored at their incubation temperatures. Additional methane and optical density measurements were taken over time.

4.3.5 Experiment 3: Exposure of *M. formicicum* to 50 mbar for 49 days

This experiment utilized only cultures of *M. formicicum* and media did not contain resazurin, as in Expt 2. Additionally, cells were washed before inoculation in order to remove residual resazurin. Two, one-month-old cultures consisting of 10 mL MSF medium were combined, then poured into two large centrifuge tubes. Tubes were centrifuged at 5000 rpm for 45 min. Next, the supernatant was poured off, and 5 mL CO_2 buffer containing 2.5% sodium sulfide (Na_2S) were added to each centrifuge tube. The tubes were shaken to redistribute cells and centrifuged again at 5000 rpm for 45 min. The supernatant was poured off and 10 mL CO_2

buffer + Na_2S was added to each centrifuge tube. The centrifuge tubes were combined to form a single inoculum source. Thirty-five test tubes containing sterile MSF medium were then inoculated with 0.5 mL of washed *M. formicicum* cells (five tubes were not inoculated to serve as blanks). Each test tube was pressurized with 2 bar H_2 and incubated at 37 °C for 7 days. After incubation, tubes were measured for methane production and optical density to determine initial growth.

Chamber procedures were similar to those for Expts. 1 and 2. Tubes were placed into the Pegasus Planetary Simulation Chamber and the chamber was evacuated to 50 mbar while CO_2 was bled into the system. The chamber was filled to atmospheric pressure with CO_2, then the CO_2 was turned off and the H_2/CO_2 gas was turned on. The chamber was evacuated again to 50 mbar, then filled to atmospheric pressure with H_2/CO_2. This cycle was repeated, the chamber pressure was lowered to 50 mbar, and the system was left to equilibrate at 50 mbar for 30 min. Next, the test tubes were punctured and allowed to equilibrate with the low pressure of the chamber for 60 min, after which the needles were removed from the test tubes and the H_2/CO_2 gas turned off. The chamber was actively maintained at 50 mbar for the duration of the experiment. After 49 days, the chamber was vented to the atmosphere and the tubes were removed. The test tubes were immediately measured for methane production and optical density. Following measurement, tubes were re-pressurized with 2 bar H_2 and incubated at 37 °C. Methane and optical density continued to be monitored over time.

4.3.6 Experiment 4: Exposure of *M. formicicum* to 50 mbar for 49 days with and without formate-supplemented media

This experiment was intended to replicate Expt. 3, with slight modification. Two sets of media were prepared: Twenty test tubes contained 10 mL MSF medium (MS medium supplemented with formate), while twenty test tubes contained 10 mL MS medium (no formate). This was enacted to determine if the methanogens are capable of using H_2 as an energy source at low pressure, or if the formate within the medium was being used as the energy source. Similarly to Expts. 2 and 3, the media did not contain the oxygen indicator, resazurin.

Cells were also washed prior to inoculation, as in Expt. 3. Three, two-month-old 10-mL stock cultures were poured into large centrifuge tubes. The tubes were centrifuged for 45 min at 5000 rpm, after which the supernatant was poured off. Ten milliliters of sterile CO_2 buffer + Na_2S were added to each centrifuge tube and the tubes were shaken to redistribute pelleted cells. The tubes were centrifuged again at 5000 rpm for 45 min. Next, the supernatant was poured off and 10 mL CO_2 buffer + Na_2S was added to each centrifuge tube. The tubes were then combined to form one inoculum source. An aliquot of 0.5 mL of washed cells was added to each of 32 test tubes (sixteen containing formate, sixteen without formate). Eight test tubes remained un-inoculated to serve as blanks. The test tubes were pressurized with 2 bar H_2 and incubated at 37 °C for 7 days. After incubation, tubes were tested for methane production and optical density to determine initial growth.

As an additional control for methane production, twelve tubes were selected to serve as heat-killed controls. After measurements for initial growth were taken, twelve tubes were placed in a heat block for 1.5 h, where temperatures ranged between 80-86 °C, within each of the twelve

reservoirs. After heating, optical density measurements were taken again for these twelve replicates.

Chamber procedures were similar to those for Expt. 3. Tubes were placed within test tubes racked, assorted randomly. The chamber door was closed, sealed with duct seal putty, and the palladium catalyst box was turned on. The procedures for the initial evacuation of the chamber and the equilibration of the low-pressure tubes to the low pressure atmosphere of the chamber were identical to those in Expt. 3. After 49 days, the chamber was vented to the atmosphere and the tubes were removed. The low-pressure test tubes were immediately filled to just above atmospheric pressure (~0.07 bar) with CO_2 gas. This was conducted for two reasons: 1. To bring cultures to atmospheric pressure for headspace analysis and 2. To minimize oxygen contamination when headspace samples were removed from the test tubes. All test tubes were then equilibrated for 2 hours before methane production was measured via gas chromatography. Following measurement, all tubes were re-pressurized with 2 bar H_2 and incubated at 37 °C. Methane and optical density continued to be monitored over time.

4.3.7 Statistical procedures

Experimental replicates consisted of individual anaerobic Balch tubes containing 10 mL methanogen culture per tube. Experiments consisted of n = 3 to n = 16 per species per experiment. The specific number of replicates are given in Section 4.4 Results, as well as in figure captions.

Statistics were conducted for all experiments using GraphPad Prism version 6.01 (GraphPad Software, Inc., La Jolla, CA, USA). All experiments were analyzed by analysis of variance (ANOVA) followed by Šídák's multiple comparisons test ($P \leq 0.05$). Each species was

analyzed independently for each experiment (Expts. 1, 2). Data were subjected to different power transformations in order to induce homogeneity of variances (specific transformations are given in 4.8 Appendix A). Data in figures represent untransformed values.

4.4 Results

The number of replicates for each species within each experiment are given as n=#, below. In cases where optical density measurements were below zero, likely due to inaccuracies in light transmission through the test tubes, or where tubes became contaminated with oxygen, data were not included in the averages given.

4.4.1 Experiment 1: Exposure of *M. barkeri, M. formicicum*, and *M. maripaludis* to 100 mbar for 28 days

Methane production by *M. formicicum* in low-pressure tubes increased significantly from 2.93±0.73% (n = 3) on the day the tubes were placed inside the chamber (Day 7) to 4.82±0.41% on the day the tubes were removed from the chamber (Day 35; after exposure to 100 mbar for 28 days; $P \leq 0.05$). Methane in control tubes increased significantly from 3.69±0.13% to 33.71±12.36% (n = 4) over the course of the experiment (Fig. 4.2; $P \leq 0.0001$). One low-pressure replicate was not adequately punctured during the experiment, and thus, not exposed to the low-pressure environment. It is not included in the data shown here.

The optical density for *M. formicicum* low-pressure replicates also increased during exposure to low pressure (0.051±0.004 to 0.100±0.013; Fig. 4.2; $P \leq 0.001$). This increase in optical density is similar to the increase in optical density for the control tubes ($P > 0.05$). It is

important to note that the blank for the low-pressure replicates of *M. formicicum* became contaminated with oxygen during the low-pressure exposure period, and so the blank for the control tubes was used to measure the optical density of the low-pressure beginning on Day 35. The only difference between the blank for the control tubes and the blank for the low-pressure tubes is that the control blank was not subjected to low pressure at any point in time. Otherwise, the two blanks were subjected to the same conditions. It is highly unlikely that the low-pressure environment altered the media within the low-pressure blank in such a way as to cause a significant increase (> 0.01) in optical density and so the use of the control blank is warranted.

Methane production by *M. barkeri* was ~1.5% higher in the low-pressure tubes than in the control tubes following the initial 7-day incubation period at 37 °C ($P \leq 0.001$). After exposure to low-pressure, methane abundance decreased in low-pressure tubes ($P \leq 0.01$) and increased in control tubes ($P \leq 0.0001$) [Fig. 4.3). Although methane did not increase in low-pressure replicates, optical density increased significantly from 0.003±0.003 to 0.012±0.006 ($P \leq 0.05$; Fig. 4.3). Optical density ranged widely for the control tubes with one replicate measuring 0.044 on Day 35 and the other three replicates measuring ~0.02. There was no significant difference between the optical density of the low-pressure replicates and the optical density of the control replicates both before and after exposure of the experimental tubes to low pressure ($P > 0.05$). As with the *M. formicicum* blank, the low-pressure blank for *M. barkeri* was also contaminated with oxygen and thus, for optical density measurements beginning on Day 35, the control blank was used with the low-pressure tubes.

Methane production increased in three out of four low-pressure replicates for *M. maripaludis* over the period of exposure, but by very small amounts (0.33±0.04% to 0.93±0.21%). The methane abundance within one low-pressure replicate decreased slightly,

resulting in a shift in average methane abundance from 0.34±0.04% to 0.78±0.34% for all four replicates ($P > 0.05$). Control tubes increased in methane production by over 40% ($P \leq 0.0001$; Fig. 4.4). Optical density measurements decreased for the low-pressure replicates of *M. maripaludis* over the course of exposure to low pressure ($P > 0.05$), but increased greatly for the control replicates ($P \leq 0.0001$; Fig. 4.4).

This experiment included a second set of *M. maripaludis* cultures, initially inoculated from an older stock culture (see Table 4.1). Initial methane production was negligible (< 0.03% headspace) following the 7-day incubation period at 22 °C for both low-pressure replicates (n = 3) and control replicates (n = 2), although average values were significantly different between the two groups ($P \leq 0.05$). Methane increased by minor, yet statistically significant, amounts for the low-pressure replicates (0.62±0.20%; $P \leq 0.0001$) and to over 40% in the control tubes (Fig. 4.5; $P \leq 0.0001$). For this set, there was no blank for the control tubes and so the control blank for the first set of *M. maripaludis* cultures was used for optical density measurements throughout the duration of the experiment.

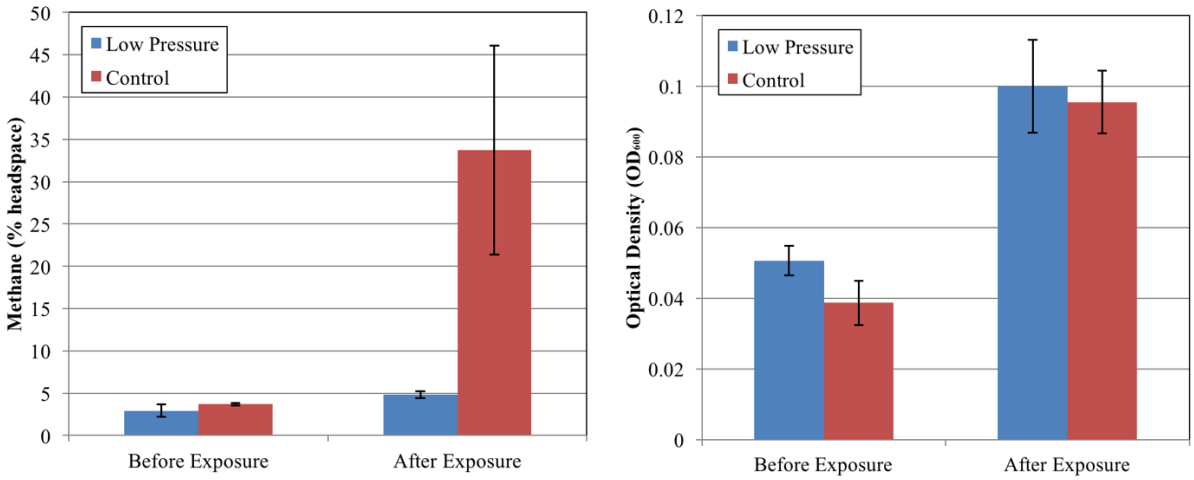

Figure 4.2 Methane production (left) and optical density (right) for *Methanobacterium formicicum* measured immediately before and immediately after exposure to low pressure (100 mbar). An initial incubation period took place at 37 °C for 7 days. Low Pressure tubes (n = 3)

were exposed to 100 mbar for 28 days. Control tubes (n = 4) were subjected to the same environmental conditions as the low-pressure tubes, except for pressure. Error bars indicate ± one standard deviation.

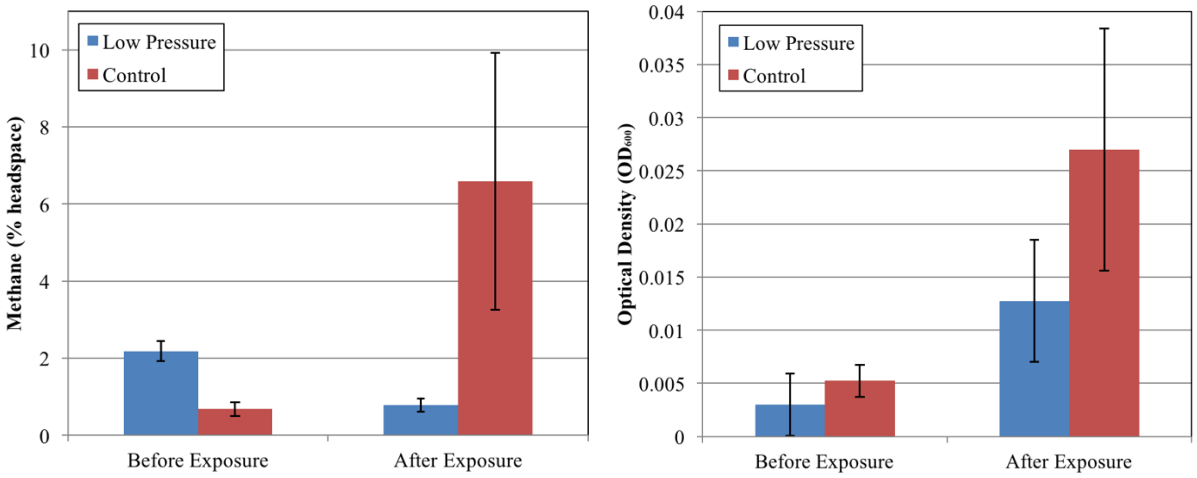

Figure 4.3 Methane production (left) and optical density (right) for *Methanosarcina barkeri* measured immediately before and immediately after exposure to low pressure (100 mbar). An initial incubation period took place at 37 °C for 7 days. Low Pressure tubes (n = 4) were exposed to 100 mbar for 28 days. Control tubes (n = 4) were subjected to the same environmental conditions as the low-pressure tubes, except for pressure. Error bars indicate ± one standard deviation.

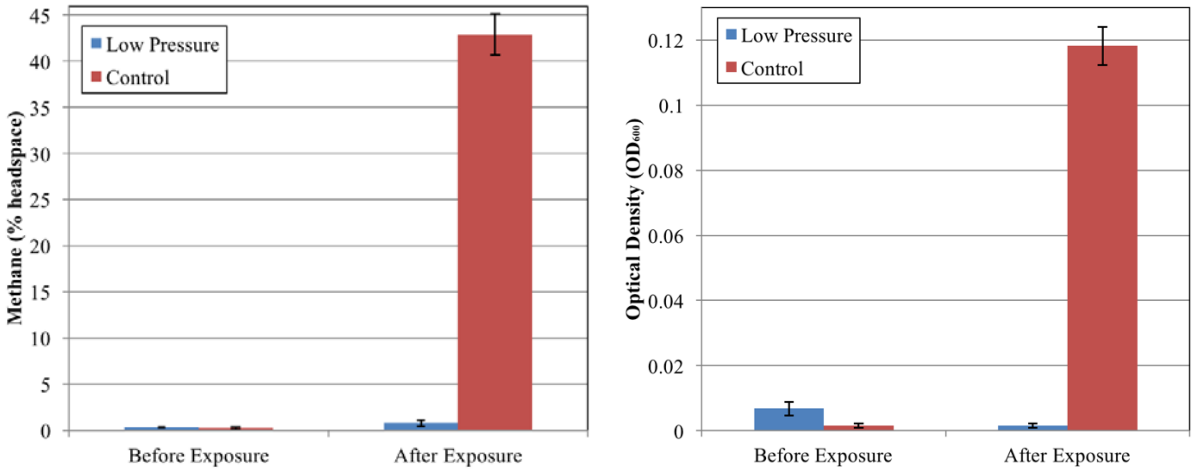

Figure 4.4 Methane production (left) and optical density (right) for *Methanococcus maripaludis* measured immediately before and immediately after exposure to low pressure (100 mbar). An initial incubation period took place at 22 °C for 7 days. Low Pressure tubes (n = 4*) were exposed to 100 mbar for 28 days. Control tubes (n = 4*) were subjected to the same environmental conditions as the low-pressure tubes, except for pressure. Error bars indicate ± one standard deviation. *Optical density measurements are n = 2 for both control and low pressure data.

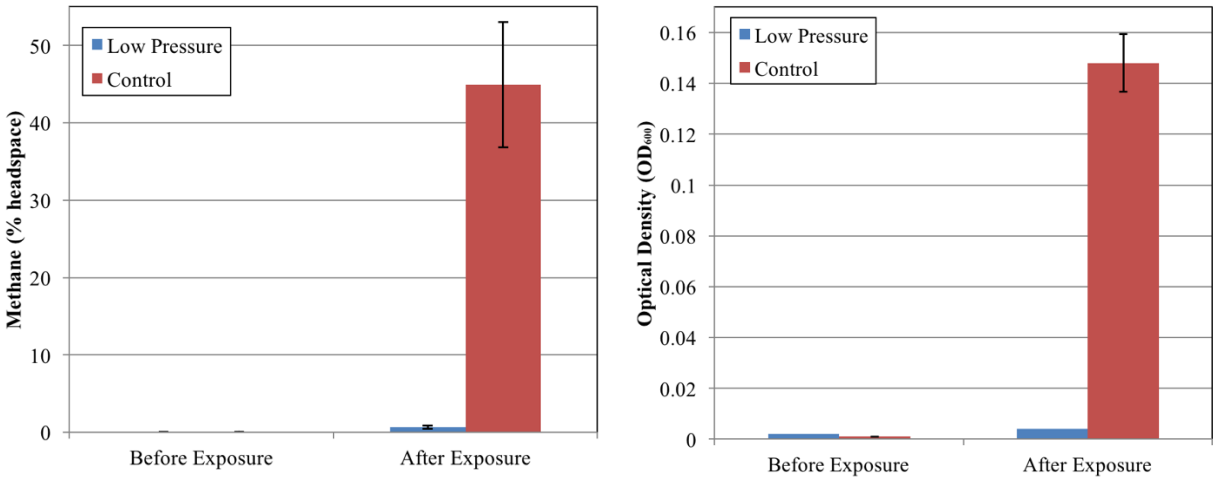

Figure 4.5 Methane production (left) and optical density (right) for *Methanococcus maripaludis* (inoculated from a 109-day-old stock culture) measured immediately before and immediately after exposure to low pressure (100 mbar). An initial incubation period took place at 22 °C for 7 days. Low Pressure tubes (n = 3*) were exposed to 100 mbar for 28 days. Control tubes (n = 2**) were subjected to the same environmental conditions as the low-pressure tubes, except for pressure. Error bars indicate ± one standard deviation. *Optical density data reflect n = 1 replicates for low-pressure tubes, and thus no error bars are shown. **Optical density data reflect n = 1 replicates for control tubes before exposure only.

4.4.2 Experiment 2: Exposure of *M. barkeri*, *M. formicicum*, and *M. maripaludis* to 50 mbar for 35 days

The media for this experiment did not include the oxygen indicator, resazurin. Therefore, possible oxygen contamination did not affect optical density values. However, the extent to which tubes may have been contaminated with oxygen is unknown.

Both methane abundance and optical density increased for cultures of *M. formicicum* exposed to 50 mbar for 35 days (Fig. 4.6). Methane within low-pressure replicates increased from 0.58±0.35% before exposure to 2.36±1.08% following exposure to 50 mbar, but these values are not statistically significant ($P > 0.05$). Methane production within control replicates was nearly identical to production within low-pressure replicates ($P > 0.05$; Fig. 4.6) and was not significantly different from initial (Day 7) values within control tubes ($P > 0.05$). Optical density

of low-pressure tubes increased from 0.023±0.015 to 0.046±0.023 during exposure to low pressure ($P > 0.05$). All four low-pressure replicates demonstrated increased methane abundance and optical density within individual tubes, but the variation amongst the four tubes accounts for the large error bars (Fig. 4.6). Surprisingly, optical density within control replicates decreased slightly during the length of the experiment (35 days), although this is not statistically significant ($P > 0.05$) after incorporating variation amongst the replicates (Fig. 4.6).

Methane abundance decreased over the course of exposure within low-pressure replicates containing *M. barkeri* ($P > 0.05$; Fig. 4.7). Optical density did increase from 0.009±0.001 to 0.022±0.014 within low-pressure tubes during the 35-day exposure to 50 mbar, but it is not significant ($P > 0.05$). Optical density only increased in three of the four low-pressure replicates, resulting in the large error bar seen in Fig. 4.7. Both methane abundance ($P \leq 0.001$) and optical density ($P \leq 0.0001$) increased significantly in control tubes over the course of the experiment (Fig. 4.7). Although there was not a significant increase in optical density values when compared to pre-exposure values, post-exposure values for the low-pressure replicates were also not significantly different from post-exposure values for the control tubes ($P > 0.05$).

Both methane abundance and optical density decreased significantly in cultures of *M. maripaludis* exposed to 50 mbar for 35 days (Fig. 4.8), whereas these values greatly increased for control tubes. Methane abundance within low-pressure tubes decreased from 2.07±0.33% to 0.82±0.05% over the course of exposure to low pressure ($P \leq 0.001$). Optical density decreased from 0.029±0.003 to 0.015±0.005 within low-pressure tubes ($P \leq 0.05$) and increased from 0.023±0.002 to 0.106±0.020 within control tubes over the course of the experiment ($P \leq 0.0001$). Methane abundance increased from 1.66±0.41% to 41.28±10.00% within the control tubes after 35 days ($P \leq 0.0001$).

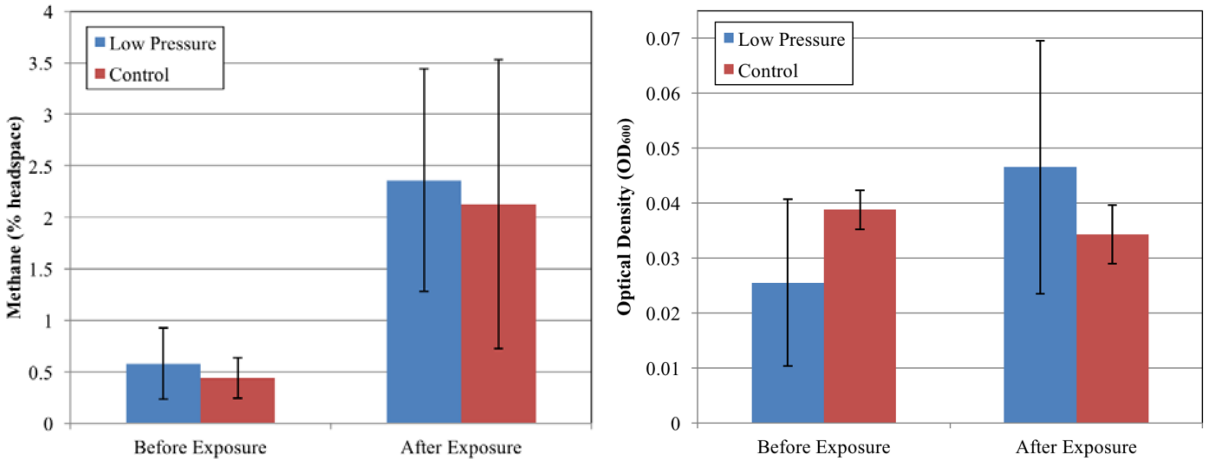

Figure 4.6 Methane production (left) and optical density (right) for *Methanobacterium formicicum* measured immediately before and immediately after exposure to low pressure (50 mbar). An initial incubation period took place at 37 °C for 7 days. Low Pressure tubes (n = 4) were exposed to 50 mbar for 35 days. Control tubes (n = 4) were subjected to the same environmental conditions as the low-pressure tubes, except for pressure. Error bars indicate ± one standard deviation.

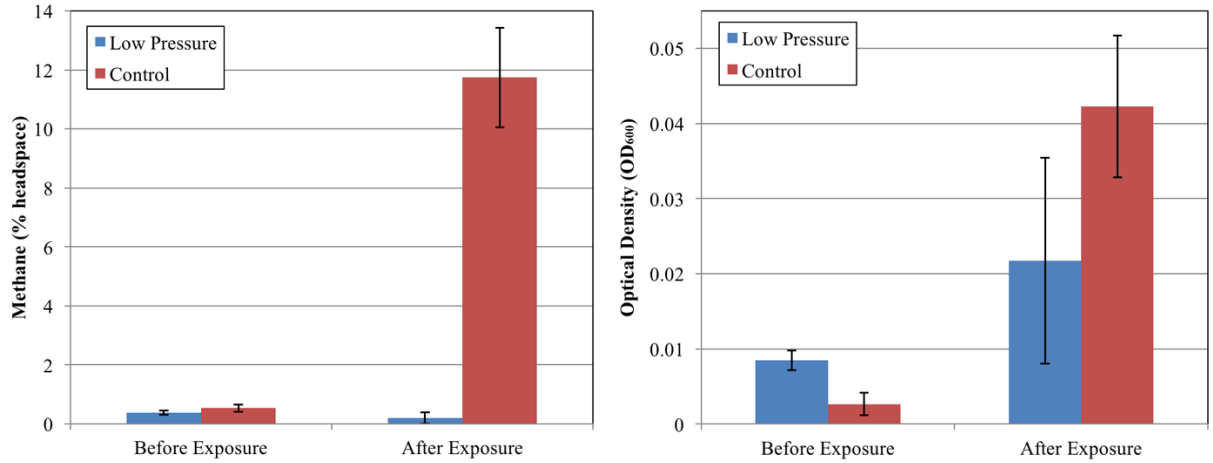

Figure 4.7 Methane production (left) and optical density (right) for *Methanosarcina barkeri* measured immediately before and immediately after exposure to low pressure (50 mbar). An initial incubation period took place at 37 °C for 7 days. Low Pressure tubes (n = 4) were exposed to 50 mbar for 35 days. Control tubes (n = 4*) were subjected to the same environmental conditions as the low-pressure tubes, except for pressure. Error bars indicate ± one standard deviation. *Optical density measurements reflect n = 3 replicates for the "Before Exposure" control tubes only.

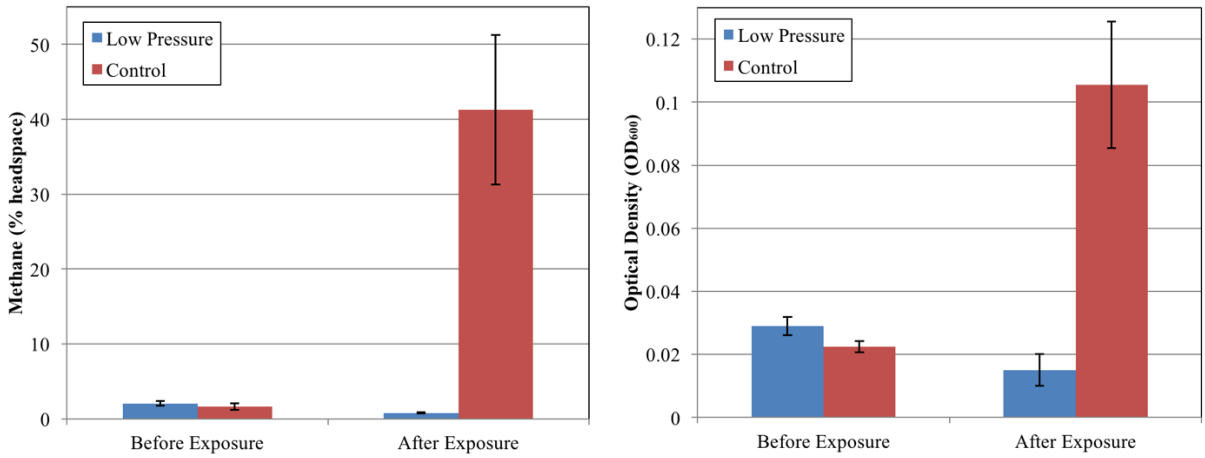

Figure 4.8 Methane production (left) and optical density (right) for *Methanococcus maripaludis* measured immediately before and immediately after exposure to low pressure (50 mbar). An initial incubation period took place at 22 °C for 7 days. Low Pressure tubes (n = 4) were exposed to 50 mbar for 35 days. Control tubes (n = 4) were subjected to the same environmental conditions as the low-pressure tubes, except for pressure. Error bars indicate ± one standard deviation.

4.4.3 Experiment 3: Exposure of *M. formicicum* to 50 mbar for 49 days

This experiment solely utilized cultures containing *M. formicicum*. There were initially 17 replicates that were exposed to low pressure, however, one tube was not sufficiently punctured to allow equilibrium between the low-pressure environment of the chamber and the test tube and so this replicate is not included in the data shown here (n = 16). There were also 16 tubes that were not exposed to low pressure that served as control replicates (n = 16). The average methane produced among the low-pressure replicates increased slightly during the exposure period (49 days) but is not statistically significant (Before: 2.87±1.64%, After: 3.37±1.26%, $P > 0.05$; Fig. 4.9). Methane increased by greater amounts in control tubes (average: 25.48±22.23%, $P \leq 0.0001$; Fig. 4.9), but with considerable variation among replicates, ranging from 5% to 57%.

Optical density increased significantly in both low-pressure replicates (0.019±0.011 to 0.050±0.017, $P \leq 0.0001$) and control replicates (0.019±0.016 to 0.085±0.033, $P \leq 0.0001$). Optical density values post-exposure (Day 56) were significantly different between low-pressure tubes and control tubes ($P \leq 0.01$).

Methane production and optical density continued to be monitored within both low-pressure tubes and control tubes following removal from the Pegasus Planetary Simulation Chamber. On Day 49, after measurements for methane production and optical density were recorded, all tubes were re-pressurized with 2 bar H_2 and incubated at 37 °C for an additional 43 days. Methane abundance and optical density continued to increase in both low-pressure tubes and control tubes (Fig. 4.10).

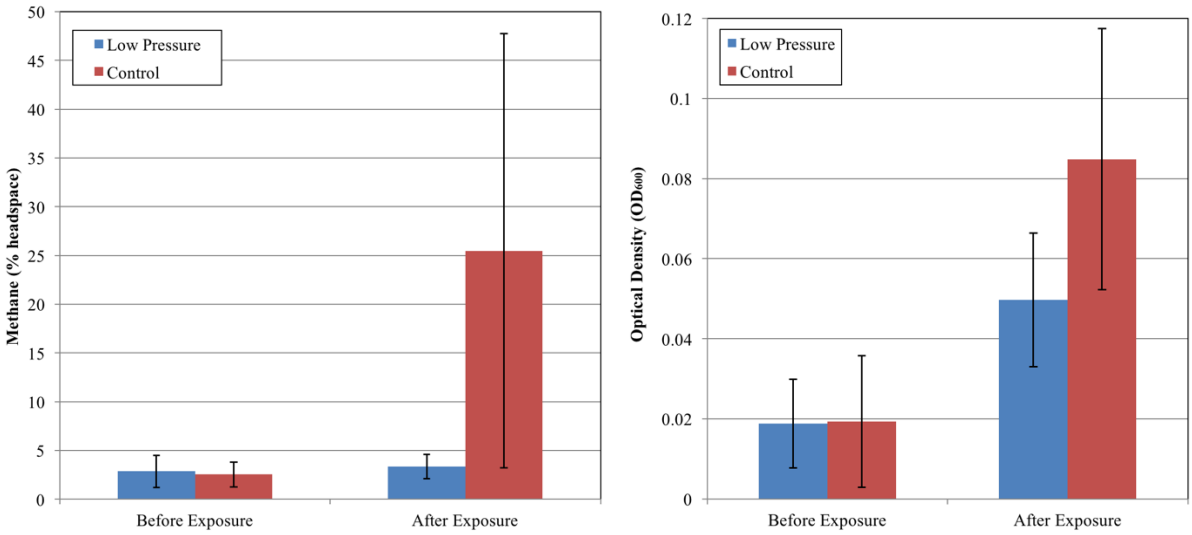

Figure 4.9 Methane production (left) and optical density (right) for *Methanobacterium formicicum* measured immediately before and immediately after exposure to low pressure (50 mbar). An initial incubation period took place at 37 °C for 7 days. Low Pressure tubes (n = 16) were exposed to 50 mbar for 49 days. Control tubes (n = 16) were subjected to the same environmental conditions as the low-pressure tubes, except for pressure. Error bars indicate ± one standard deviation.

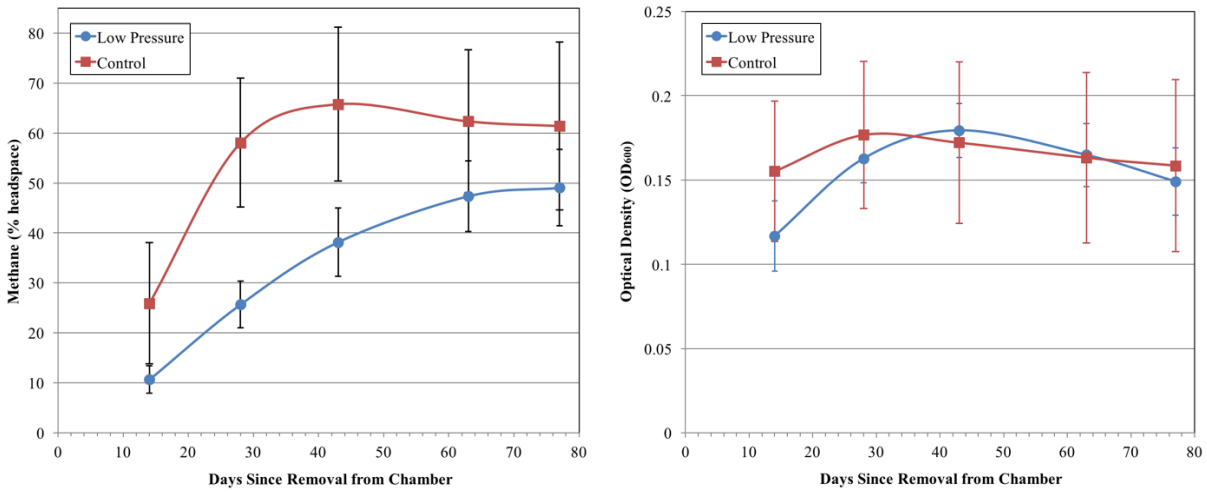

Figure 4.10 Methane production (left) and optical density (right) for *Methanobacterium formicicum* measured after exposure to low pressure (50 mbar). Low Pressure tubes (n = 16) were exposed to 50 mbar for 49 days. Control tubes (n = 16) were subjected to the same environmental conditions as the low-pressure tubes, except for pressure. Day 0 corresponds to the day all tubes were removed from the Pegasus Planetary Simulation Chamber. Error bars indicate ± one standard deviation.

4.4.4 Experiment 4: Exposure of *M. formicicum* to 50 mbar for 49 days with and without formate-supplemented media

Experiment 4 was intended to duplicate Experiment 3, but contained three major differences: 1. Inclusion of heat-killed controls, 2. Media with or without formate, and 3. Low-pressure replicates were brought to just above atmospheric pressure (~0.07 bar) with CO_2 immediately following removal from the Pegasus Planetary Simulation Chamber.

Both low-pressure groups (+formate, -formate) decreased slightly in methane concentration following exposure to 50 mbar (Fig. 4.11). Low-pressure tubes supplemented with formate decreased from 2.54±0.25% methane to 2.12±0.58% methane ($P > 0.05$) over the course of the experiment (49 days) while the low-pressure tubes without formate decreased from 1.64±0.52% to 1.08±0.54% methane during the same period ($P > 0.05$; Fig. 4.11). Both control

groups (+formate, -formate) increased in methane abundance over 49 days, increasing by about 40% methane ($P \leq 0.0001$).

Optical density increased from 0.028±0.002 to 0.040±0.013 within low-pressure replicates supplemented with formate ($P > 0.05$), while replicates lacking formate decreased slightly in optical density (0.023±0.003 to 0.019±0.011) over the period of exposure to low pressure ($P > 0.05$; Fig. 4.11). Optical density increased significantly in control tubes, increasing from 0.013±0.002 to 0.139±0.019 in replicates supplemented with formate ($P \leq 0.0001$) and from 0.022±0.005 to 0.112±0.025 in replicates lacking formate ($P \leq 0.0001$; Fig. 4.11). Methane abundance and optical density also continued to increase in all tubes (low pressure, control) following removal from the chamber, re-pressurization with 2 bar H_2 and 14 days' incubation at 37 °C (Fig. 4.11).

Controls that were supposed to be heat-killed (with and without formate) unfortunately were not killed following 1.5 hours at 80-86 °C, demonstrated by significant methane production and increasing optical density over time within certain replicates (Fig. 4.12) and within cultures subjected to a separate control study (data not shown).

All experimental data can be found in Appendix B.

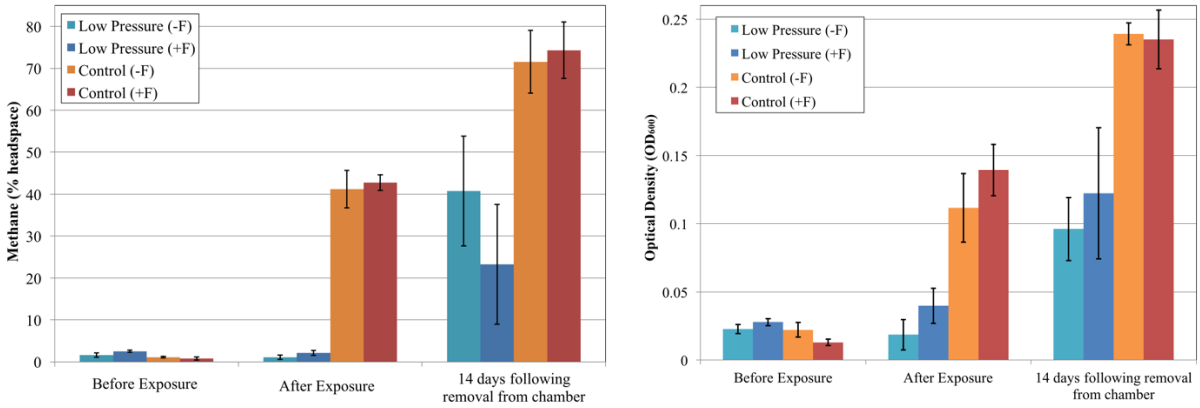

Figure 4.11 Methane production (left) and optical density (right) for *Methanobacterium formicicum* measured immediately before and immediately after exposure to low pressure (50 mbar), as well as 14 days after removal from low pressure, re-pressurization with 2 bar H_2 and incubation at 37 °C. Low Pressure tubes (n = 10) were exposed to 50 mbar for 49 days. Control tubes (n = 10) were subjected to the same environmental conditions as the low-pressure tubes, except for pressure. Both Low Pressure and Control tubes were separated into two groups: +F replicates (n = 5) contain formate in the medium, -F replicates (n = 5) lack formate. Error bars indicate ± one standard deviation.

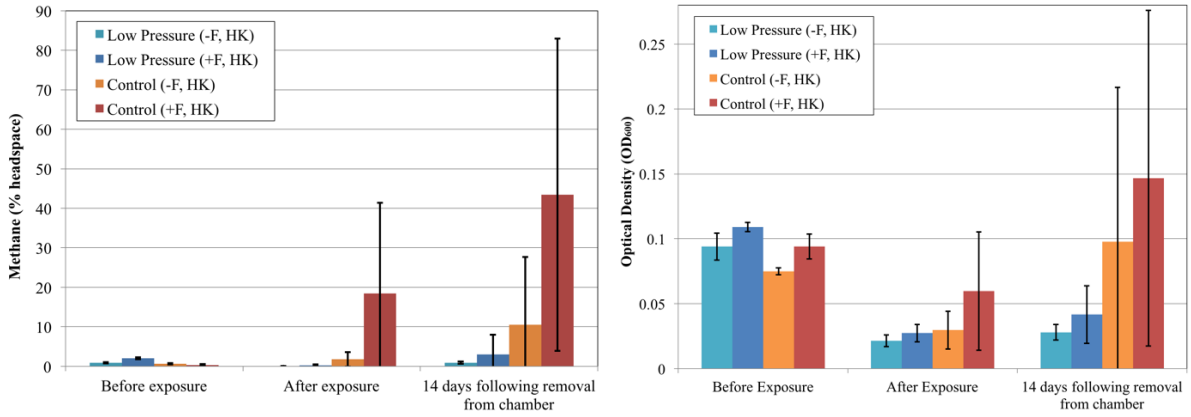

Figure 4.12 Methane production for heat-killed (HK) cultures of *Methanobacterium formicicum* measured immediately before heat treatment (before exposure to low pressure) and immediately after exposure to low pressure (50 mbar), as well as 14 days after removal from low pressure, re-pressurization with 2 bar H_2 and incubation at 37 °C. Low Pressure tubes (n = 6) were exposed to 50 mbar for 49 days. Control tubes (n = 6) were subjected to the same environmental conditions as the low-pressure tubes, except for pressure. Both Low Pressure and Control tubes were separated into two groups: +F replicates (n = 3) contain formate in the medium, -F replicates (n = 3) lack formate. Error bars indicate ± one standard deviation.

4.5 Discussion

Demonstrating active methane production within methanogenic cultures at low pressure is difficult considering methane is typically monitored via gas chromatography and obtaining and injecting a gas sample at low pressure is not ideal. In the experiments conducted here, low-pressure "microenvironments" were created by equilibrating the headspace within anaerobic test tubes with the low-pressure atmosphere inside a planetary simulation chamber. Tubes were equilibrated to low pressure (100 mbar, Expt. 1 or 50 mbar, Expts. 2-4) for 60 min using syringe needles. After the period of equilibration, the needles were removed, resealing the anaerobic test tubes and effectively creating low-pressure microenvironments within each replicate. The chamber atmosphere was actively maintained at 100 mbar (Expt. 1) or 50 mbar (Expts. 2-4) for the duration of the experiment so that there was no change in pressure in the event of an unsealed test tube. Further, visual inspection during and after the exposure period ensured that microenvironments were intact as no evaporation was detected from the individual cultures. Additionally, in Expts. 1-3, negative pressure within each replicate (as headspace samples were removed for methane detection) further demonstrated that each individual test tube was under low pressure. Low pressure tubes in Expt. 4 were also verified as being under low pressure by the ability to add ~0.07 bar CO_2 to cultures following removal from the chamber.

Methane abundance within anaerobic test tubes was measured by removing a 0.5 mL sample of gas from the headspace and injecting this into a gas chromatograph. In Expts. 1-3, following exposure to low pressure, headspace samples were removed from the test tubes while still under low pressure. Since the test tubes were themselves below atmospheric pressure, it is possible that air began to enter each test tube as soon as the external pressure rose above 50 mbar (or 100 mbar, Expt. 1). The test tubes remained sealed with aluminum crimps and rubber

stoppers, although it is possible that air began to seep into each tube through pores within the stoppers or if the seal between the stopper and the test tube was not adequately robust. Despite whether or not air is able to seep into the test tubes themselves following removal from the chamber, it is known that air will rush into the syringe when a headspace sample is removed from the test tube and transferred to the gas chromatograph. Airtight syringes were not used in this research. If airtight syringes had been used, the same effect would have occurred. Once the sample had been injected into the gas chromatograph, air would have diluted the sample in the injection port. Thus, the samples removed from the low-pressure tubes were diluted.

In the case of Expt. 1, the dilution would occur at a factor of ~10 between the experimental pressure (100 mbar) and atmospheric pressure (~1013 mbar). For Expts. 2-4, the dilution factor is ~20 (1013 mbar/50 mbar). Although methane concentration did increase within low-pressure replicates for *M. formicicum* as measured in Expt. 1, incorporating the 10x dilution factor into the post-exposure methane abundances for the low-pressure tubes indicates that methane production within low-pressure tubes may be greater than that within control tubes for this species (Fig. 4.13). Interestingly, the incorporation of the dilution factor into the post-exposure methane values perhaps more accurately aligns with the optical density measurements which showed a slightly higher average value than control tubes (Fig. 4.2). In Expt. 2, both methane production and optical density were nearly identical ($P > 0.05$) for low-pressure cultures and control cultures (Fig. 4.6); incorporating a 20x dilution factor would indicate that methane production is actually much higher in tubes at 50 mbar than from cultures at atmospheric pressure (data not shown).

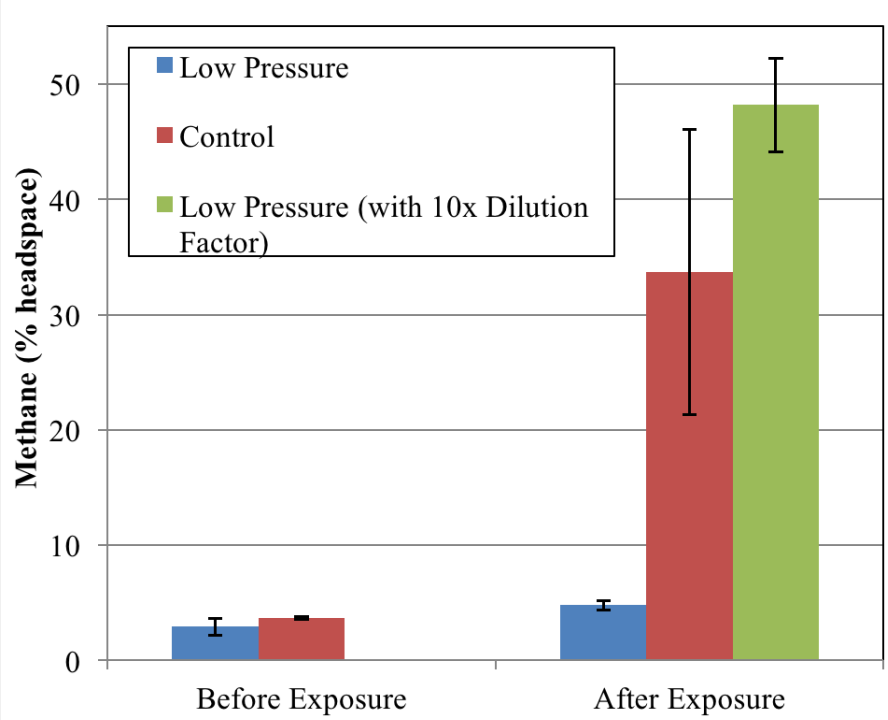

Figure 4.13 Methane production by *Methanobacterium formicicum* measured immediately before and immediately after exposure to low pressure (100 mbar). An initial incubation period took place at 37 °C for 7 days. Low Pressure tubes (n = 3) were exposed to 100 mbar for 28 days. Control tubes (n = 4) were subjected to the same environmental conditions as the Low Pressure tubes, except for pressure. The green bar incorporates a dilution factor of 10 to the average methane measured in the low pressure replicates after exposure to 100 mbar. Data in this figure is the same data in Figure 4.2. Error bars indicate ± one standard deviation.

Further analysis of data from Experiment 3 (exposure of *M. formicicum* to 50 mbar for 49 days) reveals that there are two distinct groupings within both the low-pressure replicates (designated “group a” [n = 9] and “group b” [n = 7]) and the control replicates (designated “group c” [n = 7] and “group d” [n = 9]). Figure 4.14 shows distinct groupings within both sets with the most obvious difference being between group c and group d within the control replicates following the length of the experiment (49 days). The amount of methane within group c replicates on Day 56 was 49.28±7.78%, while the methane abundance averaged 6.97±0.87% within the group d replicates. Initial optical density measurements also varied between the four

groups (Fig. 4.15). Group a of the low-pressure replicates and group c of the control replicates were most similar with initial optical density values of 0.027±0.006 and 0.035±0.011 on Day 7, respectively. Values for group b of the low-pressure replicates and group d of the control replicates were also nearly identical, measuring initial optical density values of 0.008±0.001 and 0.007±0.007, respectively. After the length of the experiment (49 days), optical density increased in all four groups (Fig. 4.15).

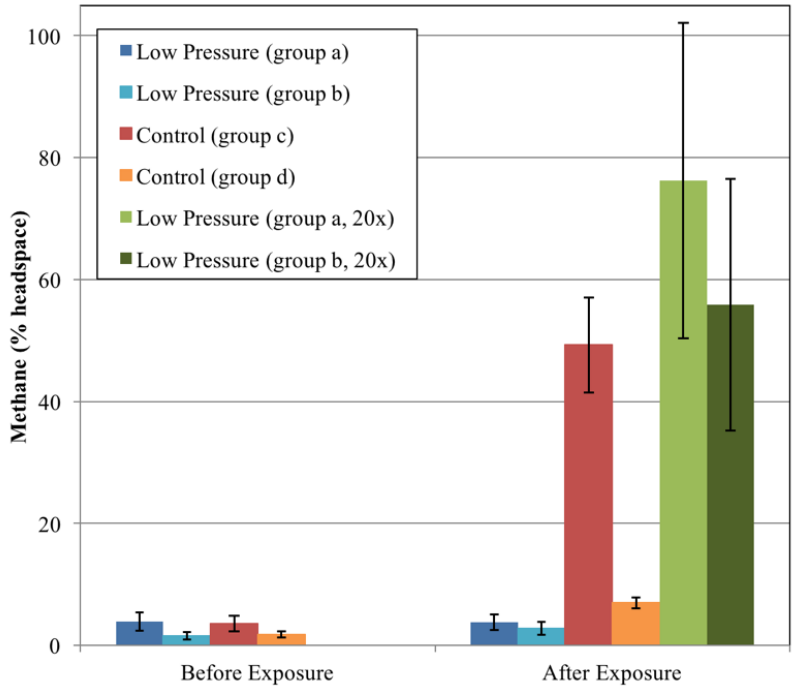

Figure 4.14 Methane production by *Methanobacterium formicicum* measured immediately before and immediately after exposure to low pressure (50 mbar). An initial incubation period took place at 37 °C for 7 days. Low Pressure tubes (n = 16) were exposed to 50 mbar for 49 days. Control tubes (n = 16) were subjected to the same environmental conditions as the Low Pressure tubes, except for pressure. The green bars incorporate a dilution factor of 20 to the average methane measured in the low pressure replicates after exposure to 50 mbar. Data in this figure is the same data in Figure. 4.9, but separated into two distinct groups for both the Low Pressure tubes (groups a and b) and the Control tubes (groups c and d). Error bars indicate ± one standard deviation.

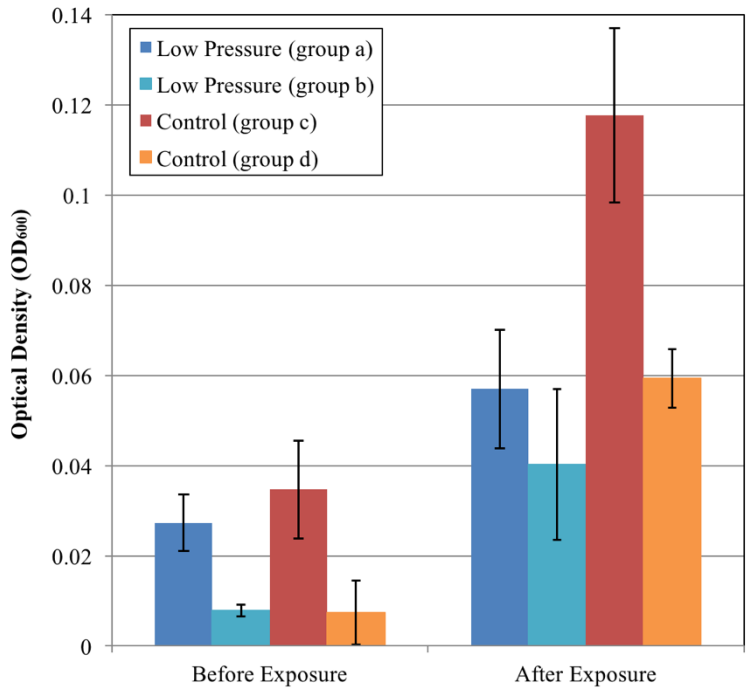

Figure 4.15 Optical density for cultures of *Methanobacterium formicicum* measured immediately before and immediately after exposure to low pressure (50 mbar). An initial incubation period took place at 37 °C for 7 days. Low Pressure tubes (n = 16) were exposed to 50 mbar for 49 days. Control tubes (n = 16) were subjected to the same environmental conditions as the Low Pressure tubes, except for pressure. Data in this figure are the same data in Figure. 4.9, but separated into two distinct groups for both the Low Pressure tubes (groups a and b) and the Control tubes (groups c and d). Error bars indicate ± one standard deviation.

Application of the 20x dilution factor into the post-exposure methane abundances for both low-pressure groups is shown in Fig. 4.14. Of interest is the effect of the dilution factor on group b within the low-pressure replicates: after the dilution factor is applied, methane abundance within group b of the low-pressure replicates is very similar to the methane abundance with the group c control replicates (Fig. 4.14). However, evidence against the legitimacy of the dilution factor is apparent in the optical density values for the low-pressure replicates and the control replicates following exposure. Post-exposure optical density values for the low-pressure groups (a and b) are more similar to the optical density values for control group d values, than for control group c (Fig. 4.14). Thus, a general correlation between methane

production and optical density would expect post-exposure methane abundances to be most similar to this group as well, whereas the dilution factor results in methane abundances much larger than those for control group d, as well as control group c (Fig. 4.14).

The explanation for the separation of the low pressure replicates and the control replicates into two distinct groups within each set is unknown. All media were prepared identically and all tubes were inoculated from the same starting culture. As there were 36 replicates to inoculate, it is possible that through the course of inoculations, as the starting culture was exposed to aerobic conditions, that remaining cells were killed by exposure to oxygen and that later and later inocula contained fewer and fewer cells. These tubes with fewer cells then happened to form half of the replicates for the low-pressure set and half of the replicates for the control set. However, inoculations were conducted swiftly and McAllister and Kral (2006) have previously demonstrated that cells of this species are capable of withstanding exposure to aerobic conditions for 1.5 h during washing procedures. This scenario would also anticipate a continuous decrease in cell number, and thus methane production/optical density, between the first tube inoculated and the last. However, the initial methane production and initial optical density measurements more specifically indicate two distinct groups. It was also considered that the sets of media comprising these replicates may have lacked formate within the media and this exclusion could result in the different methane abundances and optical density values. As such, Expt. 4 utilized media both with and without formate, which, unfortunately, did not replicate the distinct groupings within the low-pressure and control sets seen in Expt. 3 (Expt. 3, Fig. 4.14; Expt. 4, Fig. 12), although initial methane production within the 7-day incubation period was both varied and low. These data appear to possibly indicate a continuous decrease in methane production per replicate likely based on cell death due to oxygen exposure

over the period of inoculation. The inoculation procedure was the same as that for Expt. 3, except that 30 mL total were used as a starting inoculum instead of 20 mL total. Unrelated experiments utilizing the same species have subjected the organisms to oxygen for longer periods of time (more wash cycles) without any deleterious effect on methane production (Mickol et al., 2016).

An interesting aspect to this discrepancy within sets is the extent of optical density and methane production within both low-pressure and control tubes for *M. formicicum* in Expt. 2. In this experiment, optical density and methane production were highly similar ($P > 0.05$) between low-pressure replicates and control replicates. The abundance of methane within control tubes after 35 days (~2%) is, however, extremely low for a typical *M. formicicum* culture. In Expts. 1 and 3, 2% methane was reached within the initial 7-day incubation period (Figs. 4.2, 4.9).

M. formicicum was the only methanogen out of the three species to demonstrate both an increase in methane production and an increase in optical density during exposure to low pressure. Increases in methane were not statistically significant in low-pressure tubes, when methane abundance in tubes before exposure was compared to methane abundance in tubes after exposure to low pressure. These increases may not be significant since the pre- and post-exposure values were very similar (e.g., Expt 3: Before: 2.87±1.64%, After: 3.37±1.26%). However, when the tubes were punctured to equilibrate them with the low-pressure chamber atmosphere, the methane initially contained within each test tube would escape. Thus, the post-exposure methane values are essentially increasing from zero. Although post-exposure abundances are not significantly different from pre-exposure values, an increase of ~3%, along with an increase in optical density, indicates active metabolism.

In Expts. 1 and 2, *M. barkeri* cells increased in optical density during 28 days' exposure to 100 mbar and 35 days' exposure to 50 mbar, respectively, but a concurrent increase in methane was not seen (Figs. 4.3, 4.7). Cells of *Methanosarcina* spp. typically form irregular multicellular aggregates, especially under stressed conditions (Maestrojuan and Boone, 1991), which may account for the increase in optical density seen here. Although *M. barkeri* and *M. maripaludis* did not demonstrate active growth under low-pressure conditions, methane production resumed during the post-exposure incubation period and cultures also increased in optical density (data not shown). However, survival was likely not difficult as cells remained within a 10 mL water column for the duration of the experiment. Mickol and Kral (2016) also note that as the tubes were upright and the cells congregated at the bottom of the test tubes, the pressure at the bottom of the water column was, in actuality, about 6 mbar higher than the experimental pressure (50 mbar or 100 mbar) due to the weight of the water. The production of methane likely did not increase the headspace pressure within the test tubes based on the destruction of five molecules of gas to the creation of one:

$$4H_2 + CO_2 \rightarrow CH_4 + 2H_2O \qquad (1)$$

Due to the variation amongst replicates under identical conditions, future experiments may need to utilize additional growth proxies besides methane concentration and optical density. The anaerobic nature of methanogens, the high number of replicates within most experiments and the slow doubling time of the organisms makes cell counting or MPN procedures a daunting task. However, accurate cell counts would provide a necessary comparison to methane abundances and optical densities.

It is important to note that on Day 30 (of 49) for Expt. 4 (49 days at 50 mbar), the pressure control valve malfunctioned and dropped the internal chamber pressure to ~0.8 mbar.

The individual test tubes remained sealed at this point, and there was no evidence of extensive leakage (evaporation) of the media. Thus, it is believed that the microenvironments remained intact at ~50 mbar for the following 19 days of the experiment, despite the lower pressure of the chamber. As the cultures were not subjected to this lower pressure, the data were analyzed without alteration.

4.6 Conclusions

M. formicicum is capable of active growth at 50 mbar as verified by concurrent methane production and increased optical density. Although *M. barkeri* and *M. maripaludis* did not demonstrate growth during exposure to low pressure, all cultures produced methane and increased in optical density during the post-exposure incubation period, indicating that all species survived the exposure to low pressure. Results suggest that low pressure may not have an effect on methane production by *M. formicicum* at 50-100 mbar. However, variation amongst replicates under identical conditions warrants further investigation to the effect of low pressure on methanogenesis and cell growth.

4.7 References

Boone, D.R., Johnson, R.L., Liu, Y. (1989) Diffusion of the interspecies electron carriers H_2 and formate in methanogenic ecosystems and its implications in the measurement of K_m for H_2 or formate uptake. *Applied and Environmental Microbiology* 55, 1735-1741.

Conrad, R. (2009) The global methane cycle: recent advances in understanding the microbial processes involved. *Environmental Microbiology Reports* 1, 285-292.

Fajardo-Cavazos, P., Waters, S.M., Schuerger, A.C., George, S., Marois, J.J., Nicholson, W.L. (2012) Evolution of *Bacillus subtilis* to Enhanced Growth at Low Pressure: Up-Regulated

Transcription of *des-desKR*, Encoding the Fatty Acid Desaturase System. *Astrobiology* 12, 258-270.

Fonti, S., Marzo, G.A. (2010) Mapping the methane on Mars. *Astronomy and Astrophysics* 512.

Formisano, V., Atreya, S., Encrenaz, T., Ignatiev, N., Giuranna, M. (2004) Detection of methane in the atmosphere of Mars. *Science* 306, 1758-1761.

Geminale, A., Formisano, V., Giuranna, M. (2008) Methane in Martian atmosphere: average spatial, diurnal, and seasonal behaviour. *Planetary and Space Science* 56, 1194-1203.

Geminale, A., Formisano, V., Sindoni, G. (2011) Mapping methane in Martian atmosphere with PFS-MEX data. *Planetary and Space Science* 59, 137-148.

Hess, S.L., Henry, R.M., Tillman, J.E. (1979) The seasonal variation of atmospheric pressure on Mars as affected by the south polar cap. *Journal of Geophysical Research: Solid Earth (1978–2012)* 84, 2923-2927.

Hess, S.L., Ryan, J.A., Tillman, J.E., Henry, R.M., Leovy, C.B. (1980) The annual cycle of pressure on Mars measured by Viking landers 1 and 2. *Geophysical Research Letters* 7, 197-200.

IPCC (2013) *Climate Change 2013: The Physical Science Basis: Working Group I Contribution to the Fifth Assessment Report of the Intergovernmental Panel on Climate Change* [Stocker, T.F., D. Qin, G.-K. Plattner, M. Tignor, S.K. Allen, J. Boschung, A. Nauels, Y. Xia, V. Bex and P.M. Midgley (Eds.)]. Cambridge University Press, Cambridge, United Kingdom and New York, NY, USA, pp. 1535.

Kendrick, M.G., Kral, T.A. (2006) Survival of methanogens during desiccation: implications for life on Mars. *Astrobiology* 6, 546-551.

Kral, T.A., Altheide, T.S. (2013) Methanogen survival following exposure to desiccation, low pressure and martian regolith analogs. *Planetary and Space Science* 89, 167-171.

Kral, T.A., Altheide, T.S., Lueders, A.E., Schuerger, A.C. (2011) Low pressure and desiccation effects on methanogens: Implications for life on Mars. *Planetary and Space Science* 59, 264-270.

Krasnopolsky, V.A., Bjoraker, G.L., Mumma, M.J., Jennings, D.E. (1997) High-resolution spectroscopy of Mars at 3.7 and 8 μm: A sensitive search for H_2O_2, H_2CO, HCl, and CH_4, and detection of HDO. *Journal of Geophysical Research* 102, 6525.

Krasnopolsky, V.A., Maillard, J.P., Owen, T.C. (2004) Detection of methane in the martian atmosphere: evidence for life? *Icarus* 172, 537-547.

Maestrojuán, G.M., Boone, D.R. (1991) Characterization of *Methanosarcina barkeri* MS^T and 227, *Methanosarcina mazei* $S\text{-}6^T$, and *Methanosarcina vacuolata* $Z\text{-}761^T$. *International Journal of Systematic and Evolutionary Microbiology* 41, 267-274.

Maguire, W.C. (1977) Martian isotopic ratios and upper limits for possible minor constituents as derived from Mariner 9 infrared spectrometer data. *Icarus* 32, 85-97.

McAllister, S.A., Kral, T.A. (2006) Methane production by methanogens following an aerobic washing procedure: simplifying methods for manipulation. *Astrobiology* 6, 819-823.

Mickol, R., Craig, P., Kral, T. (2016) *Nontronite and Montmorillonite as Nutrient Sources for Life on Mars*, poster presented as part of: Biosignature Preservation and Detection in Mars Analog Environments, Lake Tahoe, NV.

Mickol, R., Kral, T. (2016) Low Pressure Tolerance by Methanogens in an Aqueous Environment: Implications for Subsurface Life on Mars. *Origins of Life and Evolution of Biospheres*, 1-22.

Mumma, M.J., Villanueva, G.L., Novak, R.E., Hewagama, T., Bonev, B.P., DiSanti, M.A., Mandell, A.M., Smith, M.D. (2009) Strong release of methane on Mars in northern summer 2003. *Science* 323, 1041-1045.

Ni, S., Boone, D.R. (1991) Isolation and characterization of a dimethyl sulfide-degrading methanogen, *Methanolobus siciliae* HI350, from an oil well, characterization of *M. siciliae* T4/M^T, and emendation of *M. siciliae*. *International Journal of Systematic Bacteriology* 41, 410-416.

Nicholson, W.L., Fajardo-Cavazos, P., Fedenko, J., Ortíz-Lugo, J.L., Rivas-Castillo, A., Waters, S.M., Schuerger, A.C. (2010) Exploring the low-pressure growth limit: evolution of *Bacillus subtilis* in the laboratory to enhanced growth at 5 kilopascals. *Applied and Environmental Microbiology* 76, 7559-7565.

Nicholson, W.L., Krivushin, K., Gilichinsky, D., Schuerger, A.C. (2013) Growth of *Carnobacterium* spp. from permafrost under low pressure, temperature, and anoxic atmosphere has implications for Earth microbes on Mars. *Proceedings of the National Academy of Sciences of the United States of America* 110, 666-671.

Schirmack, J., Böhm, M., Brauer, C., Löhmannsröben, H.-G., de Vera, J.-P., Möhlmann, D., Wagner, D. (2014) Laser spectroscopic real time measurements of methanogenic activity under simulated Martian subsurface analog conditions. *Planetary and Space Science* 98, 198-204.

Schuerger, A., Nicholson, W. (2006) Interactive effects of hypobaria, low temperature, and CO_2 atmospheres inhibit the growth of mesophilic *Bacillus* spp. under simulated martian conditions. *Icarus* 185, 143-152.

Schuerger, A.C., Nicholson, W.L. (2016) Twenty Species of Hypobarophilic Bacteria Recovered from Diverse Soils Exhibit Growth under Simulated Martian Conditions at 0.7 kPa. *Astrobiology* 16, 964-976.

Schuerger, A.C., Ulrich, R., Berry, B.J., Nicholson, W.L. (2013) Growth of *Serratia liquefaciens* under 7 mbar, 0 degrees C, and CO_2-enriched anoxic atmospheres. *Astrobiology* 13, 115-131.

Spiga, A., Forget, F., Dolla, B., Vinatier, S., Melchiorri, R., Drossart, P., Gendrin, A., Bibring, J.P., Langevin, Y., Gondet, B. (2007) Remote sensing of surface pressure on Mars with the Mars Express/OMEGA spectrometer: 2. Meteorological maps. *Journal of Geophysical Research: Planets (1991–2012)* 112.

Waters, S.M., Robles-Martínez, J.A., Nicholson, W.L. (2014) Exposure of *Bacillus subtilis* to low pressure (5 kilopascals) induces several global regulons, including those involved in the SigB-mediated general stress response. *Applied and Environmental Microbiology* 80, 4788-4794.

Waters, S.M., Zeigler, D.R., Nicholson, W.L. (2015) Experimental Evolution of Enhanced Growth by *Bacillus subtilis* at Low Atmospheric Pressure: Genomic Changes Revealed by Whole-Genome Sequencing. *Applied and Environmental Microbiology* 81, 7525-7532.

Webster, C.R., Mahaffy, P.R., Atreya, S.K., Flesch, G.J., Mischna, M.A., Meslin, P.-Y., Farley, K.A., Conrad, P.G., Christensen, L.E., Pavlov, A.A., Martín-Torres, J., Zorzano, M.P., McConnochie, T.H., Owen, T., Eigenbrode, J.L., Glavin, D.P., Steele, A., Malespin, C.A., Archer Jr., P.D., Sutter, B., Coll, P., Freissinet, C., McKay, C.P., Moores, J.E., Schwenzer, S.P., Bridges, J.C., Navarro-Gonzalez, R., Gellert, R., Lemmon, M.T., MSL Science Team (2015) Mars methane detection and variability at Gale crater. *Science* 347, 415-417.

4.8 Appendix A: Statistical Procedures

This appendix provides additional information regarding the statistical procedures utilized above.

4.8.1 Experiment 1: Exposure of *M. barkeri, M. formicicum*, and *M. maripaludis* to 100 mbar for 28 days

Methane data for *M. formicicum* were log-log-transformed (i.e. log(log(methane)) in order to induce homogeneity of variance according to the Brown-Forsythe test. Optical density data were not transformed. Methane data for *M. barkeri* were log-transformed and optical density data were square-root-transformed to induce homogeneity of variance according to the

Brown-Forsythe test and Bartlett's test. Methane data for the first set of *M. maripaludis* cultures were square-root-transformed to induce homogeneity of variance according to the Brown-Forsythe test and Bartlett's test, while the optical density data did not require transformation. Methane data for the second set of *M. maripaludis* cultures were log-transformed to induce homogeneity of variance according to the Brown-Forsythe test. There were not sufficient data to run statistical analyses on the optical density data for the second set of *M. maripaludis*.

4.8.2 Experiment 2: Exposure of *M. barkeri*, *M. formicicum*, and *M. maripaludis* to 50 mbar for 35 days

Methane data for *M. formicicum* were log-transformed to induce homogeneity of variance according to the Brown-Forsythe test and Bartlett's test. The optical density data for *M. formicicum* were subjected to a reciprocal transformation (1/y) in order to induce homogeneity of variance according to the Brown-Forsythe test and Bartlett's test. Methane data for *M. barkeri* were subjected to a log transformation to induce homogeneity of variance according to the Brown-Forsythe test. There were no transformations or double-transformations that satisfied both the Brown-Forsythe test and Bartlett's test for these data. The optical density data for *M. barkeri* were also log-transformed to induce homogeneity of variance according to the Brown-Forsythe test. For *M. maripaludis*, the methane data were log-transformed and the optical density data were square-root-transformed to induce homogeneity of variance according to the Brown-Forsythe test and Bartlett's test.

4.8.3 Experiment 3: Exposure of M. formicicum to 50 mbar for 49 days

Methane data were subjected to a reciprocal (1/y) transformation, then to a square-root transformation in order to induce homogeneity of variance according to the Brown-Forsythe test and Bartlett's test. Optical density data were subjected to a square-root transformation to induce homogeneity of variance according to the Brown-Forsythe test and Bartlett's test.

4.8.4 Experiment 4: Exposure of *M. formicicum* to 50 mbar for 49 days with and without formate-supplemented media

Due to the failure to adequately sterilize the heat-killed controls, these cultures were not subjected to statistical analysis. The methane data for this experiment were subjected to a square-root transformation to induce homogeneity of variance according to the Brown-Forsythe test and Bartlett's test. The optical density data were subjected to a power transformation of one-fourth to induce homogeneity of variance according to the Brown-Forsythe test and Bartlett's test.

4.9 Appendix B: Data

4.9.1 Experiment 1: Exposure of *M. barkeri, M. formicicum*, and *M. maripaludis* to 100 mbar for 28 days

Table 4.2 Data for Experiment 1: Exposure of *M. barkeri*, *M. formicicum*, and *M. maripaludis* to 100 mbar for 28 days

Experiment	Medium[a]	Tube	Type[b]	Day[c]	Methane[d]	OD[e]
1	MSF	1	E	0	0	0
1	MSF	3	E	0	0	0
(continued)						

Experiment	Medium[a]	Tube	Type[b]	Day[c]	Methane[d]	OD[e]
1	MSF	4	E	0	0	0
1	MSF	1	C	0	0	0
1	MSF	2	C	0	0	0
1	MSF	3	C	0	0	0
1	MSF	4	C	0	0	0
1	MS	1	E	0	0	0
1	MS	2	E	0	0	0
1	MS	3	E	0	0	0
1	MS	4	E	0	0	0
1	MS	1	C	0	0	0
1	MS	2	C	0	0	0
1	MS	3	C	0	0	0
1	MS	4	C	0	0	0
1	MSH	1	E	0	0	0
1	MSH	2	E	0	0	0
1	MSH	3	E	0	0	0
1	MSH	4	E	0	0	0
1	MSH	1	C	0	0	0
1	MSH	2	C	0	0	0
1	MSH	3	C	0	0	0
1	MSH	4	C	0	0	0
1	MSH2[f]	1	E	0	0	0
1	MSH2	2	E	0	0	0
1	MSH2	3	E	0	0	0
1	MSH2	4	E	0	0	0
1	MSH2	1	C	0	0	0
1	MSH2	2	C	0	0	0
1	MSF	1	E	7	2.146	0.046
1	MSF	3	E	7	3.066	0.054
1	MSF	4	E	7	3.569	0.052
1	MSF	1	C	7	3.757	0.048
1	MSF	2	C	7	3.819	0.037
1	MSF	3	C	7	3.538	0.035
1	MSF	4	C	7	3.634	0.035
1	MS	1	E	7	1.812	0.006
1	MS	2	E	7	2.406	0.001
1	MS	3	E	7	2.215	0.005
(continued)						

Experiment	Medium[a]	Tube	Type[b]	Day[c]	Methane[d]	OD[e]
1	MS	4	E	7	2.304	0
1	MS	1	C	7	0.803	0.004
1	MS	2	C	7	0.551	0.004
1	MS	3	C	7	0.511	0.007
1	MS	4	C	7	0.866	0.006
1	MSH	1	E	7	0.325	0.005
1	MSH	2	P	7	0.373	0.005
1	MSH	3	P	7	0.282	0.008
1	MSH	4	P	7	0.37	0.009
1	MSH	1	C	7	0.101	ND[g]
1	MSH	2	C	7	0.253	ND
1	MSH	3	C	7	0.175	0.001
1	MSH	4	C	7	0.386	0.002
1	MSH2	2	E	7	0.009	ND
1	MSH2	3	E	7	0.008	ND
1	MSH2	4	E	7	0.009	0.002
1	MSH2	1	C	7	0.023	0.001
1	MSH2	2	C	7	0.021	ND
1	MSF	1	E	35	5.195	0.086
1	MSF	3	E	35	4.389	0.112
1	MSF	4	E	35	4.872	0.102
1	MSF	1	C	35	23.314	0.086
1	MSF	2	C	35	46.827	0.104
1	MSF	3	C	35	23.009	0.102
1	MSF	4	C	35	41.691	0.09
1	MS	1	E	35	0.537	0.02
1	MS	2	E	35	0.843	0.012
1	MS	3	E	35	0.937	0.013
1	MS	4	E	35	0.82	0.006
1	MS	1	C	35	11.366	0.044
1	MS	2	C	35	5.157	0.021
1	MS	3	C	35	3.731	0.023
1	MS	4	C	35	6.095	0.02
1	MSH	2	E	35	0.345	ND
1	MSH	3	E	35	1.011	0.002
1	MSH	4	E	35	1.077	0.001
1	MSH	1	C	35	40.832	0.123
(continued)						

Experiment	Medium[a]	Tube	Type[b]	Day[c]	Methane[d]	OD[e]
1	MSH	2	C	35	45.458	0.11
1	MSH	3	C	35	41.183	0.122
1	MSH	4	C	35	43.985	0.118
1	MSH2	2	E	35	0.425	ND
1	MSH2	3	E	35	0.722	ND
1	MSH2	4	E	35	0.808	0.004
1	MSH2	1	C	35	39.232	0.14
1	MSH2	2	C	35	50.636	0.156
1	MSF	1	E	70	34.596	0.212
1	MSF	3	E	70	24.375	0.218
1	MSF	4	E	70	26.817	0.185
1	MSF	1	C	70	64.476	0.186
1	MSF	2	C	70	71.907	0.202
1	MSF	3	C	70	60.87	0.204
1	MSF	4	C	70	63.175	0.193
1	MS	2	E	70	2.392	0.014
1	MS	3	E	70	1.747	0.015
1	MS	4	E	70	2.295	0.005
1	MS	1	C	70	11.288	0.048
1	MS	2	C	70	11.106	0.04
1	MS	3	C	70	9.645	0.042
1	MS	4	C	70	13.7	0.035
1	MSH	2	E	70	11.836	0.024
1	MSH	3	E	70	18.968	0.092
1	MSH	4	E	70	20.653	0.046
1	MSH	1	C	70	57.565	0.185
1	MSH	2	C	70	52.178	0.126
1	MSH	3	C	70	60.03	0.162
1	MSH	4	C	70	73.714	0.155
1	MSH2	2	E	70	16.756	0.075
1	MSH2	1	C	70	55.902	0.186
1	MSH2	2	C	70	61.525	0.19
1	MSF	1	E	84	47.3	0.22
1	MSF	3	E	84	40.813	0.224
1	MSF	4	E	84	45.475	0.2
1	MSF	1	C	84	65.284	0.178
1	MSF	2	C	84	71.974	0.208
(continued)						

Experiment	Medium[a]	Tube	Type[b]	Day[c]	Methane[d]	OD[e]
1	MSF	3	C	84	70.689	0.203
1	MSF	4	C	84	73.892	0.198
1	MS	2	E	84	3.908	0.014
1	MS	3	E	84	4.002	0.026
1	MS	4	E	84	4.678	0.023
1	MS	1	C	84	20.665	0.054
1	MS	2	C	84	15.875	0.038
1	MS	3	C	84	13.181	0.044
1	MS	4	C	84	17.101	0.039
1	MSH	2	E	84	20.119	0.016
1	MSH	3	E	84	30.414	0.101
1	MSH	4	E	84	31.884	0.03
1	MSH	1	C	84	74.081	0.093
1	MSH	3	C	84	74.176	0.085
1	MSH	4	C	84	79.427	0.075
1	MSH2	2	E	84	26.551	0.096
1	MSH2	3	E	84	8.926	0.046
1	MSH2	1	C	84	76.444	0.126
1	MSH2	2	C	84	82.693	0.154
1	MSF	1	E	126	59.074	0.192
1	MSF	3	E	126	68.112	0.198
1	MSF	4	E	126	52.743	0.192
1	MSF	1	C	126	50.025	0.165
1	MSF	2	C	126	62.746	0.195
1	MSF	3	C	126	70.421	0.195
1	MSF	4	C	126	60.693	0.185
1	MS	1	E	126	4.647	0.048
1	MS	2	E	126	9.764	0.067
1	MS	3	E	126	12.193	0.086
1	MS	4	E	126	13.581	0.08
1	MS	1	C	126	49.53	0.07
1	MS	2	C	126	47.664	0.072
1	MS	3	C	126	44.625	0.075
1	MS	4	C	126	43.355	0.051
1	MSH	3	E	126	34.95	0.173
1	MSH	4	E	126	42.215	0.068
1	MSH	1	C	126	74.552	0.016
(continued)						

Experiment	Medium[a]	Tube	Type[b]	Day[c]	Methane[d]	OD[e]
1	MSH	3	C	126	78.15	0.027
1	MSH	4	C	126	73.623	0.021
1	MSH2	2	E	126	31.689	0.014
1	MSH2	3	E	126	27.955	0.058
1	MSH2	1	C	126	73.326	0.047
1	MSH2	2	C	126	88.983	0.042

[a]Medium corresponds to the specific medium within the test tube, as well as the specific organisms used: MSF = *Methanobacterium formicicum*; MS = *Methanosarcina barkeri*; MSH = *Methanococcus maripaludis* (see 4.3.1 Microbial Procedures for the specific components of each medium).
[b]Type refers to whether the test tube was within the Experimental set ("E") or the Control set ("C"). Experimental tubes were exposed to low pressure (100 mbar) for 28 days. Control tubes were subjected to the same temperature as Experimental tubes.
[c]Days refers to the days elapsed since the cultures were first inoculated. Experimental tubes were subjected to low pressure between Day 7 and Day 35.
[d]Methane is given in % headspace.
[e]OD = Optical Density (600 nm).
[f]There were also two separate sets of test tubes for unique *M. maripaludis* cultures (MSH, MSH2; see Table 4.1 for a description).
[g]ND = No Data.

4.9.2 Experiment 2: Exposure of *M. barkeri*, *M. formicicum*, and *M. maripaludis* to 50 mbar for 35 days

Table 4.3 Data for Experiment 2: Exposure of *M. barkeri*, *M. formicicum*, and *M. maripaludis* to 50 mbar for 35 days

Experiment	Medium[a]	Tube	Type[b]	Day[c]	Methane[d]	OD[e]
2	MSF	1	E	0	0	0
2	MSF	2	E	0	0	0
2	MSF	3	E	0	0	0
2	MSF	4	E	0	0	0
2	MSF	1	C	0	0	0
2	MSF	2	C	0	0	0
2	MSF	3	C	0	0	0
2	MSF	4	C	0	0	0
2	MS	1	E	0	0	0
(continued)						

Experiment	Medium[a]	Tube	Type[b]	Day[c]	Methane[d]	OD[e]
2	MS	2	E	0	0	0
2	MS	3	E	0	0	0
2	MS	4	E	0	0	0
2	MS	1	C	0	0	0
2	MS	2	C	0	0	0
2	MS	3	C	0	0	0
2	MS	4	C	0	0	0
2	MSH	1	E	0	0	0
2	MSH	2	E	0	0	0
2	MSH	3	E	0	0	0
2	MSH	4	E	0	0	0
2	MSH	1	C	0	0	0
2	MSH	2	C	0	0	0
2	MSH	3	C	0	0	0
2	MSH	4	C	0	0	0
2	MSF	1	E	7	0.467	0.021
2	MSF	2	E	7	0.475	0.017
2	MSF	3	E	7	0.284	0.016
2	MSF	4	E	7	1.082	0.048
2	MSF	1	C	7	0.322	0.034
2	MSF	2	C	7	0.318	0.041
2	MSF	3	C	7	0.395	0.042
2	MSF	4	C	7	0.732	0.038
2	MS	1	E	7	0.288	0.01
2	MS	2	E	7	0.338	0.007
2	MS	3	E	7	0.425	0.008
2	MS	4	E	7	0.436	0.009
2	MS	1	C	7	0.396	ND[f]
2	MS	2	C	7	0.531	0.001
2	MS	3	C	7	0.518	0.003
2	MS	4	C	7	0.678	0.004
2	MSH	1	E	7	2.382	0.029
2	MSH	2	E	7	1.927	0.025
2	MSH	3	E	7	2.296	0.03
2	MSH	4	E	7	1.682	0.032
2	MSH	1	C	7	1.099	0.02
2	MSH	2	C	7	2.059	0.024
(continued)						

Experiment	Medium[a]	Tube	Type[b]	Day[c]	Methane[d]	OD[e]
2	MSH	3	C	7	1.829	0.023
2	MSH	4	C	7	1.637	0.023
2	MSF	1	E	42	2.139	0.027
2	MSF	2	E	42	3.184	0.034
2	MSF	3	E	42	0.921	0.046
2	MSF	4	E	42	3.199	0.079
2	MSF	1	C	42	1.593	0.028
2	MSF	2	C	42	3.664	0.04
2	MSF	3	C	42	0.453	0.037
2	MSF	4	C	42	2.807	0.032
2	MS	1	E	42	0.398	0.012
2	MS	2	E	42	0.038	0.033
2	MS	3	E	42	0.018	0.034
2	MS	4	E	42	0.344	0.008
2	MS	1	C	42	9.671	0.029
2	MS	2	C	42	13.131	0.046
2	MS	3	C	42	11.07	0.043
2	MS	4	C	42	13.099	0.051
2	MSH	1	E	42	0.788	0.02
2	MSH	2	E	42	0.798	0.016
2	MSH	3	E	42	0.891	0.016
2	MSH	4	E	42	0.794	0.008
2	MSH	1	C	42	50.479	0.101
2	MSH	2	C	42	27.471	0.094
2	MSH	3	C	42	40.918	0.092
2	MSH	4	C	42	46.265	0.135
2	MSF	1	E	70	23.922	0.382
2	MSF	2	E	70	30.931	0.277
2	MSF	3	E	70	11.564	0.24
2	MSF	4	E	70	5.094	0.093
2	MSF	1	C	70	45.788	0.082
2	MSF	2	C	70	19.696	0.052
2	MSF	3	C	70	9.731	0.063
2	MSF	4	C	70	16.669	0.065
2	MS	1	E	70	1.169	0.002
2	MS	2	E	70	0.085	0.06
2	MS	3	E	70	0.007	0.052
(continued)						

Experiment	Medium[a]	Tube	Type[b]	Day[c]	Methane[d]	OD[e]
2	MS	4	E	70	3.862	0.065
2	MS	1	C	70	26.548	0.072
2	MS	2	C	70	23.762	0.083
2	MS	3	C	70	24.668	0.085
2	MS	4	C	70	17.013	0.082
2	MSH	1	E	70	0.873	0.011
2	MSH	2	E	70	25.54	0.083
2	MSH	3	E	70	4.735	0.017
2	MSH	4	E	70	27.018	0.078
2	MSH	1	C	70	22.844	0.132
2	MSH	2	C	70	51.848	0.139
2	MSH	3	C	70	82.783	0.113
2	MSH	4	C	70	93.18	0.193
2	MSF	1	E	91	52.393	0.266
2	MSF	2	E	91	48.912	0.221
2	MSF	3	E	91	18.991	0.16
2	MSF	4	E	91	6.171	0.059
2	MSF	1	C	91	54.631	0.135
2	MSF	2	C	91	41.626	0.066
2	MSF	3	C	91	20.714	0.098
2	MSF	4	C	91	26.345	0.053
2	MS	1	E	91	2.266	0.013
2	MS	2	E	91	0.125	0.043
2	MS	3	E	91	0.006	0.039
2	MS	4	E	91	9.209	0.07
2	MS	1	C	91	29.46	0.059
2	MS	2	C	91	32.121	0.06
2	MS	3	C	91	24.048	0.064
2	MS	4	C	91	22.088	0.067
2	MSH	1	E	91	0.674	0.001
2	MSH	2	E	91	30.974	0.123
2	MSH	3	E	91	21.568	0.03
2	MSH	4	E	91	31.785	0.117
2	MSH	1	C	91	16.37	0.095
2	MSH	2	C	91	47.114	0.037
2	MSH	3	C	91	73.085	0.097
2	MSH	4	C	91	81.815	0.152
(continued)						

Experiment	Medium[a]	Tube	Type[b]	Day[c]	Methane[d]	OD[e]
2	MSF	1	E	105	47.481	0.272
2	MSF	2	E	105	41.694	0.222
2	MSF	3	E	105	21.386	0.159
2	MSF	4	E	105	5.675	0.057
2	MSF	1	C	105	62.598	0.108
2	MSF	2	C	105	56.88	0.102
2	MSF	3	C	105	54.497	0.132
2	MSF	4	C	105	30.923	0.06
2	MS	1	E	105	4.15	0.024
2	MS	2	E	105	0.174	0.04
2	MS	3	E	105	0.007	0.038
2	MS	4	E	105	7.951	0.086
2	MS	1	C	105	35.101	0.059
2	MS	2	C	105	38.604	0.057
2	MS	3	C	105	29.561	0.058
2	MS	4	C	105	25.167	0.068
2	MSH	1	E	105	0.892	0.001
2	MSH	2	E	105	23.39	0.139
2	MSH	3	E	105	18.992	0.044
2	MSH	4	E	105	30.955	0.134
2	MSH	1	C	105	17.861	0.091
2	MSH	2	C	105	46.401	0.036
2	MSH	3	C	105	78.803	0.106
2	MSH	4	C	105	78.087	0.116

[a]Medium corresponds to the specific medium within the test tube, as well as the specific organisms used: MSF = *Methanobacterium formicicum*; MS = *Methanosarcina barkeri*; MSH = *Methanococcus maripaludis* (see 4.3.1 Microbial Procedures for the specific components of each medium).

[b]Type refers to whether the test tube was within the Experimental set ("E") or the Control set ("C"). Experimental tubes were exposed to low pressure (50 mbar) for 35 days. Control tubes were subjected to the same temperature as Experimental tubes.

[c]Day refers to the days elapsed since the cultures were first inoculated. Experimental tubes were subjected to low pressure between Day 7 and Day 42.

[d]Methane is given in % headspace.

[e]OD = Optical Density (600 nm).

[f]ND = No Data.

4.9.3 Experiment 3: Exposure of *M. formicicum* to 50 mbar for 49 days

Table 4.4 Data for Experiment 3: Exposure of *M. formicicum* to 50 mbar for 49 days

Experiment	Medium[a]	Tube	Type[b]	Day[c]	Methane[d]	OD[e]
3	MSF	101	E	0	0	0
3	MSF	102	E	0	0	0
3	MSF	103	E	0	0	0
3	MSF	104	E	0	0	0
3	MSF	105	E	0	0	0
3	MSF	107	E	0	0	0
3	MSF	108	E	0	0	0
3	MSF	109	E	0	0	0
3	MSF	110	E	0	0	0
3	MSF	131	E	0	0	0
3	MSF	132	E	0	0	0
3	MSF	133	E	0	0	0
3	MSF	134	E	0	0	0
3	MSF	135	E	0	0	0
3	MSF	136	E	0	0	0
3	MSF	137	E	0	0	0
3	MSF	111	C	0	0	0
3	MSF	112	C	0	0	0
3	MSF	113	C	0	0	0
3	MSF	114	C	0	0	0
3	MSF	115	C	0	0	0
3	MSF	116	C	0	0	0
3	MSF	117	C	0	0	0
3	MSF	121	C	0	0	0
3	MSF	122	C	0	0	0
3	MSF	124	C	0	0	0
3	MSF	125	C	0	0	0
3	MSF	126	C	0	0	0
3	MSF	127	C	0	0	0
3	MSF	128	C	0	0	0
3	MSF	129	C	0	0	0
3	MSF	130	C	0	0	0
3	MSF	101	E	7	4.179	0.027
(continued)						

Experiment	Medium[a]	Tube	Type[b]	Day[c]	Methane[d]	OD[e]
3	MSF	102	E	7	1.756	0.026
3	MSF	103	E	7	3.013	0.026
3	MSF	104	E	7	4.286	0.024
3	MSF	105	E	7	1.921	0.017
3	MSF	107	E	7	4.633	0.032
3	MSF	108	E	7	3.446	0.023
3	MSF	109	E	7	5.127	0.032
3	MSF	110	E	7	6.393	0.039
3	MSF	131	E	7	2.263	0.008
3	MSF	132	E	7	1.461	0.007
3	MSF	133	E	7	0.545	0.006
3	MSF	134	E	7	2.182	0.007
3	MSF	135	E	7	1.198	0.008
3	MSF	136	E	7	2.105	0.009
3	MSF	137	E	7	1.417	0.01
3	MSF	111	C	7	4.06	0.049
3	MSF	112	C	7	2.353	0.028
3	MSF	113	C	7	1.736	0.03
3	MSF	114	C	7	4.208	0.021
3	MSF	115	C	7	2.682	0.027
3	MSF	116	C	7	4.911	0.041
3	MSF	117	C	7	4.871	0.047
3	MSF	121	C	7	2.281	0.006
3	MSF	122	C	7	1.313	0.002
3	MSF	124	C	7	0.967	0.011
3	MSF	125	C	7	1.312	0.005
3	MSF	126	C	7	2.48	0.003
3	MSF	127	C	7	2.315	0.004
3	MSF	128	C	7	1.503	0.006
3	MSF	129	C	7	1.899	0.004
3	MSF	130	C	7	2.063	0.025
3	MSF	101	E	56	4.456	0.059
3	MSF	102	E	56	3.352	0.058
3	MSF	103	E	56	3.163	0.071
3	MSF	104	E	56	1.457	0.025
3	MSF	105	E	56	3.836	0.053
3	MSF	107	E	56	6.264	0.065
(continued)						

Experiment	Medium[a]	Tube	Type[b]	Day[c]	Methane[d]	OD[e]
3	MSF	108	E	56	3.838	0.058
3	MSF	109	E	56	4.561	0.066
3	MSF	110	E	56	3.372	0.058
3	MSF	131	E	56	3.454	0.055
3	MSF	132	E	56	3.263	0.043
3	MSF	133	E	56	3.978	0.05
3	MSF	134	E	56	2.53	0.031
3	MSF	135	E	56	2.348	0.053
3	MSF	136	E	56	0.806	0.007
3	MSF	137	E	56	3.175	0.043
3	MSF	111	C	56	51.258	0.158
3	MSF	112	C	56	52.572	0.126
3	MSF	113	C	56	33.19	0.109
3	MSF	114	C	56	49.453	0.102
3	MSF	115	C	56	57.048	0.112
3	MSF	116	C	56	47.25	0.112
3	MSF	117	C	56	54.18	0.105
3	MSF	121	C	56	6.731	0.075
3	MSF	122	C	56	7.562	0.061
3	MSF	124	C	56	7.131	0.062
3	MSF	125	C	56	7.054	0.058
3	MSF	126	C	56	8	0.055
3	MSF	127	C	56	7.179	0.058
3	MSF	128	C	56	7.395	0.055
3	MSF	129	C	56	6.805	0.053
3	MSF	130	C	56	4.9033	0.057
3	MSF	101	E	70	15.084	0.142
3	MSF	102	E	70	12.397	0.125
3	MSF	103	E	70	13.029	0.135
3	MSF	104	E	70	9.027	0.107
3	MSF	105	E	70	11.638	0.111
3	MSF	107	E	70	14.045	0.135
3	MSF	108	E	70	10.578	0.107
3	MSF	109	E	70	10.901	0.123
3	MSF	110	E	70	12.165	0.14
3	MSF	131	E	70	9.725	0.141
3	MSF	132	E	70	12.83	0.129
(continued)						

Experiment	Medium[a]	Tube	Type[b]	Day[c]	Methane[d]	OD[e]
3	MSF	133	E	70	8.956	0.11
3	MSF	134	E	70	5.1	0.077
3	MSF	135	E	70	7.2	0.099
3	MSF	136	E	70	6.722	0.076
3	MSF	137	E	70	10.384	0.112
3	MSF	111	C	70	45.921	0.242
3	MSF	112	C	70	42.975	0.206
3	MSF	113	C	70	38.375	0.187
3	MSF	114	C	70	43.2	0.19
3	MSF	115	C	70	37.652	0.177
3	MSF	116	C	70	27.774	0.172
3	MSF	117	C	70	29.281	0.177
3	MSF	121	C	70	17.678	0.14
3	MSF	122	C	70	19.771	0.13
3	MSF	124	C	70	10.913	0.105
3	MSF	125	C	70	17.517	0.121
3	MSF	126	C	70	9.147	0.072
3	MSF	127	C	70	17.636	0.138
3	MSF	128	C	70	18.273	0.144
3	MSF	129	C	70	16.49	0.14
3	MSF	130	C	70	22.015	0.142
3	MSF	101	E	84	32.153	0.186
3	MSF	102	E	84	28.447	0.175
3	MSF	103	E	84	26.612	0.167
3	MSF	104	E	84	21.896	0.146
3	MSF	105	E	84	32.215	0.141
3	MSF	107	E	84	30.481	0.162
3	MSF	108	E	84	22.02	0.145
3	MSF	109	E	84	22.521	0.162
3	MSF	110	E	84	26.962	0.175
3	MSF	131	E	84	29.305	0.181
3	MSF	132	E	84	23.116	0.164
3	MSF	133	E	84	30.47	0.17
3	MSF	134	E	84	15.906	0.139
3	MSF	135	E	84	21.134	0.162
3	MSF	136	E	84	24.976	0.176
3	MSF	137	E	84	22.253	0.154
(continued)						

Experiment	Medium[a]	Tube	Type[b]	Day[c]	Methane[d]	OD[e]
3	MSF	111	C	84	80.117	0.288
3	MSF	112	C	84	71.327	0.248
3	MSF	113	C	84	81.62	0.198
3	MSF	114	C	84	74.274	0.198
3	MSF	115	C	84	62.416	0.202
3	MSF	116	C	84	51.85	0.179
3	MSF	117	C	84	51.181	0.172
3	MSF	121	C	84	53.525	0.169
3	MSF	122	C	84	55.838	0.146
3	MSF	124	C	84	52.988	0.147
3	MSF	125	C	84	56.598	0.137
3	MSF	126	C	84	32.681	0.107
3	MSF	127	C	84	51.975	0.161
3	MSF	128	C	84	54.886	0.161
3	MSF	129	C	84	49.738	0.163
3	MSF	130	C	84	48.082	0.153
3	MSF	101	E	99	44.251	0.195
3	MSF	102	E	99	42.422	0.181
3	MSF	103	E	99	33.979	0.185
3	MSF	104	E	99	41.411	0.159
3	MSF	105	E	99	38.354	0.156
3	MSF	107	E	99	46.997	0.183
3	MSF	108	E	99	39.785	0.19
3	MSF	109	E	99	35.07	0.192
3	MSF	110	E	99	38.538	0.197
3	MSF	131	E	99	39.553	0.19
3	MSF	132	E	99	33.365	0.176
3	MSF	133	E	99	46.931	0.184
3	MSF	134	E	99	23.065	0.16
3	MSF	135	E	99	28.991	0.163
3	MSF	136	E	99	46.503	0.205
3	MSF	137	E	99	31.21	0.155
3	MSF	111	C	99	72.422	0.275
3	MSF	112	C	99	95.144	0.245
3	MSF	113	C	99	78.446	0.198
3	MSF	114	C	99	87.25	0.194
3	MSF	115	C	99	76.971	0.224
(continued)						

Experiment	Medium[a]	Tube	Type[b]	Day[c]	Methane[d]	OD[e]
3	MSF	116	C	99	81.717	0.203
3	MSF	117	C	99	79.86	0.191
3	MSF	121	C	99	52.774	0.148
3	MSF	122	C	99	52.258	0.131
3	MSF	124	C	99	57.953	0.132
3	MSF	125	C	99	53.949	0.118
3	MSF	126	C	99	53.477	0.113
3	MSF	127	C	99	52.515	0.142
3	MSF	128	C	99	58.824	0.152
3	MSF	129	C	99	51.62	0.152
3	MSF	130	C	99	47.56	0.137

[a]Medium corresponds to the specific medium within the test tube, as well as the specific organisms used: MSF = *Methanobacterium formicicum* (see 4.3.1 Microbial Procedures for the specific components of the medium).
[b]Type refers to whether the test tube was within the Experimental set ("E") or the Control set ("C"). Experimental tubes were exposed to low pressure (50 mbar) for 49 days. Control tubes were subjected to the same temperature as Experimental tubes.
[c]Day refers to the days elapsed since the cultures were first inoculated. Experimental tubes were subjected to low pressure between Day 7 and Day 56.
[d]Methane is given in % headspace.
[e]OD = Optical Density (600 nm).

4.9.4 Experiment 4: Exposure of *M. formicicum* to 50 mbar for 49 days with and without formate-supplemented media

Table 4.5 Experiment 4: Exposure of *M. formicicum* to 50 mbar for 49 days with and without formate-supplemented media

Experiment	Medium[a]	Tube	Type[b]	Formate[c]	Heatkill[d]	Day[e]	Methane[f]	OD[g]
4	MSF	200	E	Y	N	0	0	0
4	MSF	201	E	Y	N	0	0	0
4	MSF	202	E	Y	N	0	0	0
4	MSF	203	E	Y	N	0	0	0
4	MSF	204	E	Y	N	0	0	0
4	MSF	210	C	Y	N	0	0	0
4	MSF	211	C	Y	N	0	0	0
(continued)								

Experiment	Medium[a]	Tube	Type[b]	Formate[c]	Heatkill[d]	Day[e]	Methane[f]	OD[g]
4	MSF	212	C	Y	N	0	0	0
4	MSF	213	C	Y	N	0	0	0
4	MSF	217	C	Y	N	0	0	0
4	MSF	214	C	Y	Y	0	0	0
4	MSF	215	C	Y	Y	0	0	0
4	MSF	216	C	Y	Y	0	0	0
4	MSF	205	E	Y	Y	0	0	0
4	MSF	206	E	Y	Y	0	0	0
4	MSF	207	E	Y	Y	0	0	0
4	MSF	220	E	N	N	0	0	0
4	MSF	221	E	N	N	0	0	0
4	MSF	225	E	N	N	0	0	0
4	MSF	226	E	N	N	0	0	0
4	MSF	227	E	N	N	0	0	0
4	MSF	232	C	N	N	0	0	0
4	MSF	233	C	N	N	0	0	0
4	MSF	234	C	N	N	0	0	0
4	MSF	235	C	N	N	0	0	0
4	MSF	239	C	N	N	0	0	0
4	MSF	222	E	N	Y	0	0	0
4	MSF	223	E	N	Y	0	0	0
4	MSF	224	E	N	Y	0	0	0
4	MSF	236	C	N	Y	0	0	0
4	MSF	237	C	N	Y	0	0	0
4	MSF	238	C	N	Y	0	0	0
4	MSF	200	E	Y	N	7	2.845	0.028
4	MSF	201	E	Y	N	7	2.231	0.027
4	MSF	202	E	Y	N	7	2.463	0.024
4	MSF	203	E	Y	N	7	2.416	0.03
4	MSF	204	E	Y	N	7	2.762	0.03
4	MSF	210	C	Y	N	7	1.38	0.016
4	MSF	211	C	Y	N	7	0.66	0.014
4	MSF	212	C	Y	N	7	0.406	0.014
4	MSF	213	C	Y	N	7	0.808	0.011
4	MSF	217	C	Y	N	7	0.586	0.01
4	MSF	214	C	Y	Y	7	0.026	0.088
4	MSF	215	C	Y	Y	7	0.436	0.089
(continued)								

Experiment	Medium[a]	Tube	Type[b]	Formate[c]	Heatkill[d]	Day[e]	Methane[f]	OD[g]
4	MSF	216	C	Y	Y	7	0.516	0.105
4	MSF	205	E	Y	Y	7	2.065	0.11
4	MSF	206	E	Y	Y	7	2.212	0.112
4	MSF	207	E	Y	Y	7	1.764	0.105
4	MSF	220	E	N	N	7	1.028	0.025
4	MSF	221	E	N	N	7	1.667	0.02
4	MSF	225	E	N	N	7	1.215	0.019
4	MSF	226	E	N	N	7	2.231	0.027
4	MSF	227	E	N	N	7	2.043	0.023
4	MSF	232	C	N	N	7	1.388	0.021
4	MSF	233	C	N	N	7	1.008	0.028
4	MSF	234	C	N	N	7	1.132	0.027
4	MSF	235	C	N	N	7	1.159	0.02
4	MSF	239	C	N	N	7	0.928	0.015
4	MSF	222	E	N	Y	7	0.705	0.089
4	MSF	223	E	N	Y	7	0.963	0.106
4	MSF	224	E	N	Y	7	1.041	0.087
4	MSF	236	C	N	Y	7	0.479	0.073
4	MSF	237	C	N	Y	7	0.743	0.078
4	MSF	238	C	N	Y	7	0.65	0.074
4	MSF	200	E	Y	N	56	2.922	0.058
4	MSF	201	E	Y	N	56	1.378	0.022
4	MSF	202	E	Y	N	56	2.353	0.042
4	MSF	203	E	Y	N	56	1.836	0.037
4	MSF	204	E	Y	N	56	2.129	0.04
4	MSF	210	C	Y	N	56	41.345	0.161
4	MSF	211	C	Y	N	56	43.823	0.153
4	MSF	212	C	Y	N	56	41.694	0.142
4	MSF	213	C	Y	N	56	41.343	0.125
4	MSF	217	C	Y	N	56	45.501	0.116
4	MSF	214	C	Y	Y	56	0.0368	0.016
4	MSF	215	C	Y	Y	56	11.232	0.056
4	MSF	216	C	Y	Y	56	44.105	0.107
4	MSF	205	E	Y	Y	56	0.068	0.035
4	MSF	206	E	Y	Y	56	0.485	0.023
4	MSF	207	E	Y	Y	56	0.104	0.024
4	MSF	220	E	N	N	56	0.498	0.01
(continued)								

Experiment	Medium[a]	Tube	Type[b]	Formate[c]	Heatkill[d]	Day[e]	Methane[f]	OD[g]
4	MSF	221	E	N	N	56	0.829	0.014
4	MSF	225	E	N	N	56	1.2	0.017
4	MSF	226	E	N	N	56	1.934	0.038
4	MSF	227	E	N	N	56	0.962	0.014
4	MSF	232	C	N	N	56	34.448	0.094
4	MSF	233	C	N	N	56	46.4	0.155
4	MSF	234	C	N	N	56	39.963	0.1
4	MSF	235	C	N	N	56	43.35	0.097
4	MSF	239	C	N	N	56	41.835	0.112
4	MSF	222	E	N	Y	56	0.059	0.026
4	MSF	223	E	N	Y	56	0.029	0.021
4	MSF	224	E	N	Y	56	0.057	0.017
4	MSF	236	C	N	Y	56	0.451	0.018
4	MSF	237	C	N	Y	56	0.958	0.025
4	MSF	238	C	N	Y	56	3.859	0.046
4	MSF	200	E	Y	N	70	23.53	0.165
4	MSF	201	E	Y	N	70	20.603	0.175
4	MSF	202	E	Y	N	70	12.669	0.117
4	MSF	203	E	Y	N	70	12.173	0.06
4	MSF	204	E	Y	N	70	47.194	0.095
4	MSF	210	C	Y	N	70	64.463	0.206
4	MSF	211	C	Y	N	70	74.778	0.237
4	MSF	212	C	Y	N	70	72.013	0.249
4	MSF	213	C	Y	N	70	77.66	0.223
4	MSF	217	C	Y	N	70	82.542	0.261
4	MSF	214	C	Y	Y	70	0.022	0.013
4	MSF	215	C	Y	Y	70	52.891	0.156
4	MSF	216	C	Y	Y	70	77.421	0.271
4	MSF	205	E	Y	Y	70	0.024	0.032
4	MSF	206	E	Y	Y	70	8.787	0.067
4	MSF	207	E	Y	Y	70	0.074	0.026
4	MSF	220	E	N	N	70	34.007	0.092
4	MSF	221	E	N	N	70	51.494	0.123
4	MSF	225	E	N	N	70	49.246	0.103
4	MSF	226	E	N	N	70	20.794	0.06
4	MSF	227	E	N	N	70	48.208	0.103
4	MSF	232	C	N	N	70	75.19	0.241
(continued)								

Experiment	Medium[a]	Tube	Type[b]	Formate[c]	Heatkill[d]	Day[e]	Methane[f]	OD[g]
4	MSF	233	C	N	N	70	72.383	0.243
4	MSF	234	C	N	N	70	58.419	0.225
4	MSF	235	C	N	N	70	76.199	0.244
4	MSF	239	C	N	N	70	75.535	0.243
4	MSF	222	E	N	Y	70	1.175	0.035
4	MSF	223	E	N	Y	70	0.629	0.025
4	MSF	224	E	N	Y	70	0.924	0.024
4	MSF	236	C	N	Y	70	0.615	0.027
4	MSF	237	C	N	Y	70	0.676	0.031
4	MSF	238	C	N	Y	70	30.317	0.235
4	MSF	200	E	Y	N	86	56.874	0.176
4	MSF	201	E	Y	N	86	51.702	0.18
4	MSF	202	E	Y	N	86	32.283	0.132
4	MSF	203	E	Y	N	86	46.496	0.112
4	MSF	204	E	Y	N	86	48.941	0.093
4	MSF	210	C	Y	N	86	75.793	0.198
4	MSF	211	C	Y	N	86	67.769	0.211
4	MSF	212	C	Y	N	86	73.496	0.228
4	MSF	213	C	Y	N	86	71.507	0.208
4	MSF	217	C	Y	N	86	77.218	0.231
4	MSF	214	C	Y	Y	86	0.023	0.015
4	MSF	215	C	Y	Y	86	63.494	0.184
4	MSF	216	C	Y	Y	86	80.867	0.238
4	MSF	205	E	Y	Y	86	0.024	0.025
4	MSF	206	E	Y	Y	86	48.995	0.113
4	MSF	207	E	Y	Y	86	0.227	0.026
4	MSF	220	E	N	N	86	48.529	0.1
4	MSF	221	E	N	N	86	46.577	0.098
4	MSF	225	E	N	N	86	49.557	0.096
4	MSF	226	E	N	N	86	17.711	0.057
4	MSF	227	E	N	N	86	46.173	0.09
4	MSF	232	C	N	N	86	75.385	0.236
4	MSF	233	C	N	N	86	71.023	0.22
4	MSF	234	C	N	N	86	71.855	0.211
4	MSF	235	C	N	N	86	72.619	0.212
4	MSF	239	C	N	N	86	74.204	0.215
4	MSF	222	E	N	Y	86	19.147	0.086
(continued)								

Experiment	Medium[a]	Tube	Type[b]	Formate[c]	Heatkill[d]	Day[e]	Methane[f]	OD[g]
4	MSF	223	E	N	Y	86	9.971	0.047
4	MSF	224	E	N	Y	86	18.243	0.05
4	MSF	236	C	N	Y	86	1.096	0.029
4	MSF	237	C	N	Y	86	0.581	0.027
4	MSF	238	C	N	Y	86	57.004	0.219

[a]Medium corresponds to the specific medium within the test tube, as well as the specific organisms used: MSF = *Methanobacterium formicicum* (see 4.3.1 Microbial Procedures for the specific components of the medium).
[b]Type refers to whether the test tube was within the Experimental set ("E") or the Control set ("C"). Experimental tubes were exposed to low pressure (50 mbar) for 49 days. Control tubes were subjected to the same temperature as Experimental tubes.
[c]Media were prepared with and without sodium formate. "Y" refers to tubes with media containing formate and "N" refers to tubes with media lacking formate.
[d]Attempts were made to sterilize certain cultures as an additional control. "Y" refers to tubes that were subjected to 1.5 h at 80-86 ºC ("heat-killed") and "N" refers to tubes that did not receive this treatment.
[e]Day refers to the days elapsed since the cultures were first inoculated. Experimental tubes were subjected to low pressure between Day 7 and Day 56.
[f]Methane is given in % headspace.
[g]OD = Optical Density (600 nm).

Chapter 5. Magnesium Sulfate Salt Solutions and Ices Fail to Protect *Serratia liquefaciens* from the Biocidal Effects of UV Irradiation under Martian Conditions

Rebecca L. Mickol[1], Jessica L. Page[2], Andrew C. Schuerger[3]

[1]Center for Space and Planetary Sciences, University of Arkansas, Fayetteville, Arkansas 72701.

[2]Department of Physics and Space Science, Florida Institute of Technology, Melbourne, Florida 32901.

[3]Department of Plant Pathology, University of Florida, Merritt Island, FL 32953.

Contributions of authors: The overall writing of this manuscript was performed by R.L.M. and A.C.S. Experiment 1 and analyses of all experiments were conducted by R.L.M., with significant contributions from A.C.S. Experiments 2-4 were conducted by J.L.P. under the guidance of A.C.S.

This chapter has been published.
Mickol, R. L., J. L. Page, and A. C. Schuerger (2017) Magnesium Sulfate Salt Solutions and Ices Fail to Protect *Serratia liquefaciens* from the Biocidal Effects of UV Irradiation under Martian Conditions. *Astrobiology*, 17(5).

5.1 Abstract

The growth of *Serratia liquefaciens* has been demonstrated under martian conditions of 0.7 kPa (7 mbar), 0 °C, and CO_2-enriched anoxic atmospheres (Schuerger *et al*., 2013, Astrobiology, 13, 115-131), but studies into the survivability of cells under hypersaline conditions that are likely to be encountered on Mars are lacking. *Serratia liquefaciens* cells were suspended in aqueous $MgSO_4$ solutions, or frozen brines, and exposed to terrestrial (i.e., 101.3 kPa, 24 °C, O_2/N_2-normal atmosphere) or martian (i.e., 0.7 kPa, -25 °C, CO_2-anoxic atmosphere) conditions to assess the roles of $MgSO_4$ and UV irradiation on the survival of *S. liquefaciens*. Four solutions were tested for their capability to attenuate martian UV irradiation in both liquid and frozen forms: sterile deionized water (SDIW), 10 mM PO_4 buffer, 5% $MgSO_4$, and 10% $MgSO_4$. None of the solutions provided enhanced protection against martian UV irradiation in either liquid or frozen forms. Sixty minutes of UV irradiation reduced cell densities from 2.0 x 10^6 cells/mL to less than 10 cells/mL for both liquid and frozen solutions. In contrast, 3-4 mm of a martian analog soil was sufficient to attenuate 100% of UV irradiation. Results suggest that terrestrial microorganisms may not survive on sun-exposed surfaces on Mars, even if the cells are embedded in frozen martian brines composed of $MgSO_4$. However, if dispersed microorganisms can be covered by only a few millimeters of dust or regolith, long-term survival is probable.

5.2 Introduction

The proximity of Mars and the likelihood of a warmer, wetter past (Pollack et al., 1987) make the planet an obvious target in the search for life outside Earth. The numerous rovers and

missions sent to Mars over the last 40 years, along with ongoing discoveries of extremophilic life on Earth, hasten the need for sufficient experiments to demonstrate the ability of Earth microorganisms to withstand interplanetary travel and planetary colonization. Results of such experiments may require enhanced planetary protection measures for spacecraft in order to limit the forward contamination of Mars.

The currently cold and dry conditions on Mars seem inhospitable to terrestrial life (Rummel et al., 2014), but recent work has demonstrated that at least a few microorganisms are capable of growth under simulated Mars surface conditions of 0.7 kPa, 0 °C, and CO_2-enriched anoxic atmospheres (Nicholson et al., 2013; Schuerger et al., 2013). Thus, it is not unreasonable that Earth microorganisms may persist on spacecraft, survive the conditions in space, and find a conducive environment on the martian surface. The varieties of microorganisms that have been isolated from spacecraft cleanrooms (La Duc et al., 2007; Moissl et al., 2007; Moissl-Eichinger, 2010; Moissl-Eichinger et al., 2012; Probst et al., 2010; Satomi et al., 2006; Stieglmeier et al., 2009; Venkateswaran et al., 2003; Venkateswaran et al., 2014) suggest that, even with multiple sterilization and cleaning techniques, it is generally not possible to completely sterilize spacecraft before launch. Interplanetary microbial survival studies (de Vera, 2012; de Vera et al., 2002, 2004; Horneck et al., 2012; Horneck et al., 2001; Nicholson et al., 2012b; Onofri et al., 2012; Vaishampayan et al., 2012) have demonstrated the hardiness of Earth microorganisms and suggest the possibility that viable cells on launched spacecraft may endure the transfer between Earth and Mars.

For any terrestrial microorganism to persist and grow on Mars, liquid water is required (Rummel et al., 2014). In the polar region of Mars, the Phoenix lander uncovered a water-ice layer protected from sublimation by a layer of regolith (Rennó et al., 2009). In addition, the

presence of gullies and recurring slope lineae (RSL) on Mars suggests that near-surface water sources may be present, which are hypothesized as brines in shallow subsurface seeps or surface runoffs from elevated sites on steep crater walls (Malin and Edgett, 2000, 2003; 2014; McEwen et al., 2011; Ojha et al., 2015; Rennó et al., 2009). Salts can absorb water, lower evaporation rates, and depress freezing points of liquids on Mars, thereby increasing the stability of fluids on the martian surface (Rennó et al., 2009; Zorzano et al., 2009). In the context of life, the relatively higher water activity of sulfate solutions, as compared to chloride solutions, suggests the possibility of habitable environments on Mars (Crisler et al., 2012). Furthermore, Crisler et al. (2012) conducted experiments testing the growth of halotolerant organisms in ~50% $MgSO_4$ solutions subjected to multiple stresses of salinity, pH, and temperature. Although the numbers of microbial species in diverse terrestrial ecosystems capable of growth under martian conditions are low, active growth of at least some terrestrial microorganisms appears possible on Mars, and thus, microbial activity under simulated martian conditions warrants further study.

Recent experiments have tested the ability of two common spacecraft isolates, *Escherichia coli* and *Serratia liquefaciens*, to withstand a variety of Mars-like conditions including hypersaline solutions (e.g., $MgSO_4$, $MgCl_2$, NaCl) between 5 and 20% and temperatures from 5-30 °C (Berry et al., 2010). Both organisms were capable of growth in all three salts at concentrations up to 5%, with greater growth rates achieved at higher temperatures. However, at higher salt concentrations, both *S. liquefaciens* and *E. coli* grew only in 10% $MgSO_4$ at 5 and 10 °C, with no growth observed at 10% or 20% in $MgCl_2$ and NaCl, or in 20% $MgSO_4$ at any of the temperatures tested.

The objectives of the current work were (1) to characterize the effects of liquid and frozen $MgSO_4$ brines on the survival of cells of *S. liquefaciens* under Mars equatorial UV fluence

rates, (2) to identify whether frozen brines of $MgSO_4$ are stable near 0 °C under martian conditions, and (3) to determine whether embedded cells in frozen $MgSO_4$ brines can be protected from solar UV irradiation by the ice matrix. The bacterium *S. liquefaciens* was selected for the current study because members of the genus *Serratia* have been recovered from spacecraft hardware and cleanrooms (Moissl et al., 2007; Novikova, 2004; Venkateswaran et al., 2014), and *S. liquefaciens* has been shown to be capable of growth under stable hydrated conditions maintained at 0.7 kPa, 0 °C, and in a CO_2-dominated anoxic atmosphere (Schuerger et al., 2013).

5.3 Materials and Methods

5.3.1 Mars Simulation Chamber

All experiments were conducted in the Mars Simulation Chamber (MSC) at the Space Life Sciences Lab, Kennedy Space Center, FL (Schuerger et al., 2008; 2011). The MSC is capable of simulating five components of the martian surface environment including (1) pressures down to 0.01 kPa, (2) UVC, UVB, and UVA irradiation between 200 and 400 nm, (3) dust loading in the atmosphere at optical depths between 0.1 (dust-free sky) and 3.5 (global dust storm), (4) temperatures between -100 °C and 30 °C, and (5) an atmospheric mixture comprised of the top five gases in the martian atmosphere [CO_2 (95.53%), N_2 (1.9%), Ar (1.9%), O_2 (0.13%), and H_2O (0.03%)].

Solar irradiation within the MSC system was simulated by one, 1000 W xenon arc lamp (model 6269; Newport Corp., Mountain View, CA, USA). The UV irradiation at the upper surfaces of the samples was calibrated for an optical depth of *tau* = 0.3 for equatorial Mars (Schuerger et al., 2003; 2006; 2008) and yielded UVC (200-280 nm), UVB (280-320 nm), and

UVA (320-400 nm) fluence rates of 4.4, 6.4, and 13.0 W/m^2, respectively. The visible (VIS; 400-700 nm) photon flux was approximately 80-100 W/m^2. A 6-cm water filter was placed in the light path of the xenon lamp to absorb mid-infrared irradiation above 1100 nm (Schuerger et al., 2008). All experiments with UV irradiation were conducted by using a simulated Mars equatorial UV flux calibrated at the upper surfaces of the samples (Schuerger et al., 2003; 2008).

Microbial samples were placed on the upper surface of a liquid nitrogen (LN_2) thermal control plate (model TP1265; Sigma Systems Corp., San Diego, CA, USA). Samples were equilibrated for 30 min to martian environmental conditions (0.7 kPa, 0 °C) prior to exposure to the martian UV-enriched light beam. After exposure and the UV beam turned off, an additional 30 min were required to equilibrate the MSC to room conditions (i.e., 101.3 kPa, 25 °C) before the MSC could be vented with filtered room air passed through a 0.3 μm pore-size HEPA filter.

5.3.2 Microbial procedures

Experiments utilized cells of the bacterium *Serratia liquefaciens* ATCC 27592 (type strain), which has been previously shown to grow under martian conditions of 0.7 kPa, 0 °C, and a CO_2-enriched atmosphere (Schuerger et al., 2013). Bacteria were maintained on trypticase soy agar (TSA; Thermo Fisher Scientific, Inc., Pittsburg, PA, USA). Vegetative cells of *S. liquefaciens* were grown at 30 °C for 24 h on TSA. The experimental unit for each assay was a 6-cm glass petri dish in which various solutions were added at the rate of 12 mL per dish.

A Most Probable Numbers (MPN) procedure (Koch, 1994; Mancinelli and Klovstad, 2000; Schuerger et al., 2003) was used to estimate the numbers of viable cells in all solutions. Briefly, 1 mL of each sample was transferred per time-step to a sterile test tube containing 9 mL

sterile deionized water. A series of six, 10-fold dilutions were performed for all samples. Twenty microliters of each dilution were transferred into each of 16 wells of a 96-well plate. The wells were previously filled with 180 μL of tryptic soy broth per well (TSB; Thermo Fisher Scientific, Inc., Pittsburg, PA, USA). The MPN assay plates were incubated at 30 °C for 24 h, at which time the number of wells showing positive growth were counted and the MPN values estimated.

5.3.3 Experiment 1: Mars UV irradiation of *S. liquefaciens* cells in liquid brines under lab conditions

Log-phase cells of *S. liquefaciens* were prepared at optical densities (OD) of 0.005 at 400 nm and dispensed at the rate of 2 x 10^6 cells/mL in the following solutions: sterile deionized water (SDIW; 18 MΩ mega-ohm resistance), 10 mM PO_4 buffer, 5% $MgSO_4$, or 10% $MgSO_4$. Twelve milliliters were dispensed into each of two 6-cm petri dishes and placed on independent magnetic stirring devices within the MSC. After being placed in the MSC and the magnetic stir pads turned on, each dish was immediately assayed in order to quantify the number of cells within each solution prior to UV-exposure (T = 0).

After the initial assay was completed, the liquid solutions were exposed to martian UV irradiation for periods of 0.17, 0.5, 1, 5, 10, 20, 30, or 60 min (cumulative). A 1 mL sample was removed from each of the two dishes following each time-step and assayed via the MPN procedure. The samples were exposed to Mars-normal UV irradiation but at Earth-normal lab conditions of 101.3 kPa (average Earth sea level pressure), 24 °C and an O_2/N_2 atmosphere (21% and 78%, respectively).

5.3.4 Experiment 2: Mars UV irradiation of *S. liquefaciens* cells in ices under martian conditions

Cells of *S. liquefaciens* were prepared as described above, and 12 mL were added to each of the following solutions: SDIW, 10 mM PO_4 buffer, 5% $MgSO_4$, and 10% $MgSO_4$ at densities of 2 x 10^6 viable cells/mL of solution. Cell suspensions were transferred to 6-cm glass petri dishes, which were then placed on the upper surface of the LN_2 cold plate in the MSC. To aid in ice crystallization of the frozen solutions, ~0.1 g of Hawaiian palagonite was added to each treatment to serve as ice nuclei (Fig. 5.1C). The chamber was closed and equilibrated to 0.7 kPa, -25 °C, and a CO_2-enriched anoxic atmosphere. The equilibration process took approximately 60 min. Although all solutions froze between 0 and -5 °C, the $MgSO_4$ solutions exhibited a thin layer of hypersaline liquid on the upper surfaces of the samples until the chamber temperature was lowered to -18 to -20 °C. Thus, all experiments were run at -25 °C to ensure that all portions of the salt solutions were frozen.

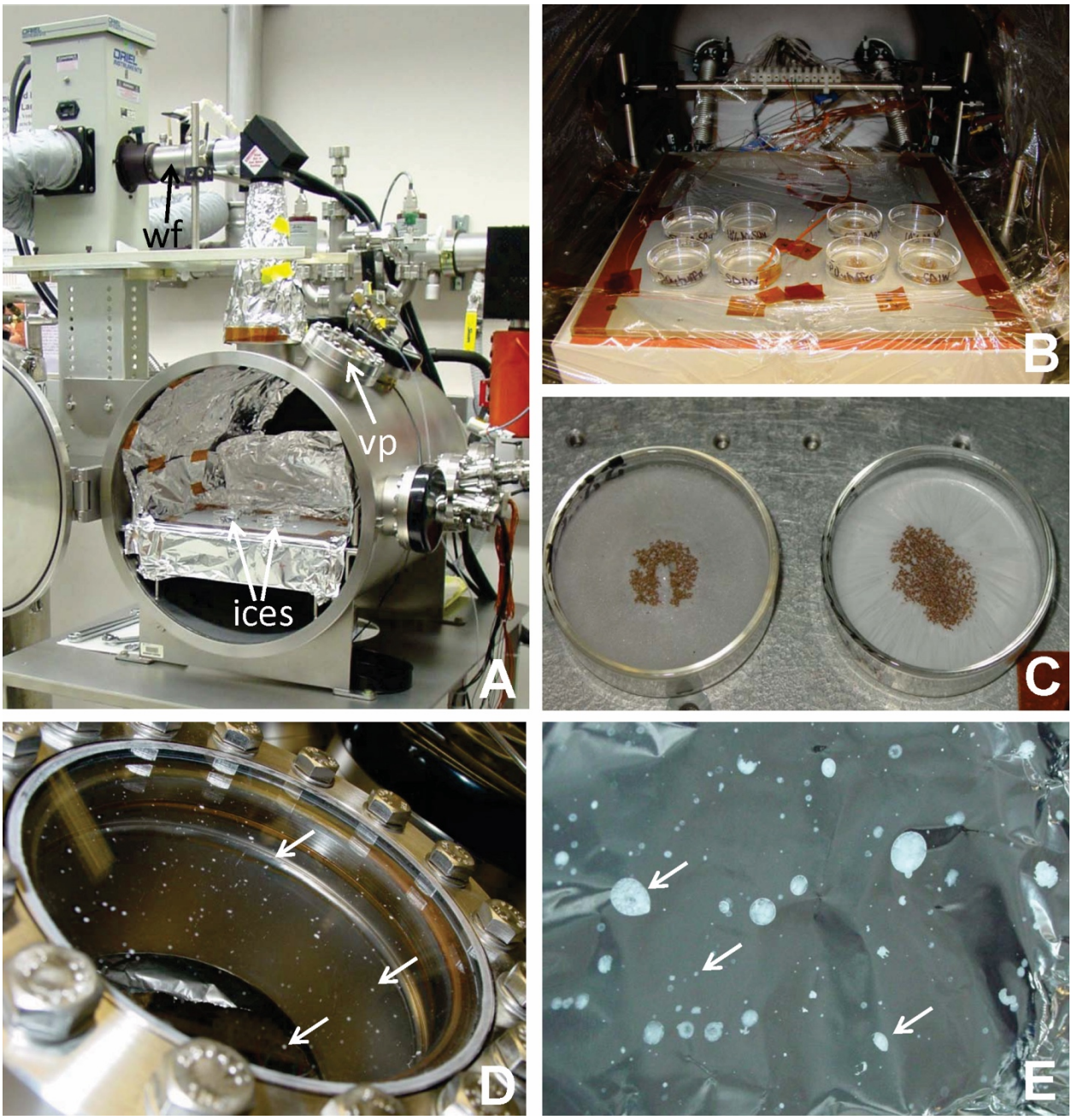

Figure 5.1 Mars Simulation Chamber (MSC) experimental setup and slush-sputtering results for Experiment 2. Aluminum foil (**A**) or clear cellophane wrap (**B**) were used to cover the inside of the Mars Simulation Chamber (MSC) in order to mitigate slush-sputtering of the water/ice/cells/salt slurries in Experiment 2. The 6-cm water filter (wf; Fig. 5.1**A**) for UV attenuation measurements (Table 5.2) was placed immediately after the xenon lamp housing on top of the MSC. The 6-cm water filter contained filtered (0.45 µm) double-deionized (18 MΩ) water for all other experiments. (**C**) Frozen samples of $MgSO_4$ brines in Experiment 2 were dispensed in 6-cm glass dishes and placed within the central part of the UV beam (28-cm wide) on top of the LN_2 cold plate. Approximately 0.1 g of Hawaiian palagonite was added to each salt solution to provide nuclei for crystallization of the ices. (**D**) Right-side view port (vp in Fig.

5.1**A**) on the MSC with salt deposits on the inside surface of the glass port. (**E**) Salt deposits were frequently observed on the aluminum foil within the MSC during Experiment 2. The dried salt slurries created salt deposits that were primarily 0.5 to 3 mm in diameter.

The frozen cells were exposed to a Mars equatorial UV flux for 0, 0.17, 1, 10, or 60 min. The MSC was held under martian conditions for 180 min (see below) to expose all treatments to identical time periods at -25 °C; during this time, samples were exposed to the UV time-steps listed above. After UV exposures, the MSC was equilibrated to lab conditions, the chamber vented, and the cells processed by the MPN method to estimate the numbers of surviving cells. A second set of petri dishes was similarly prepared, placed on the rear section of the LN_2 cold plate within the MSC, shielded from UV irradiation by placing aluminum foil over the petri dishes, and exposed to all other Mars conditions. Each assay was run for a total of 180 min under martian conditions in which the first 60 min was used to equilibrate the samples to the Mars conditions listed above, up to 60 min was used for exposing the cells in the frozen brines to UV irradiation, and 60 min was used to thaw and equilibrate the samples to lab conditions prior to venting the MSC.

Special care was taken to cover the internal walls of the MSC with either aluminum foil or clear cellophane wrap (Fig. 5.1A and 5.1B, respectively) to protect the stainless steel surfaces from salt and microbial contamination, which occurred during repressurization of the melting ices (see Results section). The ices exhibited a tendency to sputter ice/salt/cells/water droplets from the $MgSO_4$ frozen samples onto the MSC walls during the thawing process near 0 °C (Fig. 5.1D and 5.1E). The process was akin to the sputtering of metal droplets during welding and is henceforth called slush sputtering because of the undefined nature of the sputtered mixtures. The aluminum foil and cellophane protective shields were removed every two or three experiments to minimize salt and microbial contamination within the MSC.

5.3.5 Experiment 3: Survival of *S. liquefaciens* cells in liquid brines and ices

The effect of salt solutions on survival was examined under frozen and non-frozen conditions. Log-phase cells of *S. liquefaciens* were prepared and added to 36 mL of each of the following solutions: SDIW, 10 mM PO_4 buffer, 5% $MgSO_4$, and 10% $MgSO_4$ at densities of approximately 2 x 10^6 viable cells/mL of solution. For each solution, 12 mL were immediately processed by using the MPN procedure (T = 0 controls), 12 mL were transferred to sterile 6-cm glass petri dishes and incubated for 24 h at 24 °C, and 12 mL were transferred to sterile 6-cm glass petri dishes and incubated for 24 h at -20 °C. All samples were maintained at a lab-normal pressure of 101.3 kPa, and processed after 24 h by the MPN procedure.

5.3.6 Experiment 4: Mars UV irradiation of *S. liquefaciens* cells in $MgSO_4$ ice under martian conditions and covered with Mars analogs

Cells of *S. liquefaciens* were prepared and added to 5% $MgSO_4$ solutions, as described above, to final densities of 2 x 10^6 cells/mL. Cell suspensions were dispensed in 6-cm glass petri dishes at the rate of 12 mL per dish.

An Hawaiian palagonite (Allen et al., 1981) and crushed basalt (Schuerger et al., 2012) were autoclaved twice on separate days at 121 °C and 1.1 kg/cm^2 for 45 min cycles. Both the 5% $MgSO_4$ solutions and Mars analog soils were frozen separately at -20 °C for 16 h. Frozen analog soils were then dispersed on the upper surfaces of the 5% $MgSO_4$ ices to depths of 3-4 mm. The analog soils and the 5% $MgSO_4$ ices remained unmixed for the duration of the experiment. To prevent scattered UV photons from entering through the sidewalls of the 6-cm glass petri dishes, 2-mil thick Kapton tape was applied to all exterior surfaces of the dishes. Previously, Schuerger

et al. (2011) demonstrated that Kapton tape can attenuate UV photons between 200 and 400 nm down to 4-5 orders of magnitude below the Mars equatorial UV flux used here.

To insert the analog-covered 5% $MgSO_4$ ices into the MSC without thawing, a rapid and precise protocol was followed. First, the LN_2 cold plate in the MSC was lowered to 0 °C and the chamber pressure adjusted to 2.5 kPa. Without raising the LN_2 temperature, the MSC was vented to lab conditions with the room atmosphere passing through 500 cc of a desiccant (Secador Desiccant, Bel-Art Products, Wayne, NJ), preventing frost build-up on the upper surface of the LN_2 cold plate. Once at lab pressure (101.3 kPa), the soil-covered ices were quickly transferred from a lab freezer to the top of the LN_2, the MSC door closed, and the vacuum system engaged. One-half of the soil-covered ices were covered with aluminum foil to prevent UV irradiation from reaching the upper surfaces of the analog soils. The second-half of the samples were placed in the center of the UV beam within the MSC. The MSC conditions were equilibrated for 60 min at -25 °C, 0.7 kPa, and Mars atmosphere. After UV exposures of 60 min, the LN_2 cold plate was warmed to 0 °C, the MSC vented to lab pressure, and the samples collected prior to melting. Immediately upon removing the frozen analog-covered ices, most of the analog soils were removed by aseptically inverting the petri dishes; some residual analog soil particles adhered to the ice surfaces and ended up in the MPN assays. The ices remained frozen as the analog soils were removed by inversion and no loss of the ices occurred. Thus, no losses of bacteria were expected. Once extracted from the MSC, and analog soils removed, all samples were allowed to thaw and were then processed by the MPN procedure as described above.

5.3.7 UV transmission through salt solutions

To predict UV transmission into ices, salt solutions were used to characterize the attenuation of UV or VIS bands in the xenon lamp spectrum. It was assumed that UV transmittance through solutions would approximate the UV transmittance through ices of the same composition that are free of analog dusts or regolith. Approximately 120 mL each of SDIW, 10 mM PO_4 buffer, 5% $MgSO_4$, and 10% $MgSO_4$ solutions were transferred separately into the internal void space of a 6-cm water filter [Fig. 5.2 here; and see Schuerger et al. (2008)] placed in the xenon lamp light path. The UV lamp was turned on with the optics previously calibrated to deliver an equatorial Mars-normal UV-VIS spectrum (200 to 700 nm) at the top of the detectors placed on the upper surface of the LN_2 cold plate. Photon fluence rates (W/m^2) were measured for UVC, UVB, UVA, and VIS for each solution with a series of light sensors from International Light (Newburyport, MA, USA).

5.3.8 Statistical procedures

Experimental replicates were composed of individual 6-cm petri dishes with 12 mL of cell suspensions per dish. Treatments were placed in the MSC in a completely randomized design in which treatments were conducted 3 to 6 times per experiment. Data are presented as N/No values in which N equaled the values for each replicate divided by No, which was the average for T = 0 controls. Statistics were conducted for all experiments with the PC-based Statistical Analysis System (SAS) version 9.4 (SAS Institute, Inc., Cary, NC, USA). All experiments were analyzed by analysis of variance (ANOVA) followed by protected least-squares mean separation tests ($P \leq 0.05$). Each solution was analyzed independently for each

experiment (Figs. 5.2, 5.3, 5.4, and 5.5). Data sets were subjected to different power transformations to induce similar homogeneities of treatment variances; specific transformations are given in figure legends. Data in figures are presented as untransformed values. Linear regression models and F_{10} values were estimated with R software (Mac version 3.1.3) for cell inactivation rates versus UVC flux and time for each solution in Fig. 5.2 between 0 and 0.5 min. Inserted plots in Fig. 5.2 represent the comparison between cell inactivation and UVC flux. Table 5.1 presents data for both sets of models.

Table 5.1 Linear regression models for *Serratia liquefaciens* cells (from Figure 5.2) exposed to UVC irradiation for 0 to 0.5 min.

Treatment	Linear models[a] for Time	r^2 (Time)	F_{10} (sec)	Linear models[a] for UVC flux	r^2 (UVC)	F_{10} (kJ/m^2)
SDIW[b]	y = -0.174x – 0.396	0.949	5.7	y = -39.72x – 0.467	0.938	0.025
10 mM PO_4	y = -0.16x – 0.475	0.872	6.3	y = -36.51x – 0.541	0.860	0.027
5% $MgSO_4$	y = -0.126x – 0.597	0.779	7.9	y = -28.48x – 0.657	0.759	0.035
10% $MgSO_4$	y = -0.134x – 0.688	0.852	7.5	y = -30.36x – 0.750	0.835	0.033

[a]Linear models were estimated with R software; Mac version 3.1.3.
[b]SDIW = Sterile deionized water; mM = millimolar; PO_4 = phosphate buffer; $MgSO_4$ = magnesium sulfate.

5.4 Results

5.4.1 Experiment 1: Mars UV irradiation of *S. liquefaciens* in liquid brines under Mars equatorial UV flux but at Earth-lab conditions of temperature and pressure

Serratia liquefaciens cells in the four solutions were exposed to a simulated equatorial UV fluence rate for Mars in time-steps up to 60 min. The most dramatic reductions in cell viability were observed for all solutions between 0 and 0.5 min of UV-exposure, with a more gradual decline thereafter (Fig. 5.2). Cell numbers decreased significantly for 0.17 and 0.5 min time-steps by 2.5 orders of magnitude (henceforth logs) and by 4-5 logs, respectively, compared to T = 0 controls (Fig. 5.2; $P \leq 0.05$). Cell numbers recovered in the MPN assays for the SDIW

samples remained relatively constant at 9 ± 5 cells/mL for UV exposure times between 0.5 and 30 min. For UV exposure times of 0.5 and 5 min, cell numbers for all solutions ranged between 1 and 1 x 10^2 cells/mL (average: 65 ± 90 cells/mL). After 5 min, the extremely low numbers of surviving cells fluctuated between non-detectable (asterisks in Fig. 5.2) and 5 x 10^1 cells/mL, except for the 5% $MgSO_4$ solution at 30 min, which reached a level of 2.25 x 10^2 cells/mL. At 60 min of UV exposure, 4 ± 9 cells/mL and 9 ± 14 cells/mL were still viable for both the 10 mM PO_4 buffer and 10% $MgSO_4$ solutions, respectively. There was no evidence that the fluctuations between 1 and 60 min were anything but random fluctuations in the numbers of recovered cells in the liquid assays.

Linear regression models were generated for the first 0 to 0.5 min of UV-inactivation of *S. liquefaciens* cells for all solutions in Fig. 5.2. From the linear models (Table 5.1), F_{10} values were estimated for both UVC fluence rates and time to achieve 1-log reductions in cell survival under the equatorial Mars UV spectrum and fluence rates used here. The F_{10} rates for the UVC flux increased slightly from the high-purity SDIW solution (0.025 kJ/m^2) to 10% and 5% $MgSO_4$ solutions (0.033 to 0.035 kJ/m^2, respectively). The F_{10} values for time ranged from a low of 5.7 sec for SDIW to a high of 7.9 sec for 5% $MgSO_4$.

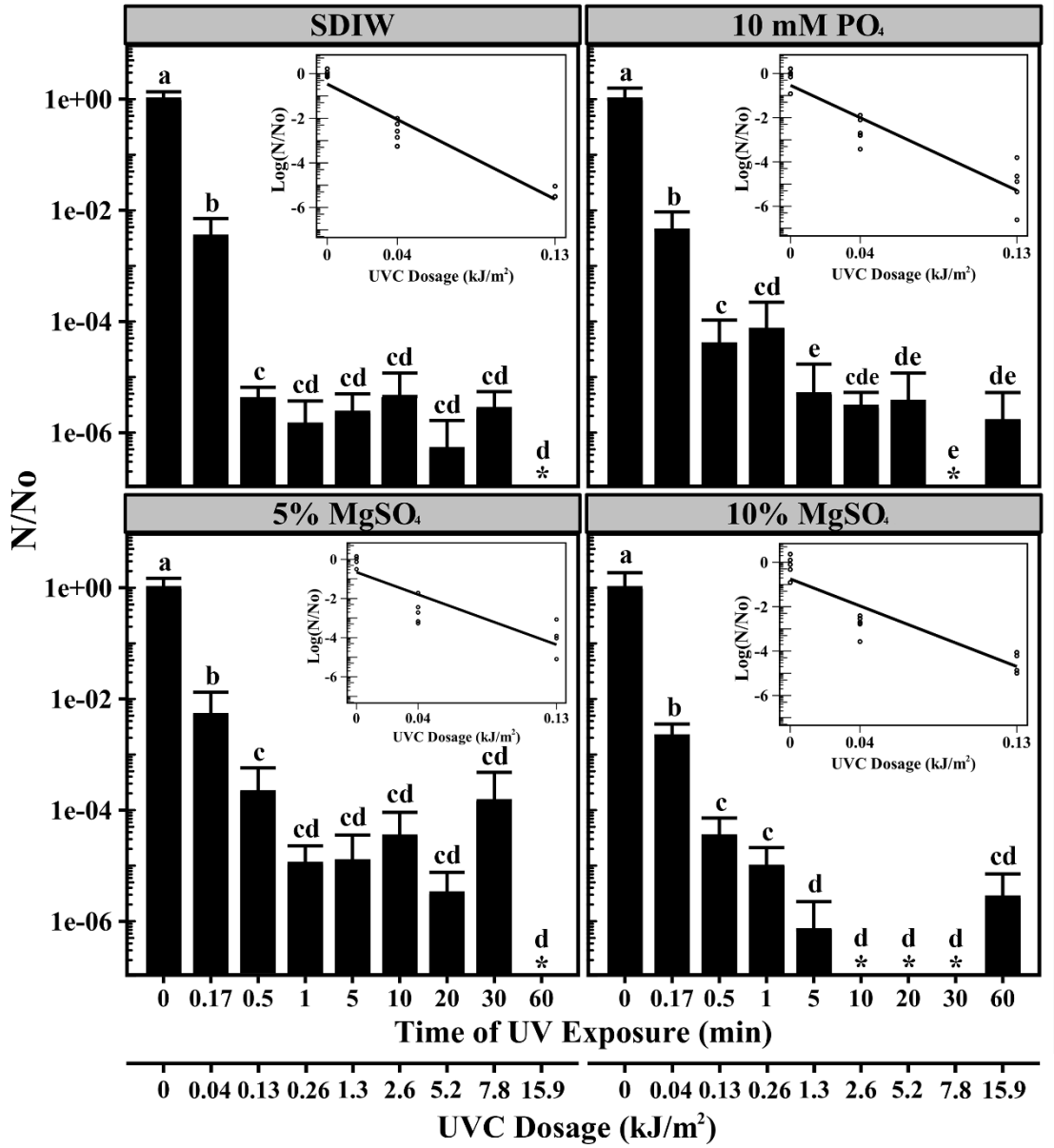

Figure 5.2 Kill curves for *Serratia liquefaciens* cells in SDIW and liquid brines exposed to Mars equatorial UV fluence rates at 101.3 kPa. Cells of *S. liquefaciens* were inoculated into SDIW, 10 mM PO_4 buffer, 5% $MgSO_4$, or 10% $MgSO_4$ solutions at densities of ~2 x 10^6 cells/mL and exposed to UV irradiation for 0, 0.17, 0.5, 1, 5, 10, 20, 30, or 60 min (cumulative). Surviving cells (N/No) decreased 4- to 5-logs between 0 and 0.5 min, with a slower decline noted thereafter. Data from each solution were transformed independently to induce homogeneity of treatment variances (i.e., SDIW and 5% $MgSO_4$ = 0.20 power transformation; 10 mM PO_4 = 0.125 power transformation; 10% $MgSO_4$ = 0.10 power transformation). Different letters indicate significant differences among treatment means for each solution based on separate ANOVA and protected least-squares mean separation tests (n = 5; $P \leq 0.05$); bars represent standard deviations of the means. Inserted graphs represent Log(N/No) values for each solution against UVC dosage (kJ/m^2) for time-steps 0, 0.17, and 0.5 min and were used to generate F_{10} values for UVC flux (shown

above) and time (data not plotted). Linear models, F_{10} values, and r^2 data for UVC flux and time are given in Table 5.1.

5.4.2 Experiment 2: UV irradiation of *S. liquefaciens* cells in ices under martian conditions

Vegetative cells of *S. liquefaciens* were held at -25 °C for a series of assays on the biocidal effects of UV irradiation on cells embedded within frozen solutions of SDIW, 10 mM PO_4 buffer, 5% $MgSO_4$, and 10% $MgSO_4$. In general, both UV-irradiated (+UV) and non-irradiated (-UV) samples exhibited significant reductions in the recovery of viable cells of *S. liquefaciens* for the frozen solutions at most time-steps compared to T = 0 samples (Fig. 5.3; $P \leq 0.05$). Most non-irradiated (-UV) samples exhibited reductions in viable cell counts between 0.5-2 logs, suggesting the reduced viabilities of cells were caused by freeze/thaw cycles encountered during the experiments. For UV-exposed treatments, viable cell numbers decreased by 3-4 logs after 0.17 min (10 sec) of UV exposure, and no viable cells were recovered from ices after 60 min of UV exposure. Reductions in cell viabilities for the [+] UV treatments were similar for all solutions and time-steps tested, suggesting that the different ices failed to attenuate UV irradiation and, thus, failed to protect *S. liquefaciens* cells in dust-free frozen SDIW or brines.

During the experiments, small droplets of water/ice/cells/salts were observed dispersed from the thawing samples (Fig. 5.1C) and deposited on fused-silica glass viewing ports (Fig. 5.1D) and walls (Fig. 5.1E) of the Mars chamber. Because the dried salt crystals likely contained viable cells of *S. liquefaciens*, aluminum foil or cellophane was placed on all internal surfaces of the MSC system. After two or three experiments, aluminum foil and cellophane protective

materials were removed and handled as biohazardous waste. The internal walls and equipment were then surface-sterilized with 70% isopropanol, and new aluminum foil or cellophane applied to the MSC walls. Although the slush sputtering process was an operational nuisance, it must be considered in future Mars simulations with frozen salt or ice mixtures in order to mitigate against human exposure to the biological agents being tested.

To evaluate the loss of ice/slush material during the slush-sputtering process, we applied salt solutions to aluminum foil in droplets from 1 to 100 µL and dried them at 0.7 kPa for 2 h in the Mars chamber to determine the volumes in the solutions likely present in the droplets observed in Fig. 5.1E. In total, droplets ≤ 1-2 µL were found to create the < 1 and up to 3 mm in diameter dried salt encrustations observed in Fig. 5.1E (data not shown). Results suggest that approximately 100 µL of the slush materials may have been ejected from each sample dish of 1.2 x 10^4 µL of the salt solutions. Losses of 100 µL of the slush/fluid droplets would yield ~0.8% reductions in the cell densities per sample. Although the physical removal of cells from the thawing salt-ice samples would bias the results in Fig. 5.3 to slightly lower levels, the overall UV-induced biocidal effects were observed to be in the range of 2-5 orders of magnitude below the T = 0 controls. Thus, we conclude that the data in Fig. 5.3 for UV-induced biocidal effects on cell survival in ices are almost exclusively influenced by UV irradiation. Because the [-] UV treatments were covered by glass petri dish tops and aluminum foil, cell losses from the samples due to slush sputtering were believed to be negligible.

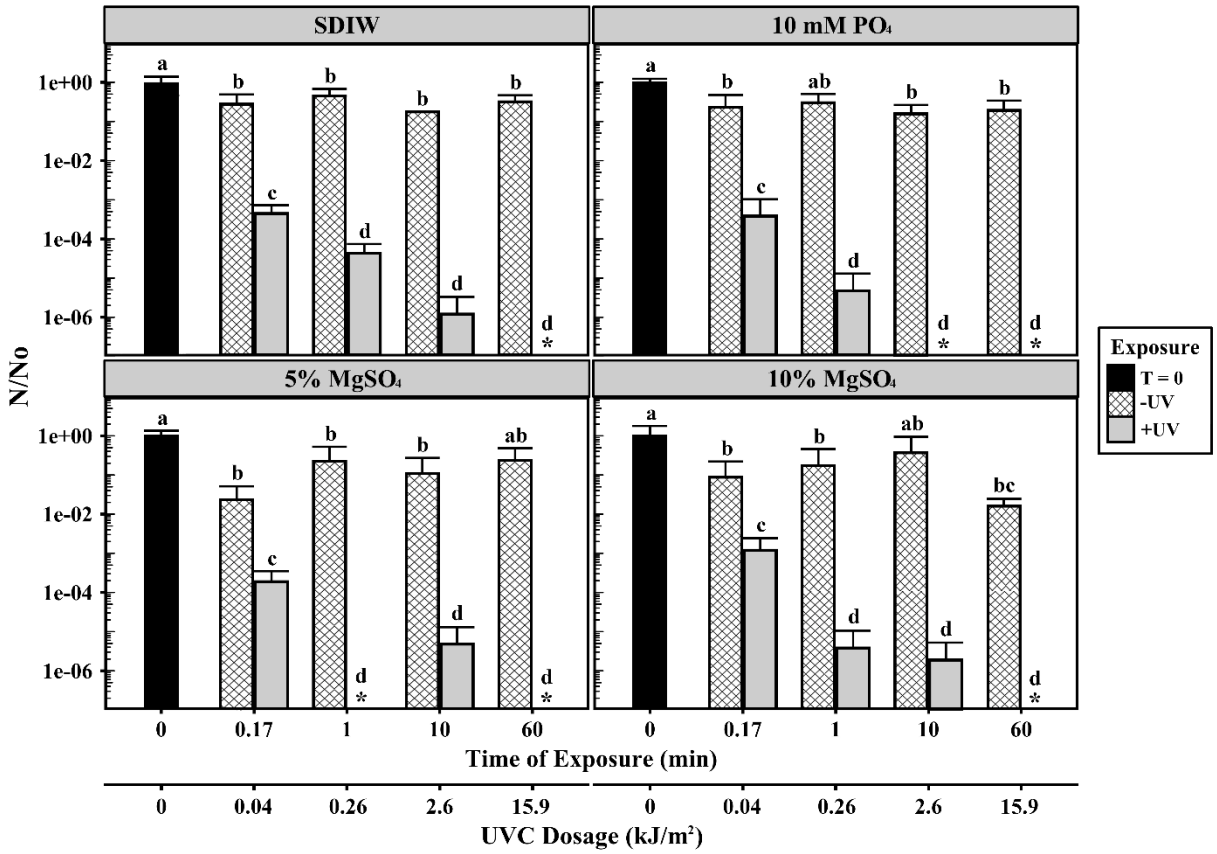

Figure 5.3 Kill curves for *Serratia liquefaciens* cells in SDIW and brine ices under martian conditions. Cells of *S. liquefaciens* were inoculated into SDIW, 10 mM PO_4 buffer, 5% $MgSO_4$, or 10% $MgSO_4$ solutions at densities of ~2 x 10^6 cells/mL. Cell suspensions were exposed to a Mars equatorial UV flux for 0, 0.17, 1, 10, or 60 min. A second set of petri dishes were similarly prepared but shielded from UV irradiation. Results here on the inactivation of *S. liquefaciens* cells embedded in the ices were very similar to the results in Fig. 5.2 obtained in liquid assays. The most dramatic declines in the numbers of surviving cells (N/No) were observed between 0 and 1 min for all treatments. Combined results from Fig. 5.2 and here suggest that the $MgSO_4$ solutions and ices failed to attenuate UV irradiation under simulated martian conditions. Data from all solutions were transformed independently to induce homogeneity of treatment variances (i.e., SDIW and 10 mM PO_4 = 0.10 power transformation; 5% $MgSO_4$ and 10% $MgSO_4$ = 0.067 power transformation). Different letters indicate significant differences among treatment means for each solution based on separate ANOVA and protected least-squares mean separation tests (n = 3; $P \leq 0.05$); bars represent standard deviations of the means.

5.4.3 Experiment 3: Survival of *S. liquefaciens* cells in liquid brines and ices

Cells of *S. liquefaciens* were inoculated into four solutions (SDIW, 10 mM PO_4 buffer, 5% $MgSO_4$, 10% $MgSO_4$) at densities of ~2 x 10^6 cells/mL to characterize the effects of freezing on the survival of cells. For each solution, one dish of cells was maintained at 24 °C for 24 h, and one dish of cells was kept at -20 °C for 24 h. Cells of *S. liquefaciens* maintained at 24 °C were generally similar to T = 0 controls (Fig. 5.4; $P > 0.05$) indicating that no losses in viability were observed for cells of *S. liquefaciens* maintained at a lab-normal temperature. Furthermore, the numbers of viable cells recovered in the 10% $MgSO_4$ solution frozen at -20 °C for 24 h were not significantly different than the T = 0 controls ($P > 0.05$). However, viable cells of *S. liquefaciens* incubated at -20 °C in SDIW, 5% $MgSO_4$, and 10 mM PO_4 exhibited significant reductions between 1 and 2 logs when compared to the T = 0 controls (Fig. 5.4; $P \leq 0.05$).

5.4.4 Experiment 4: Mars UV irradiation of *S. liquefaciens* in 5% $MgSO_4$ ices covered with Mars analog regolith

A final experiment was designed to determine whether two Mars analog soils (Allen et al., 1981) placed above frozen SDIW or brines containing *S. liquefaciens* cells might attenuate UV irradiation and yield increased survival rates for bacteria. Cells of *S. liquefaciens* were inoculated into 5% $MgSO_4$ at densities of ~2 x 10^6 cells/mL (T = 0, Fig. 5.5), frozen at -20 °C, assay dishes covered separately by two Mars analogs, and exposed to a Mars simulation at -25 °C, as described above. After the simulations, surviving cell numbers were not significantly different for the [-] UV and [+] UV exposed dishes for each Mars analog soil (Fig. 5.5, $P > 0.05$), indicating that the 3-4 mm thick layers of Mars analogs fully attenuated the UV irradiation

in the assays. The cell densities recovered for the basalt and palagonite Mars analog treatments were not significantly different ($P > 0.05$), even though there was a slight decrease in the recovered cells for the palagonite ($6.4 \pm 5.7 \times 10^4$ cells/mL) versus basalt ($1.9 \pm 1.0 \times 10^5$ cells/mL) assays (Fig. 5.5). However, there was a significant reduction in the number of viable cells recovered from the two analog soils when compared to the T = 0 controls (Fig. 5.5, $P \leq 0.05$). The recurring reduction of viable cell numbers in frozen but non-irradiated samples for Experiments 2, 3, and 4 indicates that the freezing process has a slight (~1 log) biocidal effect on *S. liquefaciens* cells.

5.4.5 UV transmittance through buffers and salt solutions

The UV transmittance through the three buffer and salt solutions decreased slightly by ~12% for UVC and UVB irradiation in the two $MgSO_4$ solutions compared to either SDIW or 10 mM PO_4 buffer (Table 5.2). In contrast, the VIS fluence rates were unchanged across the four solutions assayed. No solutions were found to attenuate enough UV irradiation to affect the biocidal nature of the simulated Mars UV conditions tested here.

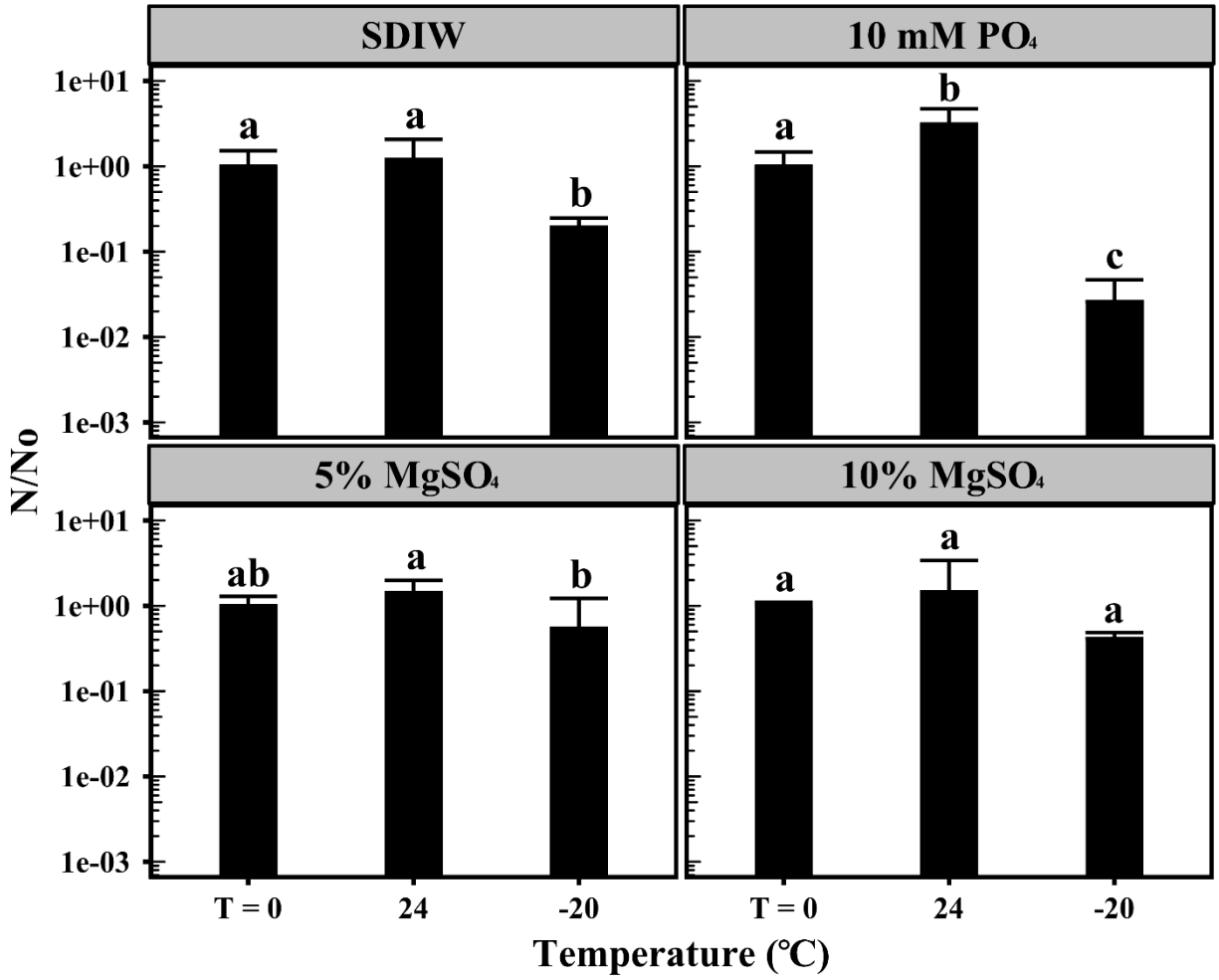

Figure 5.4 Survival of *Serratia liquefaciens* in salt solutions under frozen (-20 °C) and non-frozen (24 °C) conditions. Cells of *S. liquefaciens* were added to SDIW, 10 mM PO_4 buffer, 5% $MgSO_4$, or 10% $MgSO_4$ solutions at densities of ~2 x 10^6 viable cells/mL and exposed to either -20 or 24 °C for 24 h. Results indicate that freezing the SDIW and brine solutions at -20 °C had minimal (~1 log), but significant, effects on cell survival (N/No), except for the -20 °C 10 mM PO_4 buffer treatment which exhibited a slight decrease of 1.5 logs compared to the T = 0 controls. Data from each solution were transformed independently to induce homogeneity of treatment variances (SDIW, 10% $MgSO_4$ = log transformations; 10 mM PO_4 = 0.25 power transformation; 5% $MgSO_4$ = no transformation). Different letters indicate significant differences among treatment means for each solution within individual solutions based on separate ANOVA and protected least-squares mean separation tests (n = 4; $P \leq 0.05$); bars represent standard deviations of the means.

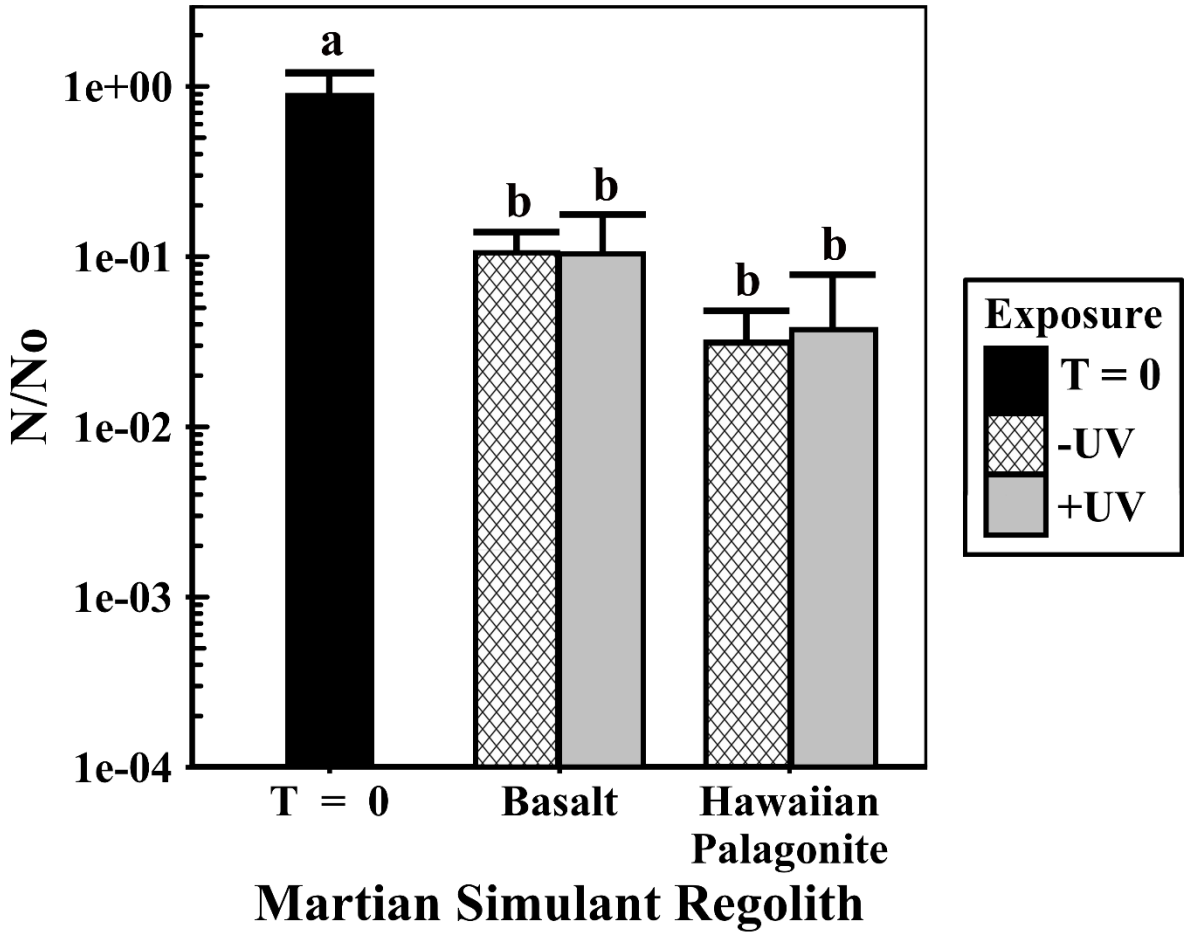

Figure 5.5 Effects of UV attenuation by Mars analog soils on the survival of *Serratia liquefaciens*. Cells of *S. liquefaciens* were added to 5% $MgSO_4$ solutions at ~2 x 10^6 cells/mL and frozen overnight for 16 h at -20 °C. Mars analog soils (i.e., basalt and Hawaiian palagonite) also were frozen at -20 °C for 16 h. The ice/analog assay dishes were exposed to a Mars UV flux for 60 min, removed, thawed, and processed with the MPN assay. Survival of *S. liquefaciens* cells (N/No) was reduced approximately 1-log and 1.5-logs for the basalt and palagonite analogs, respectively, when compared to the T = 0 controls (one T = 0 control for both analogs). Results indicate that 3-4 mm of each Mars analog completely attenuated the UV irradiation incident upon the upper surfaces of the ice/analog assays. Data were transformed with a 0.5 power transformation to induce homogeneity of treatment variances. Different letters indicate significant differences among treatment means based on separate ANOVA and protected least-squares mean separation tests (n = 6; $P \leq 0.05$); bars represent standard deviations of the means.

Table 5.2 UV Absorption (W/m^2) through sterile deionized water and three salt solutions.

	UVC[a]	UVB	UVA	VIS
SDIW[b]	4.18	5.97	12.37	81.1
10 mM PO_4	4.24	6.06	11.90	83.9
5% $MgSO_4$	3.74	5.35	11.77	83.5
10% $MgSO_4$	3.70	5.28	11.54	82.4

[a]UVC: 200-280 nm, UVB: 280-320 nm, UVA: 320-400 nm, VIS: 400-700 nm
[b]SDIW = Sterile deionized water; mM = millimolar; PO_4 = phosphate buffer; $MgSO_4$ = magnesium sulfate.

5.5 Discussion

Serratia liquefaciens exhibited a typical UV biocidal kill curve for vegetative cells of a non-spore-forming species (Fig. 5.2). Inactivation rates were between 2- to 3-logs for cells after only 0.17 min (10 sec) of UV irradiation, and 4- to 5-logs after 0.5 to 1 min of exposure. Furthermore, ultra-fast UVC inactivation rates with F_{10} values estimated for time between 5.7 and 7.9 sec for SDIW and 5% $MgSO_4$, respectively, support the conclusion that the UV environment on Mars is extremely biocidal to *S. liquefaciens*. The response is much faster than UV biocidal kill curves reported for spore-forming species in the genus *Bacillus* (Horneck et al., 2012; Horneck et al., 2001; Link et al., 2004; Moeller et al., 2012; Schuerger et al., 2003; Schuerger et al., 2005; 2006; Tauscher et al., 2006) in which endospores are much more resistant to UV irradiation than vegetative cells (Nicholson et al., 2000; Nicholson et al., 2005). The non-spore-forming bacterium, *S. liquefaciens*, was used in these experiments based on its ability to actively grow at 0.7 kPa (Schuerger et al., 2013) and within various hypersaline solutions at Mars-relevant temperatures (Berry et al., 2010). Previous experiments determined that the highest salt concentration conducive for growth of *S. liquefaciens* cells was 10% $MgSO_4$ at temperatures down to 10 °C, and that pressures down to 2.5 kPa had no effect on the growth of *S. liquefaciens* in 5% solutions of NaCl, $MgCl_2$ or $MgSO_4$ (Berry et al., 2010). Here, we

demonstrate the survival of *S. liquefaciens* in liquid or frozen SDIW and brines of 10 mM PO_4 buffer, 5% $MgSO_4$, and 10% $MgSO_4$ maintained down to 0.7 kPa and -25 °C.

There was no apparent protective effect against UV irradiation observed for *S. liquefaciens* cells when frozen in any of the four ices tested (i.e., SDIW, 10 mM PO_4, 5% $MgSO_4$, 10% $MgSO_4$; Fig. 5.3). Although the ices were visually opaque when frozen, the martian UV irradiation penetrated to the bottoms of the assay dishes (depths of 1 cm). All of the ices (Fig. 5.3) appeared to yield similar reactions to liquid assays (Fig. 5.2) with 3-log decreases in the numbers of surviving cells/mL recovered following 0.17 min (10 sec) of UV irradiation.

Our results on tolerance to hypersaline solutions are consistent with recent studies that demonstrate bacterial survival and growth in $MgSO_4$ solutions up 10% for *S. liquefaciens* (Berry et al., 2010), and up to 2 *M* solutions for halophilic species in the genera *Bacillus*, *Halomonas*, *Halobacillus*, and *Salibacillus* (Crisler et al., 2012). In contrast, the failure of $MgSO_4$ ices to protect against the biocidal effects of UV irradiation was somewhat surprising given the opacity of the frozen solutions. It was initially anticipated that the opacity would scatter the UV irradiation and, thus, reduce the total UV flux hitting cells in the ices. However, failure to attenuate biocidal UV photons by $MgSO_4$ in the current study may not reflect all potential liquid or frozen brines on Mars. For example, three recent studies demonstrate enhanced microbial survival in UV-absorbing conditions involving ferric iron solutions (Gómez et al., 2007), iron/silicate precipitates around bacterial cells (Phoenix et al., 2001), and iron-sand mixtures (Crawford et al., 2003). All three studies suggest that ferric iron may have played a role in protecting cells during the evolution of early life on Earth or Mars. Furthermore, only 12% lower UVC and UVB fluence rates were observed through the 5% or 10% $MgSO_4$ solutions

compared to SDIW (Table 5.2), and thus, the UV attenuations by the $MgSO_4$ solutions were not significant.

The observation of stable liquid perchlorate brines in active RSL features on Mars (Ojha et al., 2015) suggests that liquid habitable zones might be close to the surface in regions that are accessible by current levels of rover technologies. Magnesium sulfate solutions and ices were chosen for the current study based on the wide occurrence of $MgSO_4$ salts in martian terrains (Gendrin et al., 2005; Golden et al., 2005; Ming et al., 2006). Future work needs to expand the research to include spacecraft-relevant microorganisms in diverse salt mixtures, concentrations, and solar UV fluence rates relevant to surface conditions on Mars. For example, *Bacillus subtilis* 168 was shown to tolerate soil solution extracts from a Phoenix analog soil containing 1.5 wt% sodium perchlorate (Nicholson et al., 2012a), which is similar to the levels of perchlorates found in active RSL features (Ojha et al., 2015). But no data are available on the UV attenuation of 1.5 wt% sodium perchlorate brines under simulated martian conditions.

Previous studies have shown that relatively thin (0.5 to 2 mm thick) layers of regolith are capable of shielding cells from UV irradiation (Cockell et al., 2005; Mancinelli and Klovstad, 2000; Schuerger et al., 2012; Schuerger et al., 2003). How much shielding, however, depends in part on the mineralogical composition and layer thickness of the overburden protecting viable microorganisms. For example, when dark crushed iron-rich basalt was used to measure UV attenuation, 1-2 mm thick layers of basalt attenuated between 6 and 7 orders of magnitude of UVC and UVB irradiation, but thinner 0.5 mm layers permitted the transmission of nearly 4 orders of magnitude greater UV flux through the basalt (Schuerger et al., 2012). The UV-shielding attributes of regolith may help to preserve viable cells transferred from a rover or

lander to the martian terrain, but further research is required to identify the most UV-attenuating minerals, soil particle-size distributions, and salt species detected on Mars.

During Experiment 2, an unexpected result was the observation of sputtering of semi-liquid and slushy droplets splashed onto the internal Mars chamber walls during the thaw cycles of the brines (Fig. 5.1D and 5.1E). Based on the distances that the ice crystals were found on the side and rear walls of the MSC, and assuming that each droplet was at the apex of its arch during dispersal, we estimate that slush-sputtering of partially frozen water/ice/salt/cell slurries might attain distances up to 1.5 to 2 m on Mars. The slush-sputtering occurred when samples were thawed at 0.7 kPa and may have been due to the internal pressures within ice inclusions formed when the ices were frozen at lab pressures at 101.3 kPa. However, we have noted similar slush-sputtering when ices were frozen and thawed at 0.7 kPa (Schuerger, unpublished). A similar sputtering process was invoked to explain the occurrence of low albedo dust streaks and dark spots on the upper surfaces of CO_2 ices in the martian southern polar regions during spring thaws (Kieffer et al., 2006). The small-scale slush-sputtering process described here requires additional research to identify the internal pressures built up within ice inclusions when irradiated by solar illumination, and to clarify how far such slush ejections might disperse liquids and cells away from thawing ice or salt inclusions. Slush-sputtering may constitute an unanticipated dispersal mechanism in which terrestrial microorganisms deposited into polar ices might be moved significant distances over time through a series of sputtering events.

Terrestrial microorganisms are likely to survive the journey from Earth to Mars aboard a rover or lander and may be dispersed onto martian terrains surrounding landing sites (e.g., RSL regolith, ground ice, salt deposits, caves) [see reviews by Horneck et al., (2012); Rummel et al., (2014)]. Results of spacecraft microbial surveys suggest that a rich diversity of viable terrestrial

microorganisms are present on spacecraft at the time of launch (La Duc et al., 2007; Moissl et al., 2007; Moissl-Eichinger, 2010; Moissl-Eichinger et al., 2012; Probst et al., 2010; Satomi et al., 2006; Stieglmeier et al., 2009; Venkateswaran et al., 2003; Venkateswaran et al., 2014). Despite the harsh conditions associated with interplanetary travel, certain microorganisms, especially those that produce spores, have shown resistance to high vacuum and ionizing radiation in space (Horneck et al., 2001; 2012). Although many studies have identified solar UV irradiation as the dominant biocidal factor in space and on the martian surface (Horneck et al., 2012; Schuerger et al., 2013), UV photons can only inactivate exposed cells. Thus, a percentage of launched bioloads that are embedded within protected niches on spacecraft are likely to remain viable during the transit to Mars. Thus, martian gullies (Malin and Edgett, 2000, 2003) and active RSL features (McEwen et al., 2011; 2014; Ojha et al., 2015) represent near-surface hydrated locations that may offer terrestrial microorganisms potential habitable environments on Mars. Pure liquid water is generally unstable on the current surface of Mars, so gullies and RSL are likely formed through the presence of liquid brines. Results presented here suggest that future missions that intend to explore Special Regions with liquid brines on Mars (Ojha et al., 2015) may have to undergo a more thorough cleaning and sterilization process than rovers or landers targeted for desiccated terrains.

5.6 Acknowledgements

Rebecca Mickol was supported by the NASA Astrobiology: Exobiology and Evolutionary Biology Program (grant #NNX12AD90G), and worked in A. Schuerger's lab during the spring 2014 under a grant from NASA's Planetary Protection Office (#NNX12AJ84G). We also thank the Florida Space Grant Consortium and Space Florida for

their co-funding of J. Page for a summer 2014 internship at the Space Life Sciences Lab,

Kennedy Space Center, FL.

5.7 References

Allen, C.C., Gooding, J.L., Jercinovic, M., Keil, K. (1981) Altered basaltic glass: A terrestrial analog to the soil of Mars. *Icarus* 45, 347-369.

Berry, B.J., Jenkins, D.G., Schuerger, A.C. (2010) Effects of simulated Mars conditions on the survival and growth of *Escherichia coli* and *Serratia liquefaciens*. *Applied and Environmental Microbiology* 76, 2377-2386.

Cockell, C.S., Schuerger, A.C., Billi, D., Friedmann, E.I., Panitz, C. (2005) Effects of a simulated martian UV flux on the cyanobacterium, *Chroococcidiopsis* sp. 029. *Astrobiology* 5, 127-140.

Crawford, R.L., Paszczynski, A., Allenbach, L. (2003) Potassium ferrate [Fe (VI)] does not mediate self-sterilization of a surrogate Mars soil. *BMC Microbiology* 3, 4.

Crisler, J.D., Newville, T.M., Chen, F., Clark, B.C., Schneegurt, M.A. (2012) Bacterial growth at the high concentrations of magnesium sulfate found in martian soils. *Astrobiology* 12, 98-106.

de Vera, J.-P. (2012) Lichens as survivors in space and on Mars. *Fungal Ecology* 5, 472-479.

de Vera, J.-P., Horneck, G., Rettberg, P., Ott, S. (2002) The potential of the lichen symbiosis to cope with extreme conditions of outer space I. Influence of UV radiation and space vacuum on the vitality of lichen symbiosis and germination capacity. *International Journal of Astrobiology* 1, 285-293.

de Vera, J.-P., Horneck, G., Rettberg, P., Ott, S. (2004) The potential of the lichen symbiosis to cope with the extreme conditions of outer space II: germination capacity of lichen ascospores in response to simulated space conditions. *Advances in Space Research* 33, 1236-1243.

Gendrin, A., Mangold, N., Bibring, J.-P., Langevin, Y., Gondet, B., Poulet, F., Bonello, G., Quantin, C., Mustard, J., Arvidson, R. (2005) Sulfates in martian layered terrains: the OMEGA/Mars Express view. *Science* 307, 1587-1591.

Golden, D.C., Ming, D.W., Morris, R.V., Mertzman, S.A. (2005) Laboratory- simulated acid-sulfate weathering of basaltic materials: Implications for formation of sulfates at

Meridiani Planum and Gusev crater, Mars. *Journal of Geophysical Research: Planets (1991–2012)* 110.

Gómez, F., Aguilera, A., Amils, R. (2007) Soluble ferric iron as an effective protective agent against UV radiation: Implications for early life. *Icarus* 191, 352-359.

Horneck, G., Moeller, R., Cadet, J., Douki, T., Mancinelli, R.L., Nicholson, W.L., Panitz, C., Rabbow, E., Rettberg, P., Spry, A. (2012) Resistance of bacterial endospores to outer space for planetary protection purposes—experiment PROTECT of the EXPOSE-E mission. *Astrobiology* 12, 445-456.

Horneck, G., Rettberg, P., Reitz, G., Wehner, J., Eschweiler, U., Strauch, K., Panitz, C., Starke, V., Baumstark-Khan, C. (2001) Protection of bacterial spores in space, a contribution to the discussion on panspermia. *Origins of Life and Evolution of the Biosphere* 31, 527-547.

Kieffer, H.H., Christensen, P.R., Titus, T.N. (2006) CO_2 jets formed by sublimation beneath translucent slab ice in Mars' seasonal south polar ice cap. *Nature* 442, 793-796.

Koch, A. (1994) Most probable numbers. *Methods for General and Molecular Bacteriology (Gerhardt, P., Murray, RGE, Wood, WA and Krieg, NR, Eds.)*, 257-260.

La Duc, M.T., Dekas, A., Osman, S., Moissl, C., Newcombe, D., Venkateswaran, K. (2007) Isolation and characterization of bacteria capable of tolerating the extreme conditions of clean room environments. *Applied and Environmental Microbiology* 73, 2600-2611.

Link, L., Sawyer, J., Venkateswaran, K., Nicholson, W. (2004) Extreme spore UV resistance of *Bacillus pumilus* isolates obtained from an ultraclean spacecraft assembly facility. *Microbial Ecology* 47, 159-163.

Malin, M.C., Edgett, K.S. (2000) Evidence for recent groundwater seepage and surface runoff on Mars. *Science* 288, 2330-2335.

Malin, M.C., Edgett, K.S. (2003) Evidence for persistent flow and aqueous sedimentation on early Mars. *Science* 302, 1931-1934.

Mancinelli, R.L., Klovstad, M. (2000) Martian soil and UV radiation: microbial viability assessment on spacecraft surfaces. *Planetary and Space Science* 48, 1093-1097.

McEwen, A.S., Dundas, C.M., Mattson, S.S., Toigo, A.D., Ojha, L., Wray, J.J., Chojnacki, M., Byrne, S., Murchie, S.L., Thomas, N. (2014) Recurring slope lineae in equatorial regions of Mars. *Nature Geoscience* 7, 53-58.

McEwen, A.S., Ojha, L., Dundas, C.M., Mattson, S.S., Byrne, S., Wray, J.J., Cull, S.C., Murchie, S.L., Thomas, N., Gulick, V.C. (2011) Seasonal flows on warm martian slopes. *Science* 333, 740-743.

Ming, D.W., Mittlefehldt, D.W., Morris, R.V., Golden, D., Gellert, R., Yen, A., Clark, B.C., Squyres, S.W., Farrand, W.H., Ruff, S.W. (2006) Geochemical and mineralogical indicators for aqueous processes in the Columbia Hills of Gusev crater, Mars. *Journal of Geophysical Research: Planets (1991–2012)* 111.

Moeller, R., Schuerger, A.C., Reitz, G., Nicholson, W.L. (2012) Protective role of spore structural components in determining *Bacillus subtilis* spore resistance to simulated mars surface conditions. *Applied and Environmental Microbiology* 78, 8849-8853.

Moissl, C., Osman, S., La Duc, M.T., Dekas, A., Brodie, E., DeSantis, T., Venkateswaran, K. (2007) Molecular bacterial community analysis of clean rooms where spacecraft are assembled. *FEMS Microbiology Ecology* 61, 509-521.

Moissl-Eichinger, C. (2010) Archaea in artificial environments: their presence in global spacecraft clean rooms and impact on planetary protection. *The ISME journal* 5, 209-219.

Moissl-Eichinger, C., Rettberg, P., Pukall, R. (2012) The first collection of spacecraft-associated microorganisms: a public source for extremotolerant microorganisms from spacecraft assembly clean rooms. *Astrobiology* 12, 1024-1034.

Nicholson, W.L., Krivushin, K., Gilichinsky, D., Schuerger, A.C. (2013) Growth of *Carnobacterium* spp. from permafrost under low pressure, temperature, and anoxic atmosphere has implications for Earth microbes on Mars. *Proceedings of the National Academy of Sciences of the United States of America* 110, 666-671.

Nicholson, W.L., McCoy, L.E., Kerney, K.R., Ming, D.W., Golden, D.C., Schuerger, A.C. (2012a) Aqueous extracts of a Mars analogue regolith that mimics the Phoenix landing site do not inhibit spore germination or growth of model spacecraft contaminants *Bacillus subtilis* 168 and *Bacillus pumilus* SAFR-032. *Icarus* 220, 904-910.

Nicholson, W.L., Moeller, R., the Protect Team, Horneck, G. (2012b) Transcriptomic responses of germinating *Bacillus subtilis* spores exposed to 1.5 years of space and simulated martian conditions on the EXPOSE-E experiment PROTECT. *Astrobiology* 12, 469-486.

Nicholson, W.L., Munakata, N., Horneck, G., Melosh, H.J., Setlow, P. (2000) Resistance of *Bacillus* Endospores to Extreme Terrestrial and Extraterrestrial Environments. *Microbiology and Molecular Biology Reviews* 64, 548-572.

Nicholson, W.L., Schuerger, A.C., Setlow, P. (2005) The solar UV environment and bacterial spore UV resistance: considerations for Earth-to-Mars transport by natural processes and human spaceflight. *Mutation Research/Fundamental and Molecular Mechanisms of Mutagenesis* 571, 249-264.

Novikova, N. (2004) Review of the knowledge of microbial contamination of the Russian manned spacecraft. *Microbial Ecology* 47, 127-132.

Ojha, L., Wilhelm, M.B., Murchie, S.L., McEwen, A.S., Wray, J.J., Hanley, J., Massé, M., Chojnacki, M. (2015) Spectral evidence for hydrated salts in recurring slope lineae on Mars. *Nature Geoscience* 8, 829-832.

Onofri, S., de la Torre, R., de Vera, J.-P., Ott, S., Zucconi, L., Selbmann, L., Scalzi, G., Venkateswaran, K.J., Rabbow, E., Sánchez Iñigo, F.J. (2012) Survival of rock-colonizing organisms after 1.5 years in outer space. *Astrobiology* 12, 508-516.

Phoenix, V., Konhauser, K., Adams, D., Bottrell, S. (2001) Role of biomineralization as an ultraviolet shield: Implications for Archean life. *Geology* 29, 823-826.

Pollack, J.B., Kasting, J.F., Richardson, S.M., Poliakoff, K. (1987) The case for a wet, warm climate on early Mars. *Icarus* 71, 203-224.

Probst, A., Vaishampayan, P., Osman, S., Moissl-Eichinger, C., Andersen, G.L., Venkateswaran, K. (2010) Diversity of anaerobic microbes in spacecraft assembly clean rooms. *Applied and Environmental Microbiology* 76, 2837-2845.

Rennó, N.O., Bos, B.J., Catling, D., Clark, B.C., Drube, L., Fisher, D., Goetz, W., Hviid, S.F., Keller, H.U., Kok, J.F., Kounaves, S.P., Leer, K., Lemmon, M., Madsen, M.B., Markiewicz, W.J., Marshall, J., McKay, C., Mehta, M., Smith, M., Zorzano, M.P., Smith, P.H., Stoker, C., Young, S.M.M. (2009) Possible physical and thermodynamical evidence for liquid water at the Phoenix landing site. *Journal of Geophysical Research: Planets (1991–2012)* 114.

Rummel, J.D., Beaty, D.W., Jones, M.A., Bakermans, C., Barlow, N.G., Boston, P.J., Chevrier, V.F., Clark, B.C., de Vera, J.-P.P., Gough, R.V. (2014) A New Analysis of Mars "Special Regions": Findings of the Second MEPAG Special Regions Science Analysis Group (SR-SAG2). *Astrobiology* 14, 887-968.

Satomi, M., La Duc, M.T., Venkateswaran, K. (2006) *Bacillus safensis* sp. nov., isolated from spacecraft and assembly-facility surfaces. *International journal of systematic and evolutionary microbiology* 56, 1735-1740.

Schuerger, A.C., Clausen, C., Britt, D. (2011) Methane evolution from UV-irradiated spacecraft materials under simulated martian conditions: Implications for the Mars Science Laboratory (MSL) mission. *Icarus* 213, 393-403.

Schuerger, A.C., Fajardo-Cavazos, P., Clausen, C.A., Moores, J.E., Smith, P.H., Nicholson, W.L. (2008) Slow degradation of ATP in simulated martian environments suggests long residence times for the biosignature molecule on spacecraft surfaces on Mars. *Icarus* 194, 86-100.

Schuerger, A.C., Golden, D.C., Ming, D.W. (2012) Biotoxicity of Mars soils: 1. Dry deposition of analog soils on microbial colonies and survival under Martian conditions. *Planetary and Space Science* 72, 91-101.

Schuerger, A.C., Mancinelli, R.L., Kern, R.G., Rothschild, L.J., McKay, C.P. (2003) Survival of endospores of *Bacillus subtilis* on spacecraft surfaces under simulated martian environments: implications for the forward contamination of Mars. *Icarus* 165, 253-276.

Schuerger, A.C., Richards, J.T., Hintze, P.E., Kern, R.G. (2005) Surface characteristics of spacecraft components affect the aggregation of microorganisms and may lead to different survival rates of bacteria on Mars landers. *Astrobiology* 5, 545-559.

Schuerger, A.C., Richards, J.T., Newcombe, D.A., Venkateswaran, K. (2006) Rapid inactivation of seven *Bacillus* spp. under simulated Mars UV irradiation. *Icarus* 181, 52-62.

Schuerger, A.C., Ulrich, R., Berry, B.J., Nicholson, W.L. (2013) Growth of *Serratia liquefaciens* under 7 mbar, 0 degrees C, and CO_2-enriched anoxic atmospheres. *Astrobiology* 13, 115-131.

Stieglmeier, M., Wirth, R., Kminek, G., Moissl-Eichinger, C. (2009) Cultivation of anaerobic and facultatively anaerobic bacteria from spacecraft-associated clean rooms. *Applied and Environmental Microbiology* 75, 3484-3491.

Tauscher, C., Schuerger, A.C., Nicholson, W.L. (2006) Survival and germinability of *Bacillus subtilis* spores exposed to simulated Mars solar radiation: implications for life detection and planetary protection. *Astrobiology* 6, 592-605.

Vaishampayan, P.A., Rabbow, E., Horneck, G., Venkateswaran, K.J. (2012) Survival of *Bacillus pumilus* spores for a prolonged period of time in real space conditions. *Astrobiology* 12, 487-497.

Venkateswaran, K., Kempf, M., Chen, F., Satomi, M., Nicholson, W., Kern, R. (2003) *Bacillus nealsonii* sp. nov., isolated from a spacecraft-assembly facility, whose spores are γ-radiation resistant. *International Journal of Systematic and Evolutionary Microbiology* 53, 165-172.

Venkateswaran, K., Vaishampayan, P., Benardini III, J.N., Rooney, A.P., Spry, J.A. (2014) Deposition of extreme-tolerant bacterial strains isolated during different phases of Phoenix spacecraft assembly in a public culture collection. *Astrobiology* 14, 24-26.

Zorzano, M.P., Mateo-Martí, E., Prieto-Ballesteros, O., Osuna, S., Renno, N. (2009) Stability of liquid saline water on present day Mars. *Geophysical Research Letters* 36.

Conclusions

The multiple detections of methane in the martian atmosphere have fueled the study of methanogens as candidates for life on Mars. The anaerobic nature of methanogens and the use of inorganics for carbon and energy sources suggests that Mars may provide a relatively habitable environment for these microorganisms. Additionally, methanogens are non-photosynthetic, which indicates that they could exist in a subsurface environment, protected from harmful ionizing and UV radiation on the surface of the planet. The subsurface may also contain pockets of liquid water or brines, as well as offer a more stable temperature regime than the wide diurnal variations seen at the surface.

The experiments discussed here demonstrate the ability of Earth microorganisms to withstand various conditions reminiscent of the current martian environment. These include freeze/thaw cycles (Chapter 2), low pressure (Chapters 3, 4), and a combination of low temperature, brines, and UV radiation (Chapter 5). Although experiments typically focused on one condition at a time, these results still provide insight into the possibility of life on Mars. Further, these studies demonstrate that the martian environment may contain habitable niches where viable microorganisms on spacecraft could potentially colonize, should they survive the transit from Earth to Mars and the successful transfer from a rover or lander to the near martian subsurface.

5.8 Summary of Results

Chapters 2-4 focus on the growth and survivability of four methanogen species (*Methanosarcina barkeri*, *Methanobacterium formicicum*, *Methanococcus maripaludis*,

Methanothermobacter wolfeii) during exposure to freeze/thaw cycles (Chapter 2) and low pressure (Chapters 3, 4).

In Chapter 2, *M. wolfeii* and *M. formicicum* were subjected to freeze/thaw cycles over the course of months and long-term freezing over the course of years. Additionally, all four methanogens were exposed to diurnal and 48-h freeze/thaw cycles more similar to martian diurnal temperature changes. Both *M. formicicum* and *M. wolfeii* survived over 180 days' exposure to freeze/thaw cycles varying between the organisms' growth temperatures (37 °C, *M. formicicum*; 55 °C, *M. wolfeii*) and -80 °C. Surprisingly, following long-term exposure to -80 °C for over three years, *M. wolfeii*, a thermophile, proved capable of methane production following transfer to fresh medium and incubation at 55 °C.

The same was true for *M. wolfeii* cultures exposed to 24-h and 48-h temperature cycles between 22 °C and -80 °C. Following 10 or 12 days of cycling and subsequent incubation at 55 °C, cultures of *M. wolfeii* resumed methane production. Methane production was also resumed for cultures of *M. barkeri* and *M. formicicum*, although increases in the post-cycling incubation period were minimal compared to pre-cycling abundances. For *M. wolfeii*, optical density increased during freeze/thaw cycling, but remained relatively constant during post-cycling incubation. Cultures of *M. barkeri* showed increased optical density following 24-h cycling, but also demonstrated wide variation between replicates. This may be due to the formation of multicellular aggregates as is common in *Methanosarcina* species. Lastly, cultures of *M. formicicum* experienced a significant decrease in optical density during incubation following both 24-h and 48-h freeze/thaw cycling. Unfortunately, the effect of freeze/thaw cycles remains unknown for *M. maripaludis* due to explosion of test tubes during cycling. While the mechanisms for survival currently remain unknown, these results suggest that the cold

temperatures of Mars may not be lethal to non-psychrophilic microorganisms, and that metabolism may be resumed when environmental conditions are more favorable.

Chapters 3 and 4 exposed the four methanogens to pressures between 7 mbar (the average surface pressure on Mars) and 143 mbar. In Chapter 3, liquid cultures were exposed to pressure ranges between 7 and 143 mbar for lengths of time dictated by evaporation of the cultures. In all experiments, all four methanogens were capable of survival following exposure to low-pressure and subsequent evaporation of the liquid media. This chapter also included a preliminary experiment exposing the methanogens to a low-pressure "micro-environment" at 50 mbar for 21 days. In this experiment, all four methanogens also demonstrated methane production during incubation at their respective growth temperatures following exposure to low pressure.

Experiments conducted in Chapter 4 aimed to utilize microenvironments in order to demonstrate active growth at low pressure. Two experiments of different lengths (18 days, 28 days) were conducted at 100 mbar. In the 18-day experiment, none of the methanogens demonstrated an increase in methane during the exposure period. However, in the 28-day experiment, cultures of *M. formicicum* demonstrated both an increase in methane abundance and an increase in optical density during the 28-day exposure to 100 mbar. *M. barkeri* cultures also increased in optical density during the exposure period, but this may be the result of the formation of multicellular aggregates. In a third experiment lasting 35 days at 50 mbar, cultures of *M. formicicum* exposed to low pressure again showed an increase in both methane abundance and optical density over the exposure period. In this experiment, methane production and optical density in low-pressure replicates was identical to that of control replicates (not exposed to low pressure), within error. Additionally, cultures of *M. barkeri* demonstrated an increase in optical density during exposure to low pressure.

The active metabolism of *M. formicicum* at 50 mbar and 100 mbar led to two additional experiments at 50 mbar utilizing only this species. In the fourth experiment, methane production increased very slightly, but within error, for the low-pressure cultures, with a significant increase in optical density during the 49-day exposure to 50 mbar. However, replicates within this experiment appeared to form two separate groups, in terms of methane abundance and optical density values, within both the low-pressure set and the control set. The reason for the difference between replicates within both sets remains unknown, but with the data separated, both low-pressure groups still show an increase in methane production and optical density at 50 mbar. Interestingly, the separation into two groups for the control set demonstrates that the increase in methane production and optical density within the two low-pressure groups more closely resembles the methane production and optical density within one of the two control groups. The apparent division within both the control set and the low-pressure set led to a final experiment testing the inclusion of formate in the medium. *M. formicicum* can also utilize formate as an electron donor and its' normal growth medium is typically supplemented with sodium formate. This fifth experiment utilized cultures of *M. formicicum* both with and without formate. Methane production and optical density in cultures lacking formate was slightly less than cultures containing formate, but both were within error. This experiment also attempted to include heat-killed cells, in order to verify that methane is not produced from dead cells. However, this was unsuccessful and only proved that 1.5 h at 80 °C is not sufficient to kill cells of *M. formicicum*.

These low-pressure microenvironment experiments also invoke discussion regarding the comparison of methane production at low pressure with methane production within control tubes at atmospheric pressure (or potentially higher). When gas samples are removed from tubes under low pressure, air will rush into the syringe in order to equilibrate the pressure within the syringe

to that of the atmosphere. Should this not occur, when the gas sample is injected into the gas chromatograph, the carrier gas will also attempt to equilibrate this pressure difference. To eliminate this effect, low-pressure replicates in Experiment 5 were pressurized with CO_2 to just above atmospheric pressure following removal from low pressure. Thus, in any case, the actual methane (as percent headspace in the sample) will be diluted as compared to the methane within the control test tubes. This suggests that the methane abundance within low-pressure replicates is actually underestimated by a factor of ~10 (for the 100 mbar experiments) or ~20 (for the 50 mbar experiments). However, in certain cases, applying a dilution factor of 20 results in a methane abundance greater than 100% headspace. It remains, however, that this topic warrants further discussion.

Chapter 5 provides a comparison for growth and survival under specific martian conditions for a non-spore-forming bacterium, *Serratia liquefaciens*. This organism has previously been shown to grow under conditions of 7 mbar, 0 °C and a CO_2-enriched anoxic atmosphere. In the experiments discussed here, *S. liquefaciens* was exposed to martian equatorial UV irradiation within liquid and frozen brines at both Earth-normal pressures and temperatures and under martian conditions (7 mbar, -25 °C, CO_2-enriched anoxic atmosphere). Results indicate that UV irradiation is lethal within 60 min exposure for cells of *S. liquefaciens* in liquid and frozen sterile deionized water, 10 mM PO_4 buffer, or solutions of 5% and 10 % magnesium sulfate. However, 3-4 mm of martian simulant regolith (basalt, Hawaiian palagonite) were sufficient to fully attenuate martian UV irradiation.

In total, the results of the various experiments conducted here indicate that certain Earth microorganisms are able to withstand extreme conditions of temperature and pressure on Mars. This suggests that Mars may contain currently habitable microenvironments within the near sub-

surface. These results may inform future martian missions with regard to increased planetary protection measures or site selection.

5.9 Limitations and Future Work

The strictly anaerobic nature of methanogens limits the use of typical growth proxies associated with aerobic bacteria such as *Escherichia coli*. Attempts to culture these methanogens on agar plates were unsuccessful in this lab. Additionally, both cell counting and most probable number methods remain difficult and tedious, especially for the number of replicates included in most studies. For methanogens, methane production and optical density are typically used as growth proxies. However, as demonstrated in the experiments conducted here and as noted in previous studies, these two parameters are not always correlated. Additionally, the formation of multicellular aggregates by *Methanosarcina barkeri* would also hamper cell counting efforts. Regardless, future experiments may need to employ additional proxies for growth in order to verify the increases in methane production and optical density seen here.

Numerous possibilities exist for the extension of this research. Future experiments should combine both low temperature (~0 °C) and low pressure (7 mbar) conditions in order to more accurately mimic current conditions on Mars. Lower temperatures would also limit evaporation of the liquid media at these pressures. However, methanogenesis may be exceptionally slow or limited at low temperature. One possibility is to incorporate the use of a psychrophilic methanogen, such as *Methanogenium frigidum*, which has previously been shown capable of methanogenesis at ~0 °C. That being said, growth would still be fairly slow and not necessarily conducive to student research timeframes. Additionally, attempts to culture older stocks of *M. frigidum* in this lab were unsuccessful.

5.10 Additional Research

Additional research into the ability of these methanogens to survive or grow under martian conditions is also being conducted. These experiments are testing the growth of *M. barkeri* and *M. formicicum* on martian regolith simulants, which include clays such as montmorillonite, nontronite, and kaolinite, among others, as well as mixtures of these clays. *M. barkeri* and *M. formicicum* are capable of active methane production on certain clays, using only the clays, carbonate buffer, and hydrogen as nutrient sources. Following methane production over time, the materials are then shipped to Dr. Patricia Craig, currently at the Lunar and Planetary Institute, who analyzes the clays via scanning electron microscopy, energy dispersive x-ray spectroscopy, x-ray diffraction, and evolved gas analysis for potential biosignatures.